

---

# Design and Evaluation of Novel Histone Deacetylase 8 Inhibitors

---

Simon O.R. GREENWOOD

Institute of Structural and Molecular Biology  
University College London

A thesis submitted for the degree of  
Doctor of Philosophy

---

September 2015



I, Simon Oliver Richard Greenwood confirm that the work presented in this thesis is my own. Where information has been derived from other sources, I confirm that this has been indicated in the thesis.



# Abstract

Chapter One gives an introduction to the biological importance of HDACs and in particular of HDAC8. It discusses the structural features of the HDAC proteins, the different structural classes of inhibitors that have been reported and the isoform selectivity profiles of different inhibitors. The evaluation of a fluorogenic *N*-Boc-protected acetyl-lysine substrate in comparison to a commercially available acetyl-lysine containing tetrapeptide is also discussed and its suitability for inhibition assays is demonstrated.

The synthesis and evaluation of eight 1<sup>st</sup> generation  $\alpha$ -amino amide HDAC8 inhibitors is described in Chapter Two. These inhibitors were inspired by a literature compound utilizing a novel zinc-binding  $\alpha$ -amino amide group. The diversity in the inhibitors was envisaged to explore the chemical space around this novel zinc-binding group into two of the major structural features of HDAC8, the substrate tunnel and the acetate release pocket.

Nineteen 2<sup>nd</sup> generation  $\alpha$ -amino amide HDAC8 inhibitors were designed as a result of the HDAC8 inhibition assays of the 1<sup>st</sup> generation compounds. Chapter Three discusses the design, synthesis and biological activity of these compounds. The results of HDAC8 inhibition assays are rationalised using manual docking of the inhibitors into an HDAC8 crystal structure. Through calculation of binding energies investigation is carried out into the contribution of each feature of the compound to the overall potency of the molecule. A potential beneficial HDAC8-inhibitor contact is revealed, though no 2<sup>nd</sup> generation inhibitors show potencies that are similar to that of the lead compound.

Following the hypothesised interactions observed in manual docking of the most potent inhibitors from the 2<sup>nd</sup> generation of compounds, a 3<sup>rd</sup> and final round of  $\alpha$ -amino amide inhibitors was designed and synthesised. These compounds extend the isoindoline scaffold of the lead compound in an attempt to form extra contacts with a specific and conserved aspartate residue in a flexible loop at the mouth of substrate tunnel of the enzyme. In Chapter Four, two routes to obtain a substituted isoindoline ring system are evaluated and the synthesis of six substituted isoindolines is described, these isoindolines were coupled to generate  $\alpha$ -amino amide HDAC8 inhibitors which were of comparable potency to the lead compound. Two of these novel compounds show improved potency compared to the lead compound, demonstrating the importance of the key hydrogen bonding interaction and validating the hypothesis that introduction of a hydrogen bond acceptor results in improved potency. An exploratory nuclear magnetic resonance spectroscopy inhibitor bind-

ing experiment is also described which demonstrates the potential for investigations using this technique in the future.

Chapter Five describes all the experimental procedures which were followed in the biological evaluation of inhibitors and synthesis of inhibitors including physical and spectroscopic characterisation of all the synthesised compounds and intermediates.





# Acknowledgements

I would like to thank the BBSRC for funding and the ISMB for hosting me for the duration of my PhD.

Thank you to Prof. Charles Marson for taking on a biochemist and being patient with me throughout the years. My journey into organic chemistry could not have been nearly so easy and enjoyable were it not for the help and advice that was required so often by all the members of the 4<sup>th</sup> floor organic laboratory, especially to Tom Waugh and Chris Matthews who taught me the basics and kept me entertained while waiting for TLCs to run.

I would also like to thank Dr. Flemming Hansen and all the members of the Hansen Lab past and present, they made the last four years a great learning experience. Nico and Andrea for their wisdom and insight and Micha who was great help and a great laugh.

I could not have got through the last years without the support of my closest friends and family. It definitely helps to have such an (occasionally) peaceful place full of so much love to escape away to for a weekend. Finally to Anna, I do not know how she puts up with me, especially over the last few months, she has been constantly understanding and is perpetually amazing.

Thank you all.



# Contents

<b>1</b>	<b>Introduction</b>	<b>17</b>
1.1	Histone Deacetylases	17
1.1.1	Acetylation as a post translational modification	17
1.1.2	HDAC Classification	18
1.1.3	HDAC Expression	21
1.1.4	Roles of HDACs	22
1.1.5	The role of HDAC8	25
	HDAC8 in neuroblastoma	25
	HDAC8 and p53	25
1.2	Structural Features of HDAC8	26
1.2.1	HDAC8 flexibility	28
	Loop flexibility	28
	Core flexibility	29
	Substrate tunnel flexibility	30
1.2.2	Catalytic mechanism	31
1.3	Regulation of HDAC8	32
1.3.1	Regulation of subcellular location	33
1.3.2	Post translational modifications	34
1.3.3	Activation by small molecules	35
1.3.4	Regulation by cations	36
1.4	HDAC inhibitors	37
1.4.1	Effects of HDAC inhibitors	37
1.4.2	Structure of HDAC inhibitors	39
	The zinc binding group	39
	The cap-group (cyclic peptides/depsipeptides)	46
1.4.3	HDAC8 selective inhibitors	48
	Lead compound <b>4</b>	50
1.5	HDAC Activity assays	55
1.5.1	Cellular assays	55
1.5.2	<i>in vitro</i> Assays	56
1.6	Preliminary Assessment of Substrate $K_m$ values	59
1.7	Summary	63
1.8	Project goals	66

<b>2</b>	<b>1<sup>st</sup> Generation Inhibitors</b>	<b>67</b>
2.1	Introduction . . . . .	67
2.2	1 <sup>st</sup> generation $\alpha$ -amino amide inhibitor synthesis . . . . .	69
2.2.1	The amide coupling reaction . . . . .	70
2.2.2	Amide coupling to generate <i>N</i> -Boc- $\alpha$ -amino amides . . . . .	71
2.2.3	<i>N</i> -Boc deprotection of $\alpha$ -amino amides and their isolation . . . . .	71
2.3	1 <sup>st</sup> Generation $\alpha$ -amino amide inhibition assay results . . . . .	74
2.3.1	Changes to the 2,4-dichlorophenyl ARBG . . . . .	76
	Phenyl ARBG . . . . .	78
	<i>p</i> -Hydroxyphenyl ARBG . . . . .	79
2.3.2	Changes to the STBG . . . . .	80
	Tetrahydroisoquinoline STBG . . . . .	83
	Piperazine based STBGs . . . . .	86
2.4	Summary of 1 <sup>st</sup> generation inhibitor assay results . . . . .	88
<b>3</b>	<b>2<sup>nd</sup> Generation Inhibitors</b>	<b>91</b>
3.1	Introduction . . . . .	91
3.2	2 <sup>nd</sup> Generation $\alpha$ -amino amide inhibitor synthesis . . . . .	93
3.2.1	Synthesis of carbazole-3-amines . . . . .	93
3.2.2	Coupling and deprotection of 2 <sup>nd</sup> generation inhibitors . . . . .	93
3.3	2 <sup>nd</sup> Generation $\alpha$ -amino amide inhibitor assay results . . . . .	94
3.3.1	Inclusion of the ZBG . . . . .	96
3.3.2	Introducing flexibility into the STBG . . . . .	96
3.3.3	Addition of branched STBG . . . . .	97
3.3.4	Increasing length of the STBG . . . . .	100
3.3.5	Introduction of hydrogen bond acceptors . . . . .	100
3.4	Summary of 2 <sup>nd</sup> generation inhibitor assay results . . . . .	107
<b>4</b>	<b>3<sup>rd</sup> Generation Inhibitors</b>	<b>109</b>
4.1	Introduction . . . . .	109
4.2	Synthesis of 3 <sup>rd</sup> generation $\alpha$ -amino amide inhibitors . . . . .	112
4.2.1	Isindolines from reduction of phthalimides . . . . .	114
	Synthesis of substituted phthalimides . . . . .	114
	Reduction of phthalimides . . . . .	114
4.2.2	Isindolines from reduction of <i>N</i> -benzylphthalimides . . . . .	119
	Synthesis of <i>N</i> -benzylphthalimides . . . . .	119
	Reduction of <i>N</i> -benzylphthalimides . . . . .	119
4.2.3	Isindolines from cyclocondensation of <i>o</i> -xylenes . . . . .	121
4.2.4	Summary of synthesis of the isoindoline ring system . . . . .	124
4.2.5	Derivatisation of substituted isoindolines . . . . .	127
	Synthesis of <i>N</i> -benzylcarboxamido isoindolines . . . . .	127

---

	Synthesis of methyl carboxamido-isoindoline . . . . .	128
	Synthesis of carboxamido isoindoline <b>127</b> . . . . .	130
4.2.6	Debenzylation of <i>N</i> -benzylisoindolines . . . . .	130
	Synthesis of 5-((methylamino)methyl)isoindoline $\alpha$ -amino amide salt <b>144</b> . . . . .	131
	Synthesis of 4-aminoisoindoline $\alpha$ -amino amide salt <b>97</b> . . . . .	133
	Synthesis of 4-acetamido isoindolyl $\alpha$ -amino amide salts . . . . .	134
4.2.7	NMR to probe rotameric energy barriers . . . . .	134
4.3	$3^{rd}$ generation $\alpha$ -amino amide HDAC8 inhibition results . . . . .	137
4.3.1	Addition of an amine hydrogen bond donor to inhibitor <b>4</b> . . . . .	137
4.3.2	Addition of a amide hydrogen bond donor to inhibitor <b>4</b> . . . . .	140
4.4	Summary of $3^{rd}$ generation inhibitor assay results . . . . .	144
4.5	NMR spectroscopy of HDAC8- <b>4</b> binding . . . . .	145
4.6	Summary of Results . . . . .	150
4.7	Future work and perspectives . . . . .	152
4.7.1	Selectivity of $\alpha$ -amino amide HDACi . . . . .	152
4.7.2	Cellular activity of compounds . . . . .	152
4.7.3	Expanding the cap-group interactions of <b>99</b> . . . . .	153
4.7.4	<i>in silico</i> Compound screening . . . . .	154
4.7.5	NMR ligand binding studies . . . . .	155
<b>5</b>	<b>Materials and Methods</b> . . . . .	<b>157</b>
5.1	HDAC8 Sample Preparation . . . . .	157
5.1.1	Site directed mutagenesis . . . . .	157
5.1.2	Protein Purification . . . . .	158
5.1.3	HDAC8 fluorogenic activity Assay . . . . .	159
5.1.4	Manual Molecular docking . . . . .	161
5.2	NMR experiments . . . . .	161
5.2.1	Methyl-TROSY NMR . . . . .	161
5.2.2	NMR concentration measurements . . . . .	162
5.3	General Chemistry experimental . . . . .	162
5.4	Chemistry experimental procedures and characterisation . . . . .	163



# Abbreviations

AMC	Aminomethylcoumarin
AML	Acute myeloid leukaemia
AMP	Adenosine monophosphate
AMPK	AMP-activated protein kinase $\alpha$
ARBG	Acetate release pocket binding group
cAMP	Cyclic adenosine triphosphate
CBF $\beta$	Core binding factor $\beta$ subunit
CDK	Cyclin dependent kinase
CK2	Casein kinase II
COX	Cyclooxygenase
CTCL	Cutaneous T-cell lymphoma
DCM	Dichloromethane
DFT	Density functional theory
DIPEA	<i>N,N</i> -Diisopropylethylamine
DMF	Dimethylformamide
DMSO	Dimethylsulfoxide
EDC.HCl	<i>N</i> -(3-Dimethylaminopropyl)- <i>N</i> '-ethylcarbodiimide hydrochloride
ERR- $\alpha$	Estrogen related receptor- $\alpha$
Et <sub>2</sub> O	Diethyl ether
EtOH	Ethanol
FRET	Fluorescence resonance energy transfer
H <sub>2</sub> SO <sub>4</sub>	Sulfuric acid
HDAC	Histone deacetylase
HDACi	HDAC inhibitor
HIF	Hypoxia inducible factor
HPLC	High performance liquid chromatography
HOBt	Hydroxybenzotriazole
HSP	Heat shock protein
HSQC	Heteronuclear single quantum coherence
IPTG	Isopropyl- $\beta$ -D-thiogalactoside
$K_M$	Michaelis constant
kDa	kilodalton
PDB	Protein databank
Pd/C	Palladium on carbon catalyst
MD	Molecular dynamics
MeOH	Methanol
MMP	Matrix metalloprotease
mTOR	Mammalian target of rapamycin

MVC	Monovalent cation
NBS	<i>N</i> -bromosuccinimide
NCC	Neural crest cells
NMR	Nuclear magnetic resonance
PTCL	Peripheral T-cell lymphoma
PKA	Protein kinase A
PP1	Protein phosphatase 1
PTM	Post translational modification
PDB	Protein databank
RNA	Ribonucleic acid
RNAi	RNA interference
SAR	Structure-activity relationship
SDS-PAGE	Sodium-dodecyl-sulphate polyacrylamide gel electrophoresis
SMMHC	Smooth muscle myosin heavy chain
STBG	Substrate tunnel binding group
TBTU	<i>O</i> -(Benzotriazol-1-yl)- <i>N,N,N',N'</i> -tetramethyluronium tetrafluoroborate
TEA	Triethylamine
TFA	Trifluoroacetic acid
THF	Tetrahydrofuran
TLC	Thin layer chromatography
TMFO	Trifluoromethylketone
TRIS	Tris(hydroxymethyl)aminomethane
TROSY	Transverse relaxation-optimised spectroscopy
TSA	Trichostatin-A
VEGF	Vascular endothelial growth factor
ZBG	Zinc-binding group

# 1 Introduction

## 1.1 Histone Deacetylases

### 1.1.1 Acetylation as a post translational modification

Once considered a post translational modification (PTM) unique to histones, lysine acetylation is now accepted as a common and proteome wide PTM and may rival phosphorylation in its importance in the cell<sup>1</sup>. A high throughput mass spectrometry based study has concluded that there are at least 3600 lysine acetylation sites on 1700 individual proteins in the human proteome<sup>2</sup>. The covalent addition of a negatively charged acetate group ( $\text{CH}_3\text{COO}^-$ ) to a positively charged lysine sidechain neutralises it (Figure 1.1). This results in a loss of charge-dependent interactions and can act as a switch-like mechanism. This is particularly well demonstrated in the case of lysine-rich histone tail acetylation; in their unmodified form histone tails carry many positively charged lysine sidechains that wrap around the negatively charged phosphate backbone of DNA and this results in compacted, transcriptionally silent and repressed chromatin. Upon acetylation the positive charges are neutralised, the DNA is released by the histone tails and the chromatin becomes relaxed. More importantly (and now considered the major function of acetyl lysine modifications) acetyl lysine sidechains are specifically bound by proteins containing bromodomains such as histone acetyl transferases (HATs)<sup>3</sup> and the BET family of proteins<sup>4</sup> which provide binding platforms for other proteins that modify chromatin structure or facilitate transcription<sup>5</sup>.

When functioning as a switch-like modification, acetylation exists in a state of

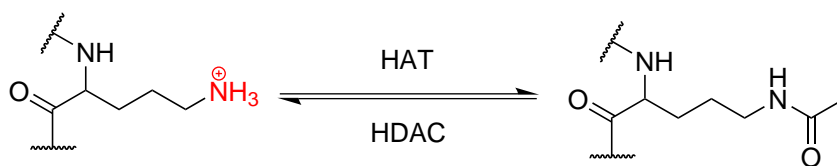


**Figure 1.1:** Acetylation and deacetylation of sidechains.

equilibrium, under constant turnover by histone acetyl-transferase (HAT) and histone deacetylase (HDAC) enzymes. Pulse-chase experiments have measured histone turnover rates with two categories of half-lives, 1-5 minutes and 30-60 minutes<sup>6</sup>. The equilibrium between the specific HAT and HDAC activities at a site determines the acetylation state as sensed by a cell, which results in a functional response. Due to the relatively fast turnover rate and wide distribution of acetylation modifications among critical functional processes, the disruption of acetylation and/or deacetylation activity (either by dysregulation, dysfunction or inhibition of HATs or HDACs) can have severe impacts on the fate of a cell.

### 1.1.2 HDAC Classification

The classical HDAC enzyme family comprises 11 enzymes divided into three phylogenetic classes (Figure 1.2b). Class I HDACs (HDAC1, HDAC2, HDAC3 and HDAC8) share homology with the yeast protein RPD3<sup>7</sup>; these proteins contain a single structured catalytic domain with a short C-terminal tail with the exception of HDAC8 which has a substantially shorter C-terminal tail than the other enzymes in this class (Figure 1.2a). This C-terminal tail is believed to be a regulatory domain and determines the specificity of the HDAC in question, indeed, replacing the HDAC1 tail with an HDAC2 sequence confers HDAC2 activity to the HDAC1 catalytic domain. HDAC1 and HDAC2 are very closely related (85% amino acid identity<sup>8</sup>) and are often found together in multiprotein complexes including: Sin3, nucleosome remodeling deacetylase (NuRD)<sup>9</sup> and corepressor for element-1-silencing transcription factor (CoREST)<sup>10</sup>. Similarly HDAC3 participates in the formation of many complexes including the silencing mediator for retinoid and thyroid receptors (SMRT) / nuclear receptor corepressor (N-CoR) complex<sup>11</sup> (Table 1.1). HDAC8 is

unique amongst class I HDACs in that it is catalytically active in a monomeric form, requiring no scaffold proteins or complexes to participate in deacetylation reactions other than its acetylated substrate.

Class II HDACs consist of HDAC4, HDAC5, HDAC6, HDAC7, HDAC9 (which occurs in three splice variants<sup>12</sup>) and HDAC10. They share homology with the yeast histone deacetylase-A (HDA1) protein, are much larger than their class I counterparts through inclusion of additional regulation and localisation domains<sup>13</sup>. Numerous interacting proteins and complexes have been identified that contain Class II HDACs including some shared with Class I HDACs such as N-CoR and SMRT<sup>14</sup>. Class II HDACs are further divided into class IIa HDACs with a single catalytic domain (HDAC4, HDAC5, HDAC7 and HDAC9) and class IIb proteins (HDAC6 and HDAC10) which have two catalytic domains, HDAC6 possesses two active catalytic domains which have different functions<sup>15</sup> and HDAC10 has a second partial catalytic domain (Figure 1.2a).

HDAC11 is the sole member of class IV and remains largely mysterious as limited research has been carried out to characterise it. HDAC11 contains some primary sequence features and activity that identify it as an HDAC but simultaneously lacks sufficient homology to either RPD3 or HDA1 to be included in either class I or II enzymes. HDAC11, like all HDACs except HDAC8, functions as part of a protein complex, one example of which is the survival of motor neuron (SMN) complex<sup>16</sup>. Class III HDAC enzymes are non-classical HDACs which require NAD<sup>+</sup> for activity; they are not related structurally to class I, II and IV HDACs and are known as sirtuins because of their homology to the yeast SIR2 protein<sup>7</sup>.

Interestingly, HDAC8 appears to have diverged from the HDAC family faster than other HDAC. The evolutionary distance between the human and zebrafish HDAC8 enzymes is similar to the human and *Drosophila melanogaster* evolutionary distances seen for other class I enzymes<sup>17</sup>. This rapid evolution is a feature that is often a result of substantial functional specialisation.

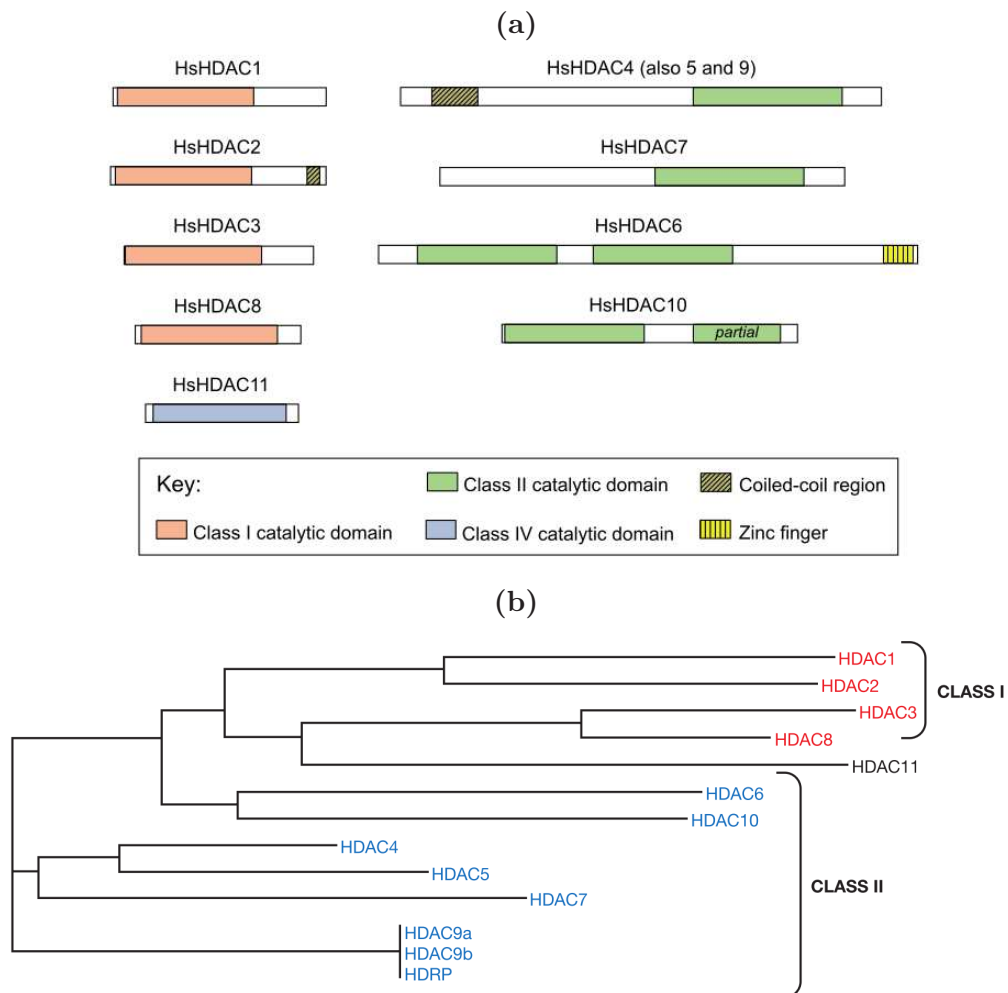


**Figure 1.2:** a) Domain architecture of Human HDAC family members (adapted from<sup>17</sup>) and b) Phylogenetic relationships within the human HDAC proteins HDRP = HDAC related protein (not to scale)<sup>7</sup>

### 1.1.3 HDAC Expression

Different members of the HDAC family are required in various cell types, cellular compartments, stages of the cell cycle and development and the expression of different HDAC isoforms consequently varies accordingly. The serial analysis of gene expression (SAGE) data for HDAC1, HDAC2, HDAC3, HDAC5, HDAC6, HDAC7 and HDAC10 suggest that they are generally expressed in all tissues examined<sup>7</sup>. The remaining HDACs are differentially expressed throughout different cell types<sup>13</sup>.

Of the class I HDACs, HDAC1 and HDAC2 are exclusively detected in the nucleus, whereas HDAC3 and HDAC8 are detected both in the nuclear and cytoplasmic cellular compartments<sup>18</sup>. All class II HDACs have been detected in cytoplasmic and nuclear fractions and also have been detected shuttling between the two; this shuttling may be part of their function and/or regulation<sup>19,20</sup>.

Conflicting data exists for the tissue distribution of HDAC8. When first characterised, low HDAC8 mRNA levels were detected in all tissues tested and very low HDAC8 mRNA levels were detected in smooth muscle (<1% of actin mRNA levels)<sup>21</sup>. Using immunofluorescence and immunoprecipitation HDAC8 was reported to be exclusively nuclear in NIH3T3 and HEK293 cells<sup>22</sup>. Subsequently HDAC8 has been seen to localise to the cytoplasmic and nuclear compartments in NIH3T3 and skin fibroblast cells<sup>23</sup> and also to the cytoskeletal fraction of smooth muscle cells<sup>24</sup>.

HDAC8 expression in nervous tissues is also the subject of debate. Some groups have reported high HDAC8 levels in the brain and pancreas<sup>25</sup> whereas others detected no expression in nervous tissues of the brain, spinal chord and periphery<sup>23</sup>. All this conflicting evidence suggests that numerous factors contribute to the expression of HDAC8 (e.g. stress levels, culture conditions, the stage of the cell cycle and the cell type)<sup>26</sup>.

### 1.1.4 Roles of HDACs

HDACs are involved in a vast array of overlapping cellular systems from metabolic regulation and cell proliferation to cell fate determination and motility. Some HDAC functions are redundant and can be compensated for by other HDACs while other HDAC functions are unique and specific to a single isoform. Their mechanisms of action are also numerous, including binding partner proteins in a protective manner, providing a scaffold for other protein interactions, recruitment of transcription factors and enzymatic deacetylation of substrate proteins. HDACs are often only characterised in disease settings because their specific roles are fundamentally involved in so many intertwined and complicated aspects of cellular life. An overview of some HDAC interaction partners and substrates is shown in Table 1.1, these numerous functions are manifested by the many different phenotypes that result from the knockout of each individual HDAC.

Mouse knockouts of HDAC1, HDAC2, HDAC3, HDAC4, HDAC7 and HDAC8 are lethal in the embryonic or perinatal stages whereas HDAC5, HDAC6, HDAC9 and HDAC11 knockout mice are viable but have defects affecting the development of various tissues, HDAC10 has yet to be successfully knocked out of the mouse genome<sup>27–38</sup>. These studies show that each HDAC plays a highly significant role within the cell and has at least one non-redundant functions which it has evolved to perform.

Many HDACs are of particular interest due to observed correlations between high expression levels in tumours and disease progression/prognosis<sup>39</sup>. All 11 Zn<sup>2+</sup> dependent HDACs have been linked to at least one process which leads to metastatic cancer<sup>39,40</sup> and many have been detected at above normal expression levels in various cancers.

When the first non-histone substrates for HDACs were identified in 2000, and HDAC1 was shown to deacetylate p53<sup>58,59</sup>, the functional roles of HDACs were greatly expanded as the possibility of other non-histone HDAC substrates became a reality. 1750 acetylated proteins have now been identified by mass spectrometry which show a change in acetylation upon treatment with HDAC inhibitors<sup>2</sup>. The number of potential HDAC substrates is therefore huge and acetylation has been suggested to rival phosphorylation in importance in the cell<sup>1</sup>, since very few sub-

**Table 1.1:** HDAC interaction partners and types (adapted from ref. [39])

Class	HDAC	interaction type	target	references
I	1, 2	active complex	Sin3, NuRd, CoREST	8,41
	1,2,3	pathway induction	HIF, VEGF	42-44
		pathway suppression	NF $\kappa$ B, mTOR, <i>BRCA2</i> & <i>RAD51</i>	11,43
	3	active complex	N-CoR-SMRT	45
	1	transcriptional repression substrate	p21 & p27	27
			AMPK,p53	46,47
	8	substrate inhibition repression degradation protection	ERR- $\alpha$ ,HSP20,SMC3	48-50
			Otx2 & Lhx1	36
p53 (mutant only)			51	
hEST1B			52	
4,5,7	regulatory transcriptional inhibition	AMPK	46	
		MEF2	7,19,54	
IIa	4	substrate interaction	GCMa, GATA-1, Hp-1	39
			ANKRA, RFXANK	39
	5	substrate interaction	Smad7, HP-1, GCMa	39
			REA, estrogen receptor	39
	7	substrate interaction	FLAG1 and 2 HIF-1 $\alpha$ , Bcl-6	39 39
9	substrate interaction	ATDC	55	
		FOX3P	39	
IIIb	6,10	substrate	HSP90	39,44,56
	6	substrate	tubulin	57
IV	11	interaction	HDAC6?	39
		active complex	SMN	16

strates have been identified as targets for specific HDACs, it is now a goal in the field to assign specific acetylation targets to each HDAC isoform.

Most class I HDACs substrate specificity is determined by the composition of their quarternary complex through assembly with specific proteins and many inhibitors have been shown to have differential inhibition depending on the complex composition<sup>60</sup>. HDAC8 is the only class I HDAC to show deacetylase activity without additional cofactors.

The observations of HDACs acting as scaffolding proteins through co-localisation without enzymatic activity gives rise to the possibility that their active site need not necessarily be the target of an inhibitor, an interaction-blocking inhibitor may not affect binding of certain substrates but may affect complex formation or regulation of activity. It may be possible to inhibit the catalytic and scaffolding functions of an HDAC independently, allowing even more intricate dissection of HDAC roles within the cell as well as more specifically targeted therapies.

Just as the importance for HDACs grew when the vast number of non-histone substrates was discovered, so their importance may grow again as there is a possibility that HDAC activity is not restricted to acetyl-lysine residues. HDAC3 has recently been shown to have some activity towards crotylated lysine residues<sup>61</sup> and a NAD<sup>+</sup> dependent deacetylase SIRT5 is a lysine demalonylase and desuccinylase<sup>62</sup>.

While these reports show no such activity for HDAC8 they suggest that HDAC substrates other than acetyl-lysines are potentially physiologically relevant. The ubiquitous role that HDACs play within cells in many cellular systems suggests that HDACs may also provide therapeutic targets in the treatment of many more widespread diseases than just cancer. These include treatments for sickle cell anaemia<sup>63</sup>,  $\alpha$ 1-antitrypsin deficiency<sup>64</sup>, cystic fibrosis<sup>65</sup>, chronic pain<sup>66</sup>, inflammatory disorders<sup>67</sup>, anthrax poisoning<sup>68</sup>, malaria<sup>69</sup>, HIV<sup>70</sup> and neurodegenerative diseases such as Alzheimer's and Parkinson's<sup>71</sup> to name a few. In a non-disease setting, HDAC inhibition shows promise as a cognitive enhancer<sup>72</sup> and has been shown to improve the efficiency of stem-cell reprogramming<sup>73</sup>.

### 1.1.5 The role of HDAC8

When originally discovered, HDAC8 was reported to have activity on the core histone proteins H2A/H2B, H3 and H4 *in vitro* when overexpressed<sup>21,22,74</sup>. Supporting this observation, hyperacetylation of histones H3 and H4 was detected when HDAC8 was inactivated by protein kinase A (PKA) phosphorylation<sup>75</sup>. However many studies since have observed that removal of HDAC8 activity by inhibition or knockdown results in no global change in histone acetylation in a cellular context<sup>76,77</sup>. HDAC8 is likely therefore to have a residual activity towards histones but this activity is only seen when overexpressed and has no significance in a physiological context. It would be interesting to know if HDAC8 shows activity towards histones in HDAC8-overexpressing neuroblastoma cell lines, as this has not been investigated.

#### HDAC8 in neuroblastoma

HDAC8 expression (but not that of other HDAC) is highly correlated with the progression of, and is a prognostic indicator in juvenile neuroblastoma<sup>76</sup>. Neuroblastoma, a cancer which arises from neural crest cells (NCCs), accounts for 7-10% of all pediatric cancers and 15% of all pediatric cancer deaths in patients <15 years old<sup>78,79</sup>. HDAC8 knockdown and selective HDAC8 inhibition with PCI-34051 (**1**) in neuroblastoma cell lines causes terminal differentiation<sup>76</sup>, suggesting that an HDAC8 specific inhibitor could be a very powerful therapeutic treatment for cases of neuroblastoma. The NCCs from which neuroblastoma arises are precursor cells that generate the skull and some nervous tissues, consequently knockout of HDAC8 causes newborn mice to die within hours of birth with severe defects in cranial tissues causing brain herniation (Figure 1.3)<sup>36</sup>.

#### HDAC8 and p53

HDAC8 also plays a crucial role in the induction of the p53 tumour suppressor through the HoxA5 transcription factor. p53 is known as the “guardian of the



**Figure 1.3:** Reconstructed skulls from micro-CT scans of wild type (left) and HDAC8 knockout (right) mice (From ref[36]).

genome” and is very important in oncology, its tumour suppressor function is mutated in over 50% of all cancers allowing unchecked proliferation of these cells<sup>80</sup>. HDAC8 (but not HDAC1, HDAC2 or HDAC3) knockdown in a variety of cancer cell lines lead to a reduction in p53 pre-mRNA expression levels. Importantly this effect was only seen in cells with a mutant p53 gene, disruption of HDAC8 activity by specific inhibition or knockdown triggered defects in proliferation of cells with a mutant but not wild type p53<sup>51</sup>. This result is important as it offers HDAC8 as a potential “personalised medicine”-type therapeutic target in many cancers with mutant p53 that would be specific for cancerous cells and not affect p53 levels healthy cells. In addition HDAC8 inhibitors may have negligible or negative effect in cancers without mutant p53.

## 1.2 Structural Features of HDAC8

Rational design of an HDAC selective inhibitor requires knowledge of the structural features of the target, specifically the features that separate it from other similar proteins. These are the features which will be useful in our drug design process.

The HDAC8 protein is a single 42 kDa  $\alpha/\beta$  domain comprising 8  $\beta$ -strands sandwiched by 12  $\alpha$ -helices. It has a high loop content which is typical of promiscuous proteins<sup>81</sup>, approximately half its residues are involved in secondary structure elements; the other half form the 9 loops which cap the top of the enzyme to form the substrate recognition surfaces and 11Å substrate binding tunnel<sup>82</sup>.

HDAC8 is structurally unique within class I HDACs - it lacks a 50-111 amino acid C-terminal domain found in other class I HDACs which is used in enzyme recruitment (a switch of HDAC1 and HDAC2 tails imparts HDAC1 activity to HDAC2) it also contains an L2 loop which is 2 residues shorter than is found in other class I HDACs<sup>82</sup>. With the exception of HDAC8 and HDAC11, HDACs have regulatory sequences in addition to the catalytic deacetylase domain, these sequences regulate HDAC activity through recruitment to different complexes or subcellular compartments as well as PTMs such as summoylation<sup>83</sup> and phosphorylation<sup>75</sup>. HDAC8 however, contains very little extraneous sequence in addition to the catalytic domain although a nuclear localisation sequence has been determined through bioinformatic analysis<sup>22</sup>.

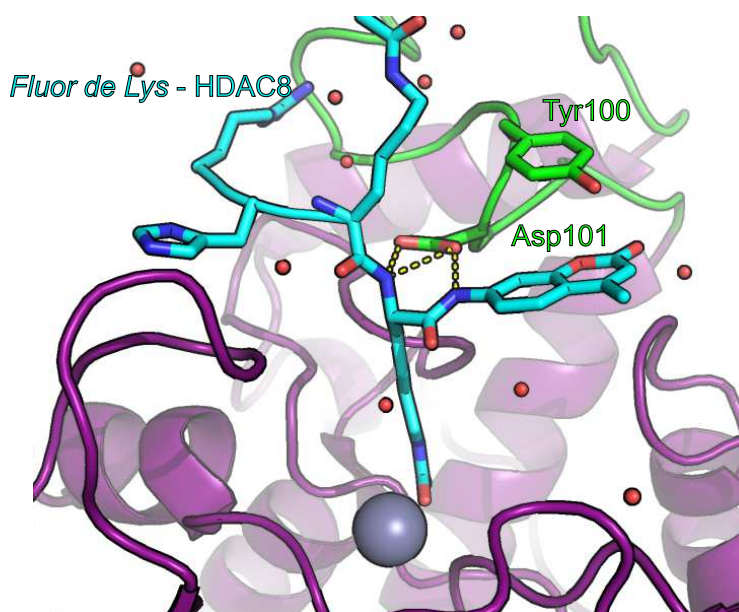


**Figure 1.4:** Structure of HDAC8 in complex with the *Fluor-de-Lys* substrate **2** showing interactions with Tyr100 and Asp101 (sticks) on the L2 loop (green) and water molecules mediating hydrogen bonds (small red spheres). PDB:2V5X.

Figure 1.4 shows a peptide substrate-bound HDAC8 structure. Asp101 is conserved throughout class I, II and IV HDACs, as part of the long L2 loop (missing from many inhibitor bound structures) forms three hydrogen bonds to the peptide backbone, and appears to lock the substrate in place<sup>84</sup>. Mutations at this position result in a dramatic loss of activity suggesting that this is the functional role of Asp101 *in*

*in vivo*. Further interactions of Asp101 and the L2 loop are mediated by a network of water molecules in the structure which may or may not occur under physiological conditions as the crystal contacts occur in this region within the asymmetric unit (Figure 1.4)<sup>85</sup>.

X-ray structures have also been solved for the deacetylase domains of HDAC2<sup>86</sup>, HDAC3<sup>87</sup>, HDAC4<sup>88</sup> and HDAC7<sup>89</sup> in complex with various ligands and cofactors. Comparison of these structures with HDAC8 structures highlights that these isoforms have a narrower substrate tunnel than HDAC8. HDAC8 also seems to have an additional “sub-pocket” within the substrate channel which has already been used as an HDAC8 specific feature in the “design” of a small molecule selective inhibitor<sup>90</sup>. This wide tunnel and sub-pocket are important features that will need consideration in the design of HDAC8 selective inhibitors.

### 1.2.1 HDAC8 flexibility

#### Loop flexibility

Each of the 32 human HDAC8 structures deposited in the Protein Databank (PDB) are in complex with an inhibitor or substrate mimic (except a single subunit in one structure which is likely an artefact of crystal packing). Protein crystallisation occurs more readily with rigid proteins and crystallisation of proteins with flexible regions is often only possible after the flexible regions have been removed, either by proteolytic cleavage or genetic alteration<sup>91</sup>, or by the addition of a ligand that stabilises a conformation that is susceptible to crystallisation. The lack of ligand-free structures suggests that HDAC8 is a dynamic and flexible protein and as such can only be crystallised when rigidified by the presence of a binding partner. When HDAC8 structures are compared, the backbone does not vary significantly within secondary structure elements but in some of the loop regions, especially the L1 and L2 substrate binding loops, there is a great deal of conformational flexibility displayed<sup>82</sup>(Figure 1.5). Interactions between these two loops are thought to have an effect on the activity by affecting substrate binding<sup>92</sup>. Electron density for the L2

loop is seen in structures with ligands that can donate hydrogen bonds to Asp101, this interaction rigidifies the loop enabling higher occupancy in the crystal and as a result electron density in the structure. Figure 1.5 shows a selection of L1 and L2 loops, the position of Tyr100 demonstrates that even when the Asp101 rigidifying interaction is present, significant flexibility in the L2 loop remains to the extent of the formation of a helix in some structures (Cyan in Figure 1.5). Additionally in many structures parts of the L2 loop still lack density. Two distinct conformations of the L1 loop are also visible.

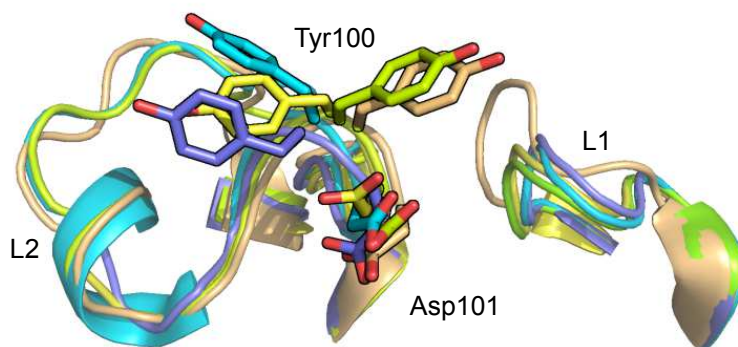


**Figure 1.5:** Five sections of structures which have electron density for the L2 loop. Asp101 and Tyr 100 are shown as sticks. PDB codes: beige - 1T64, yellow - 1W22, green - 2V5W, cyan - 2V5X, purple - 3RQD.

As the HDAC8 L2 loop is two residues shorter than the L2 loop in other class I HDACs it is quite possible that different amounts of flexibility in the L2 loop is a region of HDAC8 that could be exploited in the design of HDAC8 specific inhibitors. The flexibility within the loop could also mean that targeting of an inhibitor to the L2 loop could potentially be easy as the loop may be able to flex a small amount in order to accommodate the interaction.

### Core flexibility

An HDAC8 structure bound to the HDAC inhibitor (HDACi) trichostatin-A (TSA, **3**) shows a second inverted TSA molecule extending into the hydrophobic core of the protein (Figure 1.6a)<sup>82</sup>. A more recent HDAC8-TSA structure does not contain

this second TSA molecule<sup>93</sup> and therefore the cavity in which it binds is a transient feature of this dynamic protein. Though the cavity may possibly be a crystallisation artefact and therefore not physiologically relevant, it does demonstrate that the core of HDAC8 is flexible enough to assume such conformations. The existence of this second cavity may provide an opportunity for the design of inhibitors which can extend into this transient cavity or alternatively do not bind to the active site<sup>26</sup>.

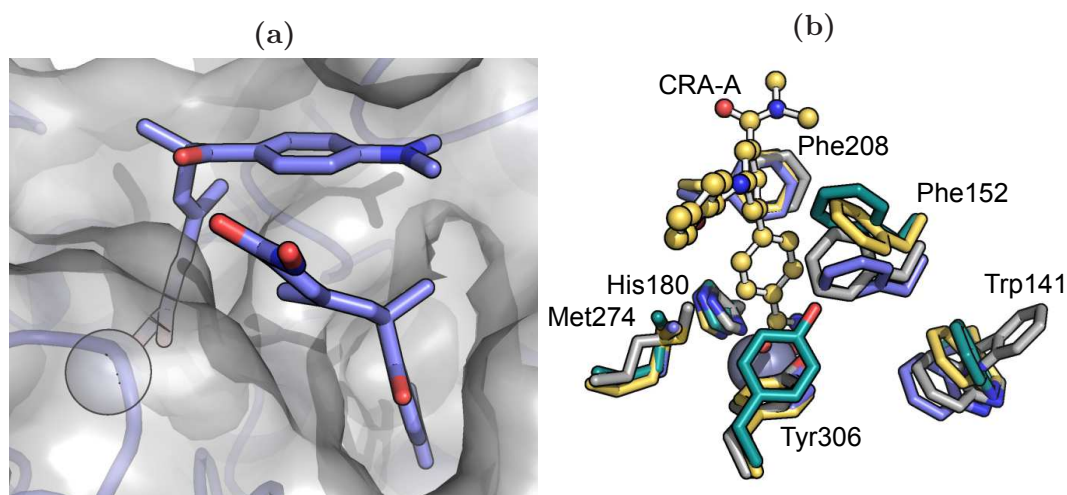


**Figure 1.6:** The flexibility of the HDAC8 substrate tunnel demonstrated by 4 structures with different ligands: (a) HDAC8-TSA (**3**) structure with a second inverted inhibitor in a separate ligand binding cavity, (b) substrate binding pockets of HDAC8 complexed with  $\alpha$ -amino amide **4** (teal), Vorinostat (**5**, grey), TSA (**3**, blue) and CRA-A (**6**, yellow balls and sticks).

### Substrate tunnel flexibility

The structure of HDAC8 with another HDACi, CRA-A (**6**) bound reveals a movement of Phe152 which usually packs against Met274 (Not shown in ). Molecular modelling and docking reinforce these data and show that the HDAC8 tunnel has a high degree of flexibility<sup>94</sup>. Phe152 in particular has been seen to assume many different orientations within the substrate binding pocket to accommodate different ligands of different sizes (see Figure 1.6b). The movement of this residue is thought to open an HDAC8 specific “sub-pocket” that has been targeted previously in the design of an HDAC8 selective inhibitor<sup>90</sup>. Fatkins and co-workers demonstrated that

in addition to an acetylated p53 peptide, HDAC8 is able to turnover an analogous thioacetylated p53 peptide which HDAC1 and HDAC2 were unable to do<sup>95</sup>. This provides evidence that despite the highly conserved nature of the catalytic pocket, the HDAC8 catalytic pocket has features that allow it to be more flexible than other HDACs and permits accommodation of the larger sulphur atom in thioacetyl-lysine.

HDAC8 has a dynamic nature that only allows crystallisation with a ligand, the resulting in the rearrangement of residues can create a potential second cavity for ligand binding. It also shows a propensity for structural rearrangement of the substrate tunnel to accommodate wide ligands and has many structures with variable conformations of loops involved with substrate and inhibitor binding. This increased flexibility of HDAC8 over other class I HDAC isoforms is a major feature of HDAC8 that I hope to be able to exploit in the design of HDAC8 selective inhibitors.

### 1.2.2 Catalytic mechanism

Generally, recombinant HDAC8 when purified under normal conditions has a  $Zn^{2+}$  ion at its catalytic centre, this is coordinated by Asp178, His180 and Asp267. The catalytic  $Zn^{2+}$  ion and His142 (acting as a general base) activates a water molecule for nucleophilic attack on the carbonyl group of the substrate. Tyr306, His142, His143 and  $Zn^{2+}$  act to stabilise a tetrahedral intermediate through hydrogen bonding and His143 (acting as a general acid - general base catalyst) then protonates the lysine leaving group completing the hydrolysis<sup>96</sup> (See Figure 1.7).

Knowledge of the chemistry that occurs within an enzyme can help in the design of inhibitors as enzymes often have evolved to function by stabilising a transition state of a reaction, this can enable very efficient binding of transition state analogues that cannot complete the intended enzymatic reaction. To some extent this has been achieved in HDACi with trifluoromethylketone analogues of existing hydroxamic acid inhibitors showing improved HDAC8 potency<sup>97</sup>. An HDAC4 structure (2VQJ) shows that when trifluoromethylketones bind to the HDAC active site they hydrate to a *gem*-diol which is stabilised by residues in the active site<sup>88</sup>.

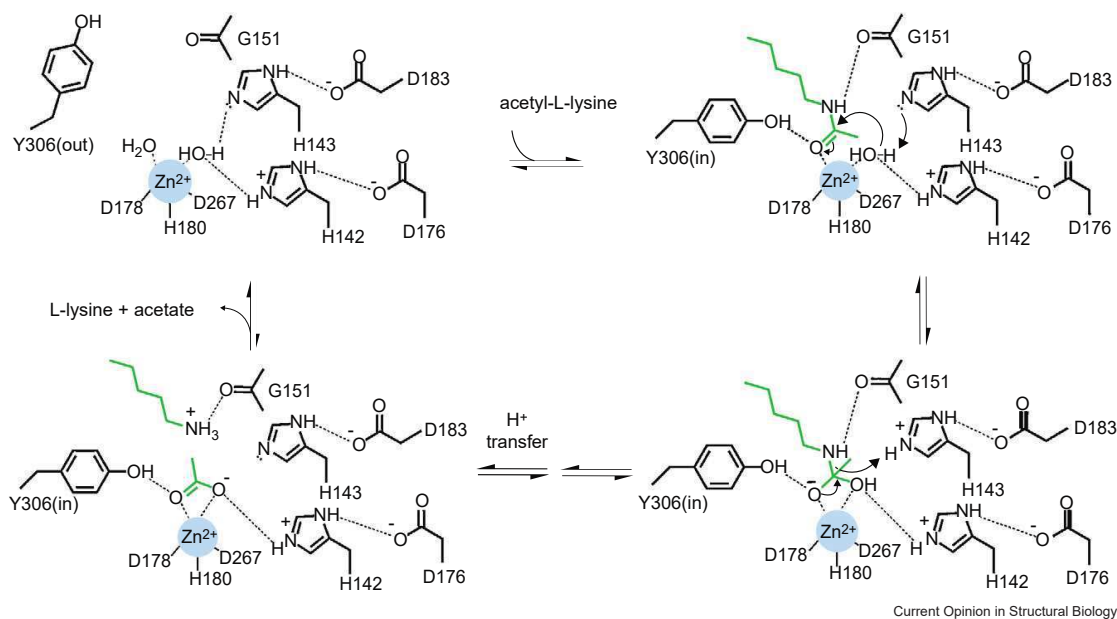


**Figure 1.7:** Proposed mechanism for HDAC catalysis. The active site transition metal ion of HDAC8 ( $\text{Zn}^{2+}$  or  $\text{Fe}^{2+}$ ) and general base His143 promote the nucleophilic attack of a metal-bound water molecule at the metal-coordinated C=O group of the acetyl-L-lysine substrate. The oxyanion of the tetrahedral intermediate and its flanking transition states are stabilized by metal coordination as well as hydrogen bond interactions with Tyr306, His143, and His142. His143 serves as a general acid catalyst to facilitate the collapse of the tetrahedral intermediate to form acetate and L-lysine after an intervening proton transfer (possibly mediated by His143), Figure taken from ref.[96].

### 1.3 Regulation of HDAC8

Included in the functions of HDACs is the regulation of many other proteins either through direct acetylation or through scaffolding interactions. HDACs in-turn are regulated through a number of different processes at many levels, from transcriptional repression to a variety of PTMs. Elucidation of the function and mechanism of action of these regulating modifications could help in understanding which parts of the protein are flexible and amenable to activity altering structural changes. With this knowledge more effective rational drug design can be undertaken by targeting naturally occurring regulatory systems. Elevated HDAC8 expression is correlated

with advanced disease progression and is a negative prognostic indicator for patients with neuroblastoma<sup>76</sup>. Direct transcriptional control of HDAC8 has been demonstrated by SOX4, a direct target gene of FRA-2 which causes elevated expression of HDAC8 in adult T-cell leukemia/lymphoma<sup>98</sup>.

### 1.3.1 Regulation of subcellular location

Substrate availability, and subsequent activity of an enzyme, can vary greatly depending on cellular compartment. Unlike HDAC1, HDAC2 and HDAC3, which are exclusively nuclear proteins, HDAC8 is often detected outside the nucleus<sup>24,53</sup>. It follows therefore that HDAC8 has non-nuclear substrates and/or interaction partners. 14-3-3 proteins are chaperones which bind some phosphorylated proteins (such as transcription factors) and translocate them into the nucleus; HDAC4, HDAC5 and HDAC7 have been identified as targets that are shuttled in this way<sup>99</sup>. HDAC8 has a nuclear localisation sequence<sup>7</sup> and may also shuttle between the nucleus and cytoplasm in a similar fashion as it has been observed as both phosphorylated and non-phosphorylated forms within cells<sup>100</sup>.

Unlike all other HDACs (with the exception of HDAC11), HDAC8 has no regulatory sequences or domains outside its core catalytic domain. The lack of these additional sequences and domains in HDAC8 suggests a more promiscuous functionality as these additional domains and sequences are a major part of selectivity in HDACs by enabling their recruitment to complexes and stabilise and strengthen protein-protein interactions. Redundancies and compensatory mechanisms in many signalling pathways also make substrate detection difficult as observed effects may not be as a direct result of HDAC8 action but a knock-on effect. Currently it is unknown what mechanisms regulate the subcellular location of HDAC8, understanding of these mechanisms may provide new directions for HDAC8 inhibition, perhaps even through indirect inhibition or activation of the HDAC8-interacting protein which regulates subcellular location.

### 1.3.2 Post translational modifications

Phosphorylation of HDAC1 and HDAC2 by casein kinase II (CK2) is an activating PTM which promotes incorporation into active complexes such as mSin3A and CoREST<sup>8,41</sup>, conversely, phosphorylation of HDAC8 has a downregulating effect. Despite having 19 predicted possible phosphorylation sites, HDAC8 is only observed to be phosphorylated at one site, Ser39, both *in vitro* and *in vivo*. Ser39 phosphorylation is only performed by cyclic adenosine monophosphate (cAMP) dependent protein kinase A (PKA) and HDAC8 is the only HDAC with a PKA phosphorylation motif<sup>100</sup>. Ser39 is conserved in HDAC8 but not found in other HDACs and so this inactivation by PKA is unique to HDAC8.

Ser39 is located 21Å from the catalytic centre of HDAC8, the inhibition therefore, cannot be a result of a simple blocking of catalysis or substrate binding. As with many other PTMs, the regulation is most likely achieved through an allosteric effect. Ser39 lies in a hydrophobic pocket so its phosphorylation may cause a structural rearrangement of the protein due to the additional charge imparted by the phosphate<sup>82</sup>. A possible explanation for the regulation involves Arg37, the acetate release “gatekeeper”<sup>101</sup>. Ser39 sits on the same  $\alpha$ -helix as Arg37 (see Figure 1.8) and phosphorylation may “shut the gate”, thereby inhibiting subsequent deacetylation reactions. Molecular dynamics simulations of HDAC8 suggest that Arg37 forms a barrier with backbone carbonyl groups restricting the access of water to the active site and the escape of acetate<sup>101</sup>.

Fifteen HDAC8 interacting proteins have been identified using a bacterial two-hybrid experiment; of which, six required HDAC8 phosphorylation<sup>52</sup>. This strongly implies that phosphorylation is key to some HDAC8 protein-protein interactions whether the phosphorylation is of HDAC8 itself or of the interacting protein. If the structural basis for this inhibition was well understood it may aid in targeting of an inhibitor that binds a stable, rigid conformation of HDAC8, possibly in a non competitive manner.

Acetylation and glycosylation are also possible HDAC8 regulatory mechanisms. The NetNGlyc 1.0 server identifies two potential glycosylation sites but does not predict

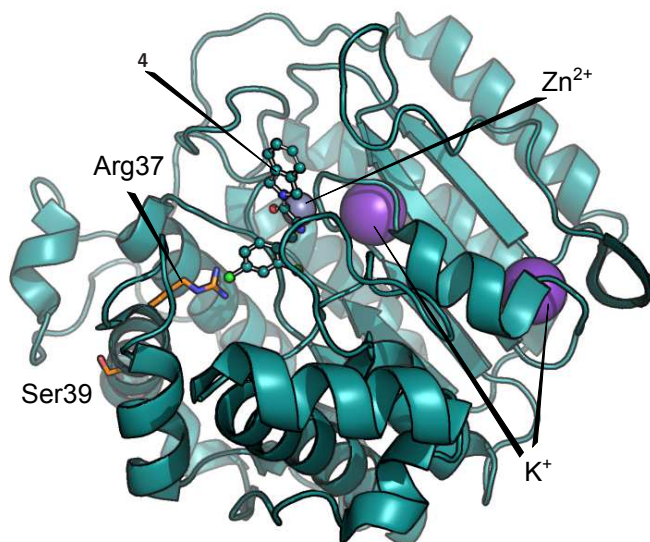


**Figure 1.8:** HDAC8-4 structure, two bound K<sup>+</sup>, the catalytic Zn<sup>2+</sup>, Ser39 and Arg37, which are all important in HDAC8 regulation are shown.

glycosylation of either site<sup>102</sup>. HDAC1 has two acetylation sites in the catalytic domain which inhibit activity towards histones<sup>103</sup>. One of these sites is conserved in HDAC8 and is close to the inhibitory monovalent cation binding site<sup>104</sup> (see Section 1.3.4), this has been suggested to be one possible mode of HDAC8 regulation but has yet to be tested<sup>26</sup>. PTMs within HDACs can play an important part in drug binding, a PTM can have a dramatic effect on the protein structure and could affect a drug binding region by completely abolishing binding or conversely cause structural change that facilitates drug binding. For example if an inhibitor could be designed to stabilise the conformation of phospho-HDAC8 through binding in this region it would be a non-competitive and highly selective HDACi.

### 1.3.3 Activation by small molecules

All known HDACi are competitive inhibitors which block access to the active site. Recently *N*-acetylthioureas have been shown to function as activators of HDAC8<sup>105</sup>. This was determined to be through a 5-fold increase in  $k_{cat}$  and lowering of the  $K_M$

by increasing the power of aromatic stacking interactions which help to bind the substrate to the mouth of substrate tunnel (determined by docking simulations).

In a physiological context some small molecule metabolites have also been found to stimulate HDAC1 and HDAC2 activity in a very specific manner such as coenzyme A derivatives and NADPH (but not NADP<sup>+</sup>, NADH or NAD<sup>+</sup>)<sup>106</sup>. Inositol phosphates have been shown to have a role in the regulation of HDAC1, HDAC2 and HDAC3, in particular, recent structures reveal the structural basis for this regulation whereby inositol phosphates mediate the formation of the HDAC complexes HDAC1-MTA1<sup>107</sup> and HDAC3-NcoR2<sup>87</sup>. Inositol phosphates and other metabolites do not have an effect on HDAC8 but these types of protein-protein contact mediating molecule sites may prove useful if they are discovered on HDAC8 in future by identifying sites that can be targeted in the design of inhibitors. These sorts of molecules may be useful in diseases correlated with low HDAC activity (eg. HDAC1 and HDAC3 in metastatic melanoma<sup>108</sup>) where an increase in HDAC activity may be beneficial to a patient.

### 1.3.4 Regulation by cations

Divalent and monovalent metal ions have been shown to have an effect on HDAC8 activity, they modulate the kinetics of catalysis but also possibly regulate activity through other mechanisms which are not fully understood.

The catalytic Zn<sup>2+</sup> in recombinantly expressed HDAC8 has been successfully exchanged with Co<sup>2+</sup>, Fe<sup>2+</sup>, Ni<sup>2+</sup> and Mn<sup>2+</sup><sup>109</sup>. Fe<sup>2+</sup> containing HDAC8 has catalytic efficiency 2.8-fold greater than HDAC8-Zn<sup>2+</sup>. It is possible that HDAC8 may exist naturally as a mixture of Fe<sup>2+</sup> and Zn<sup>2+</sup> bound enzyme as the approximate  $K_D$  values of both ions for HDAC8 (5-400 pM vs 0.2-6  $\mu$ M respectively) are in the region of the estimated cellular concentrations (5-400pM vs 0.2-0.6  $\mu$ M respectively)<sup>110</sup>. Due to difficulties expressing large amounts of other HDACs detailed analysis of the potential active site metal ions has not been undertaken. Cellular concentrations of Zn<sup>2+</sup> can change significantly in response to oxidative<sup>111,112</sup> and metal toxicity stresses<sup>113</sup>, HDAC8 activity may be regulated in part through these ionic fluxes.

In all HDAC8 crystal structures, two monovalent cations (MVC) are bound (see Figure 1.8) which have been demonstrated to have different functions. Binding at one site is activating<sup>114</sup> while the other is an inhibiting<sup>104</sup>. With peak activity occurring around the cellular concentrations of  $K^+$  (typically 139 mM<sup>115</sup>) it is possible that binding of fluctuations in  $K^+$  concentration is a *in vivo* inhibitor of HDAC8. These sites are conserved across class I and class II HDACs so this mechanism of regulation may not be unique to HDAC8<sup>104</sup>

HDAC8 activity is likely regulated by a combination of processes: concentrations of intracellular  $Zn^{2+}$ ,  $Fe^{2+}$ ,  $K^+$  and  $Na^+$ , phosphorylation of Ser39 by PKA (which is itself activated by a number of different pathways) and interactions with proteins to localise HDAC8 with substrates, binding partners or to a cellular compartment.

## 1.4 HDAC inhibitors

### 1.4.1 Effects of HDAC inhibitors

HDACs play a broad range of roles in many cellular pathways; many cancers and disease processes have been linked with overactive HDAC activity, HDACs have become an attractive target for researchers wishing to affect or halt these diseases by HDAC inhibition. A wealth of literature on HDACi has been generated over the last 20 years, but despite the drive to create HDACi that are applicable in human clinical settings only four HDACi are approved for use in human patients (with many in clinical trials).

One of the major features of HDACi treatments is their selectivity for cancerous cells. An expression profiling study has shown that, in artificially transformed cells from a number of tissue origins, over 4200 genes are differentially expressed upon treatment with non selective inhibitors Vorinostat (**5**) and Romidepsin (**7**)<sup>116</sup>. Gene ontology annotations and pathway analysis revealed that many of these genes are Bcl-2 family members which regulate the intrinsic apoptotic response<sup>116</sup>.

Class I selective HDACi seem to have the same toxicity profile as non-selective inhibitors suggesting that the effects of non-selective HDAC inhibition arise primarily from class I HDAC inhibition<sup>117</sup>. Preliminary clinical trial results are promising for a number of non-selective HDACi in leukemias and also in solid cancers when HDACi are used as part of a combination therapy. Patients do however, suffer from a wide range of undesirable side effects which have been attributed to the non-selectivity of these inhibitors. These side effects include fatigue, nausea, vomiting, diarrhoea, thrombocytopenia, and neutropenia<sup>117</sup>. These effects can be partially understood by taking into account the key role that HDACs play in the regulation of chromatin structure and expression of a huge number of proteins as well as the many non-histone HDAC substrates and interaction partners that have been reported (see Section 1.1.4). Currently the main goal in the field of HDACi research is to achieve isoform-selectivity, with an HDACi which is specific for one isoform it is hoped that side effects will be greatly reduced and efficacy in a clinical setting increased.

Trichostatin-A (TSA, **3**) is produced by *Streptomyces hygroscopicus* initially identified only as an antifungal it is now known to be a pan-HDACi<sup>118</sup>. Another historical inhibitor of HDACs is valproic acid (**8**), a prescribed treatment for bipolar disorders and some epilepsy conditions<sup>119</sup>, it has numerous targets within the cell, of which one set are HDACs with IC<sub>50</sub> in the medium to high  $\mu\text{M}$  range. The HDAC inhibitory effects of valproic acid are also potential therapies for HIV<sup>120</sup>, and various cancers<sup>121</sup>. Despite decades of research in the development of HDACi, very few have successfully exited clinical trials, often failing due to poor pharmacokinetics and high toxicity. Four HDACi are FDA approved for treatment of different cancers: Vorinostat (**5**)<sup>122</sup> and Romidepsin(**7**)<sup>123</sup> for refractory cutaneous T-cell lymphoma, Beleodaq/Belinostat (**9**) for relapsed or refractory peripheral T-cell lymphoma<sup>124</sup> and Farydak/Panobinostat (**10**) for multiple myeloma. At least 13 HDACi (including Vorinostat and Romidepsin) are currently in one (or more) clinical trials<sup>11</sup>. Because of the considerable side effects, the four approved HDACi are used mostly in combination therapies for advanced stage and relapsing patients.

Many groups report conflicting data for the inhibitory activity of some of the more widely used inhibitors. For example, the theyl ketone apicidin has been reported

to have  $IC_{50}$  vs. HDAC4 = 5 nM<sup>125</sup> and >10000 nM by another group<sup>126</sup> (see Table 1.2). The differences are likely due to the format of the assay used, but nevertheless the large discrepancy is concerning.

The disruption of HDAC containing complexes by HDACi may be a mechanism of inhibition as significant as direct inhibition of catalytic activity. As mentioned in Section 1.1.4 HDACs often form parts of complexes as both active enzymes and as scaffolding proteins which bring together other enzyme-substrate partners such as methylases, phosphatases/kinases (Table 1.1). TSA (**3**) was found to disrupt such interactions in complexes containing HDAC1, HDAC6 and HDAC10 with phosphatases<sup>127</sup>. This type of inhibition leads to HDACi affecting pathways where acetylation is not an active process and exacerbates the need for specific inhibitors that discriminate between individual isoforms and potentially even different functions of a single isoform.

## 1.4.2 Structure of HDAC inhibitors

All known HDAC inhibitors directly block access of the substrate to the active site and are as such, competitive inhibitors. HDACi are generally composed of three modules; a zinc binding group (ZBG), an aliphatic substrate tunnel binding group (STBG) which mimics the aliphatic chain of the native lysine substrate and a cap-group which interacts with the mouth and top surface of the HDAC (See Figure 1.9). Owing to the high sequence homology surrounding the active site any inhibitor selectivity is typically presumed to require modifications of the cap-group. The exterior of the protein to which the cap-group binds determines the cognate substrate specificity *in vivo* should therefore be the most differentially targetable structural feature of the protein.

### The zinc binding group

The key feature of all HDACi is the ZBG with the exception of a couple of reports<sup>134,151</sup>. Many different chemical compounds have been reported to bind zinc

**Table 1.2:** HDACi activities against the different HDACs (IC<sub>50</sub> in nM). References: <sup>a</sup>[128], <sup>b</sup>[129], <sup>c</sup> [130], <sup>d</sup>[131],<sup>e</sup>[113], <sup>f</sup>[132], <sup>g</sup>[77], <sup>h</sup>[133], <sup>i</sup>[134], <sup>j</sup>[135], <sup>k</sup>[126], <sup>l</sup>[136], <sup>m</sup>[137], <sup>i</sup>[138], <sup>n</sup>[139], <sup>o</sup>[140], <sup>p</sup>[141], <sup>q</sup>[142],<sup>r</sup>[143], <sup>s</sup>[144], <sup>t</sup>[145], <sup>u</sup>[146], <sup>v</sup>[90], <sup>w</sup>[147],<sup>x</sup>[148],<sup>y</sup>[149]

HDAC	Class I				Class II						Class IV
	1	2	3 (+NCoR2)	8	4	5	6	7	9	10	11
TSA ( <b>3</b> )	0.23 <sup>a</sup>	0.76 <sup>a</sup>	0.58 <sup>a</sup>	1100 <sup>b</sup> 25 <sup>c</sup>	12 <sup>d</sup>	16 <sup>d</sup>	13 <sup>d</sup>	22 <sup>d</sup>	38 <sup>d</sup>	7 <sup>a</sup>	15 <sup>d</sup>
Vorinostat ( <b>5</b> )	63 <sup>e</sup>	40 <sup>e</sup>	29 <sup>e</sup>	2000 <sup>f</sup> 400 <sup>g</sup>	16 <sup>g</sup> >10000 <sup>h</sup>	33 <sup>e</sup>	1 <sup>i</sup> 0.013 <sup>j</sup>	>17000 <sup>h</sup>	107 <sup>k</sup>	40 <sup>g</sup>	362 <sup>d</sup>
Entinostat( <b>11</b> ) <sup>h</sup>	45 <sup>j</sup> 300 <sup>l</sup>	250 130 <sup>j</sup>	400 <sup>h</sup> 8 <sup>l</sup>	>10000	>10000	>10000	13000	>10000	505 <sup>k</sup>	NR	NR
Mocetinostat ( <b>12</b> ) <sup>m</sup>	150	290	1660	>10000	>10000	>10000	>10000	>10000	NR	NR	>590
Apicidin ( <b>13</b> ) <sup>k</sup>	>10000 22 <sup>c</sup>	120 43 <sup>k</sup>	1.5 <sup>i</sup> 29 <sup>c</sup>	43 760 <sup>c</sup>	>10000 5 <sup>n</sup>	NR	123 <sup>i</sup> >10000 <sup>c</sup>	>10000	>10000	NR	NR
Romidepsin( <b>7</b> ) <sup>o</sup>	6700	1500	18	>50000	>50000	NR	12 200 <sup>p</sup>	>50000	>50000	NR	NR
Romidepsin( <b>7</b> )(reduced) <sup>o</sup>	5.3	3.9	5.3	26	470	NR	330	3200	1200	NR	
Tubacin ( <b>14</b> ) <sup>q</sup>	1400 995 <sup>f</sup>	6270	1270	1270 6300 <sup>f</sup>	17300	3350	4 142 <sup>f</sup>	9700	4310	3710	3790
Rocilinostat( <b>15</b> ) <sup>r</sup>	58	48	51	100	7000	5000	4.7	1400	>10000	NR	>10000
Cpd-60 ( <b>16</b> ) <sup>s</sup>	4	11	3	1020	>30000	18000	2	>30000	>30000	NR	NR
LMK-235 ( <b>17</b> ) <sup>t</sup>	320	881	NR	1278	11.9	4.22	55.7	NR	12.78	NR	852
A8B4 ( <b>18</b> ) <sup>u</sup>	3600	15000	25	NR	NR	NR	NR	NR	NR	NR	NR
Cpd2 ( <b>19</b> ) <sup>v</sup>	>100000	NR	NR	14000	NR	NR	>100000	NR	NR	NR	NR
Cpd6 ( <b>20</b> ) <sup>v</sup>	>100000	NR	NR	300	NR	NR	55000	NR	NR	NR	NR
<b>4</b> <sup>w</sup>	1700	3900	NR	90	NR	NR	>30000	NR	NR	NR	NR
PCI-34051 ( <b>1</b> ) <sup>g</sup>	4000	>50000	>50000	10	NR	NR	2900	NR	NR	13000	NR
NCC149( <b>21</b> ) <sup>x</sup>	38000	>100000	68000	70	44000	NR	24000	NR	NR	NR	NR
Farydak <sup>y</sup>											
Belinostat <sup>y</sup>											

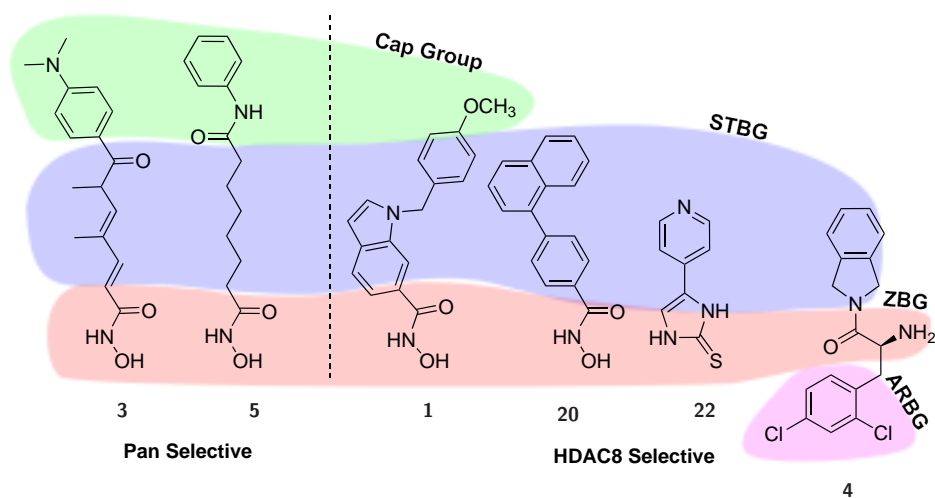


**Figure 1.9:** Two non-selective HDACi TSA - **3**<sup>118</sup> and Vorinostat - **5**<sup>150</sup> and four HDAC8 selective inhibitors PCI-34051 - **1**<sup>77</sup>, cpd6 - **20**<sup>90</sup>, SB-379278A - **22**<sup>136</sup>, and **4**<sup>147</sup>

including: thiols, carboxylic acids, barbituric acids, phosphonic acids, thiadiazoles sulfodiimes thiadiazines, hydroxamic acids, reverse hydroxamic acids,  $\alpha$ -pyrones, 2-thiopyrones, 3-hydroxypyridin-2-ones hydroxypyridine-2-thiones carbamylphosphonates, hydroxyureas, hydrazides, aminomethylbenzimidazoles, dipicolylamines,  $\beta$ -lactams and squaric acids<sup>152</sup>

The ZBG in HDACi are typically hydroxamic acids, benzamides and carboxylic acids (examples in Figure 1.10). Other ZBG found in HDACi include: ethyl ketones<sup>153</sup>, amides<sup>154</sup>, thiolates, epoxide, imidazole-2-thione<sup>77</sup>, mercaptoacetamide<sup>155</sup>, hydroxypyridine-2-thione<sup>156</sup>, oxime amide<sup>96</sup>, trifluoromethylketone<sup>157</sup>, trifluoromethylloxadiazole<sup>158</sup> and silanediol<sup>97</sup>.

Coordination of  $\text{Zn}^{2+}$  ions within the protein structures in the protein databank (PDB) repository is most commonly tetrahedral (65% of crystal structures and 98% of NMR structures) and occasionally trigonal bipyramidal/square pyramidal (15% of crystal structures and <1% NMR structures)<sup>159</sup>. The catalytic  $\text{Zn}^{2+}$  ion within HDACs is coordinated by two aspartate and one histidine residues. Therefore one (or possibly two) coordinating bonds to HDACi are available. Crystal structures of HDAC8 display both monodentate coordination (Figure 1.11a) with the thiolate

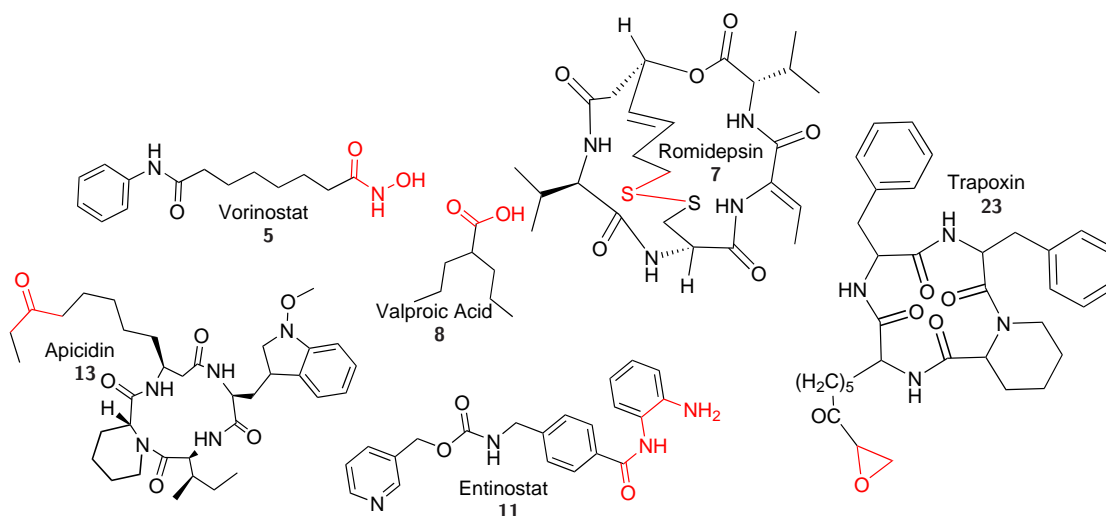


**Figure 1.10:** Examples of HDACi with  $Zn^{2+}$  binding groups common in HDACi: hydroxamic acid - Vorinostat, carboxylic acid - valproic acid, cyclic tetrapeptides with ketone - apicidin, thiolate - Romidepsin (intracellularly reduced), epoxide - trapoxin and benzamide - Entinostat.

inhibitor derived from Largazole (**24**), and bidentate coordination (Figure 1.11b) with the hydroxamic inhibitor Vorinostat (**5**).

### *Carboxylic acids*

Carboxylic acid HDACi are very weak inhibitors (Valproate (**8**)  $IC_{50} = 128 \mu M$  for HDAC2<sup>160</sup>) for this reason they are used at very high concentrations and are known to bind many other targets in addition to HDACs. Valproate is a prescribed treatment for bipolar disorders and some epilepsy conditions<sup>119</sup> and is also a potential treatment for HIV<sup>120</sup>, and various cancers<sup>121</sup>. Carboxylic acid analogues of hydroxamic acid inhibitors are occasionally used as inactive control compounds<sup>15</sup>.

### *Hydroxamic acids*

Hydroxamic acids are strong binders of  $Zn^{2+}$  and so provide significant potency to HDACi. They also however have many disadvantages such as off-target binding, in particular it has been shown that an analogue of **1** that does not inhibit HDAC8 displays the same neuroprotective characteristics as **1**<sup>161</sup>. These off target effects

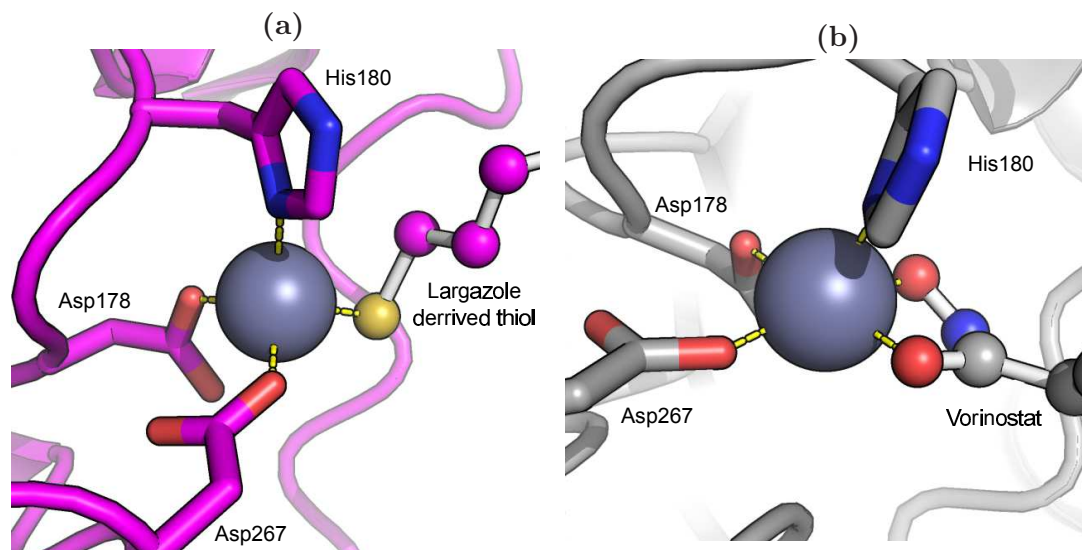


**Figure 1.11:** HDAC8  $\text{Zn}^{2+}$  ion chelated by HDAC inhibitors with two coordination geometries (a) monodentate with Largazole **24** derived thiolate inhibitor and (b) bidentate with hydroxamic acid inhibitor Vorinostat **5**

have resulted in a search for a suitable equally potent ZBG which allows for greater selectivity to specific HDACs.

Hydroxamic acids display poor pharmacokinetics in the clinic and are known to rapidly hydrolyse to give hydroxylamine and carboxylic acids<sup>162</sup>. As a result hydroxamic acid based HDACi have a fairly short half-life within the body (<100 min in cats)<sup>163</sup> and high doses are required as a result. Additionally it is thought that the hydroxamic acid group (present in the majority of HDACi) chelates catalytic  $\text{Zn}^{2+}$  ions in other zinc dependent protease enzymes such as matrix metalloprotease proteins causing “off-target” inhibition that contributes to the side effects of non selective HDACi<sup>164</sup>.

Hydroxamic acids are promiscuous metal ion chelators;  $\text{Sc}^+$ ,  $\text{Y}^{3+}$ ,  $\text{La}^{3+}$ <sup>165</sup>,  $\text{Al}^{3+}$ ,  $\text{Fe}^{3+}$ ,  $\text{Fe}^{2+}$ ,  $\text{Co}^{2+}$ ,  $\text{Co}^{3+}$ ,  $\text{Cu}^{2+}$ ,  $\text{Zn}^{2+}$ <sup>166</sup>,  $\text{Ni}^{2+}$ <sup>167</sup> and  $\text{V(IV)}$ ,  $\text{V(V)}$ <sup>168</sup> have all been reported to form hydroxamate complexes. Importantly the stability of hydroxamic acid complexes suggest that  $\text{Zn}^{2+}$  is not their preferred ion, ( $\text{Fe}^{2+} \gg \text{Cu}^{2+} > \text{Ni}^{2+} \approx \text{Zn}^{2+}$ )<sup>169</sup>. Hydroxamic acids are present in siderophores such as ferrichrome which

is synthesised by bacteria and secreted to scavenge iron from the environment, the iron-bound molecules are then imported into the cell to deliver its iron cargo<sup>170</sup>.

Hydroxamic acids are found in some drugs such as the ibuprofen prodrug Ibuprofen where hydrolysis of the hydroxamic acid is required to release the active drug, and Bufexamac, a cyclooxygenase (COX) inhibitor used as an anti-inflammatory (now withdrawn due to allergic reactions)<sup>60</sup>. Interestingly Bufexamac has also been shown to be an HDAC6 and HDAC10 specific inhibitor, COX is a haeme Fe<sup>2+</sup> containing enzyme, and it is therefore possible that if Bufexamac inhibits HDACs that COX enzymes may contribute to the off-target effects of HDACi. Hydroxamic acids have also been seen to be antioxidants, possessing radical scavenging activity<sup>171</sup>

#### *Trifluoromethylketones*

Trifluoromethylketone (TMFO) inhibitors of HDACs have fairly recently been reported<sup>172</sup> but have long been known as inhibitors of other metalloproteases<sup>173</sup>. The trifluorinated group withdraws electrons, increasing the tendency of the group to add a nucleophile such as water to become hydrated<sup>157</sup>. In this way a *gem*-diol is formed which was hypothesised to mimic the transition state in the HDAC catalytic centre and so is highly stable and tightly bound. A structure of the catalytic domain of HDAC4 bound to a TMFO inhibitor has been solved which subsequently confirmed the hydration of the inhibitor, the tetrahedral state is stabilised within the catalytic site by two histidine residues and a hydrogen bond to a backbone amide via a water molecule<sup>88</sup>.

This observation prompted synthesis of trifluoromethyl ketone inhibitors, many of which showed improved inhibition against various HDAC isoforms<sup>61</sup>. Trifluoromethylketone analogues of Vorinostat (**5**), valproic acid (**8**) and butyric acid (**25**) HDACi have been synthesised and were found to be very potent (pan-)HDACi<sup>97</sup>; in this report silanediol was also found to be a promising potential ZBG.

#### *Benzamides*

Benzamides provide a bidentate coordination with Zn<sup>2+</sup> within HDACs. Figure

1.12a shows an HDAC2 bound with benzamide inhibitor (**26**) clearly showing  $\text{Zn}^{2+}$  coordination (interatomic distances  $\leq 2.6 \text{ \AA}$ ) bonds from lone pairs on the amide oxygen and the aniline nitrogen. The amide oxygen is further stabilised through a hydrogen bond ( $2.7 \text{ \AA}$  distance) to Tyr308 (equivalent to Tyr306 in HDAC8).

The benzamide Entinostat (**11**) (Figure 1.12b) has shown good promise in phase II and phase III clinical trials<sup>174</sup>. Mocetinostat (**12**) is another benzamide class inhibitor<sup>137</sup> which is in phase II trials for various lymphomas. It shows selectivity for class I HDACs especially for HDAC1 and HDAC2 with  $\text{IC}_{50}$  values of  $150 \pm 20$  and  $290 \pm 80 \text{ nM}$  for HDAC1 and HDAC2 respectively but  $\text{IC}_{50} > 10 \text{ \mu M}$  for HDAC8 (see Table 1.2). This suggests that some feature of the HDAC8 ligand binding surface cannot accommodate the benzamide ZBG making it unsuitable for HDAC8 selective inhibitors.

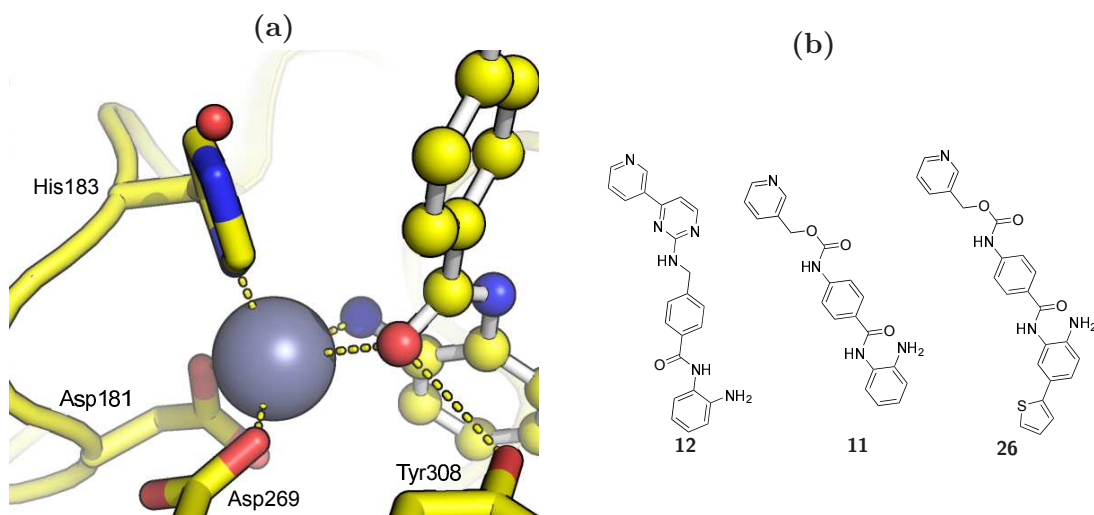
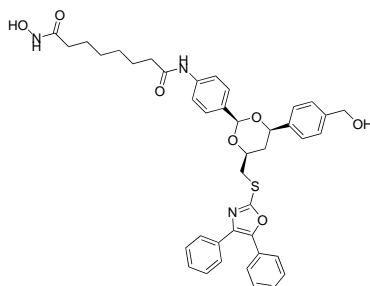


**Figure 1.12:** (a) Co-ordination of 4-(2-thiophenyl)benzamide **26** in the active site of HDAC2<sup>175</sup>, and (b) three benzamide HDACi, Mocetinostat (**12**), Entinostat (**11**) and the 4-(2-thiophenyl) substituted **26**.

Entinostat analogues with substituents at the 4-position on the anilide ring (*para* to the aniline) have been shown to have an increased affinity to HDAC1 and HDAC2. For example a  $>5$ -fold lower  $\text{IC}_{50}$  ( $0.02 \text{ \mu M}$  and  $0.1 \text{ \mu M}$ ) against HDAC1 and HDAC2 was measured with a 4-(2-thiophenyl) substituent (**26**) compared to with unsubstituted Entinostat (**11**,  $0.54 \text{ \mu M}$  and  $0.5 \text{ \mu M}$ )<sup>176</sup>.

## The cap-group (cyclic peptides/depsipeptides)

Very few of the current collection of clinical HDACi display any degree of isoform selectivity. As the HDAC substrate tunnel is relatively narrow, very few HDACi deviate from standard HDACi architecture (hydroxamic acid ZBG with aliphatic linker), the remaining unit of the HDACi from which selectivity can be achieved is therefore the cap-group. The cap-group interacts with the surface of the HDAC near to the entrance to the substrate tunnel and it is thought that if selectivity is to be achieved, it will be achieved through modification of the cap-group to provide interactions that are unique to an individual HDAC isoform. Sadly however, while many inhibitors show class selectivity few display convincing isoform selectivity. Tubacin (**14** in Figure 1.13), a fungal hydroxamic acid metabolite is one example of an HDACi which does display HDAC6 selectivity that stems from its has an extensive cap-group<sup>94</sup>.



14

**Figure 1.13:** Structure of HDAC6 selective inhibitor tubacin.

Cyclic peptides and depsipeptides (peptides with an alteration such as an ester in place of an amide) are compounds which have extensive cap-groups that form the majority of the interaction surface with the protein by binding to the surface of the HDAC near the entrance of the substrate tunnel<sup>177</sup>. Most inhibitors of this type retain a ZBG of sorts (often a thiol) attached to a “pendant sidechain” which extends into the substrate tunnel and coordinates  $Zn^{2+}$ <sup>93</sup>. Some Largazole (**24**) analogues have been synthesised that have an altered HDAC selectivity profile arising from different ZBG such as hydroxamic acids and benzamides<sup>135</sup>. The use of a large cap

group has allowed for the development of an increasingly diverse array of novel zinc binding groups.

The depsipeptide Romidepsin (**7**) is approved for treatment of CTCL. It is a prodrug whose disulfide bond is reduced intracellularly, this reduction releases a thiol group which becomes the ZBG<sup>178</sup>. The exclusively intracellular reduction avoids unwanted inhibition of matrix metalloproteases which primarily act in the oxidising environment outside the cell<sup>179</sup>. Thailandepsins are related to Romidepsin and are class I (except HDAC8) selective inhibitors<sup>180</sup>

Vaidya et al. studied HDAC inhibitors without a Zn<sup>2+</sup> coordinating hydroxamic acid moiety and suggested that the zinc-chelating moiety with hydroxamic acid group were more potent inhibitors than that of other moieties such as methyl esters and t-Bu esters that do not coordinate but rather form weaker Zn<sup>2+</sup> interactions<sup>134</sup>.

A cyclic tetrapeptide has recently been developed which has no zinc chelating group, it has sub- $\mu$ M potency against class I HDACs (HDAC8 was not tested) exclusively through interactions with the substrate binding surface of HDACs<sup>151</sup>. This inhibitor is interesting as the lack of a ZBG may allow it to have fewer side effects than the traditional hydroxamic acid inhibitors.

Trapoxin (**23**) is a natural fungal cyclic tetrapeptide product which is the only known irreversible inhibitor of HDACs; trapoxin treated HDAC remained inactive after dialysis against drug-free buffer<sup>181</sup>. Reduction of the epoxide ZBG lead to complete abolishment of inhibition implying the epoxide group binds covalently to HDAC.

A significant hindrance in studying HDAC inhibition by these cyclic peptides/depsipeptides is the low synthetic efficiency which prevents synthesis of many analogues, though some “one compound-one bead” methods are being utilised by some labs<sup>182</sup>, and this may improve throughput of screening cyclic peptides.

### 1.4.3 HDAC8 selective inhibitors

Many HDAC functions described have been identified through inhibition, knockdown or knockout of a single HDAC isoform, these functions are unaffected by disruption of other HDAC isoforms and so are thought to be non-redundant and unique to that particular HDAC. When these functions are altered and are involved with a specific disease, selective inhibition of a single HDAC isoform may prove a powerful treatment for that disease. Wider non-specific inhibition of HDACs affects multiple cellular systems causing widespread effects. Through the development of selective inhibitors, specific problematic cellular pathways can be targeted and disrupted. Having isoform specific HDAC inhibitors will also greatly benefit the scientific community by allowing dissection of the individual HDAC functions.

Four compounds that have been reported as potent and selective HDAC8 inhibitors (**1**, **20**, **21** and **4**) are shown in Figure 1.14. One feature shared by these inhibitors is the presence of an aromatic group near to the ZBG. Non selective HDAC inhibitors such as Vorinostat (**5**) and TSA (**3**) generally have long-chained aliphatic linkers between the ZBG and cap-group. Analysis of crystal structures shows that this aromatic group causes a rearrangement of substrate tunnel lining residues which allows accommodation of this aromatic ring and some stacking interactions with Phe152, possibly with Phe208 also.

The movement of Phe152 was originally seen in a crystal structure of HDAC8 complexed with CRA-A<sup>82</sup>. The hydroxamate cpd6 (**20**) was designed to target the hydrophobic sub-pocket that is opened up by this movement<sup>90</sup>. Later crystallographic evidence points to the movement of Phe152 being due to an energetically favourable edge to face stacking effect rather than hydrophobic effects<sup>147</sup>.

Another common feature amongst HDAC8 selective inhibitors is their unusually short length. As discussed above, other selective HDACi achieve specificity through modification of the cap-group (such as the HDAC6 selective inhibitor tubacin (**14**)). It seems that some HDAC8 selective inhibitors however, achieve specificity mainly through the linker region. Three potent HDAC8 selective inhibitors do not extend

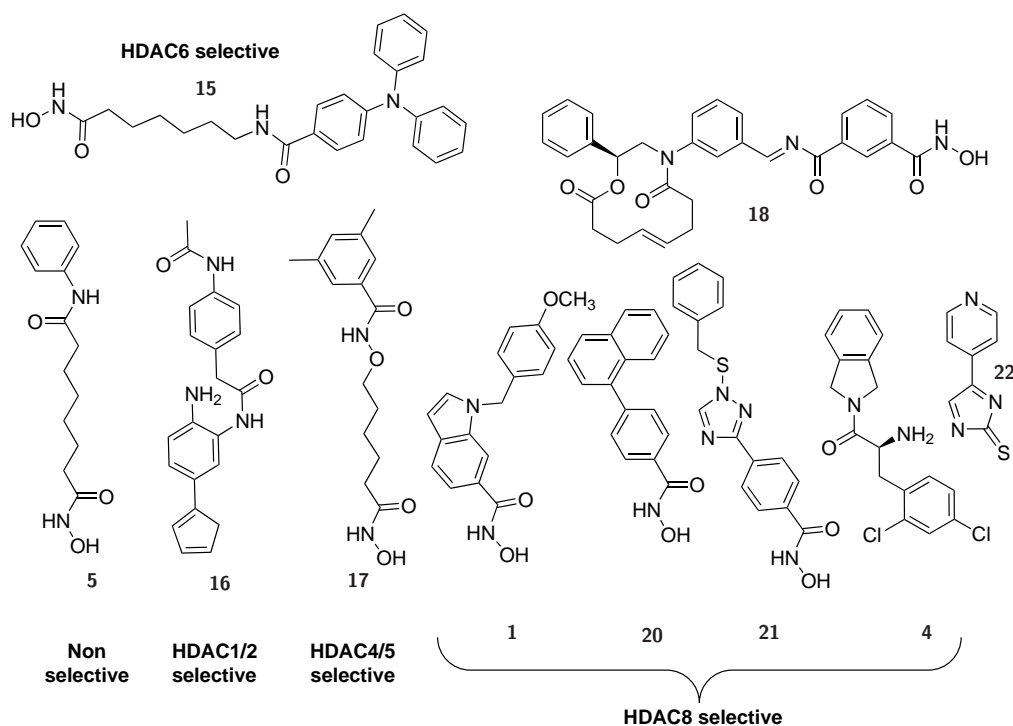


**Figure 1.14:** Non-specific HDACi Vorinostat - **5**<sup>150</sup>, HDAC1/2 selective cpd-60 - **16**<sup>144</sup>, HDAC4/5 selective LMK235 - **17**, HDAC6 selective Rocilinostat - **15** and HDAC8 selective hydroxamic acids: PCI-34051 - **1**<sup>77</sup>, cpd6 - **20**<sup>90</sup>, C149 - **21** and A8B4 - **18**<sup>148</sup> and  $\alpha$ -amino amide **4**<sup>147</sup>.

out of the substrate binding tunnel and as such, their specificity must arise from the interactions within HDAC8 rather than on the exterior surface (Figure 1.14).

PCI-34051 (**1**), NCC149 (**21**) and A8B4 (**18**) (Figure 1.14), are all potent HDAC8 selective inhibitor (>400-fold potency vs other class I HDACs) which do have a cap-group. Studies have shown PCI-34051 to be a potential therapeutic for neuroblastoma<sup>76</sup> and T-cell (but not B-cell) lymphomas by triggering caspase-dependent apoptosis via phospholipase C $\gamma$ 1 signalling, leading to mitochondrial cytochrome C release<sup>77</sup>, a more metabolically stable analogue of PCI-34051 (of undisclosed structure) is reported to reduce neuroblastoma growth in mouse models<sup>183</sup>. While they are promising potential HDAC8 selective inhibitors, PCI-34051 (and likely its stable analogue), NCC149 and A8B4 still conform to the canonical modular HDACi struc-

ture with a hydroxamic acid ZBG, they are likely to cause some side effects due to the binding many off-target proteins that arises from the hydroxamic acid ZBG.

SB-379278A (**22**, Figure 1.14) is a small inhibitor which inhibits HDAC8 with an  $IC_{50}$  500 nM and has undetectable inhibition of HDAC1 and HDAC3<sup>136</sup>, no other reports have been published on the binding of SB-379278A to other HDACs so it is difficult to draw any further conclusions. The presence of two aromatic rings does, however, reinforce the suggestion that an aromatic linker group can provide some HDAC8 selectivity. SB-379278A is a non-hydroxamate inhibitor, its mode of binding is not reported but is likely to be through the lone pair on the sulfur atom.

### Lead compound **4**

Unusually a novel  $\alpha$ -amino amide ZBG confers significant potency as a sub-unit of an HDAC8-selective inhibitor (**4**, (Figure 1.14)<sup>147</sup>. With reported  $IC_{50}$  values of 1.7, 3.9, >30 and 0.09  $\mu$ M for class I HDACs HDAC1, HDAC2, HDAC6 and HDAC8 respectively, **4** shows an 18-fold selectivity for HDAC8 over other class I HDACs (Table 1.2). This compound must therefore provide some HDAC-inhibitor interactions which can be established uniquely in HDAC8 over other HDACs in class I. Since class I enzymes are the most structurally similar to each other this selectivity is assumed to extend to class II and IV HDACs also. The HDAC8-**4** structure should guide investigation of the interactions<sup>147</sup>. Interactions between  $\alpha$ -amino amide inhibitor **4** and HDAC8 can be seen in Figure 1.15. The substrate tunnel is occupied by an isoindoline unit which makes aromatic edge to face stacking interactions with Phe152 and Phe208 with edge-to-centre distances of 3.6 and 3.7 Å respectively. Hydrophobic interactions are made with the remaining substrate tunnel lining sidechains (Met274 and Tyr306, Figure 1.15b). These interactions are permitted because of the linear structure of isoindoline which is only obtained when an amide is present at the nitrogen (Figure 1.15c), without the amide delocalising the lone pair of electrons the nitrogen atom is tetrahedral, creating a kink in the molecule.

The coordination of the catalytic  $Zn^{2+}$  ion by the  $\alpha$ -amino amide ZBG is novel;  $Zn^{2+}$

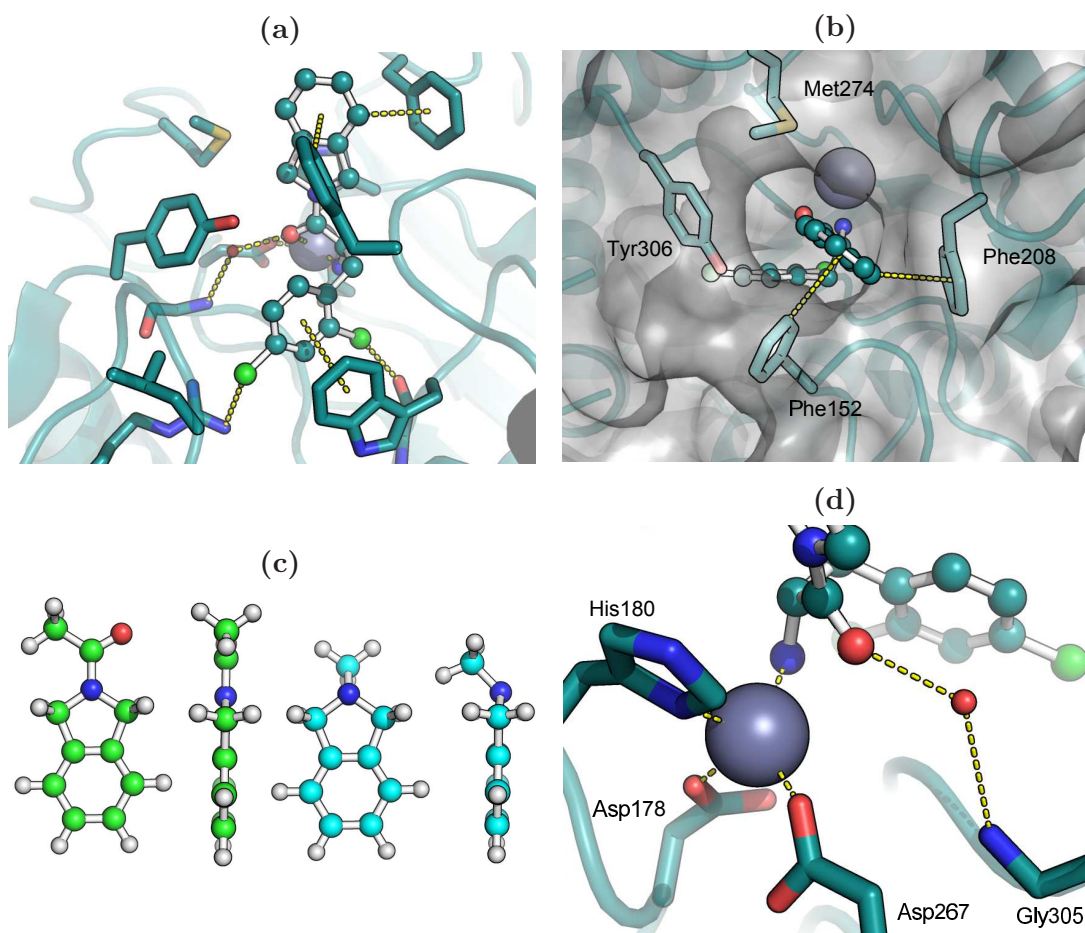


**Figure 1.15:** Interactions of 4 with HDAC8 from the structure (PDB:3SFH<sup>147</sup>). (a) an overview of the inhibitor binding site (b) interactions within the substrate tunnel (c) Energy minimised structures of 1-(isoindolin-2-yl)ethan-1-one (green carbon atoms) and *N*-methylisoindoline (cyan carbon atoms) (d) tetrahedral Zn<sup>2+</sup> coordination interactions for HDAC8-4.

coordinating bonds are made with the sidechains of Asp267 (2.0 Å), Asp178 (2.0 Å) and His180 (2.3 Å), a fourth coordinating bond is provided by the lone pair of the  $\alpha$ -amino nitrogen of the inhibitor (2.3 Å, Figure 1.15d). These four coordinating bonds sit in a preferable pseudo-tetrahedral geometry<sup>159</sup>. The amide oxygen appears to be fairly close to the  $\text{Zn}^{2+}$  ion but at 3.0 Å the distance suggests no coordination is occurring<sup>159</sup>(contradicting the report describing **4**<sup>147</sup>), the geometry of the coordination would be distorted if the oxygen was coordinating  $\text{Zn}^{2+}$ . Additional analysis of the electron density map (not shown) indicates that the amide oxygen is involved strongly in a hydrogen bonding interaction via a water molecule to the backbone nitrogen of Gly305 (visible in Figure 1.15d). This  $\text{Zn}^{2+}$  coordination differs from hydroxamate inhibitor binding which is through oxygen lone pairs of the hydroxamate resulting in penta-coordinate square pyramidal geometry around the  $\text{Zn}^{2+}$  (see Section 1.4.2).

The acetate release pocket binding group (ARBG) is a second feature of **4** which makes it unique among HDAC8 inhibitors. This chlorine substituted phenyl ring is seen to occupy a large pocket behind the catalytic ion. It is hypothesised that cleaved acetate is released into this pocket and subsequently exits the protein directly through a channel that is regulated by Arg37. Arg37 is known to be a key regulator of acetate by mediation of acetate release<sup>101,184</sup>. This pocket is much smaller and narrower in other HDAC8 structures due to a rotation of Tyr306 and Trp141 sidechains which restrict the channel (Figure 1.16) in the case of HDAC8-6 (CRA-A) the acetate release pocket is not connected at all to the substrate tunnel.

HDAC2 has been crystallised with a benzamide inhibitor **28**<sup>86</sup>, this inhibitor includes an ARBG, though inhibition of HDAC8 was not reported for this inhibitor, a crystal structure alignment reveals that the positioning of the **28** ARBG in the HDAC8 structure would result in a steric clash with Trp141 which is Leu144 in HDAC2 (Figure 1.17a). Additionally no benzamides have yet been reported which inhibit HDAC8 so this inhibitor is highly unlikely to be a potent HDAC8 inhibitor

The HDAC8-4 crystal structure shows many interactions within the acetate release pocket. Parallel displaced aromatic stacking occurs between the dichlorophenyl group of the inhibitor with Trp141 (4.0 Å center-center, Figure 1.17b). As men-

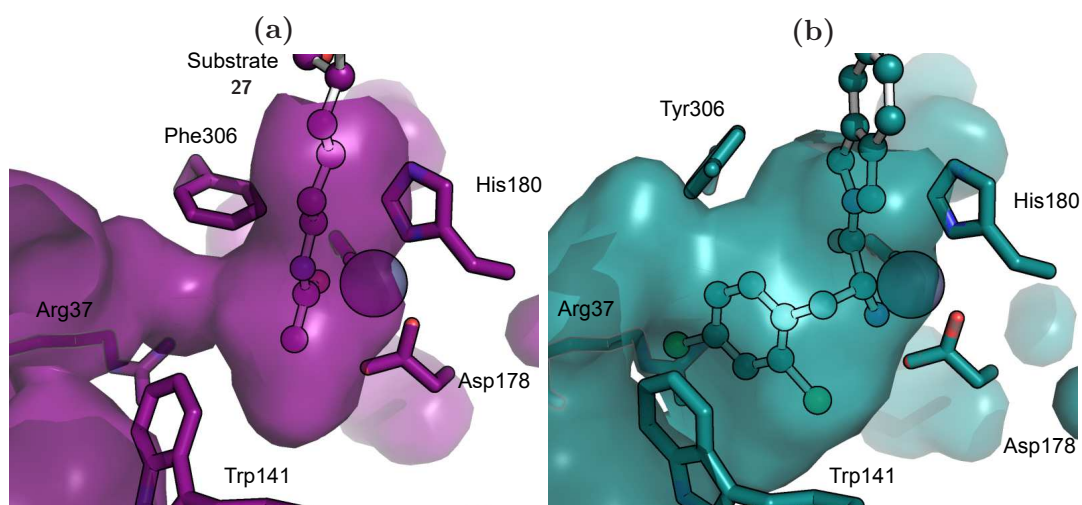


**Figure 1.16:** (a) Narrow internal cavities of HDAC8 when bound with substrate (b) much larger cavity opened up by  $\alpha$ -amino amide inhibitor **4**.

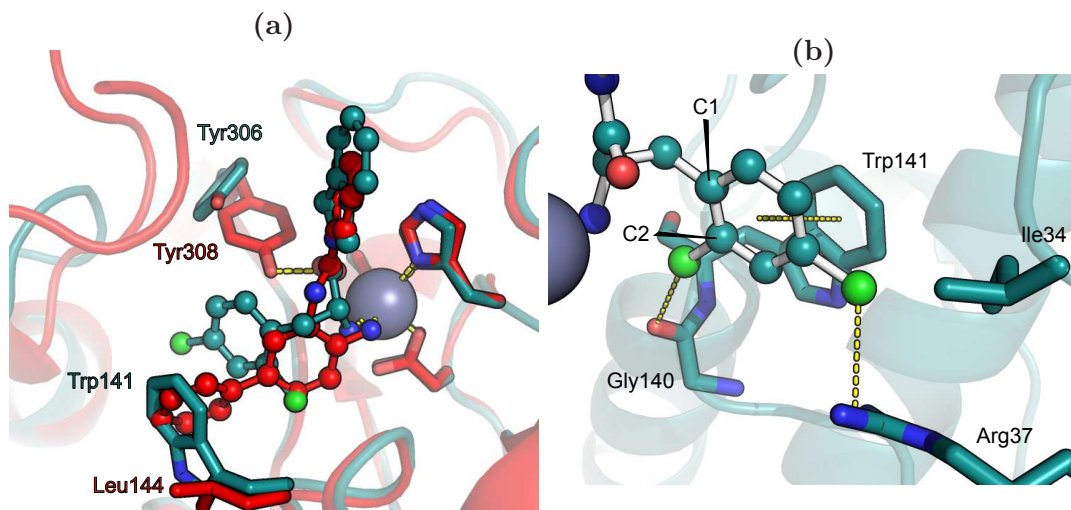


**Figure 1.17:** (a) Aligned crystal structures of HDAC8-**4** (teal) and HDAC2-**28**, a phenylbenzamide inhibitor (red) (b) acetate release pocket interactions, carbons 1 and 2 of the aromatic ring are labeled.

tioned above, Trp at this position is unique to HDAC8 and so likely provides one mechanism for the selectivity of **4** for HDAC8.

The other interactions within the ARBG are between the two aryl chlorine substituents (Figure 1.17b). To understand the two aryl chlorine-protein interactions a modern interpretation of the distribution of electrons around an aryl chlorine atom is necessary. Historically chlorine was considered an electronegative atom which acquires a  $\delta^{-ve}$  charge as a result of its electronegativity when covalently bonded to a carbon atom (since carbon is less electronegative) as seen in Figure 1.18b. This was thought to give chlorine a general Lewis base-like character. However density functional theory (DFT) models reveal that there is anisotropy of electrons surrounding the chlorine which leads to a doughnut shaped distribution of electrons about the atom and a “ $\sigma$ -hole” of electrons in the middle resulting in a  $\delta^{+ve}$  charge (Figure 1.18b)<sup>185</sup>. As a result, for interactions which occur roughly perpendicular to the C-Cl bond, the Cl atom appears to act as a Lewis base, but along the axis of the bond however the  $\sigma$ -hole in the electron density can act as a Lewis acid - this phenomenon is known as halogen bonding<sup>185</sup>.

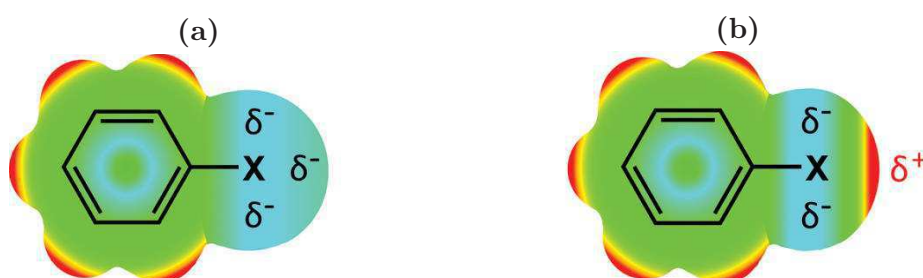


**Figure 1.18:** Electro-surface potential representations of a halogen substituted aromatic ring, the colour gradient from cyan to red represents the electrostatic potential mapped onto the electron isodensity surface. (a) The traditional view of a halogen as an electron donating Lewis base and (b) the more modern view of an aryl halogen that can also act as an electron receiving Lewis acid (taken from ref.[185]).

The chlorine at position 4 on the ring makes contact with the electrophilic sidechain of Arg37 which is side-on and therefore sees the Cl to have Lewis base character (Figure 1.17b). The chlorine at position 2 of the ring however is end-on with the backbone carbonyl oxygen of Gly140, the sigma hole of  $\delta^{+ve}$  charge can therefore

make a halogen bond with the lone pair on the oxygen atom. These two opposite types of interactions are important in the stable filling of the acetate release pocket and an  $\alpha$ -amino amide analogue with a single chlorine substitution was reported to have >2-fold higher  $IC_{50}$ <sup>147</sup>.

The presence of halogen bonding between HDAC8 and  $\alpha$ -amino amide **4** makes conventional small molecule docking algorithms ineffective at finding the lowest energy binding pose for inhibitor **4**. This is because these docking algorithms use a scoring function that calculates interactions by considering each atom as a point charge. Representing with a point charge is not a correct approximation in the case of aryl halogen atoms due their electronic anisotropy. Recently however a scoring function has been described that can accurately replicate the  $\sigma$ -hole required for halogen bonding<sup>186</sup>.

## 1.5 HDAC Activity assays

### 1.5.1 Cellular assays

The study of HDACs and their inhibition requires tools and techniques to monitor their activity. In a cellular context this usually comes in the form of detection of acetylation epitopes such as histone tails by Western blot. This is useful for investigations on the functions of HDACs when one isoform is knocked down or inhibited. Since over 1700 proteins are known to be deacetylated<sup>2</sup> detection of acetylation levels is a very rudimentary technique that may not detect a vast number of acetylation sites due to non-uniform affinity of anti-acetyl antibodies to different acetylation sites. Also cellular techniques cannot isolate individual HDAC functions since complex compensatory mechanisms exist and can cause knock-on effects. In an oncology setting the effect of HDACi on cancer cell lines is assessed much the same as other potential anticancer drugs, for example: flow cytometry, colony forming and migration assays.

### 1.5.2 *in vitro* Assays

No high affinity substrates ( $K_M > 100 \mu\text{M}$ ) are currently available for use in *in vitro* assays, this is primarily because information about the *in vivo* sequence specificity of HDAC8 is scarce.

Radiolabelling assays are an old technique used to monitor HDAC activity. Histone tails are labelled by chemically peracetylating histone tail peptides with  $^3\text{H}$ -labelled acetate<sup>187</sup>. After purification by high performance liquid chromatography (HPLC) these can be used as an HDAC substrate. Following incubation with HDACs the hydrolysed acetate can be separated from the reaction mixture by extraction into organic solvent and the amount of radioactive acetate quantified through scintillation counting. This technique only quantifies HDAC activity against histone tails and so has very limited scope given the numerous non-histone HDAC substrates, especially when considering evaluation of a specific inhibitor.

Fluorescence based HDAC assays utilising the amino methyl coumarin (AMC) fluorophore are however the most common technique used to assess HDAC activity and screen for inhibition due to their ease, speed and need for small amounts of enzyme. At the most basic level, the assay substrate MAL (**27**) consists of an aminomethylcoumarin (AMC) fluorophore conjugated to an acetylated *N*-Boc-lysine residue. Figure 1.19 shows the steps occurring during the assay, deacetylation of the substrate renders the lysine-AMC peptide bond susceptible to hydrolysis by trypsin which is added as part of a developer solution, cleavage of the AMC fluorophore is detected as an increase in fluorescence at 460 nm<sup>188</sup>. Because this is a small, single residue substrate, its  $K_M$  is very high (at  $\sim 20$  mM for HDAC8, see Section 1.6).

In a mass spectrometry based assay, HDAC8 was shown to have activity on histone H4 tail peptides, although only a longer 11 residue sequence from the H4 tail (Lys8-Arg19) produced detectable deacetylation<sup>189</sup>. This suggests that distal regions of the substrate contribute to binding of and deacetylation by HDAC8. Similar experiments have shown a fragment of the p53 tail (residues 372-389) can be a substrate for HDAC8, albeit a very poor one<sup>190</sup>.

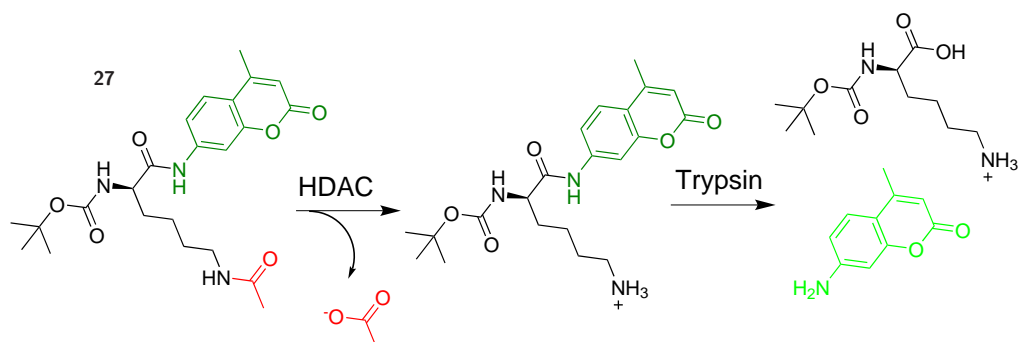


**Figure 1.19:** Steps occurring the an MAL-HDAC assay, HDAC activity removes an acetyl group from MAL (**27**) which makes the deacetylated substrate suitable for tryptic hydrolysis releasing the AMC fluorophore in the developer step.

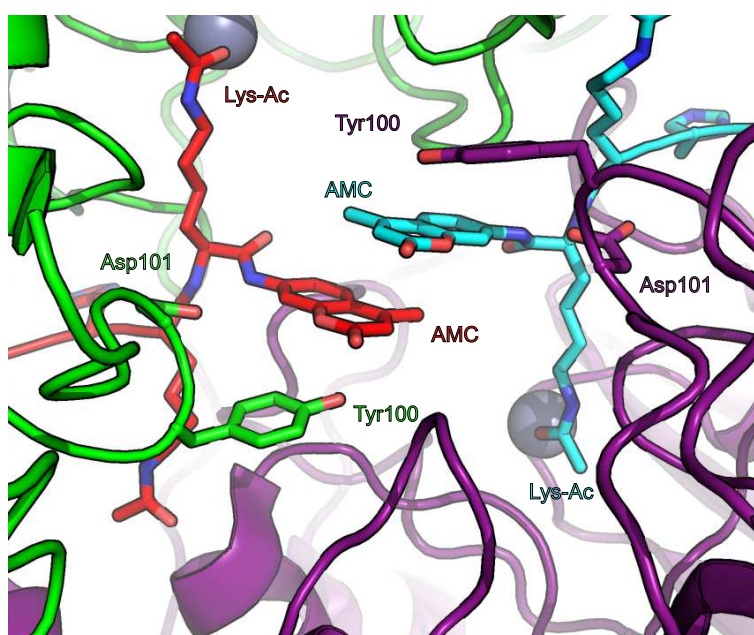


**Figure 1.20:** HDAC8-*Fluor-de-Lys* structure with aromatic stacking interactions being shared between two HDAC8 monomers and two *Fluor-de-Lys* substrate molecules

A further sequence specificity study, showed the preference of HDAC8 substrates to have Arg at the -1 position and Phe at the +1 position<sup>191</sup>. This preference of HDAC8 substrates to have an aromatic residue at the +1 position is supported by the sequence of an HDAC8 optimised assay substrate (*Fluor-de-Lys*, **2**). The *Fluor-de-Lys* substrate consists of an ArgHisLys(Ac)Lys(Ac) tetrapeptide sequence identified from the p53 tail with a C-terminal aromatic AMC reporter (at the +1 position), the inclusion of the extra ArgHisLys(Ac) sequence lowers the  $K_M$  to 1.5 mM<sup>192</sup> from ~20 mM for the MAL substrate (see Section 1.6 in results). In the absence of the aromatic AMC fluorophore however, HDAC8 is unable to deacetylate the *Fluor-de-Lys* substrate<sup>191</sup>. A structure has been solved of inactive HDAC8 mutants with the *Fluor-de-Lys* substrate Figure 1.20. In these structures the aromatic AMC fluorophore can be seen to clearly form aromatic ring stacking interactions with Tyr100<sup>85</sup> Figure 1.20. These fluorescent substrates are a useful tool in the laboratory for HDAC activity and inhibition assays but do not provide insight into bonafide *in vivo* substrates of HDAC8.

The catalytic efficiency ( $K_M/k_{cat}$ ) of HDAC8 is very low ( $7500 \text{ M}^{-1}\text{s}^{-1}$  with the *Fluor-de-Lys* substrate<sup>109</sup>) in comparison to other homologous enzymes such as HDAC1 (which are on the order of  $10^5 \text{ M}^{-1}\text{s}^{-1}$  with a Ac-GlyAlaLys-AMC HDAC1 optimised substrate)<sup>193</sup>, and is far from the diffusion limited rate seen in other enzymes of up to  $1.5 \times 10^{10} \text{ M}^{-1}\text{s}^{-1}$ <sup>194</sup>. Binding partners such as scaffolds or co-activators may play a role in increasing binding affinity and positioning of substrates (and therefore reducing their  $K_M$  and increasing the  $k_{cat}$  *in vivo*).

Development of specific HDAC inhibitors requires a tool to detect activity of single isoforms in isolation. To this end purified individual HDAC isoforms are obtained, either recombinantly expressed or immunoprecipitated from cell cultures and studied *in vitro*.

Modifications have been made to the fluorescence based HDAC assays to improve affinity<sup>195</sup>, to allow detection of inhibition by highly fluorescent inhibitors by derivatisation of deacetylated product<sup>196</sup> and both improved affinity and derivatisation of products<sup>95</sup>. A continuous protease coupled assay has also been developed that provides a more efficient method for measurement of reaction rates<sup>197</sup>. A thioacetylated

lysine peptide has been described as a novel HDAC8 specific assay substrate which quantifies released thioacetate using Elmann's reagent (5,5'-dithiobis(2-nitrobenzoate))<sup>95</sup>.

Some direct detection HDACi-binding assays have used techniques such as fluorescence resonance energy transfer (FRET) to, or fluorescence polarisation/anisotropy of, internal tryptophan residues. These techniques suffer from low signal to noise due to the fact that many inhibitors (eg. Vorinostat, **5** and TSA, **3**) do not have fluorescent groups. Fluorescent analogues are therefore required which sometimes quench the internal tryptophan fluorescence<sup>198</sup>. Given the known positive effect of coumarin on the binding of the *in vitro* HDAC substrate *Fluor-de-Lys*<sup>84</sup>, a fluorescent probe was designed adding an AMC fluorophore to Vorinostat (**5**). The fluorescence of the probe is quenched when bound to HDAC but is detectable when it is free in solution. Displacement of the probe by a competitive HDACi can therefore be detected as an increase in fluorescence. This technique also allows the detection of  $k_{on}$  and  $k_{off}$  rates of HDACi.

## 1.6 Preliminary Assessment of Substrate $K_m$ values

Having a cost-effective and reliable assay for measuring HDAC8 activity is crucial for exploring many inhibitors. To remove reliance on a commercially available enzymatic assay using the *Fluor-de-Lys* HDAC8 specific tetrapeptide-fluorophore substrate (which costs  $\sim$ £70 per 96 well plate), an acetylated lysine substrate (MAL, **27**) was used consisting of *N*-Boc-acetyl-lysine fluorophore (Figure 1.22). Enzymatic assays using the *Fluor-de-Lys* and the MAL substrates were compared in order to ensure suitability of the non-specific MAL substrate to assay inhibition of HDAC8.

The Michaelis-Menten constant ( $K_M$ ) is a measure of the binding affinity of an

enzyme-substrate interaction and is the substrate concentration ( $[S]$ ) at which the initial steady state rate ( $v_0$ ) is half the maximum rate of the enzyme ( $V_{max}/2$ ).

$$v_0 \simeq \frac{V_{max}[S]}{K_M + [S]} = \frac{[S]}{K_M + [S]} E_0 k_{cat} \quad (1.1)$$

Accurate calculation of  $K_M$  generally requires substrate concentrations both smaller than and larger than  $K_M$ . When  $[S] \ll K_M$ , the term  $\frac{[S]}{K_M + [S]} \simeq \frac{[S]}{K_M}$  therefore:

$$v_0 = \frac{k_{cat}}{K_M} E_0 [S] \quad (1.2)$$

and a plot of  $V_0$  against  $[S]$  is linear with a slope of  $E_0 k_{cat}/K_M$ . As  $E_0$  is known it is possible to extract ( $k_{cat}/K_M$ ) but not  $k_{cat}$  or  $K_M$  individually.

Kinetic parameters for the deacetylation of the *Fluor-de-Lys* substrate by HDAC8 were determined by Gantt and colleagues<sup>109</sup>. They measured the  $k_{cat}$  to be  $0.9 \text{ s}^{-1}$  and the  $K_M$  to be  $1100 \mu\text{M}$ . Calculation of the  $K_M$  for MAL requires measurement of the steady-state initial reaction rate ( $V_0$ ) at a number of concentrations of substrate including concentrations on the order of  $K_M$  or above. The MAL substrate however, is not sufficiently soluble in aqueous solutions so the calculation of  $K_M$  cannot be achieved. However, the ratio  $k_{cat}/K_M$  can be measured by plotting  $V_0$  against  $[S]$  (Figure 1.21d) as described above.

Measurement of the  $k_{cat}/K_M$  was performed for both fluorescent substrates using HDAC8 purified from recombinant *E.coli*. Fluorescence values were converted into deacetylated substrate concentrations by reference to a standard curve. This reference is the same for each substrate as the fluorophore product released during the developer step is the same for both substrates.

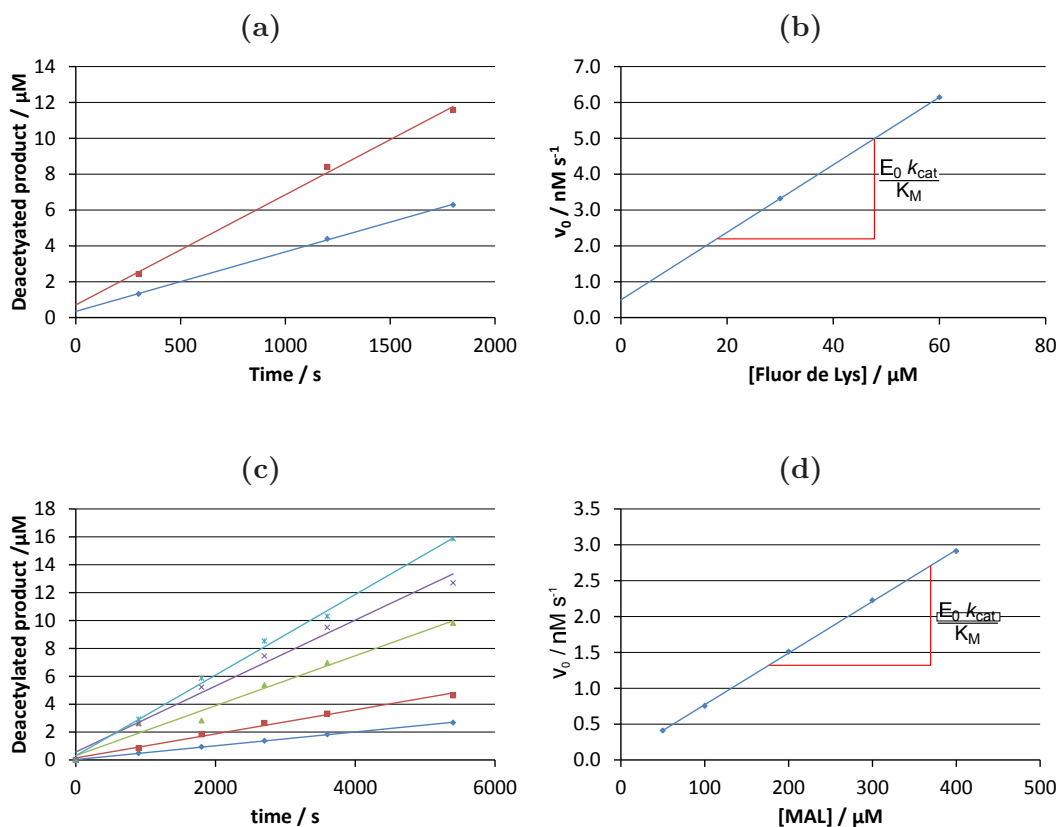


**Figure 1.21:** Comparison of *Fluor-de-Lys* and MAL assay substrates in HDAC8 activity assay using 400 nM HDAC8. (a) Initial rate of reaction at 30  $\mu\text{M}$  (blue) and 60  $\mu\text{M}$  (red) *Fluor-de-Lys* substrate, (b) Rate of reaction vs. *Fluor-de-Lys* concentration, (c) initial rate of reaction at 50  $\mu\text{M}$  (blue) 100  $\mu\text{M}$  (red), 200  $\mu\text{M}$  (green), 300  $\mu\text{M}$  (purple) and 400  $\mu\text{M}$  (cyan) MAL substrate, and (d) initial rate of reaction vs. MAL concentration.

Reaction rates for the *Fluor-de-Lys* substrate were measured using 3 timepoints (5, 20 and 30 min) using substrate concentration of 30  $\mu\text{M}$  and 60  $\mu\text{M}$  (Figure 1.21a). Reaction rates for the MAL substrate were measured at 5 timepoints (15, 30, 45, 60 and 90 mins) using substrate concentrations of 50, 100, 200, 300 and 400  $\mu\text{M}$ . The reaction rates were calculated and plotted against the substrate concentration to give  $k_{cat}/K_M$  (Figure 1.21b & 1.21b). In both cases the resultant plot is linear, indicating that  $K_M \gg [S]$ .

$k_{cat}/K_M=235 \text{ M}^{-1} \text{ s}^{-1}$  for the *Fluor-de-Lys* substrate, whereas the  $k_{cat}/K_M$  for the MAL substrate, is  $17 \text{ M}^{-1} \text{ s}^{-1}$ . If it is assumed that the  $k_{cat}$  is the same for the two substrates since the deacetylation reaction within the enzyme does not change, then the  $K_m$  of the MAL substrate is  $\sim 14$  times larger than that of *Fluor-de-Lys*, about 20 mM.

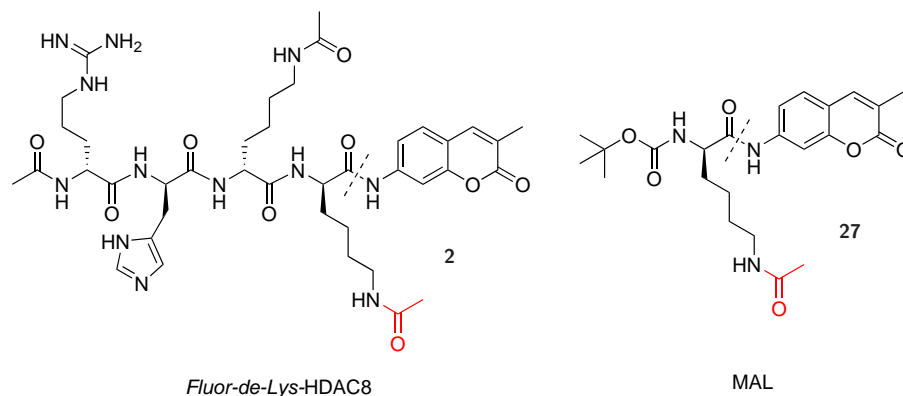


**Figure 1.22:** The commercially available *Fluor-de-Lys* substrate and the MAL HDAC substrate. Acetyl groups in red indicated are cleaved upon HDAC activity. Scissors indicate peptide bond that is hydrolysed by trypsin after deacetylation.

With competitive inhibition present the apparent  $K_M$  is modified to incorporate the fraction of total enzyme that is bound by inhibitor  $K_M^{app} = K_M(1 + \frac{[I]}{K_i})$  (Equation 1.3).

$$v_0 = \frac{E_0 k_{cat} [S]}{K_M(1 + \frac{[I]}{K_i}) + [S]} \quad (1.3)$$

Again when  $[S] \ll K_M$

$$v_0 = \frac{[S]}{K_M(1 + \frac{[I]}{K_i})} E_0 k_{cat} \quad (1.4)$$

Therefore  $v_0$  can be used as a good measure of  $K_i$  as it is proportional to  $\frac{1}{1 + \frac{[I]}{K_i}}$ , it can be used to calculate  $K_i$  as when  $[I] = K_i$ ,  $v_0 = \frac{1}{1 + \frac{[I]}{K_i}} = \frac{1}{2}$ . A plot of  $v_0$  vs.  $\log[I]$  gives

a sigmoidal curve wherefrom  $K_i$  can be determined and any differences in  $K_M$  do not matter when investigating the inhibition of the enzyme as the  $K_i$  is still reported accurately (see Figure 1.23). The MAL substrate is therefore a suitable substrate for the present work as it reports accurately the relative HDAC8 activity.

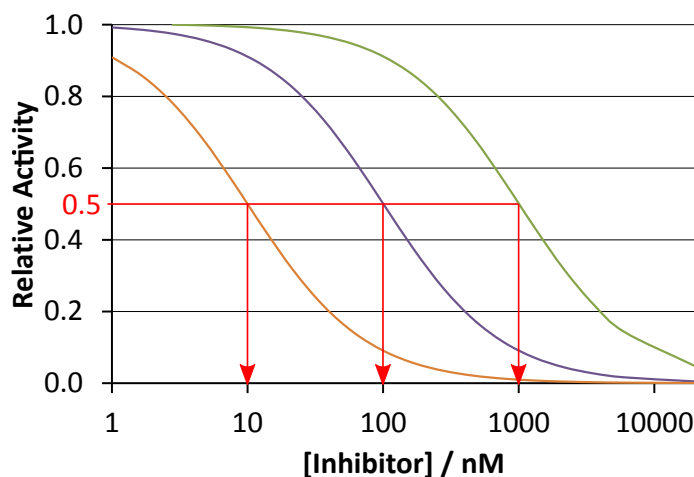


**Figure 1.23:** Simulated activity assays of an enzyme with 3 inhibitors,  $IC_{50} = 10$  nM (orange), 100 nM (purple) and 1  $\mu$ M (green),  $k_{cat} = 3$  s $^{-1}$ ,  $K_M = 100$  mM,  $E_0 = 100$  nM,  $[S] = 200$   $\mu$ M.

## 1.7 Summary

Acetylation is a major post translational modification found in over 1700 proteins within the cell, and at least 3600 acetylation sites in total that are differentially acetylated upon treatment with HDACi<sup>2</sup>. The ubiquity of the 11 Zn<sup>2+</sup> dependent HDACs across a wide range of cellular pathways and processes demonstrates their importance in life. They perform many more functions than their name suggests. In addition to deacetylating histone tails, they deacetylate non-histone proteins, both cytosolic and nuclear. Further to their role as catalytic hydrolases HDACs also mediate interactions with other proteins within multiprotein complexes. Often these complexes enable regulation of activity and substrate specificity of a particular HDAC isoform.

A great number of disease states have been linked to changes in regulation of expression (or activity) of particular HDAC isoforms or HDAC binding partner. For this reason HDACs have been major targets for the development of therapeutic treatments for decades with four HDACi currently approved for the treatment of certain cancers. The search for effective HDACi therapies has been hampered by the severe side effects caused by HDACi. These side effects are so bad that HDACi are only used in late stage cancers which have resisted previous chemotherapy. These side effects are partly a consequence of the non-isoform selectivity of HDACi meaning that all 11 Zn<sup>2+</sup> dependent HDACs are targeted in a non-selective manner. The side effects are also partly due to the promiscuous metal binding hydroxamic acid ZBG found in the majority of HDACs which are known to bind other metalloproteins. To reduce side effects associated with HDACi therapies selective HDACi must be found that can specifically target individual HDAC isoforms, additionally the selective HDACi should also utilise a ZBG that does not bind proteins other than HDACs as the hydroxamic acids that are currently used do.

The search for isoform selective HDACi has predominantly been through modification of the surface binding cap-group. This is because the internal core of the protein is thought to be fairly invariant between isoforms whereas the surface residues show a great deal less conservation. To some degree this direction of research has been successful, many class selective inhibitors have been reported and some of these class selective HDAC inhibitors are showing promise in clinical trials.

The significance of HDAC8 within the cell is becoming more apparent as more of its functions are discovered. With roles in development of the skull, p53 expression and chromatid separation, HDAC8 functions both as a deacetylase and as a scaffold, facilitating the co-localisation of other proteins. HDAC8 has been shown to play a significant role in certain types of cancer, specifically in neuroblastoma which accounts for 15% of all pediatric cancer deaths. It has been shown that abolishing HDAC8 activity in these cancers leads to cell cycle arrest, terminal differentiation and apoptosis.

Despite its class I classification HDAC8 is evolutionarily divergent from HDAC1, HDAC2, and HDAC3 and is poorly inhibited by class I specific inhibitors as a

result. It follows that those same features of HDAC8 that make it poorly inhibited by class I inhibitors should be able to be targeted to create highly selective HDAC8 inhibitors.

There is a great deal of structural information about HDAC8 to be gained from the 32 structures deposited in the PDB, ligands are bound in all these structures suggesting that HDAC8 is a flexible and dynamic protein in its ligand-free form. Certain key residues within the substrate binding tunnel and ligand binding L1 and L2 loops assume multiple conformations depending on the bound ligand, further demonstrating the dynamic nature of the protein which is thought to be significantly greater than other class I HDACs. The residues lining the substrate tunnel are thought to be more rigid in other HDACs and the L2 ligand binding loop is two residues shorter which may alter its dynamic characteristics.

HDACi have been reported which show selectivity, however these selective inhibitors are either relatively low affinity (SB-379278A, **22**) or retain the undesirable hydroxamic acid ZBG (PCI-34051, **1** and cpd6 **20**). There is a definite need for a potent non-hydroxamic acid HDAC8 selective inhibitor.

An HDAC8 selective inhibitor **4** has been reported which utilises a novel  $\alpha$ -amino amide ZBG, showing 18-fold selectivity for HDAC8 over other class I HDACs. A second novel property of this inhibitor compared to other HDAC8 inhibitors is the presence of a group which occupies the acetate release pocket. This inhibitor lacks a cap-group and so its HDAC8 selectivity must arise from the properties of the substrate tunnel and acetate release pocket which provide interactions to this unique inhibitor. Little information exists about  $\alpha$ -amino amide HDACi and so it is an ideal lead compound for rational design to improve its potency.

A commonly used fluorogenic assay substrate is suitable for assessment of inhibitor potency against HDAC8. Both the commercially available *Fluor-de-Lys* substrate and the “in-house” synthesised MAL substrate are equally suitable as they both report the relative activity of HDAC8 and show Michaelis-Menten kinetics, this makes for easy calculation of the inhibitor dissociation constants, and therefore good comparisons between inhibitors can be obtained.

## 1.8 Project goals

Since the initial publication of **4** in 2011 no other groups have explored the potential of an  $\alpha$ -amino amide HDACi. There is therefore a significant degree of chemical space to be explored around this novel ZBG. The main focus of this study is to investigate compounds based on this  $\alpha$ -amino amide ZBG through successive rounds of synthesis and measurements of HDAC8 inhibition.

The contribution of the ARBG to binding and potential chemical variability within the acetate release pocket was to be explored through synthesis of analogues. Also the ability of the substrate tunnel to accommodate alternate STBG and to identify important interactions could potentially be exploited was to be investigated. This was to be achieved by systematic substitution of the synthetically challenging isoindoline group with other aromatic groups.

Through relating the potency of an inhibitor to manual docking results, rationalisation of the effects of each STBG substitution was planned. Through this rationalisation, properties/groups/interactions that are beneficial in an  $\alpha$ -amino amide HDAC8 inhibitor would be identified as well as those which are detrimental to HDAC8 binding. A similar method was to be used to assess the importance of the 2,4-aryl substitution within the ARBG.

The final goal was to combine all the knowledge gained through exploration of the chemical space within the STBG and ARBG, and apply this knowledge to rationally design and synthesise a selective  $\alpha$ -amino amide HDAC8 inhibitor with improved potency for HDAC8 compared to lead compound **4**.

## 2 1<sup>st</sup> generation $\alpha$ -amino amide HDAC8 inhibitors - variation in ARBG and STBG

### 2.1 Introduction

Numerous HDAC inhibitors have been reported, they are all competitive inhibitors which share a common modular structure: A zinc binding group (ZBG) which coordinates the catalytic divalent zinc ion deep within the enzyme at the active site; a substrate tunnel binding group (STBG) which is a linker that occupies the substrate binding tunnel, extending from the ZBG to the surface of the HDAC and mimicking the aliphatic region of the natural acetyl-lysine substrate; and a cap-group that extends out of the substrate tunnel and interacts with the surface of the HDAC (see Section 1.4.2).

The 11 zinc-dependent HDACs have distinct roles within the cell and therefore have different substrates and interaction partners that modulate their activity and specificity<sup>2</sup>. The four FDA approved HDAC inhibitors (HDACi) (for treatment of cutaneous T-cell lymphoma, peripheral T-cell lymphoma and more recently multiple myeloma<sup>199</sup>) have a poor selectivity profile, inhibiting all HDAC isoforms in a non-selective manner. Non-selective inhibition of HDACs is not well tolerated within the body, it causes a wide range of severe adverse side effects, this is due to the diverse roles in many important cellular processes and signalling pathways that HDACs play. Non-selective HDAC inhibition therefore, causes massive cellular stress as all these

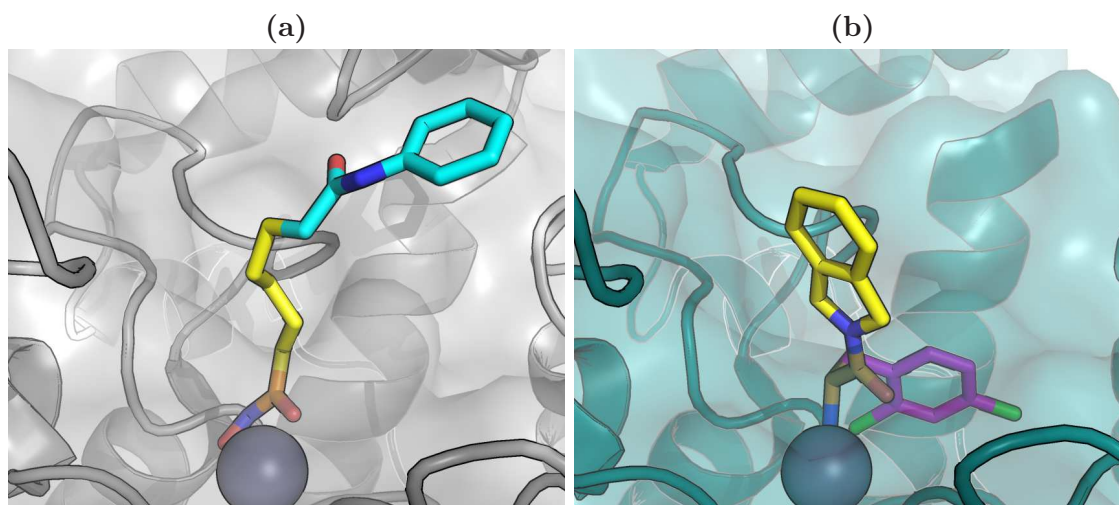


**Figure 2.1:** Structures of HDAC8 in complex with (a) Vorinostat (**5**) and (b) lead compound **4**, carbon atoms of inhibitors are coloured according to the modular HDACi structure, ZBG - orange, STBG - yellow, cap-group - cyan and ARBG magenta.

processes and pathways are perturbed simultaneously<sup>200</sup>. These severe side effects lower the benefit-risk profile of non-selective HDACi and as such, they are only used as second and third line treatments when the cancer is non-responsive or becomes resistant to other treatments.

To date it is assumed that the natural substrate of all HDACs is a protein (or peptide) with an exposed acetylated lysine, although HDAC3 has been shown to have some activity towards crotonylated lysine<sup>61</sup> (lysine crotonylation is a fairly recently discovered histone modification<sup>201</sup>). Differences in activity and substrate specificity therefore rely on the sequence and context of the acetylated lysine. This would be due to interactions between the substrate and the surface of the enzyme, especially within the residues around the mouth of the substrate tunnel. As a result of this assumption the major focus in inhibitor research has been to vary and modify the selective cap-group in order to create isoform specific interactions.

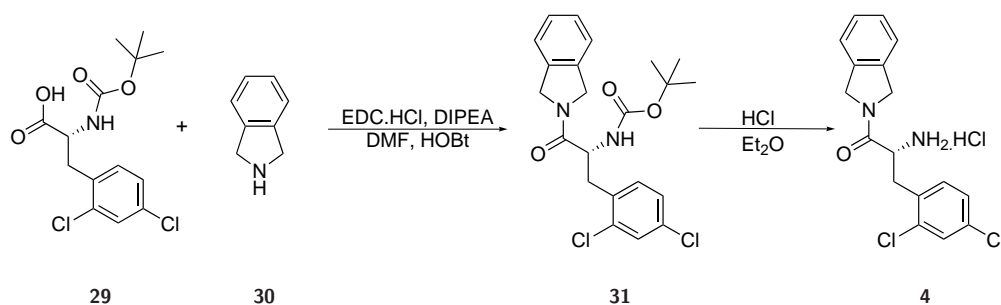
HDAC inhibitors nearly all share a common zinc binding group (ZBG) - the hydroxamic acid. Hydroxamic acids pose a large hurdle to the successful development of HDACi into effective therapies, the largest of which is the promiscuity of binding.

These compounds are known to bind to many metalloproteins such as matrix metalloproteases which cause many off-target effects which manifest as yet further side effects.

In 2011 an HDAC8 selective inhibitor was reported which deviates from the standard modular structure discussed in 1.4.3. The ZBG of **4** is a novel  $\alpha$ -amino amide zinc binding group, does not have a cap-group but instead has an acetate release pocket binding group (ARBG) which extends into a hypothesised acetate release chamber<sup>147</sup>. In order to investigate this novel zinc binding group discovered by Whitehead et al. a series of compounds was synthesised, altering both the ARBG and STBG which were not part of the the  $\alpha$ -amino amide ZBG.

## 2.2 1<sup>st</sup> generation $\alpha$ -amino amide inhibitor synthesis

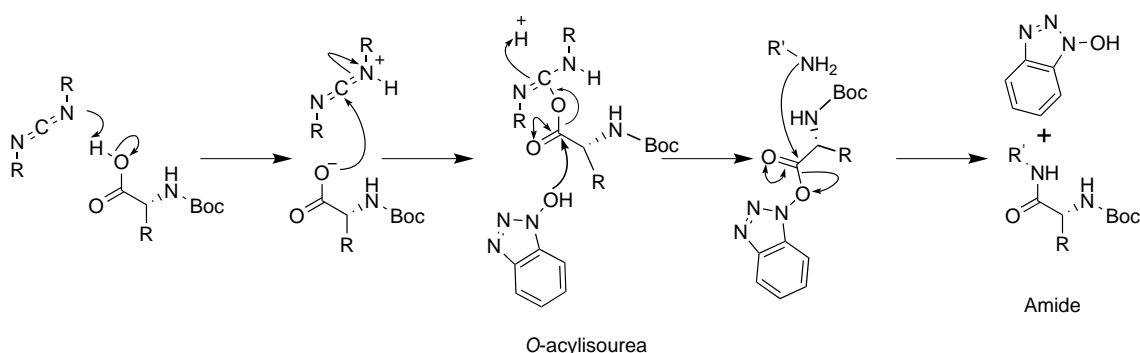
The synthetic route to lead compound **4** is shown in Scheme 2.1, this is an effective 2 step route from commercially available starting materials and was adopted for the synthesis of all  $\alpha$ -amino amides in this study. The route consists of two steps, a 1-ethyl-3-(3-dimethylaminopropyl)carbodiimide hydrochloride (EDC) activated amide coupling of *N*-Boc-(*R*)-2,4-dichlorophenylalanine with isoindoline followed by an acidic cleavage of the *N*-Boc protecting group to yield the product as a hydrochloride salt<sup>147</sup>.



**Scheme 2.1:** Route to  $\alpha$ -amino amide salt **4** as described in the literature<sup>147</sup>.

### 2.2.1 The amide coupling reaction

The mechanism of the amide coupling that was utilised is shown in Scheme 2.2. The reaction proceeds through abstraction of the carboxylic acid proton by a lone pair from the imide followed by the attack of the oxygen on the resultant imide carbocation to form an *O*-acylisourea. At this point the *O*-acylisourea can rearrange and racemise to form an unreactive *N*-acylisourea, this rearrangement is slow and can be avoided by the addition of a nucleophile (HOBT) which attacks fast but yet generates an intermediate which retains enough reactivity to couple with the amine and form the amide with a stereocentre conserved from the starting material, this fast step additionally helps to reduce side-product formation<sup>202</sup>. The choice of EDC over other carbodiimide coupling agents such as dicyclohexylcarbodiimide (DCC) or diisopropylcarbodiimide (DIC), was taken because of the solubility of the resulting urea, which in the case of EDC is a water soluble urea, allowing its removal with an aqueous workup.



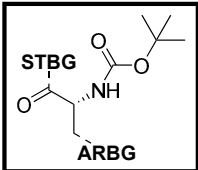
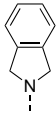
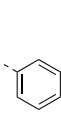
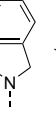
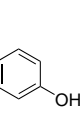
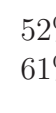
**Scheme 2.2:** Generalised mechanism for EDC activated amide coupling with HOBT

Initially 7 analogues of the lead compound **4** (shown in Table 2.1) were synthesised and their tested for HDAC8 inhibition. These analogues focused on variation of the groups either side of the  $\alpha$ -amino amide ZBG (the STBG and ARBG). The variation in STBG and ARBG was achieved by changing the *N*-Boc amino acid or the amine being coupled. Following *N*-Boc deprotection the desired compounds were successfully synthesised with good purity (>95%).

## 2.2.2 Amide coupling to generate *N*-Boc- $\alpha$ -amino amides

To investigate the effect of alterations in the STBG and ARBG the lead compound **4** and **7** analogues were synthesised with either phenyl, *p*-hydroxyphenyl or 2,4-dichlorophenyl ARBG and a selection of different STBGs (Table 2.1).

**Table 2.1:** Synthetic yields in the production of **4** and initial analogues with preliminary structural variations in the STBG and ARBG

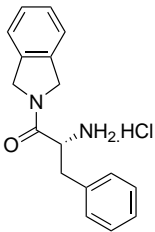
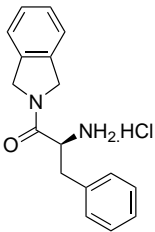
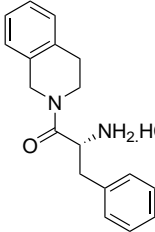
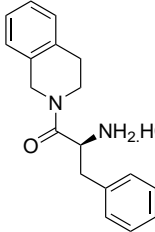
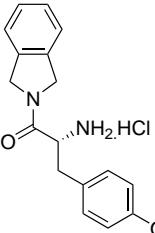
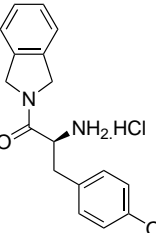
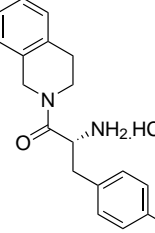
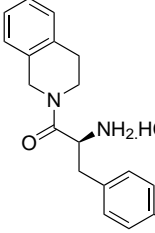
					
Coupling Deprotect	 	48% <b>32</b>	57% <b>33</b>	64% <b>34</b>	50% <b>35</b>
	 	92% <b>36</b>	85% <b>37</b>	75% <b>38</b>	98% <b>39</b>
Coupling Deprotect	 	52% <b>40</b>	32% <b>41</b>	76% <b>31</b>	68% <b>42</b>
	 	61% <b>43</b>	70% <b>44</b>	87% <b>4</b>	48% <b>45</b>

In order to confirm that the reaction was indeed proceeding without racemisation, four  $\alpha$ -amino amides (**36**, **37**, **43** and **44**) were synthesised with their corresponding enantiomers (**46**, **47**, **48** and **49** respectively) equal and opposite  $[\alpha]_D$  measurements were recorded (see Table 2.2).

## 2.2.3 *N*-Boc deprotection of $\alpha$ -amino amides and their isolation

Synthesis of *N*-Boc protected  $\alpha$ -amino amides allows facile transformation to the desired final product, an  $\alpha$ -amino amide salt through the removal of the Boc group.

**Table 2.2:**  $[\alpha]_D$  measurements of matching enantiomers.

					
$[\alpha]_D$	-30.4° <b>36</b>	+33.0° <b>46</b>		-7.8° <b>37</b>	+7.2° <b>47</b>
					
$[\alpha]_D$	34.9° <b>43</b>	+32.4° <b>48</b>		-9.0° <b>44</b>	+12.1° <b>49</b>

Removal of the Boc protecting group proceeded with ease requiring only a short treatment with ethereal hydrogen chloride (generally <2 h). The *N*-Boc- $\alpha$ -amino amides **32** and **50** were successfully deprotected following the procedure used in literature<sup>147</sup> to synthesise the lead compound **4**. Similar treatment with ethereal hydrogen chloride afforded  $\alpha$ -amino amide salts **36** and **46** in excellent yields (>90 %).

*N*-Boc protected  $\alpha$ -amino amide **47** has been *N*-Boc-deprotected previously via a similar method using trifluoroacetic acid in DCM. Following a basic workup the amine of **47** was obtained as an oil<sup>203</sup>. Solid compounds are more stable and easier to handle, in this case it was therefore desirable to obtain the hydrochloride salt for this final product (and all future cases). The oil was dissolved in diethyl ether then treated with ethereal hydrochloric acid to precipitate the insoluble hydrochloride salt.

In contrast to the easily isolable salts **36** and **46**, the hygroscopic nature of the analogues **37** and **47** (which have tetrahydroisoquinolyl STBGs) caused difficulties in isolation. Upon evaporation of the solvent from the ethereal suspension of **37** the white precipitate turned into a colourless oil with an apparent >100% yield. The

NMR spectrum of the salt revealed complete *N*-Boc deprotection but also contained a large water peak. It was therefore determined that these hydrochloride salts were hygroscopic and that the ethereal hydrochloric acid had a small amount of water which remained as the diethyl ether evaporated and was subsequently absorbed by the salt turning it into an oil. This was confirmed when trituration of the oil with dry diethyl ether to remove water did give a small amount of white hydrochloride salt.

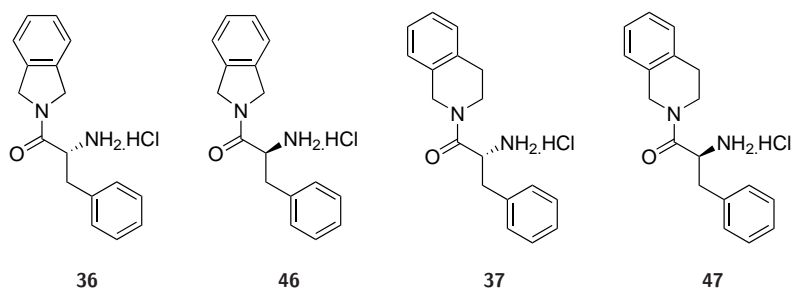


**Figure 2.2:** The non-hygroscopic (**36**, **46**) and the very hygroscopic (**37**, **47**) *N*-Boc- $\alpha$ -amino amide salts.

The salt **37** was so hygroscopic that the initial solid obtained after vacuum filtration became an oil within 5 seconds. The filtration of the hydrochloride salts was further complicated by the latent enthalpy of evaporation of diethyl ether. As the diethyl ether evaporates it cools the surrounding glassware and atmospheric water condenses on the surfaces which is absorbed by the filtered product. This problem was overcome by the use of gravity filtration over diethyl ether heated to reflux. The filter paper was then moved quickly to a warm drying cupboard to prevent the cooling of the surfaces and the resultant condensation and absorption of atmospheric water into the salt. Different levels of hygroscopicity were encountered for various other salts and so gravity filtration over boiling diethyl ether was utilised in the isolation of all subsequent salts. The solid salts were kept in a desiccator and were exposed as little as possible to open atmosphere. Yields for the deprotection of *N*-Boc  $\alpha$ -amino amides can therefore only be taken as approximate due to the unknown level of hygroscopicity for every individual hydrochloride salt.

A stronger *N*-Boc deprotection strategy was required for  $\alpha$ -amino amides **40** and **51** (Figure 2.3) with phenol ARBGs. After a 16 h treatment with ethereal hydrochloric

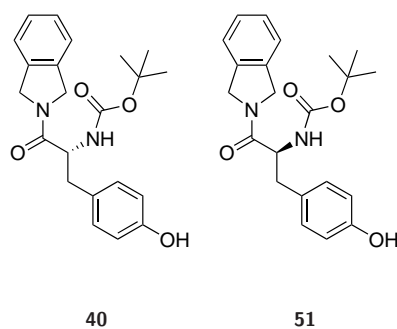


**Figure 2.3:** The  $\alpha$ -amino amides **40** & **51** which require HCl bubbling through an ethereal solution.

acid some starting material was present (as determined by TLC), and was still present after a further 2 h at reflux. A modified deprotection strategy attempted which conveniently also avoids the use of slightly wet ethereal hydrochloric acid. Hydrogen chloride is bubbled through a dry ethereal solution of the *N*-Boc- $\alpha$ -amino amide deprotecting it and forming an insoluble hydrochloride salt which can be collected by filtration as described above.

## 2.3 1<sup>st</sup> Generation $\alpha$ -amino amide inhibition assay results

Initial efforts of this study were aimed at the investigation of the chemical variability of the novel inhibitor **4** through alteration of both the STBG and ARBG components whilst keeping the  $\alpha$ -amino amide ZBG constant.

Initially exploration of the ARBG and STBG was undertaken separately to assess the possible routes to improve the potency and selectivity of the lead compound **4**. Relative initial steady-state rates collected for inhibition of HDAC8 by lead compound **4** are shown in Figure 2.4. The lead compound **4** has a measured  $IC_{50}$  of  $206 \pm 51$  nM which corresponds to a  $k_i$  of  $204 \pm 50$  nM using the Cheng-Prusoff equation (Equation 2.1)<sup>204</sup>, in this case because the  $K_M$  of the MAL substrate (17 mM) is 85 times that of the substrate concentration ( $[S]=200 \mu\text{M}$ ),  $\frac{[S]}{K_M}$  is small

and  $K_i$  values are very close to  $IC_{50}$  values. The binding energy of **4** to HDAC8 is calculated using Gibbs free energy of binding equation (Equation 2.2).

$$K_i = \frac{IC_{50}}{1 + \frac{[S]}{K_M}} \quad (2.1)$$

$$\Delta G_{binding} = -RT \ln K_i \quad (2.2)$$

The  $IC_{50}$  obtained for **4** differs slightly from the literature reported value of 90 nM<sup>147</sup>. Values reported for other inhibitors against HDAC8 can vary greatly - for example Vorinostat (**5**) has reported  $IC_{50}$  values between 49 nM<sup>205</sup> and 2185 nM<sup>206</sup>. Additionally the precise assay conditions and error values are not reported in the literature and so conclusions about this discrepancy cannot be made. Here assay conditions were kept consistent where possible and comparisons between inhibitors are therefore possible here.

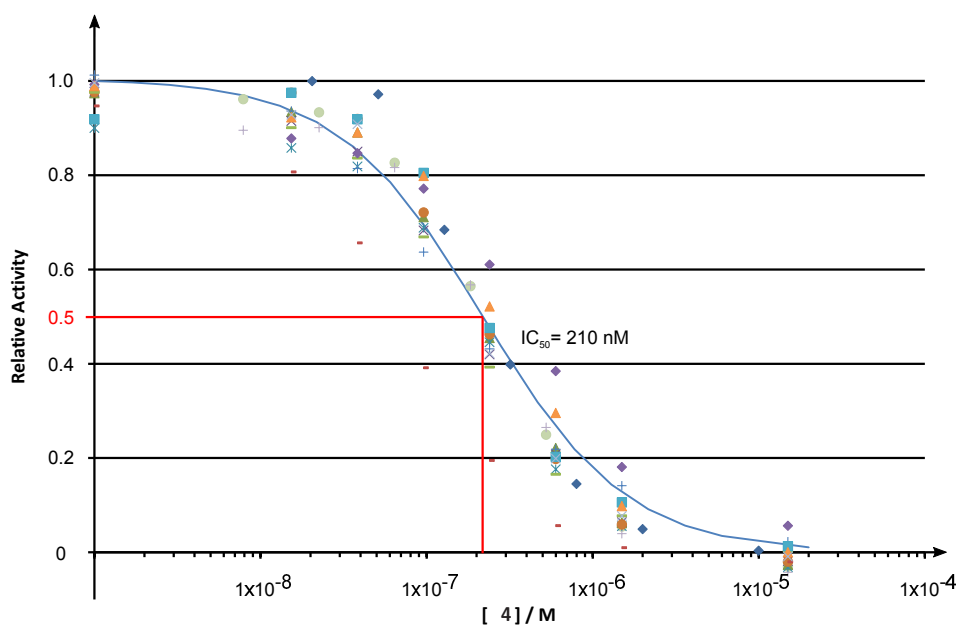


**Figure 2.4:** Experimental data points recorded for 20 HDAC8-**4** inhibition assays. Different symbols represent data from independent repeats. Fitted line is a calculated inhibition curve for  $IC_{50} = 210$  nM, the average calculated for **4**

### 2.3.1 Changes to the 2,4-dichlorophenyl ARBG

The ARBG is a key part of the novelty of the  $\alpha$ -amino amide class of HDACi. The primary interaction in this pocket is an aromatic stacking interaction with Trp141. Trp141 is unique to HDAC8 with leucine present at this position in other class 1 HDACs (Figure 2.5). The interaction with Trp141 is therefore highly likely to be contributing to the specificity of **4** for HDAC8.

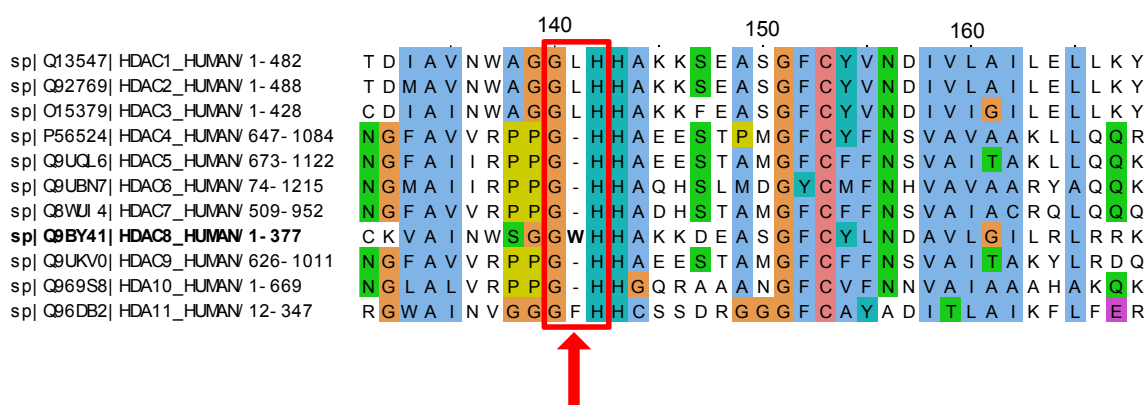


**Figure 2.5:** Alignment of all 11 human HDAC enzymes showing the unique Trp141 found in HDAC8 (performed using Mafft alignment algorithm within Jalview software).

From the HDAC8-4 structure, interactions can be seen between HDAC8 and the chlorine atoms (see Figure 2.7a). The electronic anisotropy about the chlorine atom at position 4 results in a  $\delta^{-ve}$  region facilitating an interaction with the positive Arg37 sidechain. Halogen substituents on aromatic rings have also been reported to make “halogen-bonds” to backbone carbonyl oxygen atoms, hydroxyl groups, carboxylate groups and  $\pi$  surfaces of sidechains that can all act as electron donating Lewis bases (Figure 2.6b, discussed in Section 1.4.3)<sup>185</sup>. In the HDAC8-4 structure the chlorine atom at position 2 on the aromatic ring is 3.4 Å from the peptide backbone oxygen atom of Gly140, suggesting that there is an interaction between these two atoms.

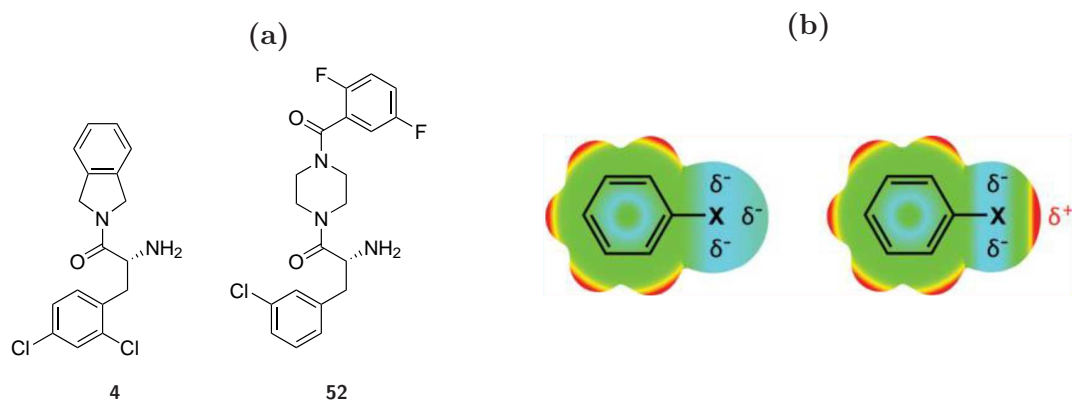


**Figure 2.6:** (a) Two reported  $\alpha$ -amino amide HDAC8 selective inhibitors, and (b, left) Traditional assumption of the halogen as a Lewis base (electron donor) with a predominantly isotropic electron distribution on the cap, (b, right) description highlighting the anisotropy of the electron density on the halogen. The color gradient from cyan to red represents the electrostatic potential mapped onto the electron isodensity surface (from [185]).

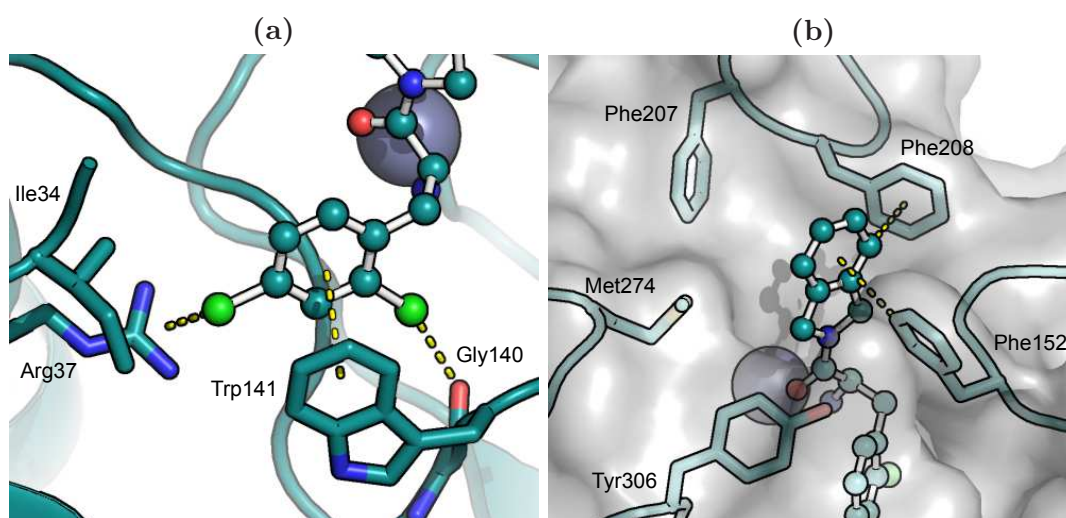


**Figure 2.7:** HDAC8-ligand interactions in (a) the ARBG, and (b) the STBG as observed in the published structure<sup>147</sup>.

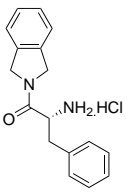
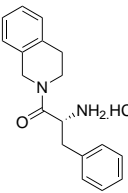
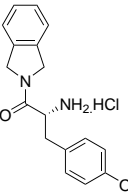
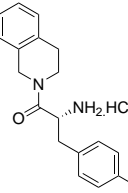
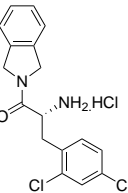
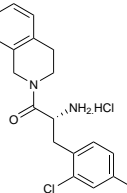
To explore the effect of the chlorinated aromatic unit, compounds were synthesised

with different ARBG as compared to the 2,4-dichlorophenyl group found in the lead compound **4**.

## Phenyl ARBG

To determine the contribution of the chlorine substitutions to the binding of **4**,  $\alpha$ -amino amide inhibitor **36** was synthesised with an unsubstituted phenyl ARBG (Table 2.3). All other protein-ligand interactions should be maintained as this variation is a removal of two chlorines rather than addition to the group. The only exception to this would be if the chlorine interactions cause a significant conformational change in the protein which alters other binding surfaces in an allosteric fashion.

**Table 2.3:** A selection of compounds synthesised to explore the possibility of varying the ARBG and STBG and their associated IC<sub>50</sub> (full results are presented in Table 2.4).

						
	<b>36</b>	<b>37</b>	<b>43</b>	<b>44</b>	<b>4</b>	<b>45</b>
IC <sub>50</sub> / $\mu$ M	1.15 $\pm 0.18$	10.7 $\pm 0.86$	4.28 $\pm 1.56$	21.0 $\pm 6.52$	0.21 $\pm 0.04$	2.06 $\pm 0.51$
$\Delta G_b$ /kcal mol <sup>-1</sup>	-8.43 $\pm 0.16$	-7.1 $\pm 0.08$	-8.24 $\pm 0.36$	-6.63 $\pm 0.31$	-9.48 $\pm 0.18$	-8.07 $\pm 0.25$

The unsubstituted ARBG containing  $\alpha$ -amino amide inhibitor **36** has a 5-fold higher IC<sub>50</sub> value than the corresponding 2,4-dichlorophenyl ARBG containing inhibitor **4** ( $1.15 \pm 0.18 \mu\text{M}$  vs.  $0.21 \pm 0.04 \mu\text{M}$ ). Using Equations 2.1 and 2.2 which convert an IC<sub>50</sub> value to a binding energy, this correlates to a binding energy loss of about  $1 \text{ kcal mol}^{-1}$  which occurs as a result of the loss of the two chlorine substituents (Table 2.3). To confirm this result, two more compounds were synthesised,

both with a tetrahydroisoquinoline substrate binding group. Compound **37** with an unsubstituted phenyl ARBG had an  $IC_{50}$  5-fold higher than the corresponding 2,4-dichlorophenyl substituted inhibitor **45**, again this energy loss corresponds to a reduction in binding energy of  $\sim 1 \text{ kcal mol}^{-1}$  indicating that the presence of the chlorine substitutions provides  $\sim 1 \text{ kcal mol}^{-1}$  to the binding energy of the lead compound **4** (see Figure 2.9). Allosteric effects are unlikely to contribute  $1 \text{ kcal mol}^{-1}$  to binding energies as the  $\Delta\Delta G_{binding}$  is the same when both isoindoline and tetrahydroisoquinoline STBG are present, therefore interactions involving the ARBG aromatic substituents as well as the  $\pi$ -stacking with Trp141 are required for tight binding.

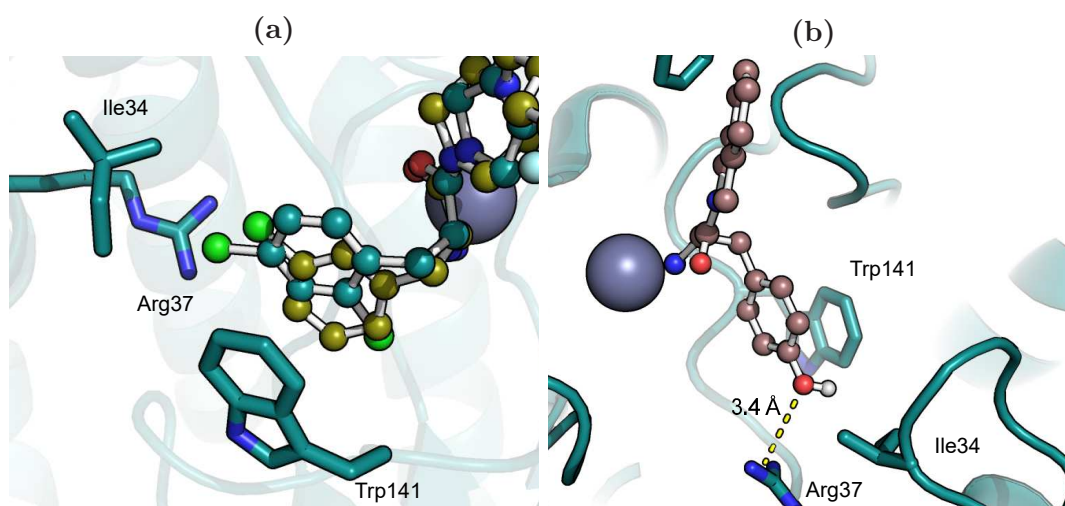


**Figure 2.8:** (a) Two aligned structures of HDAC8 bound to the literature  $\alpha$ -amino amide inhibitors **4** (teal) and **52** (olive), and (b) manual docking of *p*-hydroxyphenyl ARBG containing  $\alpha$ -amino amide **43** into HDAC8-4 structure.

### *p*-Hydroxyphenyl ARBG

Hydroxyl groups possess a lone pair of electrons and a very polar oxygen-hydrogen bond which makes them good hydrogen bond donors and acceptors and also Lewis bases. To explore the possibility of modifying the interaction between the Arg37 sidechain and a hydroxyl group, compound **43** was synthesised with a *p*-hydroxyphenyl ARBG. Manual docking of **43** into the HDAC8 structure shows that the lone pair

can be positioned in such a way as to interact with the positively charged Arg37 sidechain (Figure 2.8b). The acetate release pocket is most-likely large enough to accommodate a hydroxyl group being only slightly larger than a Cl atom.

The compound with a *p*-hydroxyphenyl ARBG (**43**) showed a reduction in binding energy of  $1.86 \pm 0.40$  kcal mol<sup>-1</sup> compared to its 2,4-dichlorophenyl ARBG containing counterpart (**4**)(Table 2.3). Again this result was confirmed through the synthesis of another compound, both with a tetrahydroisoquinoline STBG. The *p*-hydroxyphenyl ARBG containing inhibitor (**44**) has a binding energy of  $-6.63 \pm 0.31$  kcal mol<sup>-1</sup>,  $1.44 \pm 0.41$  kcal mol<sup>-1</sup> smaller than the corresponding 2,4-dichlorophenyl ARBG containing inhibitor (**45**). This loss in binding energy is close to the loss in binding energy seen when the 2,4-dichlorophenyl group is replaced with an unsubstituted phenyl ARBG (**36**→**43**, Figure 2.9,  $\sim 1$  kcal mol<sup>-1</sup>). The presence of the *p*-hydroxyphenyl group in the acetate release pocket does not re-establish interactions with the acetate release pocket, in fact there is possibly a small negative effect due to the *p*-hydroxyphenyl ARBG, possibly because of the electron-withdrawing effect of the oxygen affecting aromatic stacking with Trp141.

From these explorations of the ARBG, it appears that the 2,4-dichloro unit cannot be readily improved upon. From now on, the focus will be on exploration and optimisation of the STBG.

### 2.3.2 Changes to the STBG

Alternative aromatic ringed systems to isoindoline were explored as STBG, which would enable a more diverse series of inhibitors to be easily constructed. Such alterations include tetrahydroisoquinoline as discussed above (Section 2.3.1). Aromatic stacking interactions between inhibitor **4** and Phe152 and Phe208 are present (Figure 2.7b). These two residues have previously been mutated to all other natural amino acids in HDAC1 and were proved to be essential for activity (although a Phe208Tyr substitution partially restored some activity)<sup>207</sup>. To confirm the importance of these two residues in HDAC8 I performed site directed mutagenesis, recombinantly expressed and purified HDAC8 containing Phe152Ala and Phe208Ala mutations. No

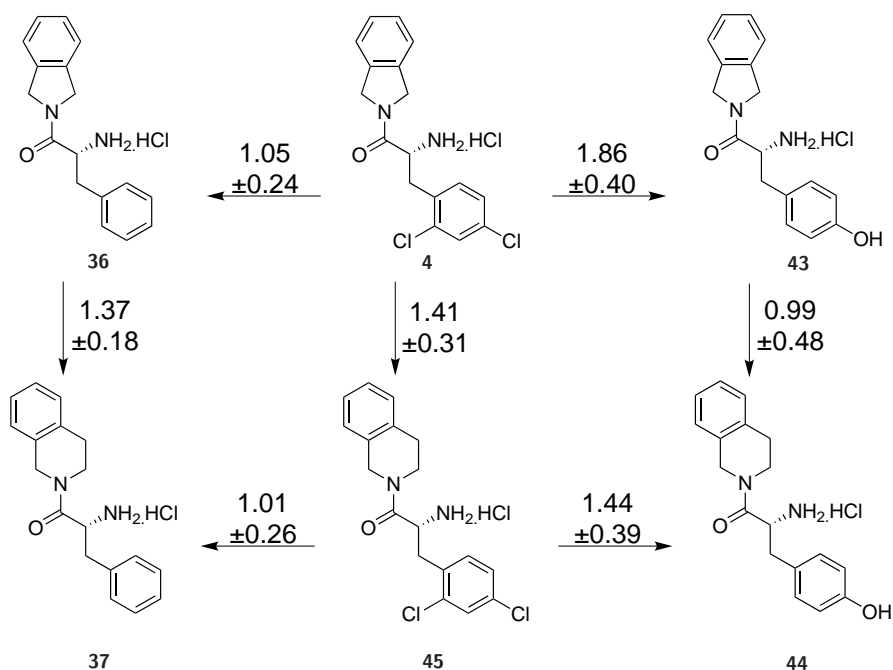


**Figure 2.9:** Losses in binding energy between 1<sup>st</sup> generation  $\alpha$ -amino amide HDAC8i. Horizontal arrows represent ARBG changes, vertical arrows represent changes in STBG. Values on arrows are  $\Delta\Delta G_{binding}$  values in kcal mol<sup>-1</sup>.

activity was detected in the mutants using the MAL substrate (results not shown). This confirms the importance of these two aromatic interactions to the binding of substrate in HDAC8.

Comparison of HDAC8 crystal structures in complex with various inhibitors shows the aromatic ring of Phe152 is able to assume many orientations in order to accommodate different ligands (Figure 2.10a<sup>82</sup>). The structural flexibility of Phe152 is such that a difference in positioning is observed even between the structures of two similar  $\alpha$ -amino amide inhibitors reported (Figure 2.6a<sup>147</sup>).

Figure 2.10a highlights the structural flexibility of Phe152 that lines the substrate tunnel of HDAC8, with a hydroxamate inhibitor CRA-A (**6**). The Phe152 sidechain can swing up to reveal a “subpocket” which is thought to be a feature unique to HDAC8. Two “linkerless” HDAC8 specific inhibitors (**19** & **53**, Figure 2.10b) have been reported which are thought to utilise this subpocket to confer HDAC8 se-

lectivity (**53**  $IC_{50} = 0.7 \mu\text{M}$ ) over HDAC1 ( $IC_{50} > 100 \mu\text{M}$ ) and HDAC6 ( $IC_{50} = 55 \mu\text{M}$ )<sup>90</sup>(though crystal structures have not been solved with these ligands which prove this). As discussed earlier in Section 1.4.3, aromatic T-stacking interactions are formed between Phe152 which is perpendicular to the substrate tunnel and the isoindoline STBG (Figure 2.7b).

The position of Phe152 when bound to the non-specific HDAC inhibitor Vorinostat (**5**), grey in Figure 2.10a) is flat against the substrate tunnel. It is possible that the ability of Phe152 to rotate is unique to HDAC8 and is a feature that can be targeted for the synthesis of HDAC8 selective inhibitors. The crystal structure shown in 2.10a has a rotated Phe152 sidechain, but the selectivity profile for this inhibitor has not been reported and so no inferences can be made in this case.

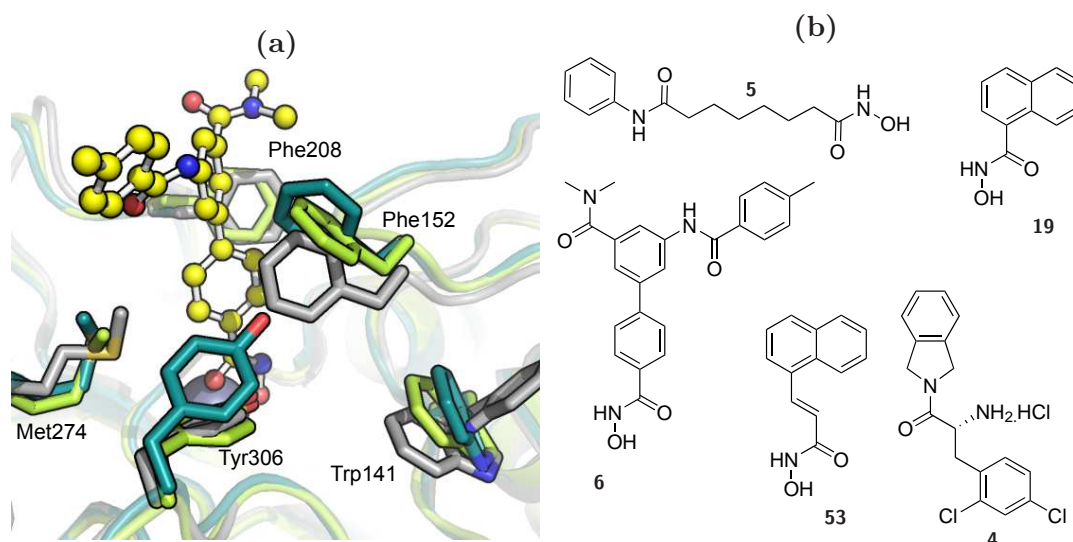


**Figure 2.10:** (a) HDAC8-4 (teal, **4** not shown) and HDAC8-Vorinostat (**5**, grey, not shown) structures superimposed onto the HDAC8-CRA-A (yellow, **6**) structure, and (b) Two “linkerless” HDAC8 inhibitors **53** and **19** which show selectivity for HDAC8 over HDAC1 and HDAC6<sup>90</sup>, Vorinostat (**5**, CRA-A (**6**) and lead compound **4**.

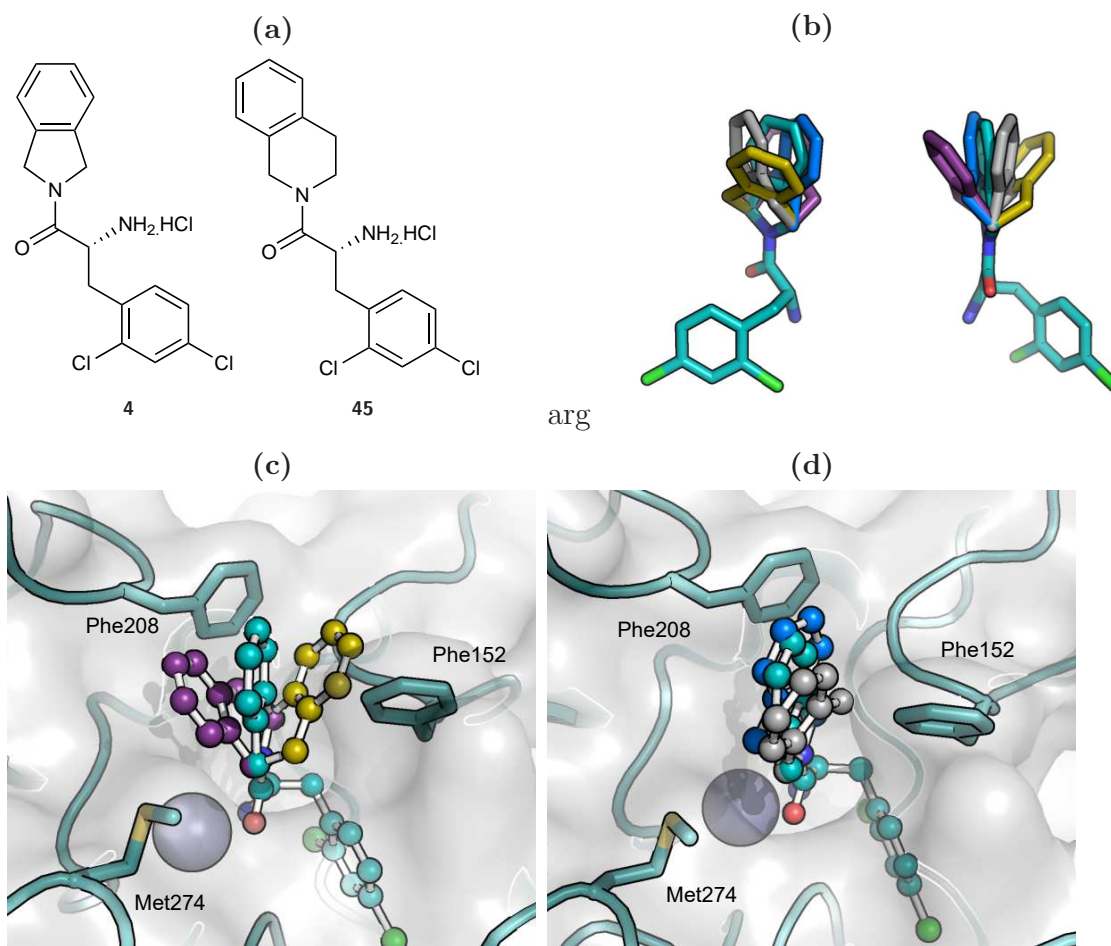
## Tetrahydroisoquinoline STBG

As discussed in Section 4.1, isoindoline is a fairly unstable molecule and substitutions around it require formation of the isoindoline system after installation of a substituent at the position desired. Tetrahydroisoquinoline was tested as a potential substitute for the isoindoline STBG as it is more stable and more readily substituted. It was hoped that due to the known flexibility of the HDAC8 substrate channel that the non-planar asymmetrical tetrahydroisoquinoline STBG would be accommodated without a large decrease in potency. If the binding affinity remained high then then modifications could be made to the tetrahydroisoquinoline system to try and introduce more interactions with the protein and improve binding affinity as a result.

The tetrahydroisoquinoline STBG can adopt one of two conformations and one of two different rotamers due to the planar amide system (Figure 2.11b). The nitrogen is sp<sup>3</sup> hybridised, but as the lone pair is delocalised into the amide bond the bonding around the nitrogen is effectively trigonal-planar. This causes the two adjacent methylene groups to be in plane with the amide bond. The remaining methylene group can assume one of two conformations, forming a more boat-like structure (Figure 2.11c) or a more chair like structure (Figure 2.11d). Both these conformations are non-planar and may cause steric clashes with the substrate channel. In addition to the non-planarity of tetrahydroisoquinoline it is also asymmetrical, the isoindoline STBG of the lead compound **4** is symmetrical about the amide bond (see Figure 2.11a). This asymmetry introduces an additional kink in the molecule causing possible steric clashes with the wall of the substrate tunnel.

Tetrahydroisoquinoline containing compounds **45**, **37** and **44** discussed above in Section 2.3.1 were assayed for HDAC8 inhibition. In all cases however, these tetrahydroisoquinoline STBG containing compounds with IC<sub>50</sub> values of 2.06 ± 0.51, 10.7 ± 0.86 and 21.3 ± 6.52 μM respectively are 5 to 10-fold less potent than their isoindoline STBG containing counterparts (**4**, **36** and **43** respectively) (IC<sub>50</sub> = 0.21 ± 0.04, 1.15 ± 0.18 and 4.28 ± 1.56 μM), this difference equates to a loss of binding energy of around 1.4 kcal mol<sup>-1</sup> (Figure 2.9). Independent of ARBG, replacement of the isoindoline

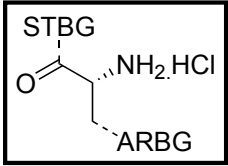
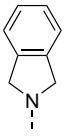
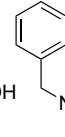
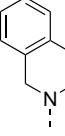
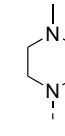
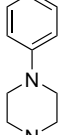
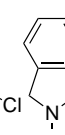
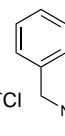
doline STBG with a tetrahydroisoquinoline STBG destabilises the HDAC8-inhibitor interaction by  $\sim 1.4$  kcal mol<sup>-1</sup>.



**Figure 2.11:** (a) Structures of  $\alpha$ -amino amide HDAC8 inhibitors **4** and **45**, (b) Overlay of four energy minimised structures of isoquinoline STBG containing **45** (yellow, purple, grey, blue) and isoindoline STBG containing **4** (teal) (c & d) manual docking of the 4 rotamers of **45**, positioning of **4** from crystal structure is shown for comparison (teal).

To explain these results, tetrahydroisoquinoline containing **45** was manually docked into the HDAC8 structure to reveal potential changes in interactions that arise from the new STBG. It was hoped that the flexibility within the substrate tunnel would allow for the accommodation of tetrahydroisoquinoline as a STBG, leaving the aromatic interactions intact. While manual docking suggests that on the whole, steric

**Table 2.4:** HDAC8 inhibition assay results for first generation compounds. Values are  $\pm$  standard deviation of >2 independent repeats ( $\Delta G_b = \Delta G_{binding}$ ).

									
	ARBG	STBG	IC <sub>50</sub> / $\mu$ M	$\Delta G_b$ /kcal mol <sup>-1</sup>		ARBG	STBG	IC <sub>50</sub> / $\mu$ M	$\Delta G_b$ /kcal mol <sup>-1</sup>
<b>36</b>			1.15 $\pm 0.18$	-8.43 $\pm 0.16$	<b>44</b>			21.3 $\pm 6.52$	-6.63 $\pm 0.31$
<b>37</b>			10.7 $\pm 0.86$	-7.1 $\pm 0.08$	<b>39</b>			11.0 $\pm 5.98$	-7.04 $\pm 0.54$
<b>38</b>			>600	>-4.6	<b>4</b>			0.21 $\pm 0.04$	-9.48 $\pm 0.18$
<b>43</b>			4.28 $\pm 1.56$	-8.24 $\pm 0.36$	<b>45</b>			2.06 $\pm 0.51$	-8.07 $\pm 0.25$

clashes should be minimal for tetrahydroisoquinoline containing **45**, comparison of **4** and **45** STBGs within the substrate tunnel reveals a potentially crucial difference between the positioning and orientation of the isoindoline and tetrahydroisoquinoline aromatic rings (Figure 2.11). The aromatic ring for isoindoline **4** is positioned for T-stacking interactions with Phe152 and Phe208 (Figure 2.7b), and despite the known conformational flexibility of Phe152 which has been seen in many positions in different structures (Figure 2.10a), it is apparent that this flexibility could not enable aromatic stacking with tetrahydroisoquinoline **45** to be maintained. The loss

in binding energy could therefore be caused by introduced steric clashes and/or loss of aromatic stacking interactions

### Piperazine based STBGs

With the loss of potency that results from the introduction of a tetrahydroisoquinoline STBG, two compounds with linear and symmetrical piperazine-based STBGs were synthesised (**39** and **38**) to further explore the possibility of replacing the isoindoline STBG with an alternative, more readily modified unit.

Similar to tetrahydroisoquinoline STBGs, piperazine based STBG are also poorly tolerated within the substrate tunnel, with IC<sub>50</sub>s of 11.0 ± 5.98 μM and >600 μM respectively both methylpiperazine **39** and phenylpiperazine **38** are poor inhibitors (Table 2.4). When manually docked into the HDAC8-4 structure the chair conformation of the piperazine ring in **39** is obvious (Figure 2.12a). In its lowest energy conformation, as calculated by an energy minimisation performed within the program Avogadro<sup>208</sup>, the methyl group lies in an equatorial position. This places the methyl group in a steric clash (1.1 Å) with Phe152 or very close (2.7 Å) to His180 (Figure 2.12a). Manual docking of the slightly less energetically favourable axial conformation of the methyl piperazine STBG allows no steric clashes with the protein. As there is a pose in which the methylpiperazine **39** can be fitted into the HDAC8 structure it is likely that the loss of potency is mainly due to the lost aromatic stacking interactions with Phe152 and Phe208. This is confirmed by comparison to the equivalent tetrahydroisoquinoline STBG containing compound **36** which has a similar potency (IC<sub>50</sub> = 10.7 ± 0.86 μM).

In an attempt to re-establish aromatic contacts in the region a phenyl ring was introduced on to the end of the methylpiperazine STBG to make the phenylpiperazine STBG containing **38**. Addition of results in a dramatic reduction in affinity of the inhibitor compared to **39** however. A 50-fold loss in potency is seen corresponding to a loss in binding energy of >2.4 kcal mol<sup>-1</sup>. The geometry of phenylpiperazine is different to that of methylpiperazine because of the delocalisation of the phenylamino nitrogen lone pair of electrons into the phenyl ring, this results in a planar

region as opposed to the approximately tetrahedral geometry of the methyl amino group.

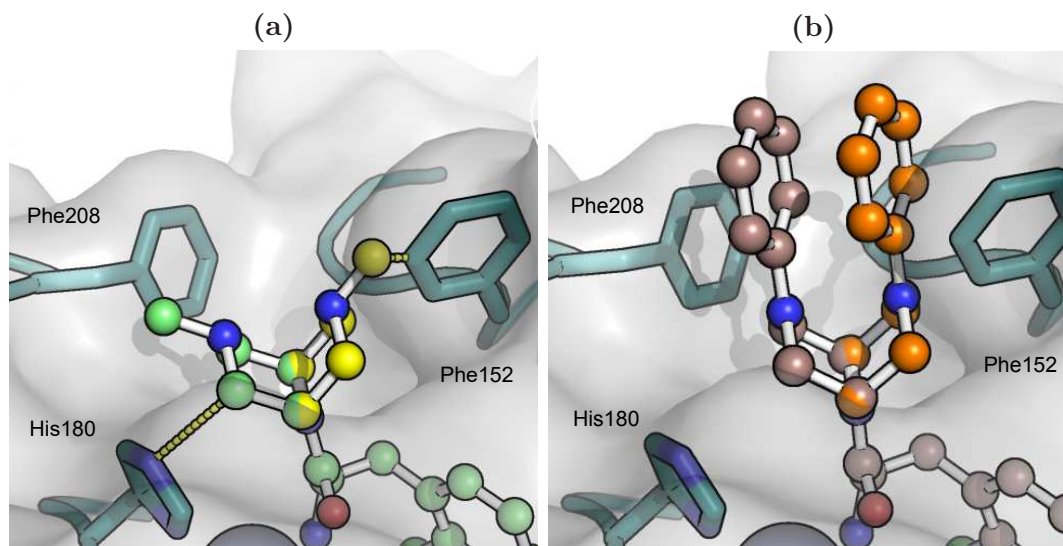


**Figure 2.12:** The two rotamers of (a)**38** with solvent exposed phenyl group & (b) **39** manually docked into HDAC8.

Of the two rotamers of **38** manually docked into the HDAC8 structure only one fits without causing steric clashes with Phe152 (brown ligand in Figure 2.12b). This conformation of **38** does not put the phenyl ring in a position to stack with any residues at the mouth of the substrate tunnel, instead it forces the phenyl ring to be exposed to the solvent. This is a very energetically unfavourable interaction and is likely the cause of the very low potency.

It is interesting that piperazine is unsuitable as a STBG as it is the STBG present in the one other known  $\alpha$ -amino amide (**52**, Figure 2.6a), this inhibitor does sit in a slightly rotated conformation in the ARBG however (Figure 2.8a), it is possible that the piperazine STBG is only compatible with a 3-chlorophenyl ARBG while isoindoline STBG is only compatible with the 2,4-dichlorophenyl ARBG due to the enforced STBG orientation governed by the identity of the ARBG. The 2,4-dichlorophenyl ARBG was pursued due to the superior reported affinity for HDAC8 of **4** (90 nM) over **52** (200 nM). Additionally **52** contains an amide on each side of

the piperazine which would significantly alter the geometry of the piperazine group (in a similar fashion as the aromatic ring of **38** was seen to do).

## 2.4 Summary of 1<sup>st</sup> generation inhibitor assay results

Eight compounds were synthesised with various ARBGs and STBGs to investigate the binding pocket of **4** in HDAC8; these compounds were tested for HDAC8 inhibition and binding energies were calculated from the measured IC<sub>50</sub> values. A tetrahydroisoquinoline group was tested in place of the isoindoline STBG of the lead compound **4**.

Chlorination of the ARBG was found to be essential as inhibitors with unsubstituted phenyl ARBG lead to a  $\sim 1$  kcal mol<sup>-1</sup> reduction in binding energy. Attempts to re-establish a contact with Arg37 by introduction of a *p*-hydroxyphenyl ARBG to act as a Lewis base resulted in a similar loss in binding energy when compared to the 2,4-dichlorophenyl ARBG.

Replacement of the isoindoline STBG for a non-planar and asymmetric tetrahydroisoquinoline STBG group lead to a loss of aromatic contacts that resulted in a  $>1$  kcal mol<sup>-1</sup> loss in binding energy that was independent of the ARBG present. In order to confirm this effect two piperazine containing inhibitors were synthesised. A similar  $\sim 1$  kcal mol<sup>-1</sup> loss in binding energy was measured for the methylpiperazine inhibitor **39** indicating that the change in binding energy is due to the loss of aromatic interactions within the substrate tunnel. Reestablishment of aromatic contacts was not successful through the addition of a phenyl ring to inhibitor **39** to give **38** with a phenylpiperazine STBG. Manual docking reveals that only one rotamer of **38** fits within the substrate tunnel without steric clashes and this conformation exposes the aromatic ring to the solvent which, being a highly unfavourable interaction reduces the binding energy by  $> 2.4$  kcal mol<sup>-1</sup> compared to the methylpiperazine STBG containing **39**.

The structure of HDAC8-4 shows very little room for additional variation within the acetate release pocket. With the observed and quantified necessity for the interactions between the two chlorine atoms and Gly140 and Arg37 it was decided that the 2,4-dichlorophenyl ARBG is unlikely to be improved upon within the time available and so subsequent efforts were focussed on exploration of possible alternative groups to occupy the substrate tunnel which is known to be flexible and contains at least one water molecule in the HDAC8-4 structure.

The acetate release pocket lies within the core of the protein and as such there is little room around it to perform modifications. Crystal structure with different ligands reveal the substrate binding tunnel is able to accommodate many different STBGs including some containing bulky and aromatic regions, in these structures conformational change is seen within residues lining the tunnel, especially Phe152 (Figure 2.10a). As a result of these observations it was decided to attempt further variation of the STBG while maintaining the 2,4-dichlorophenyl ARBG of the lead compound 4.



# 3 2<sup>nd</sup> generation $\alpha$ -amino amide HDAC8 inhibitors - further variation of the STBG

## 3.1 Introduction

Following the discovery of the necessity to have a 2,4-dichlorophenyl ARBG a series of 16 compounds were synthesised which retain the 2,4-dichlorophenyl ARBG from the lead compound but contain varying STBGs. The inhibitory activity of these compounds against HDAC8 allows us to investigate the possibility of introducing an alternative STBG (Table 3.1) and also to identify different factors that are contributing to binding of the inhibitor with a view to maximising the beneficial factors and minimising the factors which are detrimental to binding.

Entropy is a measure of disorder in a system; the more disordered a system is, the greater the entropy (the more negative the value). In small molecules a major component of entropy is the number of conformations a molecule can exist in and corresponds to the number of rotatable bonds within the molecule. Rotatable bonds add to the degrees of freedom experienced by a molecule and so add to the conformational entropy of a molecule. These factors include introducing flexibility to and extending the length of the alkyl linker to the aromatic ring, introducing heteroatoms to the ring, and adding various functional groups to the STBG.

Equation 3.1 shows the relationship between binding energy ( $\Delta G_{binding}$ ), the binding

enthalpy ( $\Delta H_{binding}$ ) and the binding entropy ( $\Delta S_{binding}$ ) where  $T$  is the absolute temperature.  $\Delta S_{binding}$  is defined in Equation 3.2 where  $S_f$  and  $S_i$  are the final and initial entropy of the molecules. For  $\Delta G_{binding}$  to be maximised  $-T\Delta S_{binding}$  must be minimised (assuming minimal change in  $\Delta H_{binding}$  remains constant). This is achieved if  $S_i$  is minimised (as there is always a reduction in conformational entropy upon binding). Therefore a reduction in conformational entropy of a free ligand will result in an increase in binding energy (all other factors being constant).

$$\Delta G_{binding} = \Delta H_{binding} - T\Delta S_{binding} \quad (3.1)$$

$$\Delta S_{binding} = S_f - S_i \quad (3.2)$$

The STBG of  $\alpha$ -amino amide **55** was designed to explore the contribution of conformational entropy to the binding of  $\alpha$ -amino amide HDACi. Comparison of STBGs of **54** and **55** is shown in Figure 3.1. The STBG of  $\alpha$ -amino amide **54** contains an ethyl linker with two rotatable bonds, transformation of this linker into an aromatic ring gives  $\alpha$ -amino amide **55** creating a rigid planar carbazole system which results in a reduction in conformational entropy of the molecule.

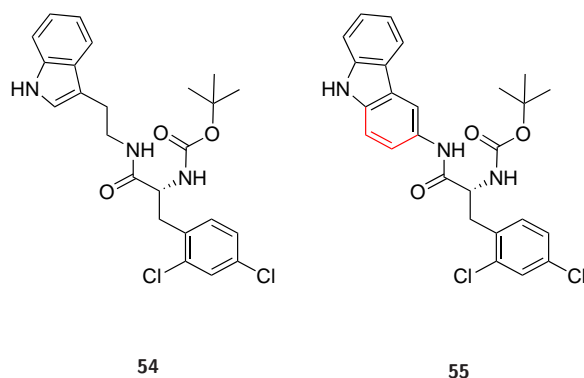
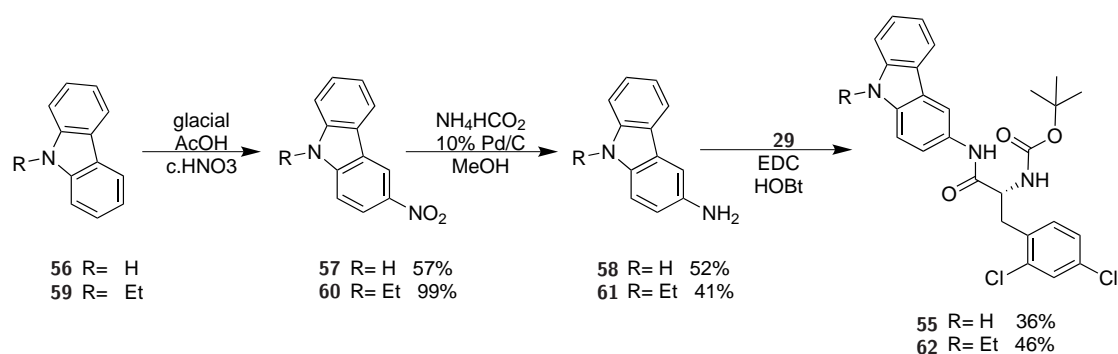


**Figure 3.1:** Comparison of the STBG of **54** and **55** with reduced conformational entropy through the addition of an aromatic ring.

## 3.2 2<sup>nd</sup> Generation $\alpha$ -amino amide inhibitor synthesis

### 3.2.1 Synthesis of carbazole-3-amines

Many of the amines coupled for the initial series of  $\alpha$ -amino amide HDAC8 inhibitors were commercially sourced. Carbazole-3-amines **58** and **61** are prohibitively expensive from commercial sources (up to \$540 /g). Both are easily synthesised in two steps from carbazoles **56** and **59** (Scheme 3.1) which are significantly cheaper (~\$1 /g). Nitration of 9-ethylcarbazole (**59**) was initially attempted as a test reaction and proceeded to give **60** with an impressive 99% yield. The analogous carbazole nitration to give **57** gave a lower yield at 57%. The subsequent reduction of **57** and **60** using ammonium formate proceeded with fairly low yields of 41% and 31% respectively. The literature describes an 80% yield for the reduction of **57** to **58** using hydrazine hydrate and a palladium catalyst<sup>209</sup>.



**Scheme 3.1:** Route taken for synthesis of  $\alpha$ -amino amides **55** and **62** via carbazole-3-amines.

### 3.2.2 Coupling and deprotection of 2<sup>nd</sup> generation inhibitors

A general trend was seen for the yield of the coupling where sterically unhindered amines (such as **63** and **83**) were coupled with a higher yield than aniline type

amines (such as **55** and **62**) that have reduced nucleophilicity because the nitrogen lone pair is delocalised into the aromatic system.

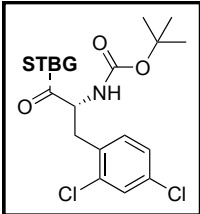
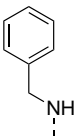
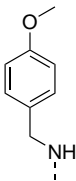
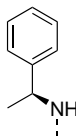
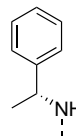
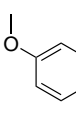
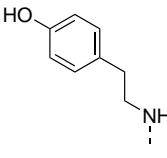
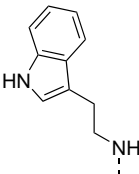
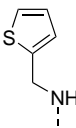
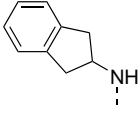
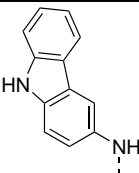
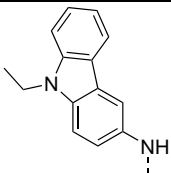
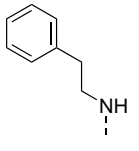
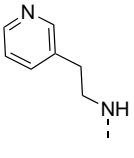
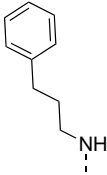
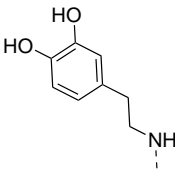
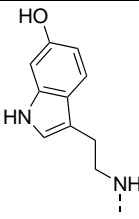
Many of the *N*-Boc- $\alpha$ -amino amides were not completely soluble in diethyl ether. A small volume of dry dichloromethane was therefore added until a complete solution was obtained before the introduction of hydrogen chloride gas. In some instances a larger amount of DCM was required (for example in the deprotection of **63** to give **68** and **67** to give **72** which required 30 mL of a 2:1 and 1:2 mixture of diethyl ether to DCM respectively). The additional DCM did not have an effect on the solubility of the resultant hydrochloride salts which remained insoluble in the diethyl ether/DCM mixture allowing filtration to proceed as before.

### 3.3 2<sup>nd</sup> Generation $\alpha$ -amino amide inhibitor assay results

To further probe the protein-ligand interactions within the substrate tunnel a number of  $\alpha$ -amino amide inhibitors were synthesised with the 2,4-dichlorophenyl ARBG but various, structurally diverse STBGs. A wide range of IC<sub>50</sub> values were measured which provide indications as to which types of groups and linkers are favoured over others within the substrate binding tunnel.

Overall, (1) linker length between the ZBG and aromatic group was varied from 0 to 3 methylene units, (2) linkers were rigidified, (3) aromatic groups were modified with *p*-methoxy and hydroxy groups and (4) a selection of heteroaromatic ring systems were tested (Table 3.2). In total 32  $\alpha$ -amino amide inhibitors were synthesised and tested for activity against HDAC8. Manual docking of inhibitors into an HDAC8 structure was performed to assess the rationale for altered potency compared to the lead compound **4**.

**Table 3.1:** Synthetic yields for  $\alpha$ -amino amide inhibitors varying in STBG only

						
STBG						
Coupling		96% <b>63</b>	71% <b>64</b>	51% <b>65</b>	94% <b>66</b>	58% <b>67</b>
Deprotect		73% <b>68</b>	55% <b>69</b>	92% <b>70</b>	63% <b>71</b>	63% <b>72</b>
STBG						
Coupling		74% <b>73</b>	77% <b>54</b>	82% <b>74</b>	54% <b>75</b>	74% <b>76</b>
Deprotect		>100% <b>77</b>	94% <b>78</b>	83% <b>79</b>	42% <b>80</b>	82% <b>81</b>
STBG						
Coupling		96% <b>82</b>	36% <b>55</b>	46% <b>62</b>	-	85% <b>83</b>
Deprotect		95% <b>84</b>	42% <b>85</b>	-	82% <b>95</b>	85% <b>86</b>
STBG						
Coupling		42% <b>87</b>	49% <b>88</b>	63% <b>89</b>	72% <b>90</b>	
Deprotect		>100% <b>91</b>	>100% <b>92</b>	95% <b>93</b>	79% <b>94</b>	

### 3.3.1 Inclusion of the ZBG

In order to test the importance of the  $\alpha$ -amino amide ZBG a compound was synthesised with a carboxylic acid in place of the amide (**95**). Compound **95** binds very poorly and has the highest  $IC_{50}$  of those tested ( $410 \pm 190 \mu\text{M}$ ) (Table 3.2). Compound **95** has no STBG, a carboxylic acid replaces the amide of the parent compound **4**, **95** therefore lacks the  $\alpha$ -amino amide ZBG. It is clear that the amide contributes a significant amount to the binding since compound **81** with the  $\alpha$ -amino amide ZBG and only a single methyl group occupying the substrate tunnel, has a greatly improved affinity,  $IC_{50} = 16.5 \pm 1.79 \mu\text{M}$ , and an increase in binding energy of  $\sim 2 \pm 0.47 \text{ kcal mol}^{-1}$  compared to **95** (Table 3.2). Both **95** and **81** have little or no extension into the substrate binding tunnel and demonstrate that contacts between the STBG and substrate tunnel are essential for tight binding of  $\alpha$ -amino amide inhibitors. Generally compounds which provide some interactions with the HDAC8 substrate tunnel have  $IC_{50} < 5 \mu\text{M}$  whereas those with obvious clashes or repulsive interactions have  $IC_{50} > 5 \mu\text{M}$ . This is in line with the generally accepted principle that increased contact surface area between two binding partners provides increased affinity as more interactions are able to be formed between the two partners<sup>210</sup>. All other compounds contain substrate tunnel binding groups with aromatic rings that occupy this tunnel and provide large hydrophobic surface area for interactions and (generally) have improved binding as a result.

### 3.3.2 Introducing flexibility into the STBG

Removal of one of the 5-membered ring methylene groups to leave a single methylene linker between the ZBG and aryl ring from **4** had an unexpectedly large effect on the binding of  $\alpha$ -amino amide inhibitor **68** (Figure 3.2). Manual docking suggests that the positioning of the STBG aromatic ring would be slightly shifted to one side (by  $1.1 \text{ \AA}$ ) but should otherwise function as the aromatic ring of **4** does, forming aromatic interactions with Phe152 and Phe208 (Figure 3.4a), Phe152 has been seen in different orientations in various structures (Figure 2.10a) and so should be able to move to accommodate the altered position of the aromatic ring.

At  $-7.62 \pm 0.28$  kcal mol<sup>-1</sup>, compound **68** with increased flexibility has a binding energy  $1.86 \pm 0.33$  kcal mol<sup>-1</sup> smaller than the lead compound **4** and IC<sub>50</sub> 20-fold higher (Table 3.2). This value corresponds to the entropy loss of approximately two rotors ( $0.6 - 1.0$  kcal mol<sup>-1</sup> per rotor<sup>211</sup>) which is what has been introduced by the removal of the 5-membered ring. As a ligand binds to a protein any rotatable bonds are fixed and the conformational entropy contained within them is lost. This manifests as a reduction in binding energy as demonstrated by Equation 3.3. The change in binding energy is therefore likely to be due to increased flexibility of the free **68** which possesses a one methylene linker with respect to **4** which has no flexibility in its rigid isoindoline group.

$$\Delta G_{binding} = \Delta H_{binding} - T\Delta S_{binding} \quad (3.3)$$

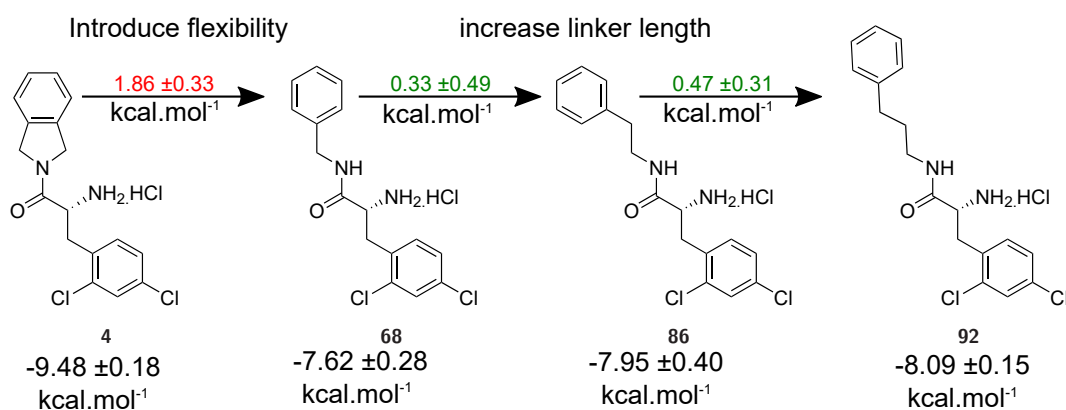


**Figure 3.2:**  $\Delta G_{binding}$  changes of  $\alpha$ -amino amide inhibitors with the introduction of flexibility and increasing length in the STBG, red values indicate reduction in binding energy and green values indicate gain in binding energy.

### 3.3.3 Addition of branched STBG

Branching in the N-amido substituent is deleterious to inhibitor binding. Two branched STBG-containing compounds (**70** and **71**) were synthesised which have IC<sub>50</sub> values of  $25.30 \pm 5.99$  and  $76.4 \pm 13.6$   $\mu$ M respectively (Table 3.2). The inclusion of a branched methyl group in the immediate vicinity of the  $\alpha$ -amino amide ZBG has a

great impact on binding by introducing steric clashes. The binding of inhibitors with these groups therefore requires an energetically unfavourable rearrangement of the hydrophobic substrate tunnel lining residues in order to be accommodated. Manual docking of **70** and **71** with the HDAC8-4 structure shows that steric clashes could be occurring with Tyr306 (for **70**, Figure 3.3a) and with His180 (for **71**, Figure 3.3b) of HDAC8. While the distances involved should allow these groups to be tolerated (2.5 Å in the case of **70** and 2.7 Å in the case of **71**), the large reduction in binding energy measured indicates that favourable interactions are being outweighed by unfavourable interactions or are being disrupted. It is possible that the presence of the methyl branching alters the positioning of the inhibitor in the pocket, distorting the Zn<sup>2+</sup> coordination geometry and also the STBG and ARBG positioning, thereby disrupting many favourable interactions, resulting in a reduced binding energy. As a result of this negative impact of a branched sidechain no further compounds were synthesised with branched sidechains.

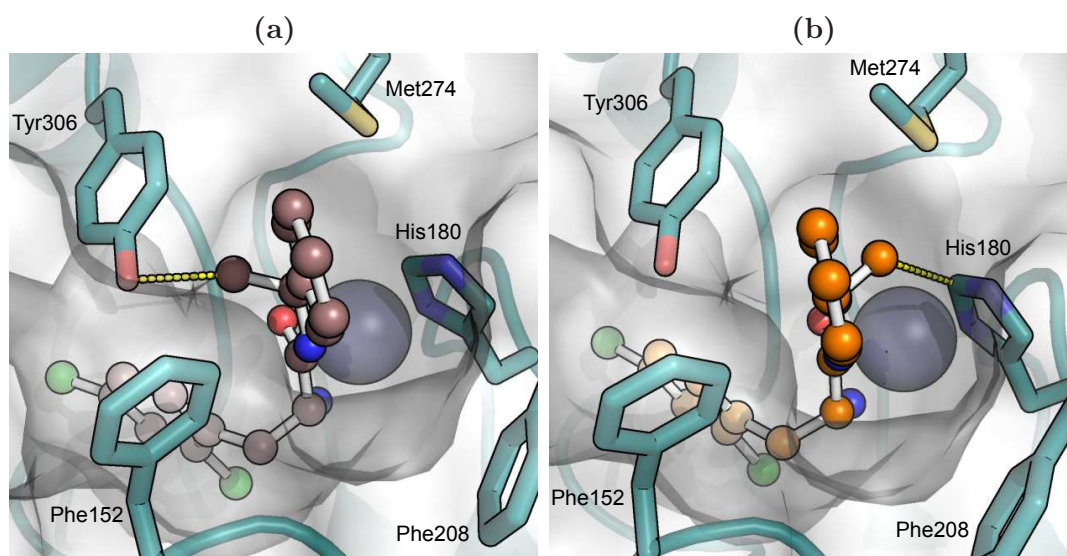
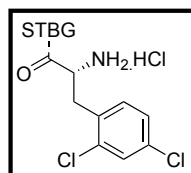


**Figure 3.3:** Manual docking poses of (a) **70**, and (b) **71** in the HDAC8 structure. Potential steric clashes are shown with dashed yellow lines.

**Table 3.2:** Inhibition assay results for second generation  $\alpha$ -amino amide HDAC8 inhibitors with varying STBG. Values are the mean of at least two independent repeats  $\pm$  standard deviation, ( $\Delta G_b = \Delta G_{binding}$ ).



	STBG	IC <sub>50</sub> / $\mu$ M	$\Delta G_b$ /kcal mol <sup>-1</sup>		STBG	IC <sub>50</sub> / $\mu$ M	$\Delta G_b$ /kcal mol <sup>-1</sup>
95		410 $\pm 190$	-4.81 $\pm 0.46$	81		16.5 $\pm 1.79$	-6.79 $\pm 0.11$
71		25.30 $\pm 5.99$	-6.53 $\pm 0.24$	70		76.4 $\pm 13.6$	-5.84 $\pm 0.18$
4		0.21 $\pm 0.04$	-9.48 $\pm 0.18$	72		2.67 $\pm 0.46$	-7.91 $\pm 0.17$
68		4.28 $\pm 1.22$	-7.62 $\pm 0.28$	69		16.6 $\pm 3.19$	-6.79 $\pm 0.19$
86		2.50 $\pm 0.99$	-7.95 $\pm 0.40$	77		1.25 $\pm 0.39$	-8.38 $\pm 0.31$
91		3.85 $\pm 0.92$	-7.69 $\pm 0.24$	93		2.07 $\pm 0.51$	-8.07 $\pm 0.25$
78		0.97 $\pm 0.34$	-8.53 $\pm 0.35$	92		2.01 $\pm 0.31$	-8.09 $\pm 0.15$
94		1.77 $\pm 0.47$	-8.16 $\pm 0.27$	85		10.5 $\pm 6.75$	-7.07 $\pm 0.64$
80		3.00 $\pm 0.76$	-7.84 $\pm 0.25$	84		8.76 $\pm 4.22$	-7.18 $\pm 0.48$

### 3.3.4 Increasing length of the STBG

Extension of the methylene linker of **68** to a two (**86**) or three methylene **92** chain (Figure 3.2) to allow more conformational flexibility slightly improves the binding affinity of the inhibitors by  $0.33 \pm 0.49$  and  $0.47 \pm 0.31$  kcal mol<sup>-1</sup> respectively (Table 3.2). These marginal improvements in binding energy suggest that the aromatic ring positioning can be improved by the greater conformational flexibility imparted by the additional rotatable bond, allowing more optimal interactions with Phe152 and Phe208, this is supported by manual docking of the inhibitors (Figures 3.4b & 3.5a). Inclusion of extra linker units increases the conformational entropy of the free inhibitor but is compensated for upon binding by the more favourable aromatic interactions.

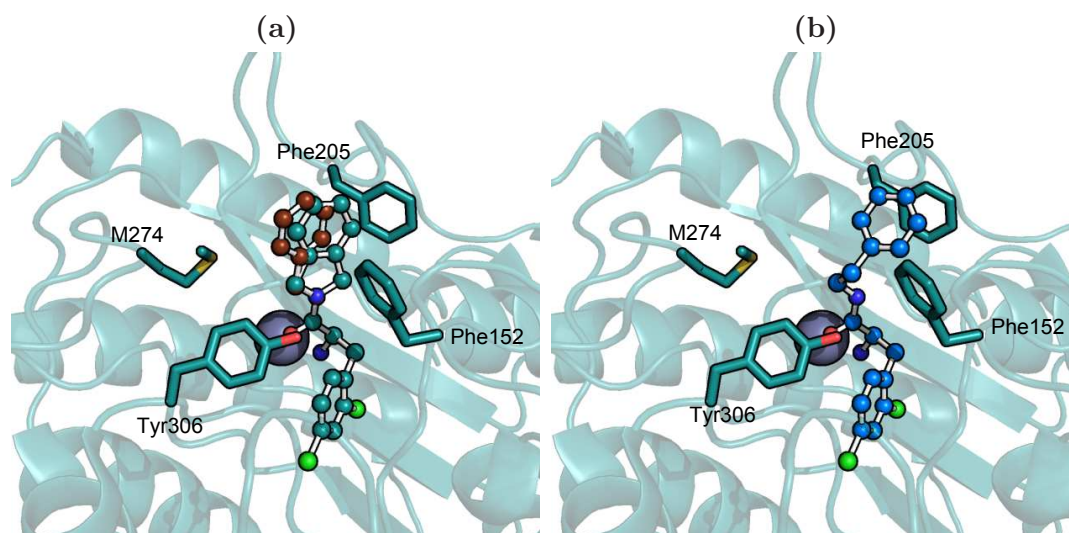


**Figure 3.4:** (a) Comparison of lead compound **4** (teal) and manual docking of **68** (brown), and (b) **86** (sky blue) manually docked into HDAC8 structure.

### 3.3.5 Introduction of hydrogen bond acceptors

A key interaction between Asp101 of HDAC8 and the peptide substrate was revealed in the crystal structure, Asp101 is conserved throughout class I and II HDACs and sits on the flexible L2 loop (which is often crystallographically unresolved) and

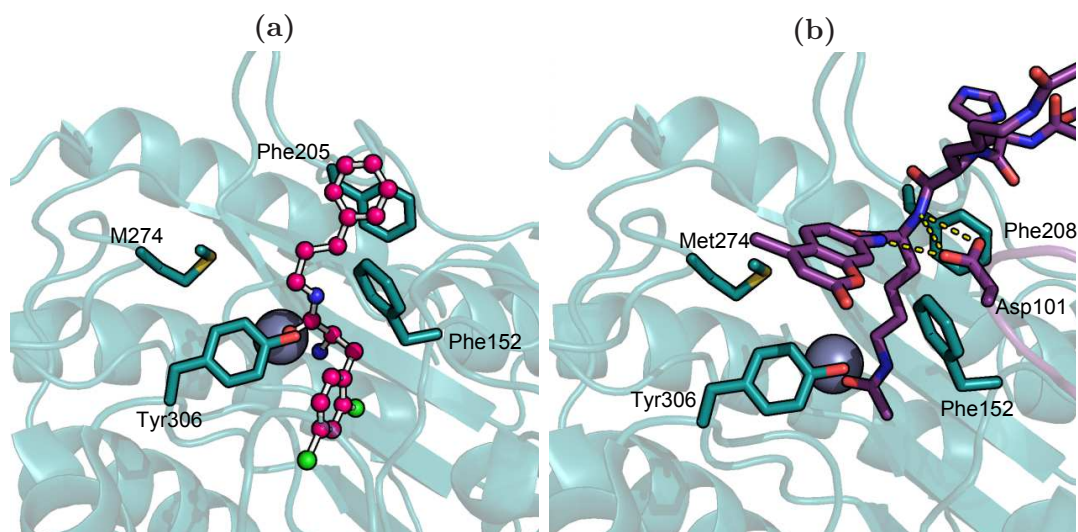


**Figure 3.5:** (a) Manual docking pose of **92** in HDAC8 and (b) HDAC8 structural overlay with *Fluor-de-Lys* substrate bound and interactions highlighted with Asp101 on the L2 loop (purple).

has been shown to be essential for substrate binding<sup>84</sup>. Asp101 facilitates substrate binding by acting as a clamp; upon association of the peptide ligand, the flexible loop can close and Asp101 forms hydrogen bonds with the backbone amide NH groups either side of the residue occupying the substrate tunnel (the acetylated lysine to be de-acetylated), this locks the peptide backbone of the substrate in a cis conformation (see Figure 3.5b), thereby reducing  $k_{off}$  and in turn  $K_i$  ( $K_i = k_{off}/k_{on}$ ). Asp101 and The L2 binding loop are unresolved in the 4-HDAC8 structure, this indicates that no interactions are occurring between the L2-loop and  $\alpha$ -amino amide inhibitor **4**. It was hypothesised therefore that introducing a hydrogen bond to Asp101 from the inhibitor would provide an improvement in affinity over inhibitors without a hydrogen bond to Asp101.

Introduction of hydrogen bond acceptors at the distal end of the STBG has a detrimental effect on the binding of the inhibitor. **69** with a *p*-methoxy group has  $IC_{50} = 16.6 \pm 3.19 \mu M$ , 5-fold higher than **68** with no methoxy group ( $IC_{50} = 4.28 \pm 0.18 \mu M$ ), this equates to a binding energy difference of  $0.83 \pm 0.34 \text{ kcal mol}^{-1}$  (Table 3.2). It is possible that this is due to a repulsion between the  $\delta^{-ve}$  *p*-methoxy oxygen and the negatively charged Asp101 as seen by manual docking (Figure 3.6a).

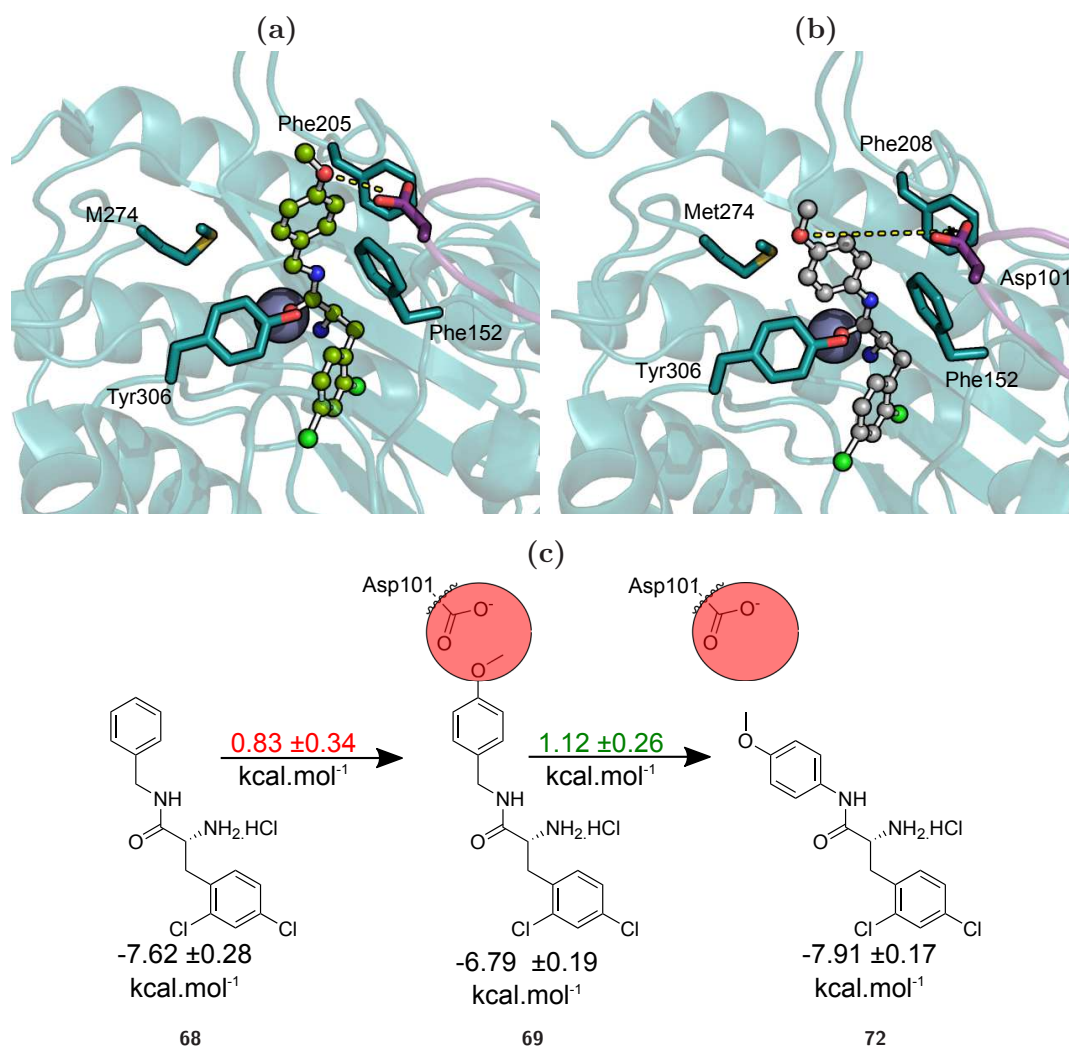


**Figure 3.6:** (a) Manual docking poses of **69**, (b) **72** in the HDAC8 structure. Flexible L2 loop and Asp101 (purple) are overlaid from substrate bound structure. (c) energy differences upon the addition of a hydrogen bond donor to Asp101, red values indicate loss in binding energy, green values indicate increase in binding energy. The red circles represent the distance over which Asp101 effects are seen.

Repulsion of the hydroxyl lone pair is supported by improved binding of **72** compared to **69**. Manual docking of **72**, a compound with a STBG which maintains the *p*-methoxy substitution but has a shortened linker was performed. In this docking the methoxy group is 7 Å from Asp101 (Figure 3.6b) such that the Asp101-*p*-methoxy

repulsion cannot take place. The binding energy of **72** is  $-7.91 \pm 0.17$  kcal mol<sup>-1</sup> which is  $1.12 \pm 0.26$  kcal mol<sup>-1</sup> better than that of **69** which has a repulsive Asp101-*p*-methoxy interaction (3.6c).

The *p*-hydroxyphenyl STBG containing **77** has two-fold lower IC<sub>50</sub> and average binding energy  $0.4 \pm 0.5$  kcal mol<sup>-1</sup> better than its phenyl counterpart **86** (Figure Table 3.2). The hydroxyl group could potentially contribute beneficial contacts to the protein-ligand interaction. Hydroxyl groups can be both hydrogen bond donors through their hydrogen, or acceptors through the lone pair on the oxygen. Manual docking of two possible poses of **77** into the HDAC8 structure reveals a possible interaction with Lys33 near the entrance to the substrate tunnel, which may contribute a hydrogen bond (Figure 3.7a), alternatively a hydrogen bond may be being donated to Asp101 (Figure 3.7b). An edge to face aromatic stacking interaction could form between the aromatic ring of the STBG and Phe152 if an interaction were to occur between the OH of **77** and Lys33 (Figure 3.7a). Lys33 is a dynamic residue, its C $\alpha$  has been seen to move by more than 0.5 nm when different inhibitors are bound to HDAC8<sup>92</sup>.

A second hydroxyl group was introduced to assess the effect a dihydroxylated aromatic ring would have on the cap group interactions (**93**). The binding energies of both mono- and dihydroxylated inhibitors (**77** and **93**) were well within the errors of each other and so the effect of the second hydroxy group is not measureable in this scenario (Table 3.2).

A heteroaromatic pyridine ring was tested as a cap group to see if this would alter binding at the entrance of the substrate tunnel (**91**). The pK<sub>a</sub> of the 4-methylpyridinium ion is 5.98<sup>212</sup> and so the pyridine nitrogen atom will be deprotonated at pH 8.0 (the pH of the fluorescent assay<sup>192</sup>). The IC<sub>50</sub> of **91** is  $3.85 \pm 0.92$   $\mu$ M corresponding to a binding energy of  $-7.59 \pm 0.24$  kcal mol<sup>-1</sup> which is very similar to that of the equivalent phenyl ringed inhibitor (**86**) so the introduction of the piperazine ring has little to no effect on the interactions of the aromatic ring.

Indole STBG containing **78** was also considerably potent of this second generation of  $\alpha$ -amino amide compounds exploring the variability STBG (IC<sub>50</sub> =  $0.97 \pm 0.34$   $\mu$ M,

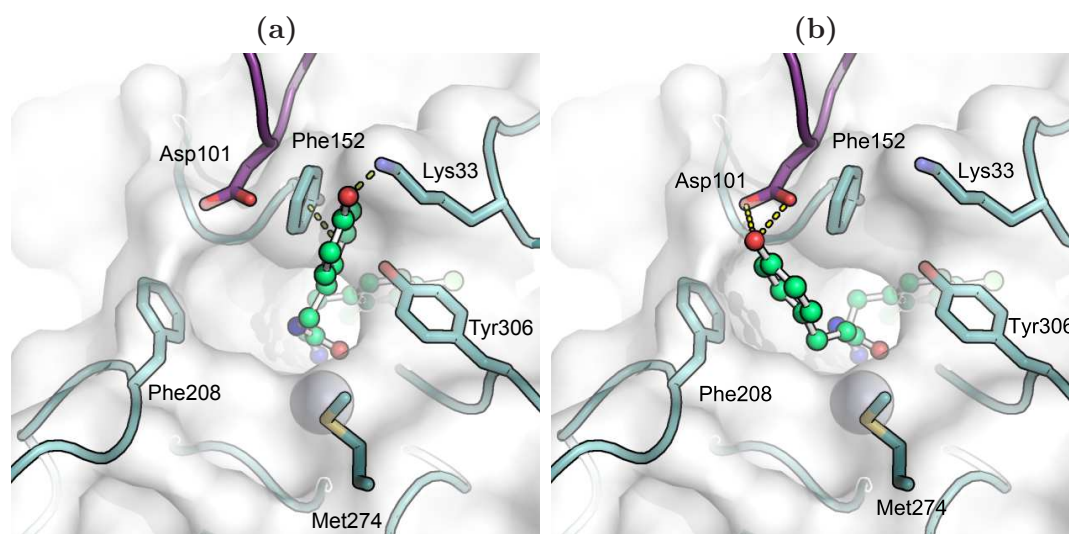


**Figure 3.7:** Two manually docked poses of **77** in HDAC8-4 structure (teal) that would allow for **77** to be (a) a hydrogen bond acceptor from Lys33 and form aromatic stacking with Phe152, and (b) a hydrogen-bond donor to Asp101.

binding energy =  $-8.53 \pm 0.35$  kcal mol<sup>-1</sup>, Table 3.2). Manual docking places the indole NH to provide a hydrogen bond to Asp101 (Figure 3.8a) in a similar manner as was seen for **77** above (Figure 3.7). This manual docking pose of a low energy conformation of **78** with its Asp101 interaction also positions the six-membered aromatic ring for an energetically favourable T-stacking interaction with Phe152. The suggestion that hydrogen bonding interactions to Asp101 could be promoting tight binding in two low IC<sub>50</sub>  $\alpha$ -amino amide inhibitors **78** and **77** suggested that the interaction could be exploited in the design of subsequent inhibitors. Addition of a hydroxyl group at the 5-position of the indole group of **78** to give **94** had little to no effect on the binding energy of **94** compared to **78** ( $-8.16 \pm 0.27$  kcal mol<sup>-1</sup> vs.  $-8.53 \pm 0.35$  kcal mol<sup>-1</sup>, Table Table 3.2).

The carbazole inhibitor **85** (Figure 3.8b) was designed with previous observations on conformational flexibility and hydrogen bonding with Asp101 in mind. A loss in binding energy of  $1.86 \pm 0.33$  kcal mol<sup>-1</sup> was observed by replacement of the rigid 5-membered ring with a methylene linker (**4**→**68**). This was attributed in the most part to increased conformational flexibility of the unbound inhibitor **68**. Compounds **78**, **77**, **93** have methylene linkers with three rotatable bonds, but with improved

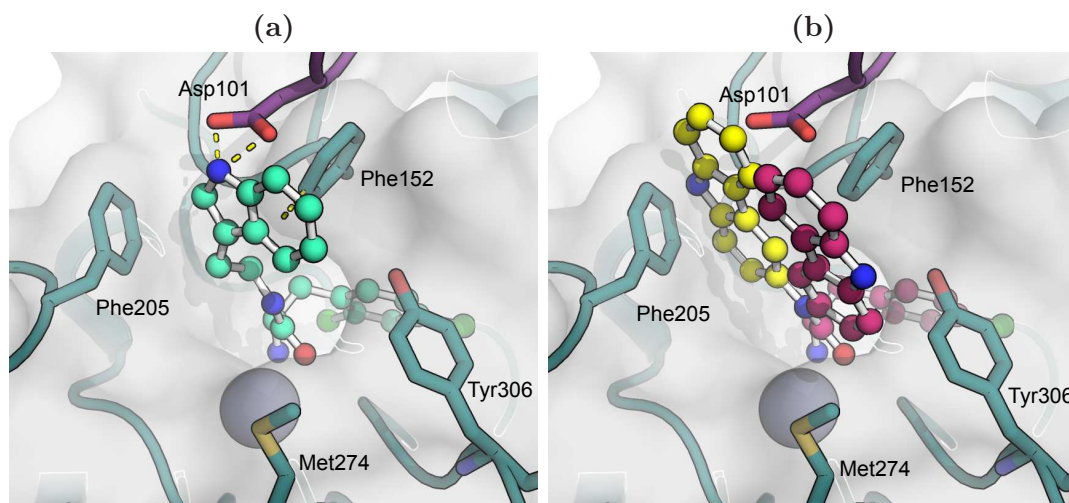


**Figure 3.8:** Manual docking poses of (a) Indole **78** and (b) carbazole **85** in two amide conformations, cis- (yellow) and trans- (magenta) the HDAC8-4 structure (teal). Flexible L2 loop and H-bond-donating Asp101 shown are overlaid from the HDAC8-*Fluor-de-Lys* structure (purple).

binding energy over **86** due to hydrogen bonding with Asp101. This suggests that the hydrogen bonding contribution is greater than the energy loss due to conformational flexibility. In order to lower the conformational flexibility of **78** the methylene linker was replaced with a rigid aromatic ring. It is known that the substrate tunnel can accommodate bulky aromatic rings close to the ZBG<sup>90</sup> as seen in Figure 2.10a.

Manual docking of carbazole **85** into the HDAC8 structure reveals the reduction in conformational flexibility actually restricts the positioning of the hydrogen bond donating nitrogen to being  $>5.0$  Å from the Asp101 acceptor (magenta in Figure 3.8b). The less energetically favourable cis-amide (yellow in Figure 3.8b) allows the carbazole nitrogen to approach 3.4 Å from Asp101, all poses of the cis-amide cause steric clashes with Phe208. The lowering of entropy was therefore cancelled out by the clashes introduced and the loss of hydrogen bonding with Asp101. The result is a significant reduction in potency ( $IC_{50} = 10.5 \pm 6.75$  μM) and in binding energy ( $1.46 \pm 0.72$  kcal mol<sup>-1</sup>), compared to indole **78**.

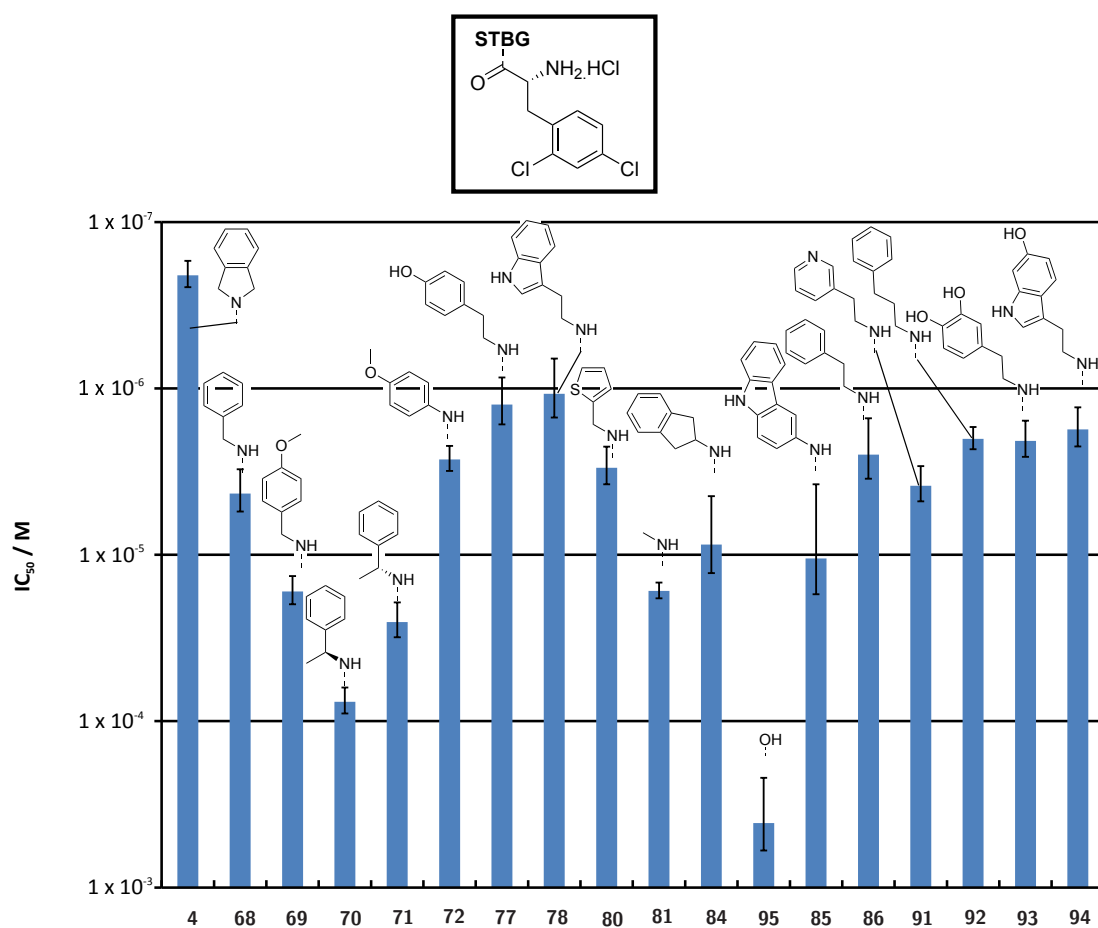


**Figure 3.9:**  $IC_{50}$  values of 2nd generation inhibitors with varying STBG, error bars are SD of >2 independent repeats. corresponding R-groups are shown above the bars.

### 3.4 Summary of 2<sup>nd</sup> generation inhibitor assay results

Second generation  $\alpha$ -amino amide compounds were designed to explore the possible groups which could occupy the substrate binding tunnel and be a good analogue for the isoindoline STBG of the lead compound **4**. Comparison of binding energies and manual docking of compounds into HDAC8 structures shows that rigidity of the STBG is essential for good binding. **4** with an isoindoline STBG remains the most potent compound ( $IC_{50} = 210 \pm 40$  nM). It appears that interactions with residues in flexible loops on the exterior of the enzyme may be important in providing extra binding contacts and therefore improved binding properties. The most potent compounds (**78** and **77**) of this generation have low energy poses that can be manually docked into the structure of the enzyme such that a hydrogen bond can form with Asp101 of HDAC8 and still form favourable aromatic stacking. The presence of hydrogen bonding between substrate and Asp101 is essential for substrate binding<sup>84</sup> and this data was subsequently used to design the 3<sup>rd</sup> generation of  $\alpha$ -amino amide inhibitors through the inclusion of a hydrogen bonding group to the lead compound **4** in an appropriate position to make this contact.



# 4 3<sup>rd</sup> generation $\alpha$ -amino amide HDAC8 inhibitors - containing isoindoline based STBG

## 4.1 Introduction

Inhibition data of the 1<sup>st</sup> and 2<sup>nd</sup> generation of  $\alpha$ -amino amide HDAC8 inhibitors were modest (see Section 2.3 & 3.3). No increase in potency was achieved with alternative ARBG or STBG and all compounds had IC<sub>50</sub> values around 10 times that of the lead compound **4** (Lit<sup>147</sup>. 90 nM). All variations of the STBG or ARBG were shown to have a detrimental effect on the binding interactions of the  $\alpha$ -amino amide inhibitors synthesised with their novel ZBG. Through manual docking simulations reasoning behind the the different degrees of inhibition of compounds with differing STBG and ARBG was reached.

The failiure to improve upon the lead compound **4** by replacement of the ARBG or STBG lead to the conclusion that existing inhibitor-protein binding interactions cannot be strengthened by the alteration of the **4** core structure, therefore in order to increase potency, new interactions must be introduced through addition to the core structure. Analysis of the HDAC8-**4** structure reveals that there is limited space inside the protein in which to add inhibitor substituents without causing steric clash with the protein (see Section 3.3.3). The remaining region that can be added to must therefore be the 5 and 6 positions on the isoindoline ring which are solvent exposed.

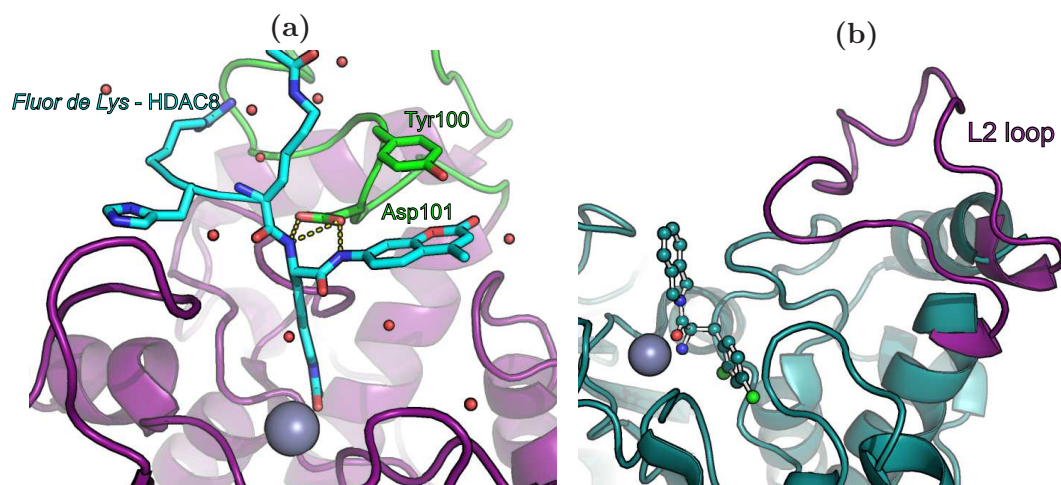


**Figure 4.1:** (a) Interactions between HDAC8 and *Fluor-de-Lys* seen from the structure<sup>84</sup>. Hydrogen bonding interactions between Asp101 on the flexible L2 loop (green) and peptide backbone of the *Fluor-de-Lys* substrate (cyan) and aromatic stacking of Tyr100 and the AMC fluorophore (b) The HDAC-4 structure (teal) with missing L2 loop from *Fluor-de-Lys* bound structure superimposed (purple).

Figure 4.1a shows the structure of HDAC8 in complex with the *Fluor-de-Lys* (**2**) substrate (PDB: 2V5W), hydrogen bonding interactions can be seen between Asp101 which resides on the flexible L2 loop and amide groups of the peptide backbone within the substrate. Asp101 is known to be an essential residue for substrate binding, mutants at this position have been measured to have three times slower  $k_{on}$  and 36 times faster  $k_{off}$  as measured by surface plasmon resonance<sup>84</sup>. The same hydrogen bonding interactions were also seen in crystal structures of HDAC8 in complex with **96**, a hydroxamate inhibitor (PDB:2V5X)<sup>84</sup>.

In the structure of HDAC8 in complex with **4** (teal in Figure 4.1b) the L2 loop is unresolved<sup>147</sup>, this indicates that the L2 loop is very flexible and has no defined regular packing in the crystal and points towards Asp101 being flexible and not involved in binding of **4** to HDAC8. It follows that if natural substrate-like interactions could be incorporated into **4**, perhaps by the introduction of hydrogen bond donor groups, that substrate mimicking L2-ligand binding interactions could be established and binding characteristics of the inhibitor improved as a result.

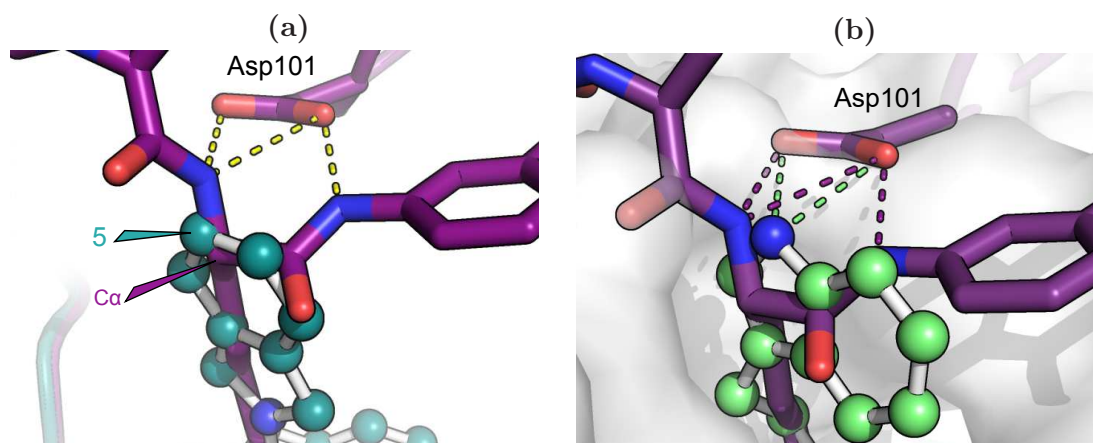


**Figure 4.2:** The crystal structure of *Fluor-de-Lys* substrate (purple) overlaid with (a) HDAC8-4 crystal structure and (b) manual docking pose of **78**, potential hydrogen bonds are displayed with dashed lines

Exploration of different STBGs highlighted the possible importance of creating a hydrogen bond between the inhibitor and Asp101 for improving binding (Section 3.3.5). In particular compound **78** was one of the highest binding novel inhibitor, manual docking of **78** into the substrate bound crystal structure allows the indole nitrogen to be positioned so as to create a hydrogen bond with Asp101, this hydrogen bonding interaction may be the reason that **78** is relatively good inhibitor compared to others synthesised with different STBGs. Despite the improvement in binding offered by the introduction of this hydrogen bond, even the most potent inhibitors synthesised with a non-isindolyl STBG (**77** and **78**) had binding energies  $\sim 1$  kcal mol<sup>-1</sup> smaller than the lead compound **4**, indicating that isindoline is the optimal STBG for  $\alpha$ -amino amide HDAC8 inhibitors, probably due to its linearity, planarity and rigidity. To improve binding of isindoline based  $\alpha$ -amino amide inhibitors, a series of inhibitors was designed and synthesised to introduce an interaction between the STBG and Asp101, essentially introducing a cap-group interaction (discussed in Section 1.4.2).

The subsequent round of  $\alpha$ -amino amide inhibitors was designed following a close inspection of the HDAC8-substrate and HDAC8-4 structures. When these two structures are aligned the C $\alpha$  of the acetylated lysine substrate lies very close ( $\sim 0.5$  Å) from the 5-position of the isindoline ring of **4** (Figure 4.2). Importantly the C $\alpha$ -N

bond orientation is approximately in plane with the aromatic ring of **4**, therefore a hydrogen bond donor at the 5-position of the aromatic ring would be in a similar position to the amide NH and so be available to provide hydrogen bonds to Asp101 in a similar manner to the substrate. Given the known flexibility of Asp101, the introduction of a hydrogen bonding interaction at the isoindoline 5-position should be well tolerated and so improve upon the binding energy of **4**. Previous reports have described the introduction of hydrogen bond donors into inhibitors in this region of the inhibitor resulting in improved binding characteristics and retaining HDAC8 selectivity<sup>213</sup>.

## 4.2 Synthesis of 3<sup>rd</sup> generation $\alpha$ -amino amide inhibitors

Compounds were envisaged with groups to provide even more “substrate-like” interactions; **98** & **99** with one amide group and **100** with two amide groups (all seen in Figure 4.3). It was hoped that these compounds would have improved binding over **4** and yet would retain the selectivity of **4**.

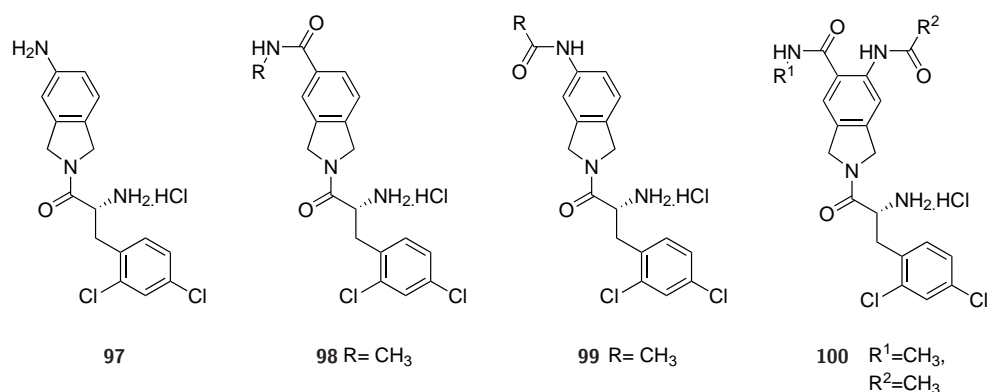


**Figure 4.3:** Structures of the mono (**97**, **98** & **99**) and disubstituted (**100**) that were designed to add “substrate-like” interactions with Asp101 on the L2 loop of HDAC8.

Establishment of synthetic routes to **97**, **98**, **99** and **100** would allow R-groups to be added which could further extend the additional binding interactions e.g. by

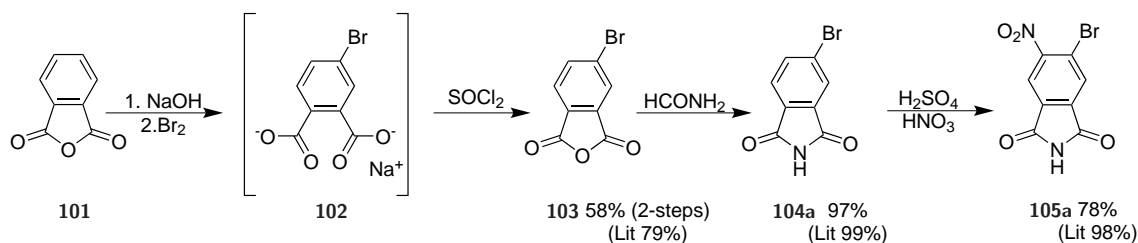


intermediate, a series of structurally diverse substituted isoindoline based  $\alpha$ -amino amide inhibitors can be synthesised.

### 4.2.1 Isoindolines from reduction of phthalimides

#### Synthesis of substituted phthalimides

The first four steps of the proposed route to generate disubstituted isoindolines requires the generation of a disubstituted phthalimide **105a** (Scheme 4.2) and are reported as a sequence from phthalic anhydride (**101**) in a patent with good yields at each step ( $>70\%$ )<sup>218</sup>. At this early stage however, the literature yields could not be obtained, over the combined steps from **101** to **103** 58% was achieved compared to the literature's 79%. Anhydride **103** underwent nucleophilic attack with ring opening and ring closing to give **104a** with 97% yield (Lit.<sup>218</sup> 99%) and the subsequent nitration with 78% yield (Lit.<sup>218</sup> 98%). As a result the combined yield over 4 steps to produce **105a** was 39% compared to 77% in the literature<sup>218</sup>. This is a large loss in yield but as the starting material is inexpensive it is not prohibitively low multigram scale production of these early intermediates is possible (5 - 10 g). This however, is dependent on relatively good yields being obtained in later steps.



**Scheme 4.2:** Route to generate 5,6-disubstituted phthalimide **105a** as described in the literature.<sup>218</sup>

#### Reduction of phthalimides

Reduction of the phthalimide carbonyl groups to generate isoindoline has been reported using electrolytic reduction<sup>219</sup> as well as many reducing agents: originally

in 1948 with  $\text{LiAlH}_4$ <sup>214</sup>, more recently with borane-THF<sup>215,220</sup> and  $\text{NaBH}_4$  and  $\text{BF}_3 \cdot \text{Et}_2\text{O}$ <sup>221</sup>.

#### *Reduction of 4-bromophthalimide*

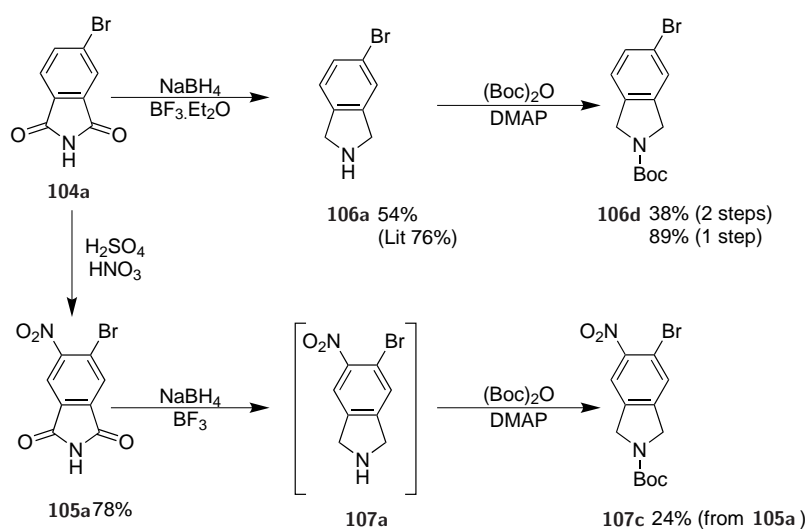
Bromophthalimide **104a** has previously been reduced in the literature using  $\text{NaBH}_4$  and  $\text{BF}_3 \cdot \text{Et}_2\text{O}$  with 76% yield<sup>221</sup> (Scheme 4.3). A lower yield of 54% was achieved on the first attempt but no product was obtained on subsequent attempts. The literature procedure describes a lengthy workup: alkaline extraction into  $\text{EtOAc}$ , drying and concentration of the organic layer, dilution in ether, acidification and extraction into the aqueous layer, basification of the aqueous layer and a second alkaline extraction before drying and evaporating. As it is known that isoindolines undergo aerial *N*-oxidation it is possible that the reduced isoindoline **106a** is degrading during the workup before it can be isolated with decent yield. In order to reduce the length of time in which degradation of the product could occur, a procedure with a shortened workup was attempted. The shortened workup consists of an alkaline extraction, a wash with brine, drying over  $\text{Na}_2\text{SO}_4$  and evaporation which did yield some crude product to take on to the next step.

The subsequent *N*-Boc protection of **106a** to **106d** is reported with 89% yield<sup>221</sup>. To minimise the degradation of isoindoline **106a** it was decided to take the product from the shortened workup and take it forward to be *N*-Boc protected without additional purification. The *N*-Boc protected product **106d** is easily purified by column chromatography resulting in a 38% overall yield from **104a**.

#### *Reduction of disubstituted phthalimides*

Following the low-yielding but successful 4-step synthesis of the disubstituted phthalimide **105a**, the reduction to give its corresponding isoindoline **107a** was pursued. The procedure used for the disubstituted phthalimide reduction (**105a** to **107a**) was the same as that used for the monosubstituted analogue (**104a** to **106a**).

When applying the  $\text{NaBH}_4/\text{BF}_3 \cdot \text{Et}_2\text{O}$  reduction procedure to the disubstituted phthalimide **105a** (Scheme 4.3), the isolation of disubstituted isoindoline **107a** proved



**Scheme 4.3:** Route to *N*-Boc protected mono- and disubstituted isoindolines

more difficult than that of monosubstituted **106a**. In addition to the rapid degradation of the product upon exposure to air it was also difficult to purify by column chromatography owing to its poor solubility. Application of the above procedure with shortened workup and direct *N*-Boc protection to **105a** gave a yet lower yield of 24% (compared to 38% for **106d**). A total 9% yield was obtained over the initial 6 steps from the starting phthalic anhydride **101** to give **107c**. This yield is not sufficient to permit the use of this route to generate sufficient amounts of the late stage intermediate **107c** which must undergo a further 6 steps in order to reach the target  $\alpha$ -amino amide salt **100**.

Many factors could be causing the low yield in the reduction of nitrophthalimide **105a** to **107a** such as a reduction in solubility of nitrophthalimide **105a** compared to unnitrated phthalimide **104a** and also the solubility of any reaction intermediates. Alternatively the presence of the electron withdrawing nitro group could be making the carbonyl bonds more polar and therefore making the reaction proceed faster than the un-nitrated analogue **104a** thereby exposing the isoindolyl product **107a** vulnerable to degradation for longer before the reaction was worked up. Conversely, nitro groups are highly polar and may be coordinating with the reducing agents, interfering with them to result in a slower, or even disrupted reduction. After the addition of  $\text{BF}_3 \cdot \text{Et}_2\text{O}$  to the reaction mixture, the disubstituted phthalimide **105a**

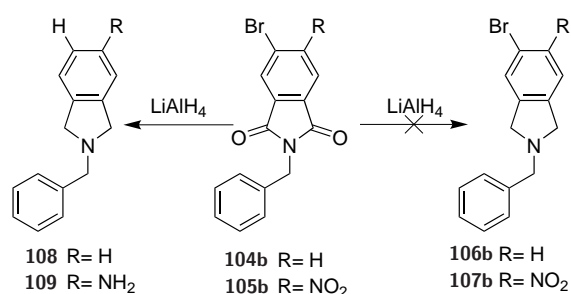
was seen to be completely consumed by TLC, therefore the reaction may be being halted at an intermediate stage.

Attempts were made to optimise the reaction by using increased volumes of solvents and varying the number of equivalents of NaBH<sub>4</sub> and BF<sub>3</sub>.Et<sub>2</sub>O. Due to the fast degradation of the product **107a**, it was very difficult to tell if the reduction yield was improved or not. Subsequent *N*-Boc protection and purification resulted in no increase of final stable product **107c**.

An alternative route to obtain **107c** was considered by nitration of the isoindoline **106d** after the reduction and protection of bromophthalimide **104a**, this is not an option however as the acidic conditions used during nitration would cleave the *N*-Boc protecting group and to give the unstable isoindoline **107a**.

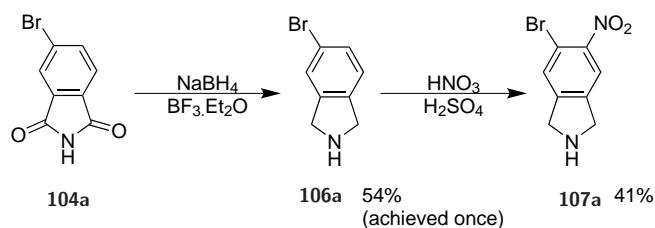
New reagents for the reduction of disubstituted phthalimide **105a** were considered. Diborane is the species that reduces the carbonyl groups in this reaction; reduction of phthalimide with borane THF has been reported to give isoindoline with good yield (78%)<sup>215</sup>, the purpose of BF<sub>3</sub>.Et<sub>2</sub>O in the reaction is to react with NaBH<sub>4</sub> generating diborane in situ, this avoids the use of what may be a deteriorated commercial sample of borane-THF (where titration for activity has not been carried out). I<sub>2</sub>, another commonly used co-reagent in the generation of diborane in situ<sup>222</sup> was tried in place of BF<sub>3</sub>.Et<sub>2</sub>O but resulted in no increase in yield. Neumeyer first observed in 1964, reduction of an *N*-(benzyl)-phthalimide is possible using LiAlH<sub>4</sub><sup>223</sup>. Using LiAlH<sub>4</sub> might also prove useful by reducing the nitro group to an amine group thereby removing the need to perform that transformation at a later stage and thereby reduce the electron withdrawing effects of the nitro group to the reduction of **105a**.

LiAlH<sub>4</sub> reduction of an *N*-benzyl protected phthalimide **104b** to *N*-benzylisoindoline **106b** is not applicable in this situation however. LiAlH<sub>4</sub> reduction was attempted on both a monosubstituted *N*-benzylphthalimide **104b** and disubstituted *N*-benzylphthalimide **105b** (Scheme 4.4). Both isoindolyl-products had an additional aromatic proton by NMR spectroscopy and so were judged to have lost their bromine substituent, this was further confirmed by mass spectrometry.



**Scheme 4.4:** Failed reduction of bromophthalimides to the analogous isoindolines using LiAlH<sub>4</sub> due to the loss of the bromine substituent.

Alternative routes were explored to reach **107a** including nitration after the reduction of the imide **104a** (Scheme 4.5) this nitration however resulted in a 41% yield and the product was difficult to handle being only sparingly soluble in MeOH and degrading rapidly.



**Scheme 4.5:** Alternative route to **107a** by nitration of **106a**.

Other alternative routes to obtain a protected substituted isoindoline were devised in order to avoid generating air sensitive unprotected isoindolines such as **106a** and **107a**. The addition of an *N*-protecting group both improves solubility and also the stability of the product by removing the possibility for the aerial oxidation of the isoindolyl product.

The introduction of an *N*-Boc group before the reduction is not feasible for this route as the Boc carbonyl bond would be reduced along with the imide when generating the isoindoline. As discussed above, *N*-benzylphthalimides undergo reduction to generate *N*-benzylisoindolines. Also *N*-benzylisoindolines have been reported to undergo debenylation to isoindolines using hydrogen and Pd/C catalysts<sup>224</sup>. The benzyl group was therefore chosen to be the phthalimide protecting group.

A hybridised method was decided on using the previously tested NaBH<sub>4</sub> / BF<sub>3</sub>·Et<sub>2</sub>O reduction conditions and 4,5-substituted *N*-benzylphthalimides as starting materials to give 5,6-substituted *N*-benzylisoindolines (numbering changes are a result of isoindoline numbering convention).

## 4.2.2 Isoindolines from reduction of *N*-benzylphthalimides

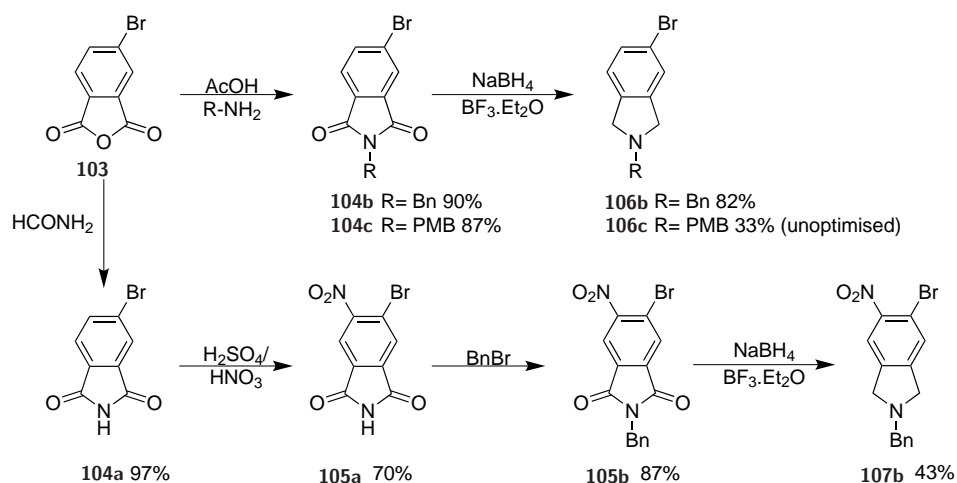
### Synthesis of *N*-benzylphthalimides

Scheme 4.6 shows the route to mono and disubstituted *N*-benzylphthalimides **104b** and **105b**. The initial steps to generate bromophthalic anhydride **103** are shared with the previously described route (Scheme 4.2). The *N*-benzylation of disubstituted phthalimide **105a** proceeds with a good yield of 70% (Lit.<sup>218</sup> 90%). Synthesis of *N*-protected bromophthalimides **104b** and **104c** were achieved directly from bromophthalic anhydride **103** in a single step by heating at reflux in acetic acid with the desired benzylamine. Both *N*-benzyl and *N*-(4-methoxybenzyl) protected bromophthalimides were achieved with very good yields (90% and 87% respectively).

Synthesis of disubstituted *N*-benzylphthalimide requires of two extra steps (discussed in Section 4.2.1), **103** → **104a** → **105a** followed by benzylation to **105b** (Scheme 4.6) these additional steps result in a 60% loss in yield compared to the monosubstituted *N*-benzylphthalimide.

### Reduction of *N*-benzylphthalimides

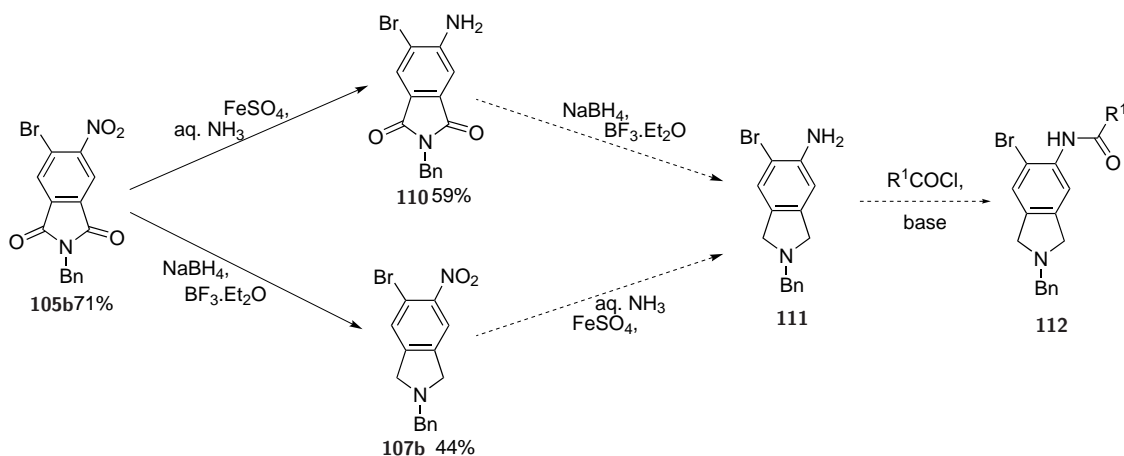
Both mono and disubstituted phthalimides **104b** and **105b** were successfully reduced to their respective isoindolines **106b** and **107b** using NaBH<sub>4</sub> and BF<sub>3</sub>·Et<sub>2</sub>O in THF. The yield for the reduction of the disubstituted benzyl-phthalimide **105b** to **107b** (43%) was nearly half that of the monosubstituted *N*-(benzyl)-phthalimide to **106b** (82%). This loss of yield proves that the nitro group is certainly having a dramatic effect on the reduction of the phthalimide, which was not possible to



**Scheme 4.6:** Route for the synthesis of mono and disubstituted *N*-benzylisoindolines.

quantify previously due to the difficulties experienced in isolating the insolindoline products (Section 4.2.1).

If the solubility of the nitro group was the cause of the poor yield when the phthalimide reduction was attempted, it follows that improving the solubility of **105b** by reduction of the nitro group to a more soluble amine (to give **110** prior to its reduction to **111**) may improve the yield over these steps (Scheme 4.7).

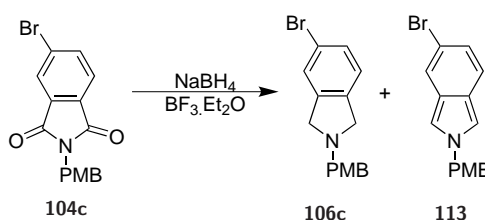


**Scheme 4.7:** Alternative routes to achieve bromo-amidoisoindolines with reduction of nitro group prior to carbonyl reduction.

Reduction of the bromonitrophthalimide **105b** proceeded with a 59% yield and the

subsequent reduction was not explored. The extra steps required to make disubstituted phthalimide **105b** mean that pursuit of optimal reducing conditions to obtain **107b** were postponed in favour of successfully synthesising and refining the route to mono-substituted isoindolines **98** and **99** (Figure 4.3).

The reduction of monosubstituted *N*-benzylphthalimide **104b** to **106b** was successful with respectable yields (43% over 4 steps from phthalic anhydride **101** to **106b**). The alternative cyclocondensation route to isoindoline ring formation was also attempted for comparison purposes (discussed in Section 4.2.3).



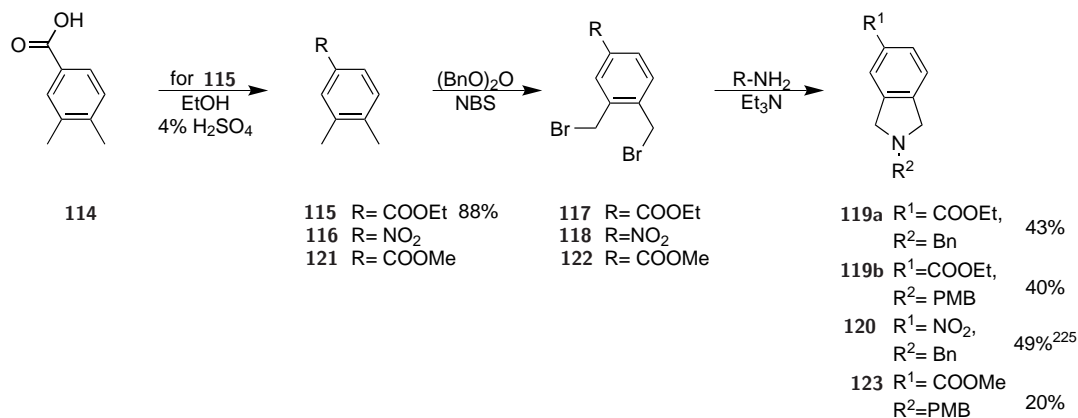
**Scheme 4.8:** 10- $\pi$  intermediate generated during reduction of phthalimide **104b**.

During purification of *N*-(4-methoxybenzyl)-isoindoline **106b** a 10  $\pi$  electron aromatic system was isolated. Column chromatography purification led to the isolation of an interesting, isoindole intermediate (**113**). Aromaticity of a molecule is a property that leads to unusually stable ring systems. Hückel's rules define aromatic ringed systems and require atoms to be arranged in one or more planar rings with a delocalised  $\pi$  electron system throughout and a number of  $\pi$  electrons  $4n+2$  where  $n$  is an integer. If these requirements are satisfied the molecule is aromatic. The isoindole **113** has a lone pair on the nitrogen that is able to contribute to the delocalised  $\pi$  electron system so the number of  $\pi$  electrons is 10 ( $4 \times$  double bonds +  $1 \times$  lone pair). It is therefore a non-benzenoid system but is still aromatic.

### 4.2.3 Isoindolines from cyclocondensation of *o*-xylenes

To determine the most efficient method for synthesis of monosubstituted isoindoline systems an alternate *o*-xylene cyclocondensation route was tested. Monosubstituted nitro (**120**) and ethylcarboxylate (**119a**) isoindoline systems were synthesised using

the ring-closure route seen in Scheme 4.9. As before, the aromatic substitutions were present before the formation of the isoindoline ring system.



**Scheme 4.9:** Synthesis of *N*-benzylisoindolines via ring-closure of a bis-bromo-*o*-xylene

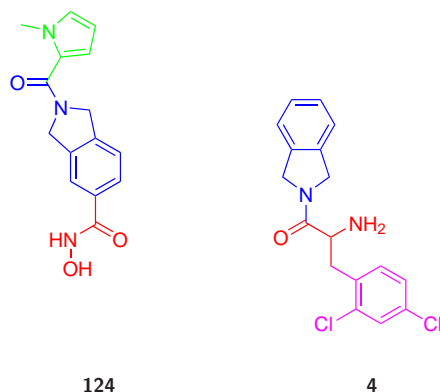


**Figure 4.4:** An isoindoline based HDAC6 inhibitor **124**<sup>225</sup> and **4**<sup>147</sup>. Green = cap-group, blue=STBG, red = ZBG, magenta = ARBG

HDAC inhibitors have previously been reported containing isoindoline ring systems generated via the ring-closure of bis-bromo-*o*-xylene methyl ester **122** which was then taken forward to generate **124**<sup>225</sup> (Figure 4.4). The isoindoline containing HDAC6 inhibitor utilises a more traditional hydroxamate ZBG that is located at the 5-position of the isoindoline ring system<sup>225</sup>, as a result the isoindoline ring system is inverted in the substrate tunnel with respect to the lead compound **4** which has an  $\alpha$ -amino amide ZBG at the 2-position. This compound inhibits HDAC6 only and has undetectable inhibition for all other class II and class I HDACs *except* HDAC8, ( $IC_{50} = 1.3 \mu\text{M}$  for HDAC8,  $IC_{50} = 0.040 \mu\text{M}$  for HDAC6) but  $IC_{50} > 50 \mu\text{M}$

against all other HDACs<sup>225</sup>. The inhibition of HDAC8 by this isoindoline containing inhibitor supports the observations that the tunnel of HDAC8 is more conformationally flexible than the substrate tunnel of other class I HDACs (HDAC1, HDAC2 and HDAC3); it also suggests that positioning of the bulky isoindoline group deep within the substrate tunnel near to the zinc binding group is possible (and possibly preferable) as it seems also to help to impart specificity of an inhibitor to HDAC8 over the other class I HDACs.

The isoindoline system contained within the HDAC6 selective inhibitor was synthesised from xylyl-methyl ester **121** (Scheme 4.9)<sup>225</sup>. Literature describes the bromination of **121** for 1.5 hours using NBS with benzoyl peroxide as a radical initiator in carbon tetrachloride at reflux. The bis-bromo intermediate **122** was obtained after filtration of the cooled mixture and dissolved in THF without purification. After treatment with triethylamine, 4-methoxybenzylamine was slowly added, generating the ring through a cyclocondensation step to give **123** with a yield of 49% (2 steps)<sup>225</sup>. The same procedure, applied to the ethyl ester **115** (synthesised through esterification of *o*-xylene-4-carboxylic acid **114**) was applied in the synthesis of isoindolines of the type **119**, slightly lower than literature yields of 40% and 43% were achieved for the *N*-benzyl (**106b**) and *N*-(4-methoxybenzyl) (**106c**) ethyl ester analogues respectively.

NMR spectroscopy of bis-brominated intermediate **117** revealed that 36% starting reactant **115** remained unbrominated, this material was therefore unavailable to participate in the subsequent cyclo-condensation step; increased yield may be possible if the bromination step was more efficient. Use of a fresher or alternative (i.e. azobisisobutyronitrile) radical initiator may also improve the efficiency of bromination as the benzoyl peroxide used was old.

Patents describe the route from nitro-*o*-xylene **116** to *N*-benzyl-5-nitroisoindoline **120** on a large scale (~40 g), obtained **120** with yields of 33%<sup>226</sup> and 22%<sup>227</sup> in a one-pot procedure. Both these procedures use a water/acetone solvent and sodium carbonate as a base for the cyclocondensation step. On the smaller (5 g) scale attempted in our hands an unoptimised 20% yield was achieved over the two steps Scheme 4.9. The procedure for the bromination of methyl ester **121** however heats

under reflux for 1.5 h<sup>225</sup>, significantly shorter than the patents describing the bromination of the nitroxylylene **116** which require heating at reflux for as much as 1 day followed by 2 further days at room temperature. The methyl ester cyclocondensation step (**122** → **123**) occurs in THF after a pretreatment with triethylamine.

The cyclocondensation of **118** for the synthesis of **120** was attempted using THF solvent and triethylamine base because difficulty was being experienced when dissolving anhydrous sodium carbonate (which was what was available at the time) and the resulting reaction mixture was a thick sludge, negligible difference in yield was observed with this alteration so triethylamine and THF were used for subsequent preparations as they make setting up the reaction easier. Improvement of initial yields was observed through the very slow addition of benzylamine to the bis-bromo intermediate (slower than 50 g benzylamine over 3 h that is described in the patents<sup>226,227</sup>), possibly because the ring-closure reaction is fairly slow and if the concentration of free benzylamine is too high then addition of a second benzylamine over ring closure can occur.

*N*-benzylnitroisindoline **120** is a photosensitive compound and must be kept in the dark. Initial purification by column chromatography removed a bright yellow impurity visible by TLC. An orange crust subsequently formed on the surface of the sample after a number of days exposed to daylight in a sealed glass sample vial. TLC analysis revealed that the bright yellow band had reappeared. Increase in yield could perhaps therefore be achieved by performing the reaction in the dark (and purification in low light conditions).

#### 4.2.4 Summary of synthesis of the isoindoline ring system

There are various advantages and disadvantages between phthalimide reduction and  $\alpha,\alpha'$ -bisbromo-*o*-xylene cyclocondensation in the generation of mono and disubstituted isoindoline systems. A comparison of the routes to obtain *N*-benzyl protected mono- and di-substituted isoindolines is shown in Scheme 4.10.

*The xylene route*

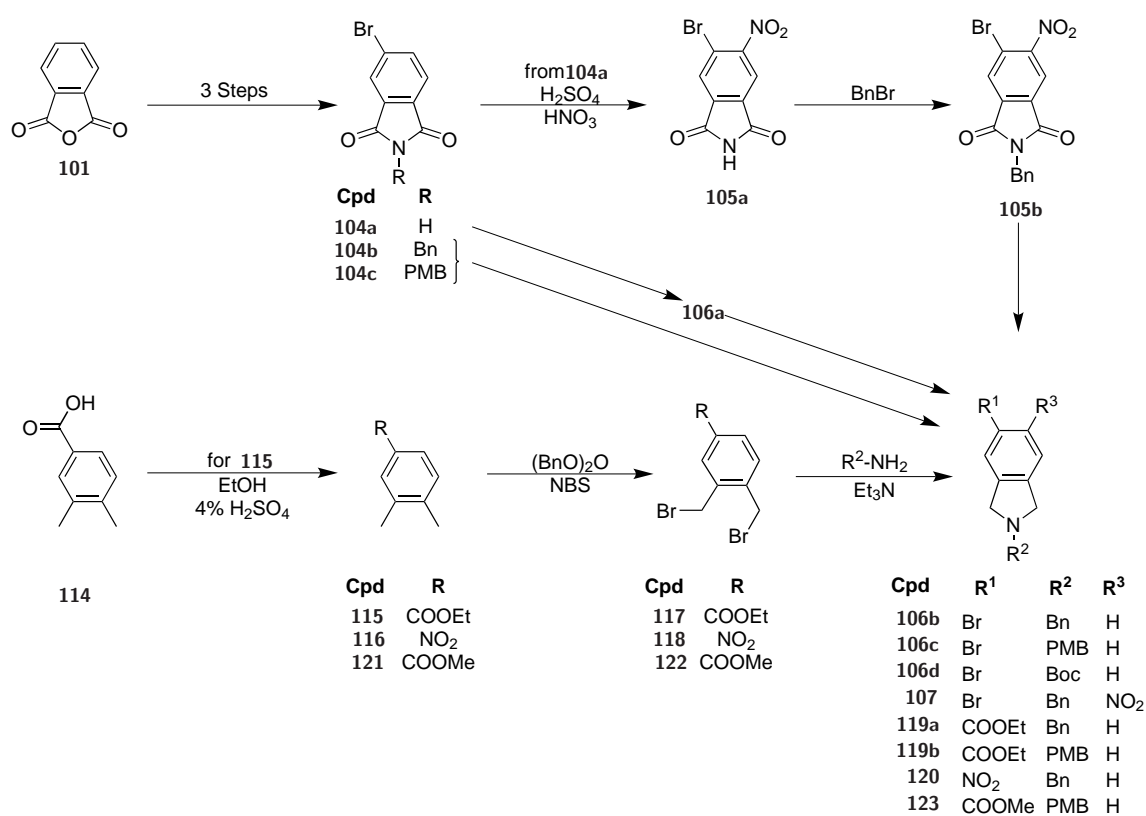
The major benefit of the cyclocondensation route to isoindolines is the short length of the route; nitro xylene **116** → **118** → **120** in a one-pot reaction gives **120** in only two steps with 20% yield. The carboxylic acid **114** → **115** (88%, unoptimised) → **117** → **119** (40% 2 steps, without isolation of the intermediate) gives the ethyl-isoindoline carboxylate in 3 steps with 35% yield.

Ethyl carboxylate **119a** is a very viscous dark brown oil. This oil is difficult to handle, therefore subsequent reactions are difficult to set up and losses are incurred during transfer between flasks and vials. Additionally the subsequent reactions to install the carboxamide group are fairly low yielding at present (Section 4.2.5). Nitroisoindoline **120** on the other hand is a bright yellow solid which (excepting its light sensitivity) is easy to handle and undergoes subsequent steps in high yields (Section 4.2.6). 4-Bromo-5-nitro-*o*-xylene has been synthesised via nitration of 4-bromo-*o*-xylene with 45% yield<sup>228</sup>, but it is impossible to know how efficient the bromination and cyclocondensation would be to form a disubstituted isoindoline without attempting the reaction.

*The phthalimide reduction route*

Reduction of phthalimides to give isoindolines **106b** and **106c** proceeded with nearly twice the yield of the cyclocondensation of *o*-xylenes (76% vs. 40%) and were white easily purifiable solids. The route to achieve the phthalimide had a yield of 52% (phthalic anhydride **101** → benzyl phthalimide **104b**, 52% over 3 steps). The phthalimide reduction vs. *o*-xylene cyclocondensation yield increase is therefore compensated for by the additional synthetic cost of obtaining the phthalimide. The literature describes the three initial steps to obtain disubstituted phthalimide **105a** with significantly higher yields than were achieved (44% vs. 77%<sup>218</sup>), if the literature could be replicated and **104a** and **105b** obtained with high yields this route would be preferable for all the desired isoindolines (although mono-substituted nitro-phthalimide reduction has not been attempted here).

Three steps are required to achieve the disubstituted phthalimide (**103** → **107b**, 60% overall yield) compared to a single high yielding step for the monosubstituted



**Scheme 4.10:** Overview of all routes to protected mono- and disubstituted isoindolines.

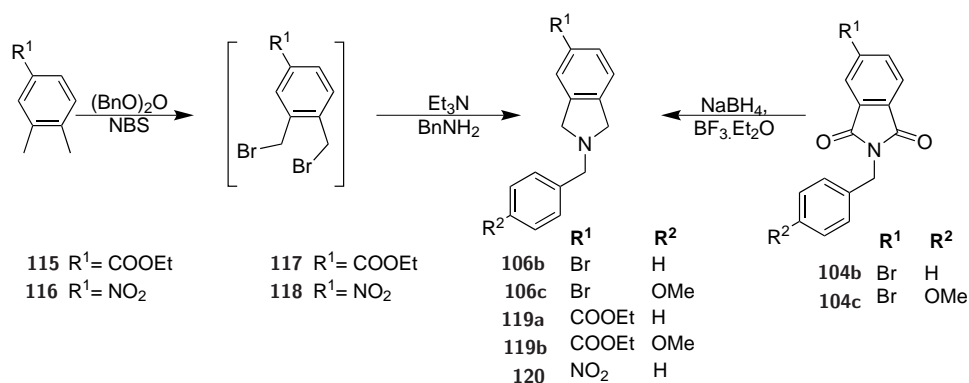
phthalimide (**103** → **104b**, 90%). The yield for the subsequent phthalimide reduction is halved for the disubstituted compared to the monosubstituted example (Scheme 4.6). Disubstituted isoindolines are however only possible using the phthalimide reduction route as 4-bromo-5-nitro-*o*-xylenes are difficult to synthesise<sup>228</sup>.

The steps to transform the bromine substitution into a carboxamide substitution are high yielding so for monosubstituted carboxamides the phthalimide reduction route is preferable to the *o*-xylene cyclocondensation route (Section 4.2.5).

## 4.2.5 Derivatisation of substituted isoindolines

### Synthesis of *N*-benzylcarboxamido isoindolines

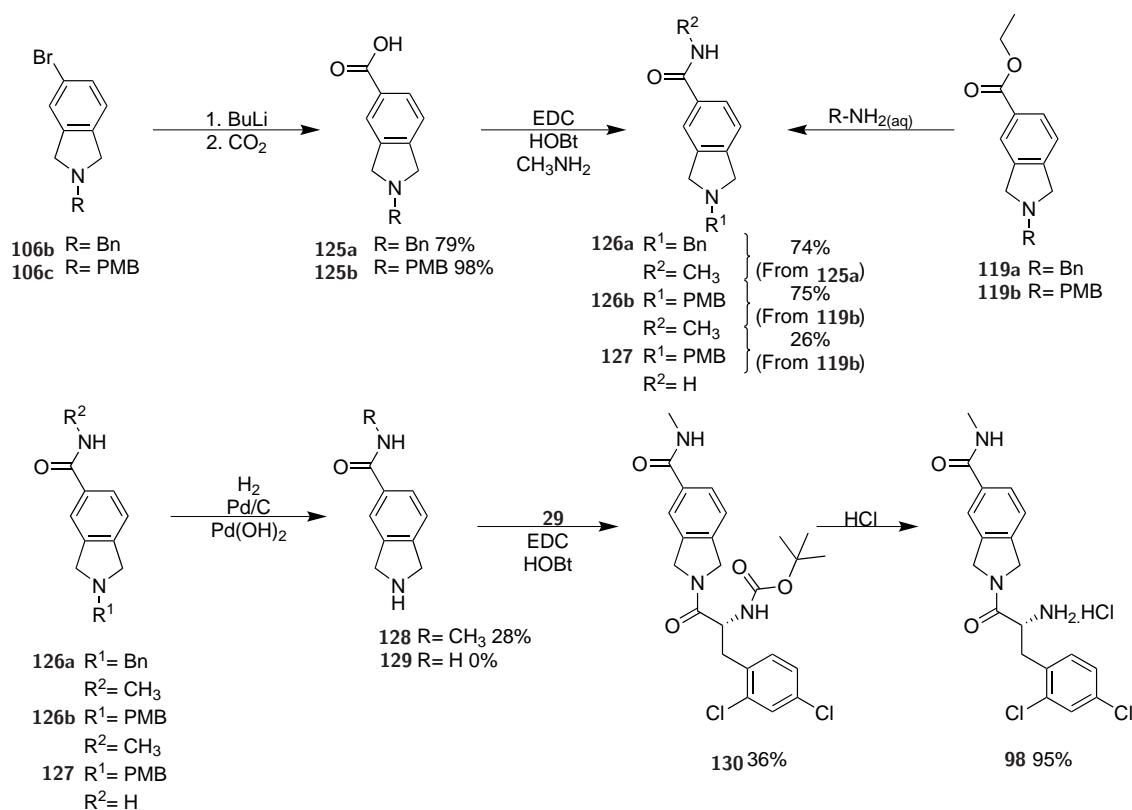
In order to obtain a series of 5 (and 5,6) -substituted isoindoline based  $\alpha$ -amino amide inhibitors, three late-stage *N*-benzylisoindoline intermediates were synthesised via two alternative routes described in Scheme 4.11: cyclocondensation of an  $\alpha$ - $\alpha'$ -bis-bromoxylene with benzylamine (**119a** & **120**) and reduction of a phthalimide with NaBH<sub>4</sub> and BF<sub>3</sub>.Et<sub>2</sub>O (**106b**).



**Scheme 4.11:** Synthetic routes to three late-stage *N*-benzylisoindoline intermediates

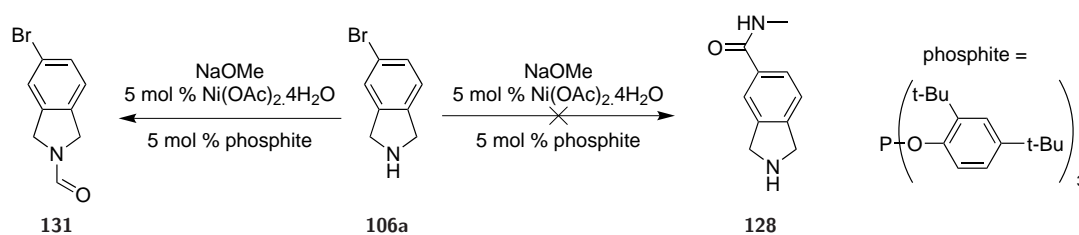
## Synthesis of methyl carboxamido-isindoline

Bromoisindolines **106b** and **119b** were derivatised to give isoindoline-5-carboxamides **126** and **127** (Scheme 4.12). The intermediate *N*-methylcarboxamide **126** is a convergence point for the two routes to the  $\alpha$ -amino amide inhibitor **98** (Scheme 4.12).



**Scheme 4.12:** Two routes to carboxamidoisindolines **126** and **127** from bromoisindolines **106** and ethylcarboxylates **119**, and subsequent steps to achieve the correlating  $\alpha$ -amino amide salt **98**.

Two synthetic routes to achieve **126** from **106** were explored. Direct transition from bromo to carboxamido aromatic substituents has been reported on a 4-bromotoluene system using a nickel acetate and phosphite coupling reaction in diglyme at 110 °C<sup>229</sup>. This procedure was attempted on the unprotected **106a** but failed (Scheme 4.13). The secondary amine within the isoindoline ring reacted to give the isoindoline-carbaldehyde **131** (confirmed by NMR and mass spectrometry). It is possible that had the reaction been attempted on an *N*-benzyl protected isoindoline that it would



**Scheme 4.13:** Attempted direct transformation of bromo-aromatic to amide **128** using a literature procedure<sup>229</sup>.

have succeeded but this route was not pursued as the alternative route proved sufficiently effective.

With the failure of a direct transformation from bromoisindoline **106** to isoindolinecarboxamide **128** an alternative method was used with a *N*-benzylisindolinecarboxylic acid intermediate (**125a** in Scheme 4.12). *N*-Benzylbromoisindoline **106b** was successfully converted to the carboxylic acid **125a** using lithium-halogen exchange followed by the addition of carbon dioxide as a nucleophile with a good yield of 79%. The analogous *N*-(4-methoxybenzyl) protected **125b** was obtained with 98% yield. Convenient purification of isoindoline carboxylic acids **125a** and **125b** was achieved by loading onto a silica plug in ethyl acetate, washing off impurities and then eluting the product with 1% acetic acid in ethyl acetate.

Coupling of **125a** with methylamine to give the *N*-methylcarboxamide **126a** using EDC was performed under similar conditions to those used for previous amide couplings (see Section 2.2.2) and proceeded well with 75% yield (Scheme 4.12)

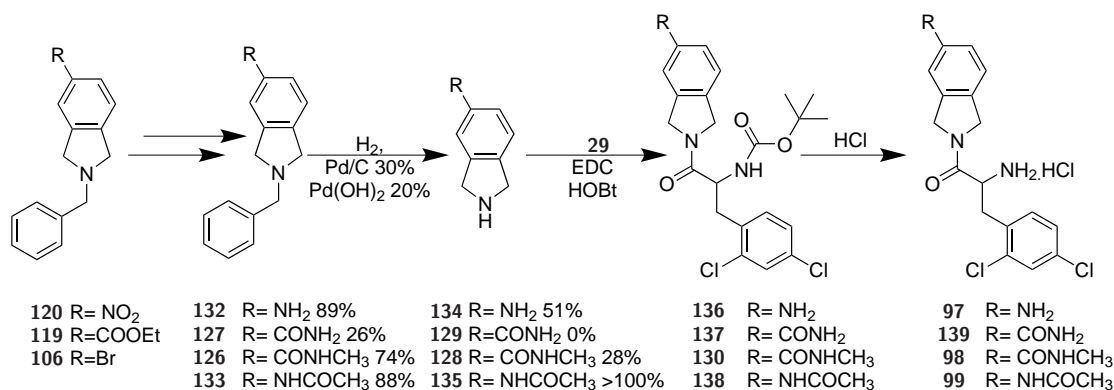
From the alternative route, conversion of the ethyl ester **119b** to the *N*-methylcarboxamide **126b** was performed in a sealed tube with 40% aqueous methylamine as has been reported previously on a tetrahydroisoquinoline system<sup>230</sup> (Scheme 4.12), a 75% yield was obtained but was difficult to repeat as methylamine is very corrosive to the rubber seals used on the sealed tubes. This strategy is also applicable to synthesis of other compounds with alternate R-groups which introduces the possibility of creating additional selective cap-group contacts.

## Synthesis of carboxamido isoindoline **127**

The steps taken to synthesise the primary carboxamide **127** were similar to those used for the synthesis of methylcarboxamide **126** (Section 4.2.5) but had a greatly reduced yield (Scheme 4.12). Heating a mixture of concentrated aqueous ammonia and **119b** at 100 °C for 16 h in a sealed tube resulted in only a 26% yield of primary amide **127** after 16 h (compared to 75% obtained for the methylcarboxamide **126**). The remaining material recovered from the reaction was the starting reactant **119b** indicating that the reaction was significantly slower.

### 4.2.6 Debenzylation of *N*-benzylisoindolines

Debenzylation of *N*-benzylisoindolines was more difficult than expected. Hydrogenolysis of isoindolineamine **120** has previously been reported and difficulty in the hydrogenolysis of the benzyl group was mentioned. Overnight hydrogenation at 50 psi with 0.6% HCl and 20 mol% Pearlman's catalyst was required for complete debenzylation to give **134**<sup>226</sup>. High pressure apparatus were not available when debenzyllating **132** and at 1 atm only 51% debenzylation was achieved after 120 h (Scheme 4.14).



**Scheme 4.14:** Generalised route from *N*-benzylisoindoline to  $\alpha$ -amino amide salt.

Multiple variations of the standard hydrogenolysis procedure (1 Atm H<sub>2</sub>, 10% Pd/C in EtOH or MeOH) were attempted for the debenzylation of **126b** to give **128**: using 5%, 10% and 30% Pd/C, Pearlman's catalyst (Pd(OH)<sub>2</sub>/C 20%), extending

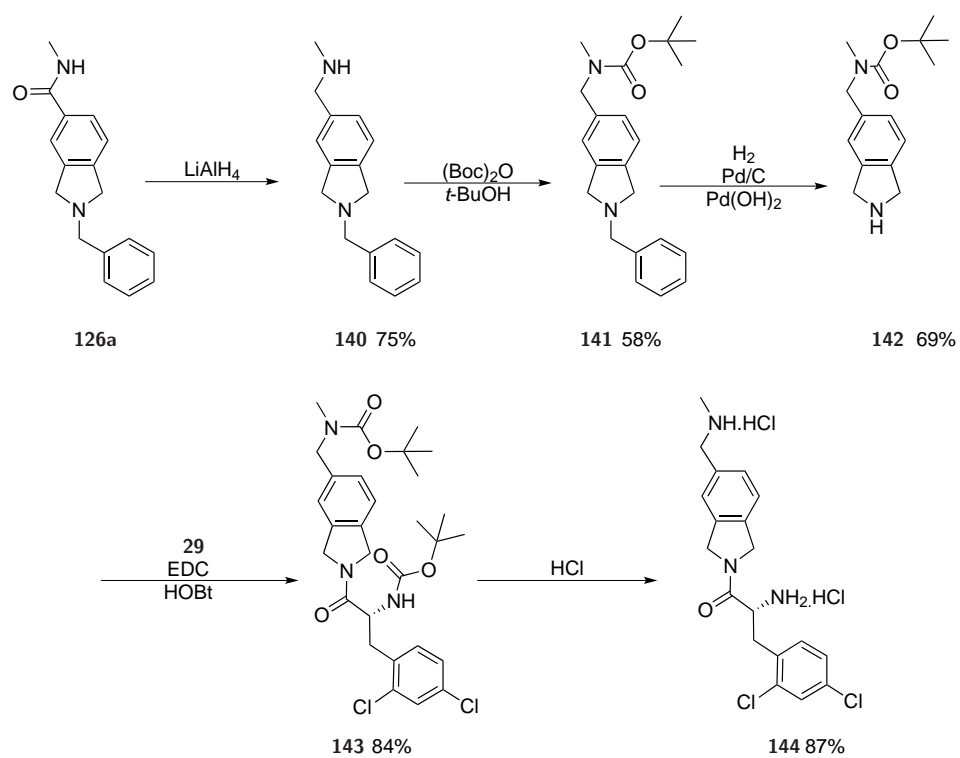
the time of the reaction to 72 h and also addition of 0.5% HCl to prevent poisoning of the catalyst. All variations resulted in yields of debenzylated product **135** of ~25%, in these cases the remainder of the starting material was recovered after silica column chromatography.

A 1:1 mixture of Pearlman's catalyst and Pd/C is reported to be an effective debenzylation strategy in cases where single catalysts are ineffective<sup>224</sup>. Efficient hydrogenolysis of **133** was achieved using a mixture of these two catalysts and heating to 30 °C, occurred in 16-20 h under only ~1 atm. hydrogen (supplied by a balloon) to give **135** (>100% crude) as seen in Scheme 4.14, in future all debenzylations should use a 1:1 mixture of pearlman's catalyst and 30% palladium on carbon.

The debenzylation of the primary carboxamido isoindoline **127** resulted in two products. Column chromatography in 5% aqueous ammonia, 5% MeOH, 90% ethyl acetate was required for the very polar amines, the less polar product (RF = 0.15) had an extra methyl group present which was detected by NMR spectroscopy, peaks corresponding to the CH<sub>2</sub> groups were also shifted, this indicates that the isoindoline had been *N*-methylated. The more polar product (RF < 0.1) seemed to be a volatile solid which sublimed during evaporation of the solvent. White needles were seen in the adapter of the rotary evaporator. Sadly, due to the sublimation, significant amounts of primary carboxamide **129** were lost and the subsequent coupling to give **137** and *N*-Boc deprotection to give **139** was not pursued.

### Synthesis of 5-((methylamino)methyl)isoindoline $\alpha$ -amino amide salt **144**

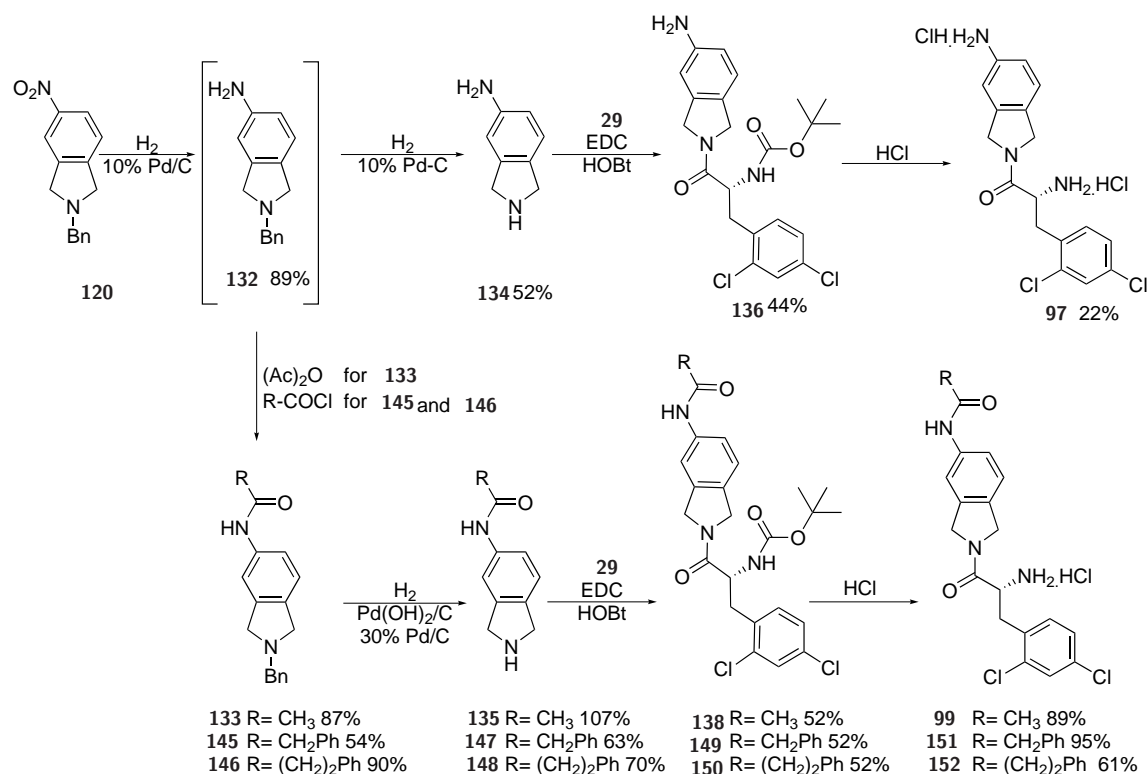
Synthesis of  $\alpha$ -amino amide **144** proceeded through carboxamido isoindoline **126a** which is an intermediate in the route to **98** (Scheme 4.12). LiAlH<sub>4</sub> reduction of the amide **126a** proceeded well to give **140** (75%) and the subsequent *N*-Boc protection of the secondary amine gave **141** with an unoptimised 58% yield (Scheme 4.15). Hydrogenolysis of the *N*-benzyl protecting group to isoindoline **142** (69%) permitted coupling with amino-acid **29** to give **143** with good yield (84%) and efficient removal of the Boc group with HCl gas bubbled through an ethereal solution of **143** resulted in  $\alpha$ -amino amide salt **144** (87%).



**Scheme 4.15:** Synthesis of  $\alpha$ -amino amide salt **144** through previously synthesised carboxamide **126a**

Synthesis of 4-aminoisoindoline  $\alpha$ -amino amide salt **97**

The preparation of  $\alpha$ -amino amide salt **97** was achieved via 5-aminoisoindoline **134** (Scheme 4.16). Hydrogenolysis of nitro and benzyl groups of *N*-benzylnitroisindoline **120** for 120 h at 20 °C using a 10% Pd/C catalyst to afford isoindolineamine **134** in a single step with fair yield (51%). The subsequent coupling of **134** to *N*-Boc-amino acid **29** proceeded to give **136** (44%). Amide coupling gave the desired product preferentially as the secondary amine of **134** is more reactive than the aniline (due to the delocalisation of the nitrogen lone pair of electrons into the aromatic ring). The removal of the Boc group with HCl (as described in Section 2.2.2) then gave **97** (22%).



**Scheme 4.16:** Derivatization of nitro-substituted *N*-benzylisindoline to achieve amino and acetamido substituted  $\alpha$ -amino amide salts.

## Synthesis of 4-acetamido isoindolyl $\alpha$ -amino amide salts

There is a vast discrepancy between the reactivity of the 5-nitro and the *N*-benzyl groups of **120** when performing palladium on carbon catalysed hydrogenolysis. *N*-Benzyl-5-nitroisoindoline (**120**) reacted to give *N*-benzylisoindoline-5-amine **132** within 2 h. (89%). Only prolonged hydrogenation with multiple catalysts and heating removed the benzyl group with acceptable efficiency (see Scheme 4.16). Selective reduction of the nitro group to an amine without debenylation to **132** is therefore possible and permits acetylation with acid chlorides or anhydrides in the presence of a base to give *N*-benzylisoindoline-acetamides with very good yields in the majority of cases: **133** (87%), **145** (54%) and **146** (90%). Following debenylation to give isoindolines **135**, **147** and **148** these isoindolines were then readily coupled with dichlorophenylalanine **29** to give **138**, **149** and **150**. Following the final deprotection step the target compounds **99**, **151** and **152** were obtained (yields given in Scheme 4.16).

### 4.2.7 NMR to probe rotameric energy barriers

Rotamers arise in compounds due to restricted rotation about certain bonds, which leads to significant populations of two conformers of a molecule, a trans and cis conformation (Figure 4.5). In the case of  $\alpha$ -amino amide HDAC8 inhibitors such as **99**, the restriction is around the amide bond within the ZBG which has partial double bond character due to delocalised electrons throughout the N, C and O atoms, thus restricting rotation around the C-N bond. For **99**, the two N-substituents are symmetrical (in the region of the amide bond) and so there is no energetic preference for one conformation over the other, therefore the two conformer populations are equal. This is manifested as equal integrations of NMR signals arising from each conformer (Figure 4.5). At equilibrium the conformational exchange rate from trans to cis ( $k_1$ ) is equal to the conformational exchange rate from cis to trans ( $k_2$ ), and the equilibrium constant  $K_{exch} = k_2/k_1 = 1$ . When a rotamer isomerises the double bond characteristics of the amide group must be overcome. The energy required to



3.  $\tau \ll 1/\Delta\nu \Rightarrow$  one narrow resonance line at  $\nu_A + \nu_B/2$ , fast exchange region

A molecule in “slow exchange” in NMR terms gives rise to two different NMR signals for each nucleus as two different rotamers are present and distinct, this occurs when a molecule has conformational lifetimes on the order of minutes. A molecule in “fast exchange” is interconverting faster than the NMR timescale (typically 10-1000 Hz) and therefore gives rise to a time-averaged signal of the two conformations rather than the two distinct signals observed at slow exchange. In between these two extremes of exchange dynamics is a grey area known as intermediate exchange - where the exchange between the two conformations is on the NMR timescale and so a mixture of averaged signals and intermediate signals are detected - this is manifested as line broadening of the two signals.)

The rate of interconversion of two conformations can be modulated by increasing the number of molecules which possess the activation energy of conformational isomerisation, i.e. by increasing the temperature of the sample. As the temperature increases there is a larger proportion of molecules with energy greater than or equal to the activation energy. This leads to greater exchange and a reduced conformational lifetime. If the isomerisation rate can be increased sufficiently to alter the exchange regime, we can estimate the amount of energy required to effect the change in exchange regimes and in turn the activation energy for the conformational isomerisation between cis and trans.

Using the Eyring equation (Equation 4.1) from transition state theory we can rearrange and substitute  $\hbar$  and  $k_B$  to obtain  $\Delta G^\ddagger$  (Equation 4.2).

A short <sup>1</sup>H NMR temperature series was recorded on **99** to investigate the energy barrier of the amide bond. Spectra were recorded at 298 K, 363 K (90 °C) and 403 K (130 °C) (Figure 4.5). At 363 K (green in Figure 4.5) rotamer peaks are clearly visible with only slight line broadening compared to the 298 K spectrum (blue in Figure 4.5, the difference in frequency between the two rotameric states ( $\Delta\nu$ ) is 23 Hz. Only at 403 K was coalescence of the peaks observed Figure 4.5, using these

values in equation 4.2 we can estimate the rotameric energy barrier to be 86.5 kJ mol<sup>-1</sup> or 20.6 kcal mol<sup>-1</sup>.

$$k = \frac{k_B T}{\hbar} e^{-\frac{\Delta G^\ddagger}{RT}} \quad (4.1)$$

$$\Delta G^\ddagger = RT[23.76 + \ln(T/k)] \quad (4.2)$$

The rate of conformational isomerisation is important in an inhibitor, if it is slow and only one conformation binds a target then the molecule will be half as potent than if the isomerisation was fast. Binding of the correct conformation of the inhibitor stabilises it thereby making it energetically favoured, shifting the equilibrium constant in favour of that binding conformation. The fraction of **99** molecules that has the energy  $> 1\Delta G^\ddagger$  at room temperature (298.15 K,  $\Delta G^\ddagger = 20.6$  kcal mol<sup>-1</sup>) is  $7.01 \times 10^{-16}$  or 1 in  $1.4 \times 10^{15}$ . The rate of isomerisation is therefore slow. It is possible that one rotameric conformation of HDAC8 inhibitor **99** has a lower  $k_i$  than the other. The inhibitor may therefore be a “slow-tight binding inhibitor” this would mean that a pre-incubation of inhibitor and enzyme would lower the apparent  $k_i$  ( $k_i^{app}$ ) as measured by an HDAC8 inhibition assay.

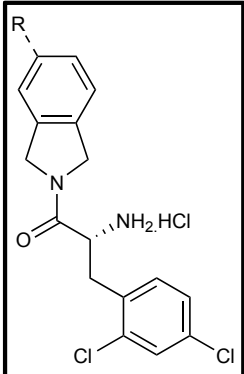
### 4.3 3<sup>rd</sup> generation $\alpha$ -amino amide HDAC8 inhibition results

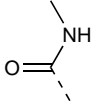
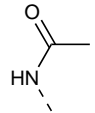
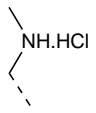
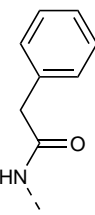
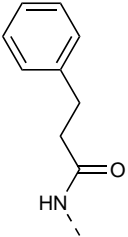
#### 4.3.1 Addition of an amine hydrogen bond donor to inhibitor

##### 4

Compounds with small substitutions that are potential hydrogen bond donors to Asp101 showed improved binding characteristics compared to the unsubstituted isoindoline containing **4**. Table 4.1 shows the IC<sub>50</sub> values measured and binding

**Table 4.1:** Inhibition assay results for 3rd generation 5-substituted isoindolyl  $\alpha$ -amino amide HDAC8 inhibitors. IC<sub>50</sub> values are the mean of at least two independent repeats  $\pm$  standard deviation. ( $\Delta G_b = \Delta G_{binding}$ ).



	R	IC <sub>50</sub> /nM	$\Delta G_b$ /kcal mol <sup>-1</sup>		R	IC <sub>50</sub> /nM	$\Delta G_b$ /kcal mol <sup>-1</sup>
<b>4</b>	H	210 $\pm 40$	-9.48 $\pm 0.18$				
<b>97</b>	NH <sub>2</sub> .HCl	130 $\pm 22$	-9.77 $\pm 0.17$	<b>98</b>		258 $\pm 63$	-9.37 $\pm 0.24$
<b>99</b>		101 $\pm 26$	-9.93 $\pm 0.26$	<b>144</b>		176 $\pm 50$	-9.59 $\pm 0.28$
<b>151</b>		232 $\pm 33$	-9.42 $\pm 0.14$	<b>152</b>		259 $\pm 67$	-9.35 $\pm 0.26$

energies calculated for  $\alpha$ -amino amide inhibitors based on **4** with Asp101 hydrogen bond donating substituents. The presence of an amino substitution at position 5 of the isoindoline STBG of **4** allows a hydrogen bond with Asp101 to be formed (Figure 4.6a). This interaction lowered the IC<sub>50</sub> from 210  $\pm$ 40 nM (**4**) to 130  $\pm$ 22 nM (**97**), with a corresponding improvement in binding energy from -9.48  $\pm$ 0.18 kcal mol<sup>-1</sup> to -9.77  $\pm$ 0.17 kcal mol<sup>-1</sup>. The hydrogen bond provided by the primary aryl-amine is not identical to the hydrogen bond provided by the amide of the *Fluor-de-Lys* substrate peptide backbone and as such the interaction of **97** with Asp101 does not truly replicate the substrate-Asp101 interaction. In the peptide, the presence of the carbonyl group increases the polarity of the amide nitrogen and so the hydrogen bond to Asp101 becomes stronger than if an amine were present.

An amide substituent was therefore installed at the 5-position to make the inhibitor-Asp101 hydrogen bonding interaction more “substrate-like”. Both 5-carboxamido (**98**) and 5-acetamido (**99**) substitutions were tested.

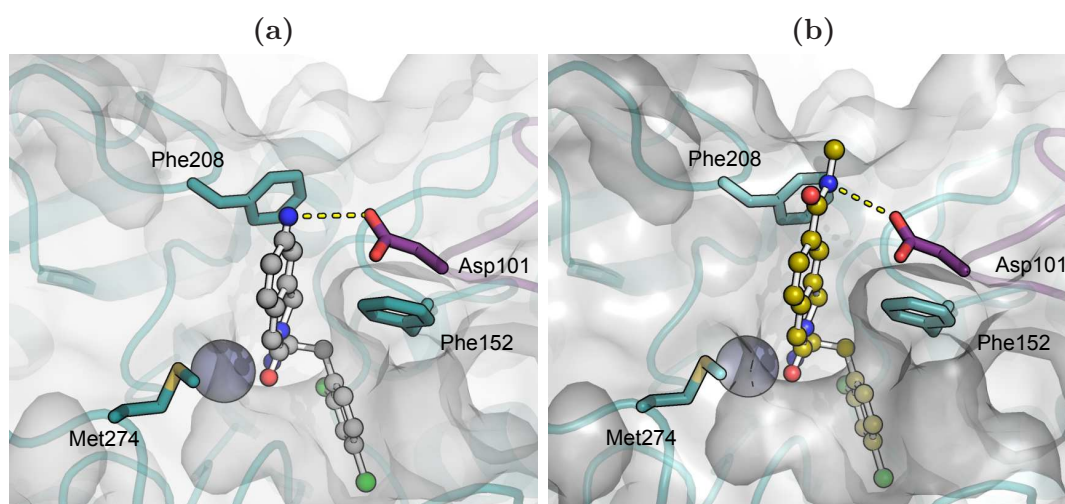


**Figure 4.6:** Manual docking poses for (a) **97** and (b) **98** in the HDAC8 structure. Flexible L2 loop and Asp101 are superimposed from HDAC8-*Fluor-de-Lys* structure (purple).

### 4.3.2 Addition of a amide hydrogen bond donor to inhibitor

#### 4

The 5-Carboxamide **98** seen in Figure 4.6b has electrons from the amide group delocalised into the aromatic ring, the hydrogen bond-donating nitrogen must therefore remain in the plane of the aromatic ring. In the most ideal manual docking pose the amide is placed 4.1 Å from the hydrogen bond accepting Asp101 and the orientation of the N-H bond is perpendicular to an ideal hydrogen bond orientation<sup>231</sup> (Figure 4.6b). As a result of this positional and orientational restriction there is no increase in potency of **98** over **4** ( $258 \pm 63$  nM vs.  $210 \pm 40$  nM, Table 4.1). The *N*-methylamine hydrochloride **144** was synthesised to enable more flexibility in the new hydrogen bond donating cap-region compared to **98**. It was hoped that with 2 rotatable bonds between the aromatic ring and the hydrogen bond donor a more optimal positioning of the nitrogen could be achieved and that this would lead to increased potency over **98** as shown in the manual docking pose in Figure 4.7a. A modest but not statistically significant increase in potency is seen for **144** over **98** ( $176 \pm 50$  nM vs.  $258 \pm 63$  nM). It is possible that the improved positioning of the hydrogen bond-donating nitrogen is offset by the increase in conformational entropy of the free ligand that comes from having two extra rotatable bonds.

5-Acetamido substituted **99** ( $101 \pm 26$  nM) showed an increase in potency over the un-substituted **4** ( $210 \pm 40$  nM), similar to that of amino substituted **97** ( $130 \pm 22$  nM) and corresponding energy increase of  $0.45 \pm 0.32$  kcal mol<sup>-1</sup> (Table 4.1). Manual docking shows that the nitrogen of **99** can closely mimic the peptide backbone of the substrate as the aryl-amide bond is superimposable with the substrate backbone. Additionally the orientation of the amide can be orthogonal to the plane of the ring (Figure 4.7b) so a stronger hydrogen bond can be formed compared to **98** where the amide is restricted to being in plane with the aromatic ring (Figure 4.6b).

Following the increase in potency of **97** and **99** over **4** which was achieved by addition of a hydrogen bond-donor, two more  $\alpha$ -amino amide inhibitors were synthesised to explore the possibility of adding more cap-group interactions with the surface of HDAC8. Three aromatic residues and one hydrophobic residue (Phe152, Phe208,

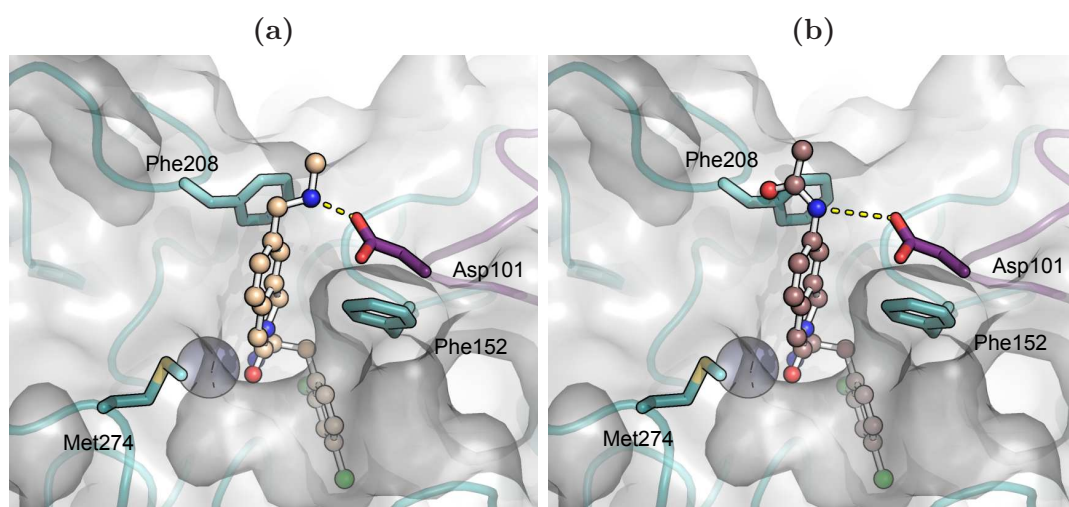


**Figure 4.7:** Manual docking poses for (a) **144** and (b) **99** in the HDAC8 structure. Flexible L2 loop and Asp101 are superimposed from HDAC8-*Fluor-de-Lys* structure (purple).

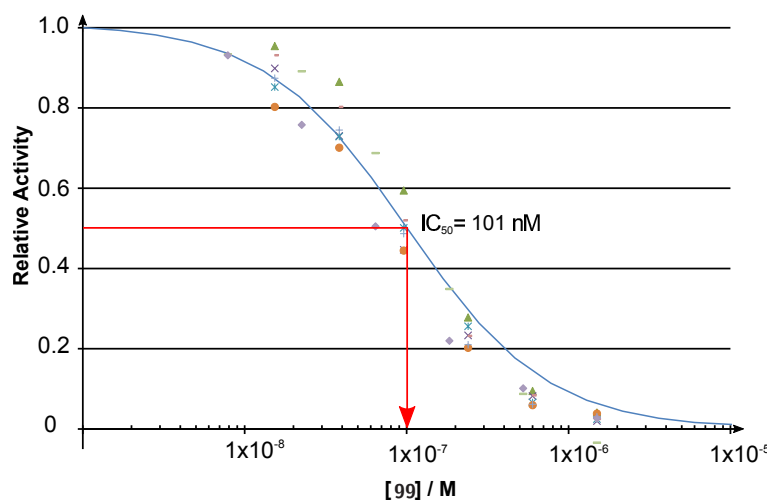


**Figure 4.8:** Experimental data points recorded for 8 HDAC8-**99** inhibition assays. Different symbols represent data collected from independent repeats. Fitted line is a calculated inhibition curve for IC<sub>50</sub> = 101 nM, the average calculated for **99**.

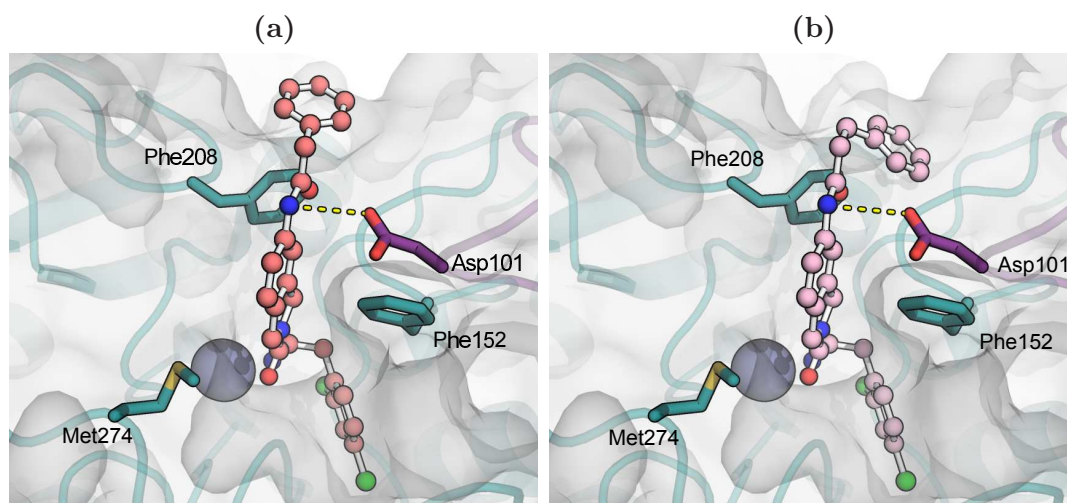


**Figure 4.9:** Manual docking poses for (a) **151** and (b) **152** in the HDAC8 structure. Flexible L2 loop and Asp101 are superimposed from HDAC8-*Fluor-de-Lys* structure (purple).

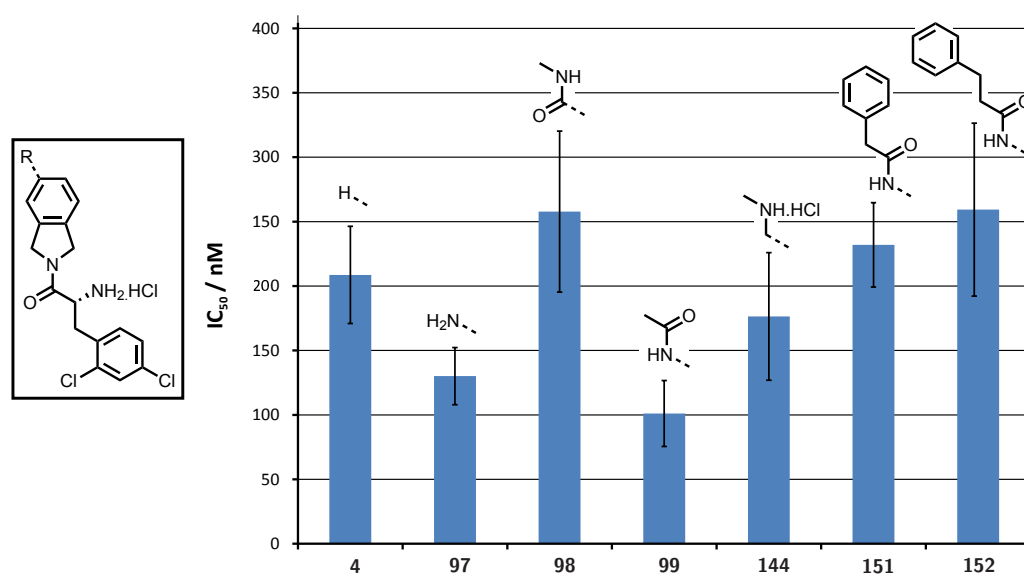


**Figure 4.10:** IC<sub>50</sub> values of HDAC8 inhibitors incorporating a hydrogen bonding group, error bars are SD of >2 independent repeats. corresponding R-groups are shown above the bars.

Tyr306 and Met274) form the entrance to the substrate channel. Phe152 and Phe208 are already known to create key contacts that are visible in the HDAC8-4 structure and mutation of these residues eliminates substrate binding (results not shown & ref [207]). The *Fluor-de-Lys* substrate has a 20-fold lower  $K_M$  than the MAL substrate and so there must be many more contacts available on the surface of the protein. The extra peptide extension of the *Fluor-de-Lys* substrate must be responsible for this increase in affinity. The exact contacts responsible for this increase are not observable from the HDAC8-substrate structure however. This is because of the face-to-face crystal packing which puts the substrate molecule in contact with a second HDAC8 monomer and means the physiologically relevant conformation of surface residues is unlikely to be present in the structure. These additional contacts are contacts that could prove very useful in dramatically increasing the potency of inhibitors and so I attempted to probe them through extension of the cap-group.

Phenylacetamide (**69**) and phenylmethylacetamide (**70**) isoindoline substitutions did not improve potency of isoindoline  $\alpha$ -amino amide inhibitor **4** against HDAC8. ( $232 \pm 33$  nM and  $259 \pm 67$  nM vs.  $210 \pm 40$  nM). Manual docking of these inhibitors suggested that possible interactions may occur between the cap-group aromatic rings and Phe208 (Figure 4.9a & b). The lack of improvement in binding over **4** suggests that the energetic contributions of any beneficial interactions (including the hydrogen bond to Asp101) are negated by other unfavourable interactions of the cap-group, perhaps through the exposure of hydrophobic surfaces to the aqueous solvent. Isoindoline  $\alpha$ -amino amide inhibitors with a small, unconjugated, hydrogen-bond-donating substitution at the 5-position (**97**, **99**, **144**) are more potent HDAC8 inhibitors than any other HDAC inhibitors reported with this novel  $\alpha$ -amino amide ZBG.

## 4.4 Summary of 3<sup>rd</sup> generation inhibitor assay results

The addition of a hydrogen bond donor in these 3<sup>rd</sup> generation of  $\alpha$ -amino amide inhibitors lead to improved binding of non-isoindoline containing  $\alpha$ -amino amide inhibitors. Manual docking of these inhibitors pointed to the possibility that interactions of these hydrogen bond donors with Asp101 could be responsible for the increased potency. Non-isoindoline from the 2<sup>nd</sup> generation of inhibitors had poor binding energies of  $>\sim 1$  kcal mol<sup>-1</sup> smaller than lead compound **4** with an isoindoline STBG. This was due to the loss of conformational restriction that was provided by isoindoline rigid, planar ring system. For the 3<sup>rd</sup> generation of inhibitors it was therefore decided to add hydrogen bond donating groups to the isoindoline group to improve the potency by adding Asp101 H-bonding interactions while maintaining the rigidity imparted by the isoindoline STBG. Hydrogen bonding groups were added at position 5 of the isoindoline ring since this position aligns nicely with the C $\alpha$  of the *Fluor-de-Lys* peptide substrate, it is therefore likely to be the most beneficial position to add a hydrogen bonding group.

5-Aminoisoindoline **97** and 5-acetamido **99** had improved potency compared to the lead compound **4** indicating that hydrogen bonds were indeed being formed between the amino group and Asp101. 5-carboxamido **98** did not show improved binding compared to **4** with an unsubstituted isoindoline STBG. This is most likely due to the orientation of the amide group which is planar with the aromatic ring since the amide electrons are delocalised into the ring, conversely the 5-acetamido group in **99** is able to rotate and provide more favourable hydrogen bonding with Asp101 since its electrons are not delocalised into the aromatic ring. **144** with a flexible amine hydrogen bond donor was synthesised to provide an improved hydrogen bond with Asp101 but did not have statistically significant improvements in binding energy over **4**, again suggesting that conformational entropy of the free ligand plays an important part in determining the potency of  $\alpha$ -amino amide inhibitors.

To further explore possible cap-group interactions two further 5-amido substituted  $\alpha$ -

amino amide inhibitors were synthesised with additional aromatic extensions (**151** and **152**). Both these inhibitors had a potency comparable to lead compound **4** suggesting that any additional favourable interactions are being cancelled out by unfavourable interactions and increased conformational entropy of the free ligand.

## 4.5 NMR spectroscopy of HDAC8-4 binding

Nuclear magnetic resonance (NMR) is a powerful technique that can be used to follow protein-protein interactions or protein-ligand interactions. <sup>1</sup>H, <sup>13</sup>C and <sup>15</sup>N nuclei give rise to NMR signals, and the position of these signals in the NMR spectrum are specific to the environment around the nucleus. Therefore of this a change in environment (i.e. by the proximity of a ligand) will alter the signal position, linewidth or intensity. This makes it an ideal tool to detect binding of ligands to proteins.

HDAC8 is 42 kDa which is large for structural studies by NMR. A uniformly <sup>1</sup>H, <sup>13</sup>C, <sup>15</sup>N isotope labelled HDAC8 gives rise to many overlapping peaks (not shown) which hampers detailed analysis. Using Transverse Relaxation Optimised Spectroscopy (TROSY), a specialised NMR technique for investigations into large proteins, the overlap in crowded spectra can be reduced<sup>232</sup>. Residue specific labelling can also greatly reduce the complexity of NMR spectra as it enables detection of signals from specifically labeled groups (or residues) against an NMR silent background<sup>233</sup>. Using these two techniques in combination it is possible to gain some insight into the binding of  $\alpha$ -amino amide HDACi to HDAC8.

An exploratory NMR experiment was performed using the Ile348Val HDAC8 mutant expressed in deuterated media with a fully deuterated amino-acid precursor ( $\alpha$ -ketobutyric acid-4-<sup>13</sup>C,3,3-<sup>2</sup>H<sub>2</sub>). This labelling strategy results in NMR spectra with peaks corresponding only to the terminal methyl groups of isoleucine sidechains as seen in Figure 4.11. HDAC8 has 25 isoleucine residues (one of which is mutated to valine in the case of HDAC8 Ile348Val) so 24 peaks should be visible in the <sup>1</sup>H-<sup>13</sup>C Methyl-TROSY HMQC spectrum (purple peaks in Figure 4.11). Spectra recorded

before and after the addition of five equivalents of  $\alpha$ -amino amide inhibitor **4** show a dramatic change in peak positions of residues lining or connected to the inhibitor binding region of the protein, a result of  $\alpha$ -amino amide inhibitor binding. Peaks assigned to Ile34, Ile284 and Ile269 have large changes in chemical shift, while the remaining 21 visible isoleucine peaks showed little to no change (Figure 4.11). These data can be rationalised by inspection of the structure shown in Figures 4.12a & b. Ile34, the most dramatically shifting peak which forms part of the acetate release pocket, is 3.3 Å away from the *para*-chlorine of **4** in the structure. Both Ile284 and Ile269 are >15 Å from **4** so do not have direct interaction with the inhibitor but their peak shifts can be explained through allosteric effects, which emanate from the change in Zn<sup>2+</sup> coordination upon inhibitor binding. The remaining isoleucine residues show little or no peak changes indicating no structural changes occur in a large part of the protein.

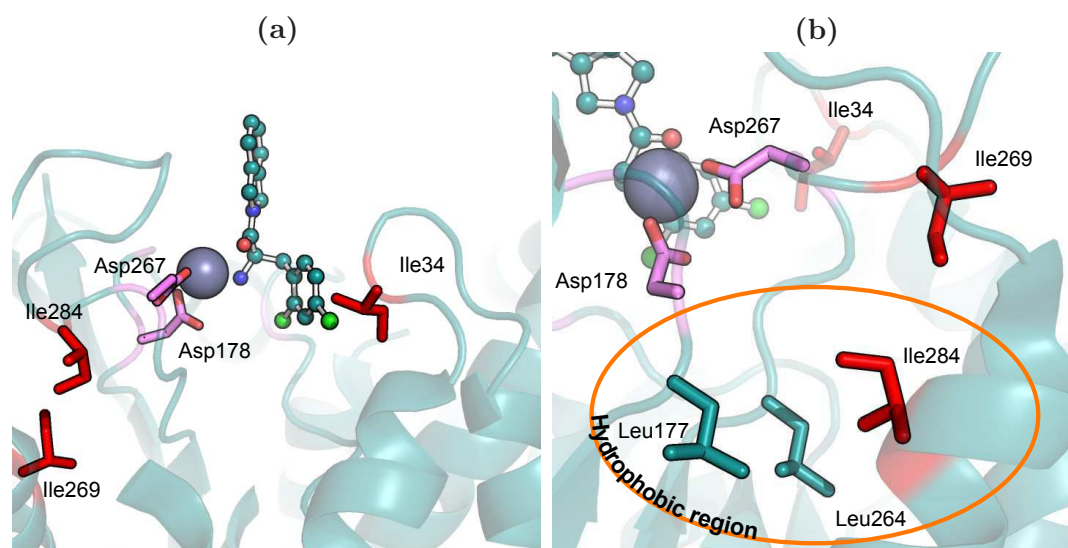


**Figure 4.12:** Effects of compound **4** binding on Ile residues. a,b) Structure of HDAC8-**4**, with Ile affected by addition of ligand (red sticks), Zn<sup>2+</sup>-coordinating aspartates (magenta sticks) and Leu residues important in transmitting change to Ile284 (teal sticks).

When substrate bound, the catalytic Zn<sup>2+</sup> ion is penta-coordinated in square pyramidal geometry by Asp178, His180, Asp267 the substrate-acetate carbonyl and a water molecule with inter atomic distances of 2.8, 2.1, 2.0, 2.0 and 2.1 Å respectively<sup>84</sup>

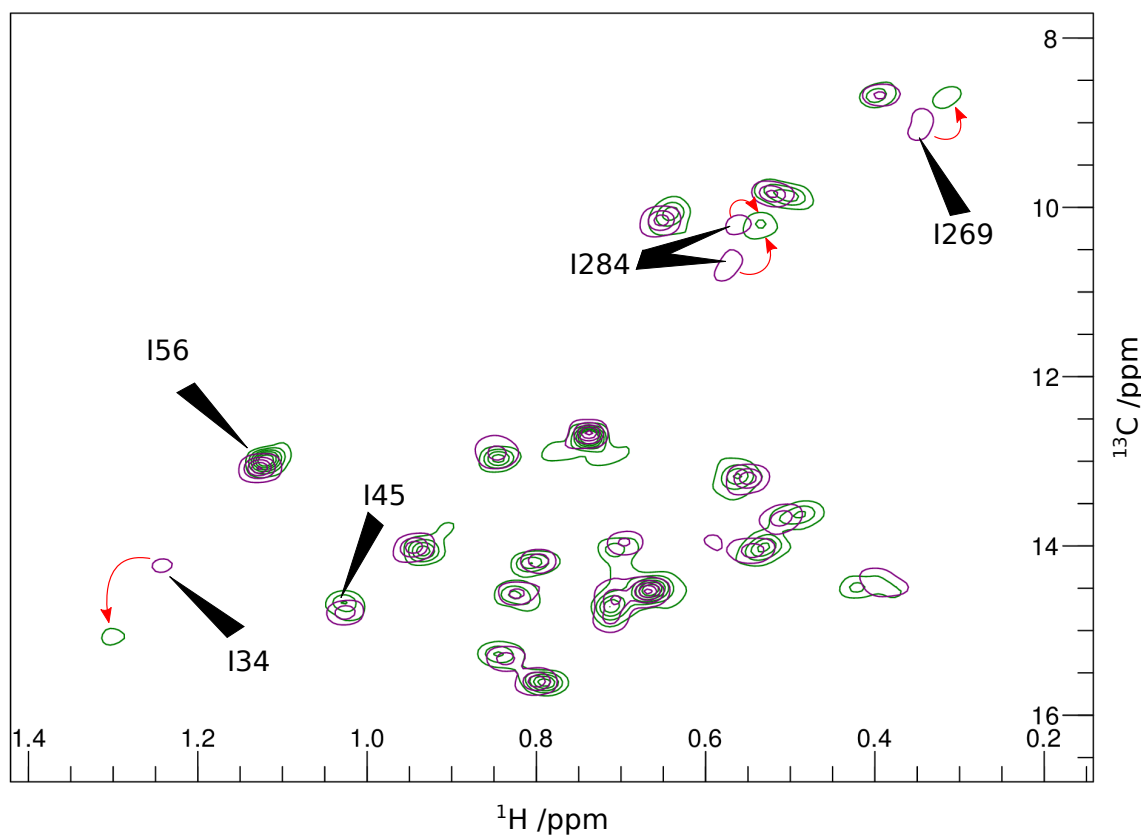


**Figure 4.11:** Methyl-TROSY HMQC spectrum of deuterated  $\delta^{13}\text{C}^1\text{H}_3\text{-Ile}$  labelled HDAC8 with 0 equivalents of **4** (purple) and with 5 equivalents **4** (green). Red arrows indicate peaks that are shifted as a result of ligand binding.

(Figure 4.13a). Zinc preferentially adopts tetrahedral coordination in proteins<sup>234</sup> and as such it is likely that in the absence of a ligand there is a single non-sidechain coordinating contact provided by an exchangeable water molecule. The lack of ligand-free HDAC8 X-ray structures suggests that in an apo-state, the region around the active site of HDAC8 is more flexible. The orientation of the mutated Tyr306Phe sidechain in this structure suggests that were the hydroxyl group of the wild-type protein present, a water-mediated coordinating bond between Tyr306 the catalytic zinc could be made in the apo-state<sup>147</sup> (Figure 4.13a).

The binding of the  $\alpha$ -amino amide inhibitor causes the replacement of the suggested exchangeable water molecule for the strong coordinating bond between the  $Zn^{2+}$  ion the lone pair on the amine  $NH_2$  (2.3 Å)(Figure 4.13b), this causes the rigidification of the local environment. The amide carbonyl of **4** contributes a weaker coordinating interaction (3.0 Å) but is mainly involved in hydrogen bonding to Gly305 via a water molecule (Figure 4.13b).

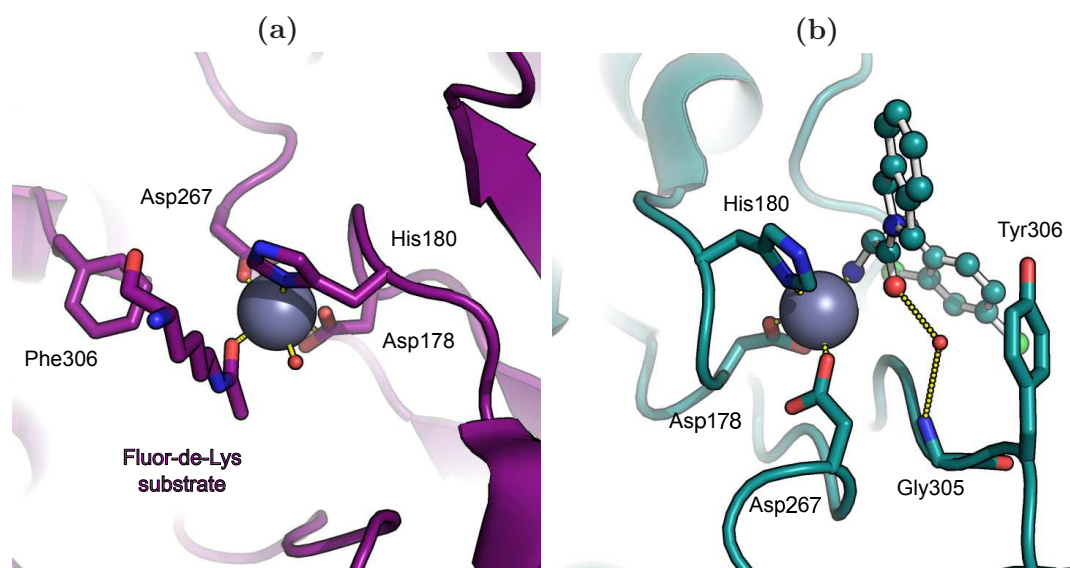


**Figure 4.13:** Coordination of the catalytic  $Zn^{2+}$  ion found in structures with (a) substrate bound square-pyramidal geometry (additional substrate residues and fluorophore not shown), and (b)  $\alpha$ -amino amide inhibitor bound tetrahedral geometry.

NMR chemical shifts were perturbed by the addition of  $\alpha$ -amino amide inhibitor **4**. The most dramatic peak shift was that of Ile34 which is located in the acetate

release pocket and sits 3.3 Å from the chlorine atom at position 4 of the ARBG (Figure 4.12a).

The rigidification of the Zn<sup>2+</sup> coordination is apparent from the chemical shift changes seen in Ile269 and Ile284. Ile269 is separated from Zn<sup>2+</sup> coordinating Asp267 by one residue. The change in Zn<sup>2+</sup> coordinating environment propagates through Asp267 to cause the change in chemical shift at Ile269 (Figure 4.12b). One possible explanation to explain the peak shift of Ile284 is also the propagation of structural changes through hydrophobic regions. Ile284 sits in a hydrophobic pocket which also contains Leu177, a residue adjacent to Zn<sup>2+</sup>-coordinating Asp178. Alteration of the Zn<sup>2+</sup> coordination sphere dynamics results in a structural stiffening that propagates through the coordinating residues Asp178 and Asp267 resulting in a change in chemical environment (and therefore peak position) of both Ile269 and Ile284 (Figure 4.12b).

The movement of the peaks in each case away from 0.8 ppm (<sup>1</sup>H dimension) and 12 ppm (<sup>13</sup>C dimension) is indicative of isoleucine residues becoming more rigid in their conformation<sup>235</sup>. Additionally, two peaks are visible in the apo-state for Ile284 suggesting the presence of two different states, upon inhibitor binding these two peaks merge into one peak suggesting a single conformation for this sidechain in the ligand-bound state. This data suggests that the environment around the Zn<sup>2+</sup> ion is altered upon **4** binding which causes a structural rearrangement and rigidification of the coordinating residues which is then propagated through nearby connected residues to Ile269 and Ile284 where the changes are detected as changes in NMR peak positions.

The shift of these peaks allows us for the first time to directly detect the binding of an inhibitor to the HDAC8 protein using NMR. This result opens the door for NMR based investigations into the binding of inhibitors and other molecules such as substrates and other binding partners to HDAC8. The residues associated with the peaks that shift in NMR titration experiments could identify residues that are important for ligand binding and even provide detailed information about  $k_{on}$  and  $k_{off}$  rates, and the specific protein-ligand interactions that contribute to them.

Current fluorescence based techniques provide only limited information about the binding of an inhibitor to HDAC8. Through utilisation of NMR experiments, precise kinetic rate constants can be obtained. Furthermore as NMR provides structural information about the protein, binding sites can be mapped onto the structure and energetic contributions of individual interactions can be calculated. Various NMR techniques have been developed that allow the detection of weak binding inhibitors<sup>236–238</sup>, multiple inhibitor fragments that bind different regions of a protein have previously been linked to create an inhibitor that binds tightly to the protein<sup>239</sup>. Lastly these experiments are independent of substrate deacetylase activity and so can be performed on mutants with limited activity (thereby reporting the effect of the mutation on ligand binding).

### *Summary*

NMR investigations with selectively labeled HDAC8 showed dramatic changes in the peak positions of certain Ile residues which can be linked to the coordination of the catalytic Zn<sup>2+</sup> and perturbation of the acetate release pocket upon saturation with **4**. This result opens the door for more in-depth ligand binding studies using NMR which are not possible with other methods.

## 4.6 Summary of Results

The exploration of the versatility of the  $\alpha$ -amino amide ZBG was initially performed by altering the ARBG and the STBG. a series of 8 inhibitors was initial synthesised using amide coupling of an *N*-Boc protected amino acid and an amine followed by acidic deprotection of the *N*-Boc protecting group. Assessment of the inhibitory activity of these compounds was performed using a fluorescent HDAC8 activity assay. It was discovered that the presence of chlorine substitutions on the aryl ARBG is essential as a  $\sim 1$  kcal mol<sup>-1</sup> loss in energy was observed when the chloro-substituted ARBG **4** was replaced with an unsubstituted ARBG **36** or *p*-hydroxy-substituted **43**. Tetrahydroisoquinoline was tested as a possible replacement for isoindoline as a STBG because it is a more chemically versatile unit than isoindoline.

Despite the reported flexibility of the HDAC8 substrate tunnel the additional bulk and deviation from the linear and planar isoindoline STBG was not well tolerated (Table 2.4).

After the initial discovery of the importance of the chlorinated aryl ARBG and the linearity and planarity of the STBG, a second generation of  $\alpha$ -amino amide inhibitors were synthesised with a constant 2,4-dichlorophenyl ARBG and varying STBG. STBGs tested included phenyl, *p*-methoxy, hydroxyphenyl and indole groups with methylene linkers as well as a methyl group and a carbazole group (Table 3.2). The most potent inhibitor from this second generation of  $\alpha$ -amino amide inhibitors was 5-fold less potent than the lead compound **4**. However, a trend was seen that suggested that hydrogen bonds were being donated from the inhibitor to HDAC8 with the most potent compounds being ethylindole **78** and ethyl-*p*-hydroxyphenyl **77**. Manual docking of the inhibitors into the HDAC8 structure suggested that the hydrogen bond acceptor was Asp101, a residue reported to be crucial for substrate binding by forming hydrogen bonds with the backbone of the peptide-substrate<sup>84</sup>. In addition to the beneficial effect of a hydrogen-bond donor, a negative effect was seen with hydrogen bond acceptor groups which was reduced by shortening of the linker chain to move the hydrogen bond acceptor away from the Asp101 residue (**69**→**72**).

Combining the observations of the initial two generations of  $\alpha$ -amino amide inhibitors a third round of  $\alpha$ -amino amide inhibitors was synthesised which added hydrogen-bond donating groups to 5-position (the distal end) of the isoindoline. Two synthetic routes were explored to reach substituted isoindoline ring systems. Both these routes were successful but neither were optimised sufficiently to give high yields, this could be improved with optimisation. Upon successful generation of the 5-substituted isoindoline ring system, a series of  $\alpha$ -amino amide inhibitors were generated and assayed for HDAC8 inhibition.

The 5-aminoisoindolyl **97** and 5-acetamido **99** had IC<sub>50</sub> values lower than the unsubstituted isoindoline inhibitor **4** with **99** having an average IC<sub>50</sub> half that of **4** equating to an improvement in binding energy of  $\sim 0.5$  kcal mol<sup>-1</sup>. 5-aminoisoindolyl **99** and 5-acetamido **97** are the most potent  $\alpha$ -amino amide HDAC8 inhibitors that have been reported to-date.

## 4.7 Future work and perspectives

### 4.7.1 Selectivity of $\alpha$ -amino amide HDACi

Currently two HDAC8 inhibitors with an  $\alpha$ -amino amide ZBG have been identified that are more potent than any other  $\alpha$ -amino amide inhibitors reported in the literature. While previous  $\alpha$ -amino amide inhibitors have been reported to be selective for HDAC8 over HDAC1, HDAC2 and HDAC6 (19 fold selectivity<sup>147</sup>), the inhibitors reported in this study are as-yet untested against other HDAC isoforms. Inhibition assays against the other 10 HDAC isoforms would confirm if selectivity for HDAC8 is retained for **99** compared to **4**.

### 4.7.2 Cellular activity of compounds

Mocetinostat (**12**), the class I selective benzamide HDACi is in phase II clinical trials for the treatment of lymphomas and leukemias<sup>240</sup>. It has a reported IC<sub>50</sub> of 150 nM and 290 nM against HDAC1 and HDAC2 respectively. The current generation of  $\alpha$ -amino amide HDAC8 inhibitors have IC<sub>50</sub>s as low as 101 nM, with successive iterations of synthesis and activity measurements (in combination with other binding studies), it is possible that this value will become lower. Therefore the potency of  $\alpha$ -amino amide HDACi is in the range of inhibitors that are currently being used as treatments.

If compounds of this  $\alpha$ -amino amide type are to become drug candidates then their cellular effects need to be investigated. It is possible that the activity of an  $\alpha$ -amino amide based HDAC8 inhibitor in a cell would not be comparable to its activity in the context of purified recombinant enzyme. This could be due to compensating mechanisms, inability to cross the cell membrane, through metabolism of the compound or a number of other reasons. For this reason it would be a good idea to attempt some assays on cell lines to determine the efficacy of **4** in a more physiological setting. From the results of these assays further rational design can be pursued, e.g. if the

compound was metabolised then knowing the metabolic products could lead to the design of a more stable inhibitor. This has been performed with the HDAC8 selective inhibitor PCI-34051 (**1**) which has been modified to be more stable in plasma for animal testing (the structure of the modified inhibitor has not been disclosed)<sup>241</sup>.

### 4.7.3 Expanding the cap-group interactions of 99

The design of an inhibitor with a single directed cap-group hydrogen bond interaction successfully lowered the binding energy by  $\sim 0.5$  kcal mol<sup>-1</sup>. It stands to reason therefore, that if additional orthogonal cap group interactions could be designed, that the binding of the inhibitor could be further improved. HDACi exist that have split cap groups<sup>15,242</sup> so a second isoindoline substitution (if designed carefully) may further improve binding to HDAC. Further investigations and manual docking of hypothetical inhibitors suggests that a second cap-group substitution at position 7 of the isoindoline ring could potentially improve binding. Previous investigations have demonstrated that the AMC fluorophore of the *Fluor-de-Lys* substrate lowers the  $K_M$  dramatically due to aromatic stacking interactions with Tyr100<sup>84</sup>, additionally studies into the sequence specificity of HDAC8 have shown a preference for a phenylalanine at the +1 position of the substrate<sup>191</sup>, finally a series of *N*-acetylthioureas have been shown to bind to HDAC8 independently of substrate and improve activity by lowering the  $K_M$  of the *Fluor-de-Lys* substrate through aromatic interactions<sup>105</sup>. These three reports strongly suggest that designing an inhibitor with an aromatic group that could form aromatic stacking interactions with Tyr100 could dramatically improve binding of a ligand to HDAC8. The inclusion of this particular could additionally increase the specificity of the  $\alpha$ -amino amide inhibitor for HDAC8 as this residue is not conserved among class I HDACs (being acidic residues in HDAC1, HDAC2 and HDAC3)<sup>84</sup>. Aromatic residues are present at this position in HDAC6 (both catalytic domains) and HDAC10 but as the lead compound **4** inhibits HDAC6 very weakly<sup>147</sup> this should not cause an issue.

#### 4.7.4 *in silico* Compound screening

To guide future chemical synthesis it would be useful to have an *in silico* method for ligand screening. many reports have performed *in silico* screening of HDAC8 inhibitors but none of these studies considered  $\alpha$ -amino amide type HDACi or considered the impact of halogen bonding<sup>243–246</sup>. Standard molecular docking algorithms use a crystal structure and allow the sidechains of residues near the binding site to be flexible, the backbone of the protein is fixed so no flexibility of the backbone is taken into account and results are limited as a result. This technique would not work well for the flexible HDAC8 protein, particularly as I have demonstrated above the significance of interactions that occur between ligand and Asp101 on the highly mobile L2 loop. The L2 loop is unresolved in the HDAC8-4 structure<sup>147</sup> that would be used as the basis for docking of any  $\alpha$ -amino amide inhibitor and so the docking would not accurately report interactions in this region even if it were modelled in as it would be considered a rigid structure. Within the lab a large amount of all-atom molecular dynamics (MD) data has been generated simulating HDAC8. Since this data has been generated I think it would be a potentially very powerful dataset for the exploration of potential inhibitors *in silico*.

By using multiple frames from the MD trajectory the flexibility of HDAC8 is accounted for and ligands can be docked into individual rigid structures. As this method removes the need to consider flexibility of sidechains, the docking algorithm is a lot less computationally intensive while having the added advantage of taking the flexibility of the full protein into account. The final difficulty in performing the docking is replicating the halogen bonding interactions that are seen in the HDAC8-4 structure. Standard forcefields used for molecular docking simulations consider each atom to be a point charge and all calculations are performed under this assumption. Due to the electronic anisotropy around the chlorine atoms in the ARBG (discussed in Section 1.4.3) this assumption is not valid. One scoring function has been described which claims to accurately replicate the effects of halogen bonding in ligand docking<sup>186</sup> but this has not been widely applied and rigorously tested. A quantum mechanics-based scoring function has recently been described which may provide a better description of the halogen bonding seen within the HDAC8-4 inter-

action. Through docking of potential inhibitors into multiple frames of an HDAC8 MD trajectory the inherent flexibility of HDAC8 can be accounted for and does not need to be considered during the docking, thereby reducing the time and computational power required. Using new scoring functions that replicate halogen bonding new potential HDAC8i could be screened *in silico* to assess their potential value as HDAC8i.

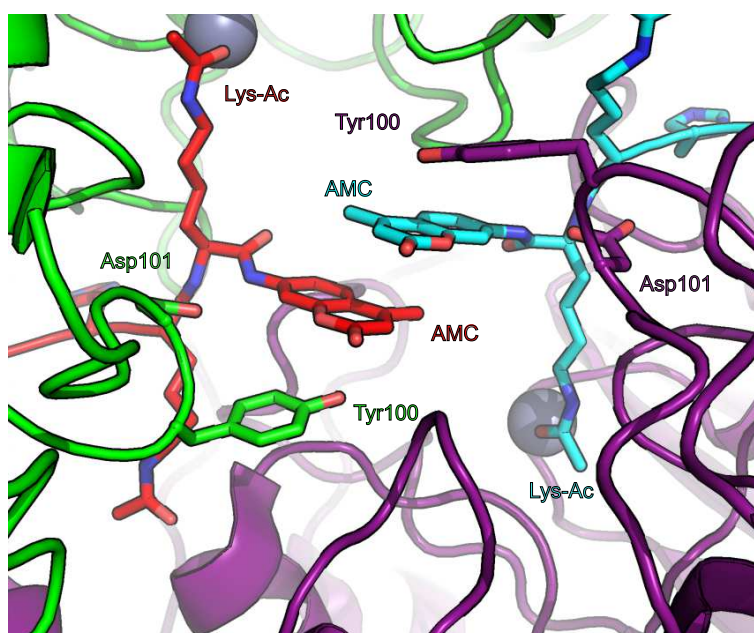


**Figure 4.14:** Crystal packing artefacts in the HDAC-*Fluor-de-Lys* substrate structure. HDAC8 (purple and green) are bound with *Fluor-de-Lys* peptide molecules (cyan and red respectively). The two AMC fluorophores are sandwiched between the two Tyr100 from each monomer.

#### 4.7.5 NMR ligand binding studies

Preliminary NMR investigations were carried out that clearly show the binding of  $\alpha$ -amino amide inhibitor **4** to HDAC8. NMR is known to be a very useful technique in the investigation of protein-ligand interactions<sup>236</sup>, and can provide dynamic, residue-specific information about protein-ligand interactions which can be used to evaluate the ligand binding surface on the protein. This is superior to X-ray crystallography because it is a solution state method and therefore avoids problems associated with

crystal packing artefacts such as is seen in the HDAC8-*Fluor-de-Lys* structure where 2 HDAC8 monomers pack face-to-face and the aromatic stacking interactions occur between the AMC fluorophores belonging to both HDAC8 monomers (Figure 4.14) but also directly estimate the strength of interactions with each residue<sup>247</sup>. Kinetic rate constants can also be calculated.

# 5 Materials and Methods

## 5.1 HDAC8 Sample Preparation

HDAC8 was expressed and purified as described in previous reports<sup>114</sup>. Ile348Val was kindly expressed and purified by Havva Yalinca using a C-terminal His-tagged construct. The protein was been expressed at 21 °C in deuterated M9 media with  $^{13}\text{C}^2\text{H}_3$   $\alpha$ -ketobutyrate (60 mg/L) added 1 hr before induction by isopropyl- $\beta$ -D-thiogalactoside (IPTG). This sample was sufficiently pure for NMR after nickel affinity purification.

The vector used for protein expression was purchased from GenScript (GenScript USA Inc., 860 Centennial Ave., Piscataway, NJ 08854, USA) and consists of a His-tag, NusA, TEV cleavage site and codon optimized human HDAC8. Protein concentrations were determined by measuring the  $A_{280}$  on a Biomate 3 spectrophotometer. The extinction coefficient  $\epsilon_{280}$  for HDAC8 was calculated to be  $53290 \text{ M}^{-1}\text{cm}^{-1}$  using the ProtParam tool at <http://expasy.org>.

### 5.1.1 Site directed mutagenesis

Site directed mutagenesis was performed using primers with optimised melting temperatures of 80°C:

HDAC8\_F152A\_f 5'- CGAAAAAAGACGAAGCCTCGGGTGCTTGTTATCTGAATGATGCG -3'

HDAC8\_F152A\_r 5'- CGCATCATTCAGATAACAAGCACCCGAGGCTTCGTCTTTTTTCG  
-3'

HDAC8\_F208A\_f 5'- TTTCCCCGGGCTTTGCCCCGGGCACCGG -3'

HDAC8\_F208A\_r 5'- CCGGTGCCCCGGGGCAAAGCCCGGGGAAA -3'

PCR was performed using KOD-hot start polymerase (Merck) and parental DNA was digested using DPN1 (New England Biolabs) before transformation into competent DH5 $\alpha$  *E. coli*. Sequences were verified by sequencing using T7\_reverse primer and a forward primer that recognises a sequence in the C-terminal of the N-terminal NusA tag

### 5.1.2 Protein Purification

BL21(DE3) pET-29b+ His-NusA-HDAC8 cells were grown in LB at 37 °C and induced with 1mM isopropyl  $\beta$  -D-1-thiogalactopyranoside (IPTG) and ZnSO<sub>4</sub> (200  $\mu$ M) when  $A_{600}$ = 0.6-1.0. The temperature was decreased to 23 °C for expression and cells were harvested after approximately 16 h.

The cells were harvested by centrifugation (4 °C, 15 min, 4k rpm). Cell pellets were resuspended in lysis buffer (50 mM Tris, pH 8.0, 500 mM KCl, 5 mM imidazole, 3 mM MgCl<sub>2</sub>, 5% glycerol, 5 mM beta-mercaptoethanol, 0.25% IGEPAL) with complete protease inhibitor, lysozyme and DNase.

Cells were lysed using sonication and the lysate centrifuged (4 °C, 50 min, 18 krpm) in a Sorvall standing centrifuge using an SS34 rotor. The lysate supernatant was filtered (0.2  $\mu$ m) and applied to a pre-equilibrated Ni-NTA column (GE Healthcare). The column was washed with washing buffer (50 mM Tris, pH 8.0, 500 mM KCl, 5 mM imidazole, 3 mM MgCl<sub>2</sub>, 5% glycerol, 5 mM beta-mercaptoethanol) and eluted with an imidazole gradient of 0 - 250 mM over 100 mL. HDAC8 containing elution fractions (as determined by SDS-PAGE) were pooled, diluted twofold and dialysed o/n at 4 °C against 2 L of TEV cleavage buffer (50 mM Tris, pH 8.0, 150 mM KCl, 5 mM beta-mercaptoethanol, 5% glycerol). To remove the NusA solubility

tag, TEV-protease was added (0.01 mg/mg protein) and incubated for 3 h at room temperature. If at this time cleavage was not complete more protease was added and incubation time was prolonged (e.g. o/n at 4 °C). The cleaved proteins were separated by a second pass over a Ni-NTA affinity column (equilibrated with washing buffer). The NusA solubility tag and TEV protease are retained on the column due to the presence of a His-tag, this step also removes other protein impurities which bound to the nickel resin and eluted in the first Ni-NTA pass. The HDAC8 containing flowthrough was concentrated and purified by gel filtration on an S75 column (GE Healthcare) equilibrated with gel filtration buffer (50 mM Tris pH 8.0, 150 mM KCl, 1 mM TCEP 5% glycerol), the relevant fractions were concentrated, and aliquotted before snap-freezing in liquid nitrogen and storage at -80°C.

### 5.1.3 HDAC8 fluorogenic activity Assay

The MAL substrate was kindly synthesised by Chris Matthews. As a single residue (rather than commercial *Fluor-de-Lys* tetrapeptide), this substrate has a higher  $K_M$  than the *Fluor-de-Lys* substrate but it is cheap and easy to synthesise, the assay is not compromised as  $[S] \gg [E]$  is still satisfied (so Michaelis Menten conditions are still met). The AMC fluorophore is used in both substrates so other parameters do not need to be modified and the same standard curve can be used to quantify deacylation in each case.

The inhibitor was diluted to 2 - 10 mM using DMSO- $d_6$  and the concentration measured using NMR (see Section 5.2.2), and was diluted to the maximum stock concentration with assay buffer: 50 mM Tris/Cl pH 8.0, 137 mM NaCl, 2.7 mM KCl, 1 mM MgCl<sub>2</sub>, 10% Polythelene glycol (PEG) (avg. MW 8000 Da), 1 mg/mL bovine serum albumin (BSA). New inhibitor dilutions were made from the DMSO- $d_6$  stock for each independent repeat. It was found that serial dilutions of inhibitor gave more consistent results than regularly distributed dilutions. Assay buffer was used to dilute all other stock solutions.

### Inhibition assays

To inhibitor (10  $\mu\text{L}$ , 5x final concentration) in a 96 well, 1/2 area, white microtitre plate (Corning), was added HDAC8 (15  $\mu\text{L}$  3.3x final concentration), 25  $\mu\text{L}$  substrate (2x final concentration, diluted in assay buffer) was then added and mixed using a multichannel pipette. The deacetylation reaction was allowed to proceed for 1 h before the addition of 50  $\mu\text{L}$  developer solution (assay buffer + 2 mg/ml trypsin and 4  $\mu\text{M}$  TSA), the TSA in the developer solution was subsequently replaced with 2  $\mu\text{M}$  **4** after the  $K_i$  of TSA was measured at 1.6  $\mu\text{M}$  and was therefore unfit for purpose as a reaction quenching agent. The stopped reactions were incubated at 20  $^\circ\text{C}$  for 15 - 45 min (the signal was seen to be stable over this time period) and then the fluorescence was read using a Fluostar Optima (BMG Labtech) plate reader  $\lambda_{ex} = 380$  nm and  $\lambda_{em} = 460$  nm.

The results of the assay were processed using a script written in MatLab<sup>®</sup>. A baseline fluorescence value was subtracted from all wells and the fluorescence values (in arbitrary fluorescence units) were normalised against an uninhibited control to give relative fluorescence values. The data were fitted to a Michaelis-Menten model using a non-linear regression using all points (Equation 5.1).

$$y = \frac{K_{cat}E_0S}{K_M(1 + I/K_i) + S} / \frac{K_{cat}E_0S}{K_M + S} \quad (5.1)$$

### Activity assays

Activity assays were performed in microcentrifuge tubes with the stated concentrations of HDAC8 and substrate. At each timepoint 50  $\mu\text{L}$  was removed from the reaction tube and quenched with 50  $\mu\text{L}$  developer solution in a 96 well, 1/2 area, white microtitre plate (Corning), the plate was incubated for 15 min. Fluorescence was subsequently measured as above and data analysed using Microsoft Excel.

### 5.1.4 Manual Molecular docking

All structural figures were made using PyMOL<sup>248</sup>. Manual docking was performed using PyMOL and Avogadro, a molecular editor<sup>208</sup>. The HDAC-4 X-ray structure (PDB:3SFH) was downloaded from the PDB and loaded into PyMOL. The ligand (**4**) was extracted and modified to make the target inhibitor in Avogadro. Atoms which are common to both the lead compound **4** and the target were then fixed and an energy minimisation was performed on the remaining atoms using the UFF forcefield with steepest decent algorithm, this process was repeated multiple times if rotamers were possible. The energy minimised ligand was loaded into the HDAC8-4 structure with the ligand removed. The newly created bonds were rotated to position relevant groups in appropriate positions using Pymol. The STBG was energy minimised a second time in the same way to ensure the dihedral angles were in allowed regions before loading into the crystal structure a final time.

## 5.2 NMR experiments

### 5.2.1 Methyl-TROSY NMR

<sup>13</sup>CH<sub>3</sub>Ile-labeled HDAC8-Ile348Val (20  $\mu$ M in 50 mM potassium phosphate, 30 mM sodium chloride, 99% D<sub>2</sub>O, pH 8.2) was mixed with **4** (10  $\mu$ L, 2.4 mM in DMSO-*d*<sub>6</sub>) in a Shigemi NMR tube at 25 °C. Methyl-TROSY HMQC spectra were recorded on a Varian 600MHz spectrometer before and after addition of **4**. The sweepwidth in the indirect dimension was 1800 Hz, 256 complex points were collected. The number of measurements in the direct dimension was 1536 real points and 768 complex points, with an acquisition time of 64 ms. The total experiment time was approximately 4 hours.

### 5.2.2 NMR concentration measurements

The mass of solid obtained from the *N*-Boc deprotection did not reliably correlate to the amount of  $\alpha$ -amino amide salt present owing to the often very hygroscopic nature of the  $\alpha$ -amino amide hydrochloride salts (as mentioned in Section 2.2.3). To account for this discrepancy, an NMR sample was made in deuterated DMSO and the concentration quantified using the quantint macro within the TopSpin NMR software (kindly set up by Dr. Abil Aliev). This method uses an external sample of a known concentration (recorded previously) to set the peak integral reference. The concentration of a sample is calculated by defining peak integral regions and running the macro which calibrates the scaling of the integral regions to give the concentration in mM of that region. Because absorbed water does not contribute to the NMR signals of the molecule (peaks away from the water signal are used for quantification), this method allows concentration measurement that is independent of any water absorbed by the compound. This method also allows greater accuracy of inhibitor concentrations within the assay as two sources of error are removed (the weighing of the solid sample and the measuring of the solvent volume). Therefore with this NMR concentration measurement greater confidence can be given to the exact inhibitor concentration within the assay.

## 5.3 General Chemistry experimental

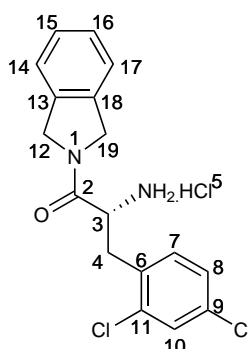
Chemicals were used as supplied from commercial sources, solvents used were reagent grade, when not purchased as anhydrous, anhydrous solvents were obtained from Anhydrous Engineering (USA) solvent systems after passing through an alumina column. Compound homogeneity was monitored by ascending thin-layer chromatography, performed on Merck 0.2 mm aluminum-backed silica gel 60 F254 plates and visualized using an alkaline potassium permanganate dip or by ultraviolet light. Flash column chromatography was performed using Merck 0.040 to 0.063 mm, 230 to 400 mesh silica gel. Evaporation refers to the removal of solvent under reduced pressure. Hydrogen chloride was generated by the dropping of concentrated sulfuric

acid into a flask containing sodium chloride equipped with a magnetic stirrer. Optical rotation measurements were performed on a Perkin Elmer 343 polarimeter using a 1 mL 10 cm pathlength cell, in the stated solvent. Melting points were measured on an electrothermal 9100 melting point apparatus. NMR spectra were recorded at 300 MHz on a Bruker AMX300 spectrometer, at 400 MHz on a Bruker AMX400, at 500 MHz on a Bruker Avance 500 spectrometer or at 600 MHz on a Bruker Avance 600 spectrometer in the stated solvent; chemical shifts are reported in  $\delta$  (ppm) relative to the lock signal of the stated solvent. Infrared spectra were recorded on a Bruker Alpha FTIR spectrometer equipped with a diamond ATR prism. Mass spectra were recorded in the UCL mass spectrometry facility on a Finnigan MAT 900XP or a capLC-MS<sup>n</sup> Thermo Finnigan LTQ spectrometer.

*note on NMR assignments:* Where ambiguous, assignments have been made using an oblique (ie. C<sub>(7)</sub>/C<sub>(9)</sub> means C<sub>(7)</sub> or C<sub>(9)</sub>), where peaks arise from more than one nucleus the assignments are separated with a comma (ie. C<sub>(7),C</sub>(9) means C<sub>(7)</sub> and C<sub>(9)</sub>).

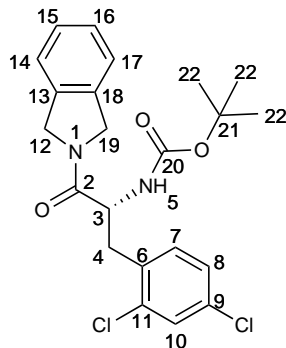
## 5.4 Chemistry experimental procedures and characterisation

(*R*)-2-Amino-3-(2,4-dichlorophenyl)-1-(isoindolin-2-yl)propan-1-one hydrochloride (4)



*N*-Boc protected amide **31** (0.15 g, 0.35 mmol) was dissolved in diethyl ether (10 mL) and hydrogen chloride was bubbled through while stirring for 2 h. The precipitate was filtered by gravity filtration through filter paper in a funnel that was on top of a flask of boiling ether **4** (114 mg, 87%) as a white solid, m.p.(decomp. 175 °C);  $[\alpha]_D^{25}$   $c=1$  methanol: -41.0°;  $\nu_{max}$  ( $\text{cm}^{-1}$ ) 3080-2680 br. (NH), 1644 (C=O);  $^1\text{H}$  NMR (500 MHz, DMSO- $d_6$ )  $\delta$  ppm 8.73 (3H, br.s, H<sub>(5)</sub>), 7.55 (1H, d,  $J=1.4$  Hz, H<sub>(10)</sub>), 7.47 (1H, d,  $J=8.1$  Hz, H<sub>(7)</sub>/H<sub>(8)</sub>), 7.33 - 7.40 (1H, m, H<sub>(8)</sub>/H<sub>(7)</sub>), 7.19 - 7.33 (4H, m, aryl), 5.04 (1H, d,  $J=13.6$  Hz, H<sub>(12)</sub>/H<sub>(19)</sub>), 4.51 (1H, d,  $J=16.0$  Hz, H<sub>(19)</sub>/H<sub>(12)</sub>), 4.36 (1H, br.s, H<sub>(3)</sub>), 4.21 (1H, d,  $J=13.6$  Hz, H<sub>(19)</sub>/H<sub>(12)</sub>), 3.17 - 3.48 (3H, m, 2H<sub>(5)</sub>, H<sub>(19)</sub>/H<sub>(12)</sub>);  $^{13}\text{C}$  NMR (126 MHz, methanol)  $\delta$  ppm 166.48 C<sub>(2)</sub>, 135.74, 135.16, 134.55, 133.55, 133.03, 131.64, 128.81, 127.64, 127.56, 122.98, 122.73, 52.08 C<sub>(12)</sub>/C<sub>(19)</sub>, 51.68 C<sub>(3)</sub>, 49.98 C<sub>(19)</sub>/C<sub>(12)</sub>, 33.30 C<sub>(4)</sub>; HRMS calcd for C<sub>17</sub>H<sub>17</sub>Cl<sub>2</sub>N<sub>2</sub>O: 435.1242, found: 435.1230.

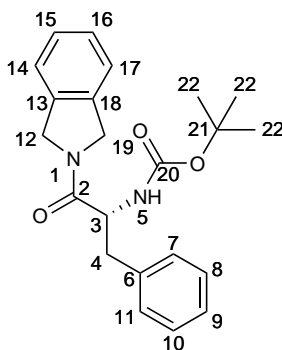
**(*R*)-tert-Butyl (3-(2,4-dichlorophenyl)-1-(2,3-dihydro-1H-inden-2-yl)-1-oxopropan-2-yl)carbamate (31)**<sup>147</sup>



To isoindoline (0.11 mL, 1.0 mmol), *N*-Boc-(*R*)-2,4-dichlorophenylalanine (344 mg, 1.0 mmol), 1-ethyl-3-(3-dimethylaminopropyl)carbodiimide (182 mg, 1.0 mmol) and anhydrous 1-hydroxybenzotriazole (203 mg, 1.5 mmol) in dimethylformamide (3.0 mL) was added *N,N*-diisopropylethylamine (1.3 mL, 7.5 mmol), the mixture was then stirred for 20 h at 20 °C. The solvent was evaporated, the residue was dissolved in ethyl acetate (20 mL) and washed with water (2 x 20 mL). The combined aqueous

fractions were re-extracted with ethyl acetate (4 x 20 mL) and the combined organic layers were washed with saturated aqueous sodium hydrogen carbonate (2 x 20 mL) and brine (20 mL) before being dried over magnesium sulfate and evaporated. The residue was purified by silica column chromatography (5% ethyl acetate in dichloromethane) to give **31** (330 mg, 76%) as a pale yellow solid, m.p. 160-162 °C;  $[\alpha]_D^{25} c=1$  CHCl<sub>3</sub> -24.7°;  $\nu_{max}$  (cm<sup>-1</sup>): 3429 (NH), 3296 (NH), 1704 (NHC=O), 1641 (CHC=O); <sup>1</sup>H NMR (500 MHz, chloroform-*d*)  $\delta$  ppm 7.30 (1H, m, aryl) 7.07 - 7.27 (6H, m, aryl), 5.67 (1H, d,  $J=9.1$  Hz, H<sub>(5)</sub>), 4.93 - 5.03 (1H, d,  $J=13.7$  Hz, H<sub>(12)</sub>/H<sub>(19)</sub>), 4.84 - 4.92 (1H, m, H<sub>(3)</sub>), 4.72 - 4.83 (1H, d,  $J=15.6$  Hz, H<sub>(19)</sub>/H<sub>(12)</sub>), 4.62 - 4.72 (1H, d,  $J=14.8$  Hz, H<sub>(19)</sub>/H<sub>(12)</sub>), 3.16 (1H, dd,  $J=13.6, 6.1$  Hz, H<sub>(4)</sub>), 3.03 (1H, dd,  $J=13.6, 8.2$  Hz, H<sub>(4)</sub>), 1.22 - 1.42 (9H, m, 3 x 3H<sub>(22)</sub>); <sup>13</sup>C NMR (126 MHz, chloroform-*d*)  $\delta$  ppm 170.22 C<sub>(2)</sub>, 155.05 C<sub>(20)</sub>, 135.85 C<sub>(13)</sub>/C<sub>(18)</sub>, 135.80 C<sub>(13)</sub>/C<sub>(18)</sub>, 135.16 C<sub>(6)</sub>, 133.62, 133.14, 132.83, 129.30, 127.97, 127.74, 127.07, 122.97, 122.80, 79.88 C<sub>(21)</sub>, 52.41 C<sub>(12)</sub>/C<sub>(19)</sub>, 52.37 C<sub>(19)</sub>/C<sub>(12)</sub>, 51.03 C<sub>(3)</sub>, 36.66 C<sub>(4)</sub>, 28.32 C<sub>(22)</sub>; HRMS calcd for C<sub>22</sub>H<sub>24</sub>Cl<sub>2</sub>N<sub>2</sub>O<sub>3</sub> 435.1242, found: 435.1230.

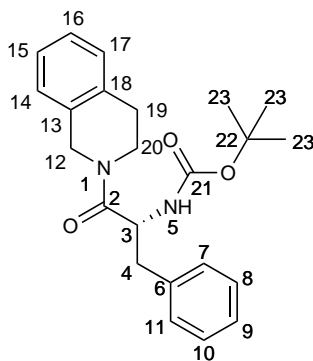
**(*R*)-tert-Butyl(1-(isoindolin-2-yl)-1-oxo-3-phenylpropan-2-yl)carbamate (32)**<sup>249</sup>



A literature procedure<sup>249</sup> using triethylamine was adapted for use with *N*-diisopropylethylamine. To isoindoline (0.11 mL, 1.0 mmol), *N*-Boc-(*R*)-phenylalanine (265 mg, 1.0 mmol), 1-ethyl-3-(3-dimethylaminopropyl)carbodiimide (182 mg, 1.0 mmol) and anhydrous 1-hydroxybenzotriazole (203 mg, 1.5 mmol) in dimethylformamide (3.0 mL) was added *N,N*-diisopropylethylamine (1.3 mL, 7.5 mmol). The mixture was

stirred for 16 h at 20 °C. The solvent was evaporated, the residue was dissolved in ethyl acetate (20 mL) and washed with water (2 x 20 mL). The combined aqueous fractions were re-extracted with ethyl acetate (2 x 20 mL) and the combined organic layers were washed with saturated sodium hydrogen carbonate solution (2 x 20 mL) and brine (20 mL) before being dried over magnesium sulfate and evaporated. The residue was purified by silica column chromatography (25% ethyl acetate/hexane) to give **32** (175 mg, 48%) as a cream solid, m.p. 156-160 °C; <sup>1</sup>H NMR (500 MHz, chloroform-*d*) δ ppm 7.20 - 7.30 (7H, aryl), 7.15 (1H, m, aryl), 7.10 (1H, m, aryl), 5.36 (1H, d, *J*=9.0 Hz, H<sub>(5)</sub>), 4.88, (1H, d, *J*=13.8 Hz, H<sub>(12)</sub>/H<sub>(19)</sub>), 4.82 (1H, d, *J*=15.9 Hz, H<sub>(19)</sub>/H<sub>(12)</sub>), 4.68 - 4.77 (1H, m, H<sub>(3)</sub>), 4.63 (1H, d, *J*=15.9 Hz, H<sub>(19)</sub>/H<sub>(12)</sub>), 4.06 (1H, d, *J*=13.8 Hz, H<sub>(12)</sub>/H<sub>(19)</sub>), 2.98 - 3.10 (2H, m, 2H<sub>(4)</sub>), 1.36 - 1.44 (9H, m, 3 x 3H<sub>(22)</sub>); <sup>13</sup>C NMR (126 MHz, chloroform-*d*) δ ppm 170.7 C<sub>(2)</sub>, 155.2 C<sub>(20)</sub>, 136.4 C<sub>(13)</sub>/C<sub>(18)</sub>, 136.0 C<sub>(18)</sub>/C<sub>(13)</sub>, 135.8 C<sub>(6)</sub>, 129.4 C<sub>(8)</sub>,C<sub>(10)</sub>, 128.5 C<sub>(7)</sub>,C<sub>(11)</sub>, 127.8 C<sub>(15)</sub>/C<sub>(16)</sub>, 127.6 C<sub>(16)</sub>/C<sub>(15)</sub>, 127.1 C<sub>(17)</sub>, 122.9 C<sub>(14)</sub>/C<sub>(9)</sub>, 122.6 C<sub>(17)</sub>/C<sub>(14)</sub>, 79.9 C<sub>(21)</sub>, 53.4 C<sub>(3)</sub>, 52.2 C<sub>(12)</sub>/C<sub>(19)</sub>, 52.1 C<sub>(12)</sub>/C<sub>(19)</sub>, 39.9 C<sub>(4)</sub>, 28.4 C<sub>(22)</sub>.

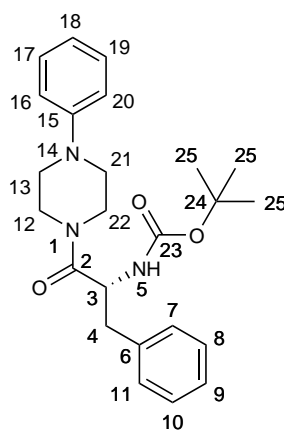
**(*R*)-tert-Butyl(1-(3,4-dihydroisoquinolin-2(1*H*)-yl)-1-oxo-3-phenylpropan-2-yl)carbamate (**33**)<sup>250</sup>**



A literature procedure<sup>250</sup> was adapted to use DMF as a solvent. To tetrahydroisoquinoline (0.13 mL, 1.0 mmol), *N*-Boc-(*R*)-phenylalanine (265 mg, 1.0 mmol), 1-ethyl-3-(3-dimethylaminopropyl)carbodiimide (182 mg, 1.0 mmol) and anhydrous 1-hydroxybenzotriazole (203 mg, 1.5 mmol) in dimethylformamide (3.0 mL) was added

*N,N*-diisopropylethylamine (1.3 mL, 7.5 mmol), the mixture was then stirred for 16 h at 20 °C. The solvent was evaporated, the residue was dissolved in ethyl acetate (20 mL) and washed with water (2 x 20 mL). The combined aqueous fractions were re-extracted with ethyl acetate (2 x 20 mL) and the combined organic layers were washed with saturated aqueous sodium hydrogen carbonate (2 x 20 mL) and brine (20 mL) before being dried over magnesium sulfate and evaporated. The residue was purified by silica column chromatography (25% ethyl acetate, 75% hexane) to give **33** (207 mg, 57%) as a colourless oil,  $\nu_{max}$  (cm<sup>-1</sup>): 4322 (NH), 3300 (NH), 1702 (NHC=O), 1635 (CHC=O); <sup>1</sup>H NMR (500 MHz, chloroform-*d*, 2 rotamers)  $\delta$  ppm 6.77 - 7.23 (9H, aryl), 5.48 - 5.65 (1H, m, H<sub>(5)</sub>), 4.84 - 4.98 (1H, m, H<sub>(3)</sub>), 4.68 - 4.77, 4.52 - 4.61, 4.43 - 4.52, 3.93 - 4.03 (2H, m, H<sub>(12)</sub>), 3.09 - 3.85 (2H, m, 2H<sub>(20)</sub>), 2.90 - 3.06 (1H, m, H<sub>(19)</sub>), 2.93 - 2.98 (1H, m, H<sub>(4)</sub>), 2.22 - 2.83 (2H, m, H<sub>(4)</sub>, H<sub>(19)</sub>), 1.41 (9H, s, 3 x H<sub>(23)</sub>); <sup>13</sup>C NMR (126 MHz, chloroform-*d*, 2 rotamers)  $\delta$  ppm 170.75 C<sub>(2)</sub>, 170.45 C<sub>(2)</sub>, 155.20 C<sub>(21)</sub>, 155.17 C<sub>(21)</sub>, 136.60, 136.36, 134.54, 134.12, 132.84, 132.17, 129.53, 129.38, 128.64, 128.50, 128.34, 128.29, 126.92, 126.86, 126.62, 126.57, 126.54, 126.30, 126.15, 79.64 C<sub>(22)</sub>, 51.88 C<sub>(3)</sub>, 51.66 C<sub>(3)</sub>, 47.06 C<sub>(12)</sub>, 44.55 C<sub>(12)</sub>, 43.09 C<sub>(20)</sub>, 40.50 C<sub>(20)</sub>, 40.40 C<sub>(4)</sub>, 40.24 C<sub>(4)</sub>, 29.15 C<sub>(19)</sub>, 28.46 C<sub>(23)</sub>, 28.35 C<sub>(19)</sub>.

**(*R*)-tert-Butyl (1-oxo-3-phenyl-1-(4-phenylpiperazin-1-yl)propan-2-yl) carbamate (34)**

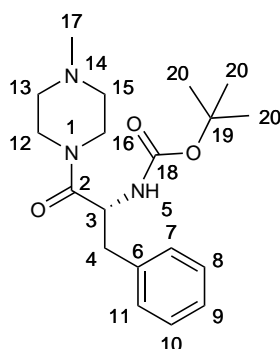


To phenylpiperazine (0.16 mL, 1.0 mmol), *N*-Boc-(*D*)-phenylalanine (265 mg, 1.0

mmol), 1-ethyl-3-(3-dimethylaminopropyl)carbodiimide (182 mg, 1.0 mmol) and anhydrous 1-hydroxybenzotriazole (203 mg, 1.5 mmol) in dimethylformamide (3.0 mL) was added *N,N*-diisopropylethylamine (1.3 mL, 1.0 mmol), the mixture was then stirred for 16 h at 20 °C. The solvent was evaporated, the residue was dissolved in ethyl acetate (20 mL) and washed with water (2 x 20 mL). The combined aqueous fractions were re-extracted with ethyl acetate (2 x 20 mL) and the combined organic layers were washed with saturated aqueous sodium hydrogen carbonate (2 x 20 mL) and brine (20 mL) before being dried over magnesium sulfate and evaporated. The residue was purified by silica column chromatography (14% ethyl acetate 86% dichloromethane) to give **34** (307 mg, 64%) as a white solid, m.p. (decomp 170 °C);  $\nu_{max}$  (cm<sup>-1</sup>): 3393 (NH), 3200-2500 br. (NH), 1648 (C=O);

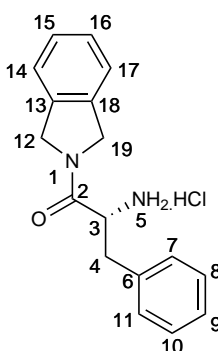
<sup>1</sup>H NMR (500 MHz, chloroform-*d*)  $\delta$  ppm 7.16 - 7.32 (7H, m, aryl), 6.87 (1H, t, *J*=7.3 Hz, aryl), 6.81 (2H, d, *J*=8.4 Hz, aryl), 5.62 (1H, d, *J*=8.8 Hz, H<sub>(5)</sub>), 4.84 - 4.94 (1H, m, H<sub>(3)</sub>), 3.60 - 3.75 (2H, m, H<sub>(12)</sub>/H<sub>(22)</sub>), 3.39 - 3.49 (1H, m, H<sub>(12)</sub>/H<sub>(22)</sub>), 2.97 - 3.19 (4H, m, H<sub>(4)</sub>,H<sub>(12)</sub>/H<sub>(22)</sub>,H<sub>(13)</sub>/H<sub>(21)</sub>), 2.87 - 2.96 (2H, m, H<sub>(4)</sub>,H<sub>(13)</sub>/H<sub>(21)</sub>), 2.39 - 2.50 (1H, m, H<sub>(13)</sub>/H<sub>(21)</sub>), 1.44 (9H, s, 3 x 3H<sub>(25)</sub>); <sup>13</sup>C NMR (126 MHz, chloroform-*d*)  $\delta$  ppm 170.20 C<sub>(2)</sub>, 155.13 C<sub>(23)</sub>, 150.79 C<sub>(15)</sub>, 136.46 C<sub>(6)</sub>, 129.65, 129.27, 128.66, 127.14, 120.61, 116.68 C<sub>(16)</sub>,C<sub>(20)</sub>, 79.88 C<sub>(24)</sub>, 51.03 C<sub>(3)</sub>, 49.32 C<sub>(13)</sub>/C<sub>(21)</sub>, 49.06 C<sub>(21)</sub>/C<sub>(13)</sub>, 45.46 C<sub>(12)</sub>/C<sub>(22)</sub>, 41.91 C<sub>(22)</sub>/C<sub>(12)</sub>, 40.57 C<sub>(4)</sub>, 28.43 C<sub>(25)</sub>.

**(*R*)-tert-Butyl(1-(4-methylpiperazin-1-yl)-1-oxo-3-phenylpropan-2-yl)-carbamate (35)**



To *N*-methylpiperazine (0.11 mL, 1.0 mmol), *N*-Boc-(*R*)-phenylalanine (265 mg, 1.0 mmol), 1-ethyl-3-(3-dimethylaminopropyl)carbodiimide (182 mg, 1.0 mmol) and anhydrous 1-hydroxybenzotriazole (203 mg, 1.5 mmol) in dimethylformamide (3.0 mL) was added *N,N*-diisopropylethylamine (1.3 mL, 7.5 mmol), the mixture was then stirred for 16 h at 20 °C. The solvent was evaporated, the residue was dissolved in ethyl acetate (20 mL) and washed with water (2 x 20 mL). The combined aqueous fractions were re-extracted with ethyl acetate (2 x 20 mL) and the combined organic layers were washed with saturated aqueous sodium hydrogen carbonate (2 x 20 mL) and brine (20 mL) before being dried over magnesium sulfate and evaporated. The residue was purified by silica column chromatography (15% methanol 85% ethyl acetate) to give **35** (174 mg, 50%) as a colourless oil,  $\nu_{max}$  (cm<sup>-1</sup>): 3297 (NH), 1704 (NHC=O), 1639 (CHC=O); <sup>1</sup>H NMR (500 MHz, chloroform-*d*)  $\delta$  ppm 7.05 - 7.22 (5H, m, aryl), 5.60 (1H, d, *J*=8.7 Hz, H<sub>(5)</sub>), 4.74 (1H, m, H<sub>(3)</sub>), 3.36 - 3.55 (2H, m, 2H<sub>(12)</sub>/2H<sub>(16)</sub>), 3.19 - 3.27 (1H, m, H<sub>(4)</sub>), 2.79 - 3.03 (3H, m, H<sub>(4)</sub>, 2H<sub>(16)</sub>/2H<sub>(12)</sub>), 2.15 - 2.29 (1H, m, H<sub>(13)</sub>/H<sub>(15)</sub>), 1.98 - 2.14 (5H, m, 1H<sub>(13)</sub>, 1H<sub>(15)</sub>, 3H<sub>(17)</sub>), 1.55 - 1.74 (1H, m, H<sub>(13)</sub>/H<sub>(15)</sub>), 1.32 (9H, s, 3 x 3H<sub>(20)</sub>); <sup>13</sup>C NMR (126 MHz, chloroform-*d*)  $\delta$  ppm 169.93 C<sub>(2)</sub>, 155.07 C<sub>(18)</sub>, 136.53 C<sub>(7)</sub>, 129.58 C<sub>(8)</sub>, C<sub>(10)</sub>, 128.50 C<sub>(7)</sub>/C<sub>(11)</sub>, 126.90 C<sub>(9)</sub>, 79.51 C<sub>(19)</sub>, 54.45 C<sub>(13)</sub>, C<sub>(15)</sub>, 54.34 C<sub>(13)</sub>/C<sub>(15)</sub>, 50.88 C<sub>(3)</sub>, 45.81 C<sub>(17)</sub>, 45.35 C<sub>(5)</sub>, 41.77 C<sub>(12)</sub>/C<sub>(16)</sub>, 40.33 C<sub>(12)</sub>/C<sub>(16)</sub>, 28.38 3C<sub>(2)</sub>.

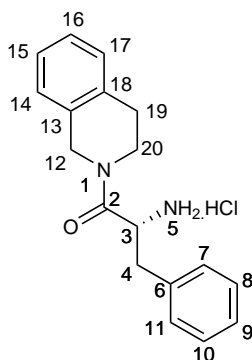
**(*R*)-2-Amino-1-(isoindolin-2-yl)-3-phenylpropan-1-one hydrochloride (36)**



*N*-Boc protected amide **32** (182 mg, 497  $\mu$ mol) was dissolved in diethyl ethereal

hydrochloric acid (10 mL, 1 M) and the mixture stirred at 20 °C for 16 h. The solvent was evaporated to give **36** as a pale brown solid (139 mg, 92%), m.p. (decomp. 220 °C);  $[\alpha]_D^{25}$   $c=1$  methanol -30.4°;  $\nu_{max}$  ( $\text{cm}^{-1}$ ): 3362 (NH), 3000-2800 br. (NH), 1650 (C=O);  $^1\text{H}$  NMR (500 MHz, DMSO- $d_6$ )  $\delta$  8.71 (3H, br.s, 3H<sub>(5)</sub>), 7.15 - 7.31 (9H, m, aryl), 4.93 (1H, d,  $J=14.0$  Hz, H<sub>(12)</sub>/H<sub>(19)</sub>), 4.69 (1H, d,  $J=16.1$  Hz, H<sub>(19)</sub>/H<sub>(12)</sub>), 4.50 (1H, d,  $J=16.1$  Hz, H<sub>(19)</sub>/H<sub>(12)</sub>), 4.32 (1H, br.s, H<sub>(3)</sub>), 3.92 (1H, d,  $J=14.0$  Hz H<sub>(12)</sub>/H<sub>(19)</sub>), 3.26 (1H, dd,  $J=13.2, 5.5$  Hz, H<sub>(4)</sub>), 3.05 (1H, dd,  $J=13.2, 9.0$  Hz, H<sub>(4)</sub>);  $^{13}\text{C}$  NMR (126 MHz, DMSO- $d_6$ )  $\delta$  166.9 C<sub>(2)</sub>, 135.9 C<sub>(13)</sub>/C<sub>(18)</sub>/C<sub>(6)</sub>, 135.1 C<sub>(13)</sub>/C<sub>(18)</sub>/C<sub>(6)</sub>, 134.8 C<sub>(13)</sub>/C<sub>(18)</sub>/C<sub>(6)</sub>, 129.5 C<sub>(10)</sub>,C<sub>(8)</sub>, 128.6 C<sub>(7)</sub>,C<sub>(11)</sub>, 127.6 C<sub>(15)</sub>/C<sub>(16)</sub>, 127.6 C<sub>(16)</sub>/C<sub>(15)</sub>, 127.3 C<sub>(9)</sub>, 123.0 C<sub>(14)</sub>/C<sub>(17)</sub>, 122.6 C<sub>(17)</sub>/C<sub>(14)</sub>, 52.0 C<sub>(3)</sub>, 51.9 C<sub>(12)</sub>/C<sub>(19)</sub>, 51.6 C<sub>(19)</sub>/C<sub>(12)</sub>, 36.5 C<sub>(4)</sub>; m/z: (CI+) 267 ([M-Cl]<sup>+</sup>, 21%) 175 ([M-Cl-CH<sub>2</sub>C<sub>6</sub>H<sub>5</sub>]<sup>+</sup>, 55%), 118, ([isoindoline]<sup>+</sup>, 34%), 120 ([C<sub>8</sub>H<sub>(10)</sub>N]<sup>+</sup>, 55%), 85 (100%); HRMS calcd for C<sub>17</sub>H<sub>20</sub>N<sub>2</sub>O requires: 267.1497, found 267.1495.

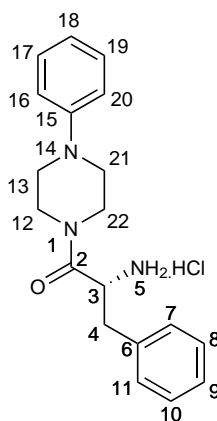
**(R)-2-Amino-1-(3,4-dihydroisoquinolin-2(1H)-yl)-3-phenylpropan-1-one hydrochloride (37)**



*N*-Boc protected amide **33** (207 mg, 54 mmol) was dissolved in ethereal hydrogen chloride (1 M, 10 mL) and stirred at 20 °C for 16 h, the solvent was evaporated to give **37** (142 mg, 85%) as a hygroscopic pale yellow solid,  $[\alpha]_D^{25}$  methanol: -7.8°;  $\nu_{max}$  ( $\text{cm}^{-1}$ ): 3200-2500 br. (NH), 1641 (C=O);  $^1\text{H}$  NMR (500 MHz, DMSO- $d_6$ , 2 rotamers)  $\delta$  ppm 8.46 (3H, br.s, 3H<sub>(5)</sub>), 6.91 - 7.36 (9H, m, aryl), 3.90 - 4.66 (2H, m, 2H<sub>(12)</sub>), 3.50 - 3.68 (2H, m, H<sub>(3)</sub>,H<sub>(20)</sub>), 3.11 - 3.24 (1H, m, H<sub>(4)</sub>), 2.91 - 3.07 (1H,

m, H<sub>(4)</sub>), 2.54 - 2.76, 2.15 - 2.36, 1.23 - 1.36 (2H, m 2H<sub>(19)</sub>); <sup>13</sup>C NMR (126 MHz, DMSO-*d*<sub>6</sub>, 2 rotamers) δ ppm 167.21 C<sub>(2)</sub>, 166.90 C<sub>(2)</sub>, 134.55, 134.29, 134.22, 134.07, 132.37, 132.33, 129.57, 129.47, 128.51, 128.33, 128.23, 127.27, 127.12, 126.58, 126.49, 126.43, 126.22, 126.09, 126.05, 50.37 C<sub>(3)</sub>, 50.18 C<sub>(3)</sub>, 46.15 C<sub>(12)</sub>, 44.03 C<sub>(12)</sub>, 42.52 C<sub>(20)</sub>, 36.99 C<sub>(4)</sub>, 36.78 C<sub>(4)</sub>, 28.34 C<sub>(19)</sub>, 27.58 C<sub>(19)</sub>. HRMS calcd for C<sub>18</sub>H<sub>21</sub>N<sub>2</sub>O: 281.1654, found 281.1650.

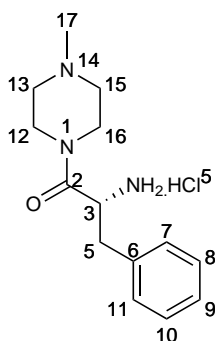
**(*R*)-2-Amino-3-phenyl-1-(4-phenylpiperazin-1-yl) propan-1-one hydrochloride(38)**



*N*-Boc protected amide **34** (307 mg, 0.75 mmol) was dissolved in dry diethyl ether (10 mL). Hydrogen chloride was bubbled through the solution with vigorous stirring for 5 h. The precipitate was filtered by gravity filtration through filter paper in a funnel that was on top of a flask of boiling ether **38** (244 mg, 75%) as a cream solid, m.p. (decomp. 170 °C);  $[\alpha]_D^{25}$  *c*=1 methanol: +37.3°;  $\nu_{max}$  (cm<sup>-1</sup>): 3393 (NH), 3200-2700 br. (NH), 1648 (C=O); <sup>1</sup>H NMR (500 MHz, DMSO-*d*<sub>6</sub>) δ ppm 8.65 (3H, br.s, 3H<sub>(5)</sub>), 7.03 - 7.59 (10H, m, aryl), 3.82 - 3.84 (1H, m, H<sub>(8)</sub>), 3.57 - 3.72 (2H, m, H<sub>(12)</sub>/H<sub>(13)</sub>/H<sub>(21)</sub>/H<sub>(22)</sub>), 3.52 (1H, br.s, H<sub>(12)</sub>/H<sub>(13)</sub>/H<sub>(21)</sub>/H<sub>(22)</sub>), 3.35 (1H, dd, *J*=14.0, 6.9 Hz, H<sub>(12)</sub>/H<sub>(13)</sub>/H<sub>(21)</sub>/H<sub>(22)</sub>), 3.23 - 3.31 (1H, m, H<sub>(12)</sub>/H<sub>(13)</sub>/H<sub>(21)</sub>/H<sub>(22)</sub>), 3.20 (1H, dd, *J*=13.0, 5.4 Hz, H<sub>(4)</sub>), 3.04 - 3.16 (1H, m, H<sub>(12)</sub>/H<sub>(13)</sub>/H<sub>(21)</sub>/H<sub>(22)</sub>), 2.93 (1H, dd, *J*=13.2, 9.2 Hz, H<sub>(4)</sub>), 2.54 - 2.74 (1H, m, H<sub>(12)</sub>/H<sub>(13)</sub>/H<sub>(21)</sub>/H<sub>(22)</sub>); <sup>13</sup>C NMR (126 MHz, DMSO-*d*<sub>6</sub>) δ ppm 166.93 C<sub>(2)</sub>, 146.01 C<sub>(15)</sub>, 134.48, 129.61,

129.44, 128.54, 127.27, 118.52  $C_{aryl}$ , 51.13  $C_{(13)}/C_{(21)}$ , 50.87  $C_{(21)}/C_{(13)}$  49.39  $C_{(3)}$ , 43.59  $C_{(12)}/C_{(22)}$ , 40.29  $C_{(22)}/C_{(12)}$ , 36.88  $C_{(4)}$ ; HRMS calcd for  $C_{19}H_{23}N_3O$  requires 309.1841, found 309.1837;

**(*R*)-2-Amino-1-(4-methylpiperazin-1-yl)-3-phenylpropan-1-one hydrochloride (**39**)**

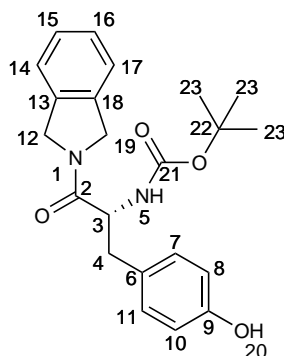


*N*-Boc protected amide **35** (174 mg, 0.5 mmol) was dissolved in ethereal hydrogen chloride (1 M, 10 mL) and stirred at 20 °C for 16 h and the solvent was evaporated. To the residue was added saturated aqueous sodium hydrogen carbonate (20 mL) and the solution was washed with ethyl acetate (2 x 20 mL) and extracted into dichloromethane (3 x 30 mL) and evaporated to give the amine,  $^1H$  NMR (500 MHz, chloroform-*d*)  $\delta$  ppm 7.07 - 7.25 (5H, m, aryl), 3.87 (1H, br.s,  $H_{(3)}$ ), 3.45 - 3.61 (2H, m,  $2H_{(12)}/2H_{(16)}$ ), 3.22 - 3.35 (1H, m,  $H_{(16)}/H_{(12)}$ ), 2.97 - 3.08 (1H, m,  $H_{(16)}/H_{(12)}$ ), 2.82 - 2.90 (1H, dd,  $J=13.1, 7.0$  Hz,  $H_{(5)}$ ), 2.70 - 2.78 (1H, dd,  $J=13.1, 7.1$  Hz,  $H_{(5)}$ ), 2.22 - 2.32 (1H, m,  $13/H_{(15)}$ ), 2.15 - 2.19 (2H, m,  $H_{(13)}/H_{(15)}$ ), 2.14 (3H, s,  $H_{(17)}$ ), 1.74 - 1.82 (H, m,  $H_{(13)}/H_{(15)}$ );  $^{13}C$  NMR (126 MHz, DMSO-*d*<sub>6</sub>)  $\delta$  ppm 173.22  $C_{(2)}$ , 137.67  $C_{(6)}$ , 129.40  $C_{(8),C_{(10)}}$ , 128.63  $C_{(7),C_{(11)}}$ , 126.83  $C_{(9)}$ , 54.63  $C_{(12)}/C_{(16)}$ , 54.50  $C_{(12)}/C_{(16)}$ , 52.33  $C_{(3)}$ , 45.93  $C_{(19)}$ , 45.08  $C_{(13)}/C_{(15)}$ , 43.18  $C_{(5)}$ , 41.85 ( $13/C_{(15)}$ );

The residue was dissolved in diethyl ether (5 mL) and ethereal hydrochloric acid (2 M, 5 mL) was added and the solvent was evaporated to give **39** (140 mg, 98%) as a

cream solid, m.p. (decomp. 150 °C);  $\nu_{max}$  (cm<sup>-1</sup>): 3391 (NH), 1650 (C=O), 1602;  $[\alpha]_D^{25}$  *c*=1 methanol: -27.0°; HRMS calcd for C<sub>14</sub>H<sub>22</sub>N<sub>3</sub>O: 248.1763, found: 248.1762.

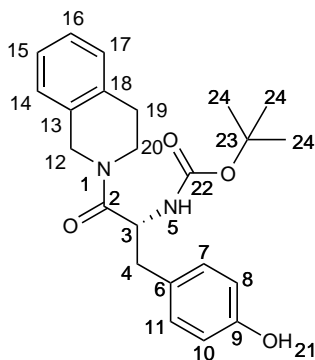
**(*R*)-*tert*-Butyl (3-(4-hydroxyphenyl)-1-(isoindolin-2-yl)-1-oxopropan-2-yl) carbamate (40)**



To isoindoline (0.11 mL, 1.0 mmol), *N*-Boc-(*D*)-tyrosine (270 mg, 1.0 mmol), 1-ethyl-3-(3-dimethylaminopropyl)carbodiimide (182 mg, 1.0 mmol) and anhydrous 1-hydroxybenzotriazole (203 mg, 1.5 mmol) in dimethylformamide (3.0 mL) was added *N,N*-diisopropylethylamine (1.3 mL, 7.5 mmol), the mixture was then stirred for 16 h at 20 °C. The solvent was evaporated, the residue was dissolved in ethyl acetate (20 mL) and washed with water (2 x 20 mL). The combined aqueous fractions were re-extracted with ethyl acetate (2 x 20 mL) and the combined organic layers were washed with saturated aqueous sodium hydrogen carbonate (2 x 20 mL) and brine (20 mL) before being dried over magnesium sulfate and evaporated, to give **40** (200 mg, 52%) as a white solid, m.p. 213-214 °C;  $[\alpha]_D^{25}$  *c*=1 Chloroform -29.8°; <sup>1</sup>H NMR (500 MHz, chloroform-*d*)  $\delta$  ppm 8.11 (1H, br.s, H<sub>(20)</sub>), 7.12 - 7.23 (3H, m, aryl), 7.04 (1H, d, *J*=8.5 Hz, aryl), 6.74 (1H, d, *J*=8.5 Hz, aryl), 5.50 (1H, d, *J*=9.0 Hz, H<sub>(5)</sub>), 4.86 (1H, d, *J*=13.7 Hz, H<sub>(12)</sub>/H<sub>(19)</sub>), 4.78 (1H, d, *J*=16.0 Hz, H<sub>(19)</sub>/H<sub>(12)</sub>), 4.67 (1H, s, H<sub>(3)</sub>), 4.58 (1H, d, *J*=16.1 Hz, H<sub>(19)</sub>/H<sub>(12)</sub>), 4.15 (1H, d, *J*=13.7 Hz, H<sub>(12)</sub>/H<sub>(19)</sub>), 2.96 (1H, dd, *J*=13.4, 8.5 Hz, H<sub>(4)</sub>), 2.89 (1H, dd, *J*=13.4, 6.0 Hz, H<sub>(4)</sub>), 1.39 (9H, s, 3 x H<sub>(23)</sub>); <sup>13</sup>C NMR (126 MHz, chloroform-*d*)  $\delta$  ppm 170.96 C<sub>(2)</sub>, 155.42 C<sub>(20)</sub>/C<sub>(21)</sub>, 155.31 C<sub>(20)</sub>/C<sub>(21)</sub>, 135.83, 135.62, 130.55 C<sub>(7)</sub>,C<sub>(11)</sub>, 127.84, 127.64, 127.62, 122.90,

122.64, 115.55 C<sub>(8)</sub>,C<sub>(10)</sub>, 80.15 C<sub>(22)</sub>, 53.51 C<sub>(3)</sub>, 52.33 C<sub>(12)</sub>/C<sub>(19)</sub>, 52.22 C<sub>(19)</sub>/C<sub>(12)</sub>, 38.76 C<sub>(4)</sub>, 28.42 C<sub>(23)</sub>; HRMS calcd for C<sub>22</sub>H<sub>26</sub>N<sub>2</sub>O<sub>4</sub>: 383.1971, found: 383.1953.

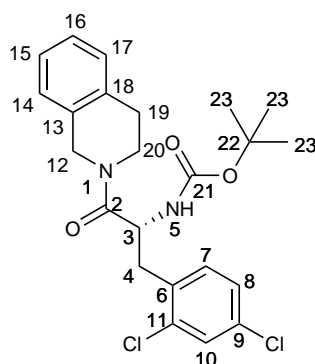
**(*R*)-*tert*-Butyl (1-(3,4-dihydroisoquinolin-2(1*H*)-yl)-3-(4-hydroxyphenyl)-1-oxopropan-2-yl)carbamate (41)**



To tetrahydroisoquinoline (0.11 mL, 1.0 mmol), *N*-Boc-(*R*)-tyrosine (281 mg, 1.0 mmol), 1-ethyl-3-(3-dimethylaminopropyl)carbodiimide (182 mg, 1.0 mmol) and anhydrous 1-hydroxybenzotriazole (203 mg, 1.5 mmol) in dimethylformamide (3.0 mL) was added *N,N*-diisopropylethylamine (1.3 mL, 7.5 mmol), the mixture was then stirred for 24 h at 20 °C. The mixture was diluted with ethyl acetate (20 mL) and washed with water (2 x 20 mL). The combined aqueous fractions were re-extracted with ethyl acetate (2 x 20 mL) and the combined organic layers were washed with saturated aqueous sodium hydrogen carbonate (2 x 20 mL) and brine (20 mL) before being dried over magnesium sulfate and evaporated. The residue was purified by silica column chromatography (50% ethyl acetate, 50% hexane) to give **41** (125 mg, 32%) as a white solid, m.p. 213-214 °C;  $\nu_{max}$  (cm<sup>-1</sup>): 3303 (NH), 2978, 1691 (NHC=O), 1630 (CHC=O); <sup>1</sup>H NMR (500 MHz, chloroform-*d*, 2 rotamers)  $\delta$  ppm 6.80 - 7.18 (6H, m, aryl), 6.66 (1H, d, *J*=8.5 Hz, aryl), 6.60 (1H, d, *J*=8.5 Hz, aryl), 5.50 (1H, d, 8.7 Hz, H<sub>(5)</sub>), 4.84 - 4.93 (1H, m, H<sub>(3)</sub>), 4.76, 4.53 (1H, d, *J*=17.2 Hz, H<sub>(12)</sub>), 4.51, 4.08 (1H, d, *J*=15.9 Hz, H<sub>(12)</sub>), 3.76 - 3.83, 3.62 - 3.70, 3.55 - 3.62, 3.16 - 3.23 (2H, m, 2H<sub>(20)</sub>), 2.84 - 2.96 (2H, m, H<sub>(4)</sub>,H<sub>(9)</sub>), 2.69 - 2.82 (2H, m, H<sub>(4)</sub>,H<sub>(9)</sub>), 2.41 - 2.48 (1H, m, H<sub>(9)</sub>), 1.37 - 1.46 (9H, m, 3 x 3H<sub>(24)</sub>); <sup>13</sup>C

NMR (126 MHz, chloroform-*d*, 2 rotamers)  $\delta$  ppm 171.19 C<sub>(2)</sub>, 170.93 C<sub>(2)</sub>, 155.94 C<sub>(9)/C<sub>(22)</sub></sub>, 155.87 C<sub>(9)/C<sub>(22)</sub></sub>, 155.55 C<sub>(22)/C<sub>(9)</sub></sub>, 155.53 C<sub>(22)/C<sub>(9)</sub></sub>, 134.46, 134.07, 132.54, 132.05, 130.56 C<sub>(7),C<sub>(11)</sub></sub>, 130.47 C<sub>(7),C<sub>(11)</sub></sub>, 128.56, 128.31, 127.21, 127.03, 126.99, 126.73, 126.57, 126.44, 126.18, 115.62 C<sub>(8)/C<sub>(10)</sub></sub>, 115.52 C<sub>(8)/C<sub>(10)</sub></sub>, 80.18 C<sub>(23)</sub>, 77.51 C<sub>(23)</sub>, 52.09 C<sub>(3)</sub>, 51.86 C<sub>(3)</sub>, 47.19 C<sub>(12)</sub>, 44.71 C<sub>(12)</sub>, 43.20 C<sub>(20)</sub>, 40.63 C<sub>(20)</sub>, 39.49 C<sub>(4)</sub>, 39.43 C<sub>(4)</sub>, 29.12 C<sub>(19)</sub>, 28.46 3C<sub>(2)</sub>, 28.29 C<sub>(19)</sub>; HRMS calcd for C<sub>22</sub>H<sub>26</sub>N<sub>2</sub>O<sub>4</sub>: 397.2127, found: 397.2133.

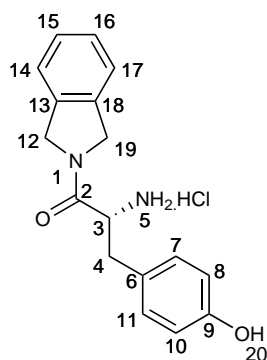
(*R*)-*tert*-Butyl (3-(2,4-dichlorophenyl)-1-(3,4-dihydroisoquinolin-2(1*H*))-yl)-1-oxopropan-2-yl)carbamate (**42**)



To tetrahydroisoquinoline (0.12 mL, 1.0 mmol), *N*-Boc-(*R*)-2,4-dichlorophenylalanine (344 mg, 1.0 mmol), 1-ethyl-3-(3-dimethylaminopropyl)carbodiimide (182 mg, 1.0 mmol) and anhydrous 1-hydroxybenzotriazole (203 mg, 1.5 mmol) in dimethylformamide (volume mL) was added *N,N*-diisopropylethylamine (1.3 mL, 7.5 mmol), the mixture was then stirred for 20 h at 20 °C. The solvent was evaporated, the residue was dissolved in ethyl acetate (20 mL) and washed with water (2 x 20 mL). The combined aqueous fractions were re-extracted with ethyl acetate (2 x 20 mL) and the combined organic layers were washed with saturated aqueous sodium hydrogen carbonate (2 x 20 mL) and brine (20 mL) before being dried over magnesium sulfate and evaporated. The residue was purified by silica column chromatography (6% ethyl acetate, 94% dichloromethane) to give **42** (308 mg, 68%) as a white solid, Mp 155-156 °C;  $\nu_{max}$  (cm<sup>-1</sup>): 3393 (NH), 3200-2700 br. (NH), 1648 (CHC=O); <sup>1</sup>H

NMR (500 MHz, chloroform-*d*, 2 rotamers )  $\delta$  ppm 6.87 - 7.42 (7H, m, aryl), 5.50 (1H, d,  $J=8.7$  Hz, H<sub>(5)</sub>), 5.46 (1H, d,  $J=8.7$  Hz, H<sub>(5)</sub>), 5.10 (1H, q,  $J=7.7$  Hz, H<sub>(3)</sub>), 5.04 (1H, q,  $J=7.7$  Hz, H<sub>(3)</sub>), 4.73 (1H, d,  $J=16.8$  Hz, H<sub>(12)</sub>), 4.64 (1H, d,  $J=16.8$  Hz, H<sub>(12)</sub>), 4.59 (1H, d,  $J=16.1$  Hz, H<sub>(12)</sub>), 4.50 (1H, d,  $J=16.1$  Hz, H<sub>(12)</sub>), 4.02 - 4.10, 3.71 - 3.81, 3.50 - 3.60, 3.41 - 3.50 (2H, m, 2H<sub>(20)</sub>), 3.12 (1H, dd,  $J=13.4, 6.4$  Hz, H<sub>(4)</sub>), 3.02 (1H d,  $J=7.4$  Hz, H<sub>(19)</sub>), 2.97 (1H, dd,  $J=13.4, 8.0$  Hz, H<sub>(4)</sub>), 2.83 - 2.92 (1H, m, H<sub>(19)</sub>), 2.65 - 2.80 (1H, m, H<sub>(19)</sub>), 1.36 - 1.42, 1.28 - 1.36 (9H, s, H<sub>(23)</sub>); <sup>13</sup>C NMR (126 MHz, chloroform-*d*, 2 rotamers)  $\delta$  ppm 170.32 C<sub>(2)</sub>, 169.92 C<sub>(2)</sub>, 154.95 C<sub>(21)</sub>, 135.18 C<sub>(18)</sub>, 134.91 C<sub>(18)</sub>/C<sub>(19)</sub>, 134.23, 133.91, 133.58, 133.53, 133.03, 132.85, 132.77, 132.64, 131.87, 129.24, 129.11, 128.82, 128.40, 127.17, 127.00, 126.94 126.81, 126.70, 126.63, 126.49, 125.92, 79.80 C<sub>(27)</sub>, 79.78 C<sub>(22)</sub>, 49.48 C<sub>(3)</sub>, 49.31 C<sub>(3)</sub>, 47.38 C<sub>(12)</sub>, 44.74 C<sub>(12)</sub>, 43.23 C<sub>(20)</sub>, 40.46 C<sub>(20)</sub>, 37.79 C<sub>(4)</sub>, 37.43 C<sub>(4)</sub>, 29.41 C<sub>(19)</sub>, 28.35 C<sub>(23)</sub>, 28.20 C<sub>(19)</sub>.

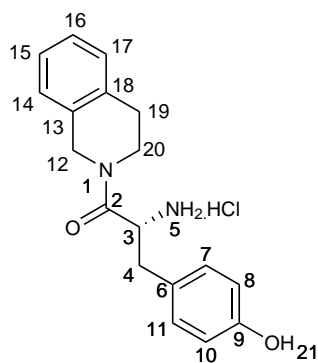
**(*R*)-2-Amino-3-(4-hydroxyphenyl)-1-(isoindolin-2-yl)propan-1-one hydrochloride (43)**



*N*-Boc protected amide **40** (100 mg, 0.26 mmol) was dissolved in dichloromethane (2 mL) and ethereal hydrochloric acid (1 M, 10 mL) was added, after 16 h the reaction was incomplete and the mixture was heated at reflux for 4 h. The reaction was still incomplete and was subsequently completed by bubbling of gaseous hydrochloric acid through the solution. The solid was filtered over boiling diethyl ether and dried to give **43** (51 mg, 61%) as a white solid, m.p. (decomp. 220 °C);  $[\alpha]_D^{25}$ : °C -34.9°;

$\nu_{max}$  ( $\text{cm}^{-1}$ ): 3225, 3049 (NH) 1649 (C=O) 1633;  $^1\text{H}$  NMR (500 MHz, chloroform-*d*)  $\delta$  ppm 9.41 (1H, s, H<sub>(20)</sub>), 8.47 (3H, s, 3H<sub>(6)</sub>), 7.30 - 7.35 (1H, m, aryl), 7.26 (2H, m, aryl), 7.17 - 7.23 (1H, m, aryl), 7.04 (2H, d,  $J=8.4$  Hz, H<sub>(7)</sub>,H<sub>(11)</sub>), 6.67 (2H, d,  $J=8.4$  Hz, H<sub>(8)</sub>,H<sub>(10)</sub>), 4.92 (1H, d,  $J=14.0$  Hz, H<sub>(12)</sub>/H<sub>(19)</sub>), 4.72 (1H, d,  $J=16.2$  Hz, H<sub>(19)</sub>/H<sub>(12)</sub>), 4.53 (1H, d,  $J=16.2$  Hz, H<sub>(19)</sub>/H<sub>(12)</sub>), 4.19 - 4.31 (1H, m, H<sub>(3)</sub>), 4.02 (1H, d,  $J=14.0$  Hz, H<sub>(12)</sub>/H<sub>(19)</sub>), 3.06 (1H, dd,  $J=13.4, 6.0$  Hz, H<sub>(4)</sub>), 2.94 (1H, dd,  $J=13.4, 7.0$  Hz, H<sub>(4)</sub>);  $^{13}\text{C}$  NMR (126 MHz, chloroform-*d*)  $\delta$  ppm, 167.08 C<sub>(2)</sub>, 156.63 C<sub>(9)</sub>, 135.95,135.14, 130.41C<sub>(7)</sub>/C<sub>(11)</sub>, 127.58 C<sub>(11)</sub>/C<sub>(7)</sub>, 127.55, 124.53, 123.01, 122.60, 115.32 C<sub>(8)</sub>,C<sub>(10)</sub>, 52.24 C<sub>(3)</sub>, 51.84 C<sub>(12)</sub>/C<sub>(19)</sub>, 51.50 C<sub>(19)</sub>/C<sub>(12)</sub>, 35.77 C<sub>(4)</sub>; HRMS calcd for C<sub>17</sub>H<sub>19</sub>N<sub>2</sub>O<sub>2</sub>: 283.1447, found: 283.1449.

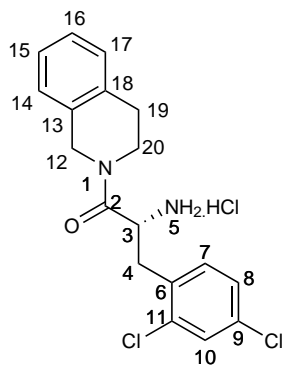
**(*R*)-2-Amino-1-(3,4-dihydroisoquinolin-2(1*H*)-yl)-3-(4-hydroxyphenyl)propan-1-one hydrochloride (44)**



*N*-Boc protected amide **41** (125 mg, 315  $\mu\text{mol}$ ) was dissolved in ethereal hydrogen chloride (1 M, 10 mL) and the mixture stirred at 20 °C for 16 h. The solvent was evaporated to give **44** (74 mg, 70%) as a white solid, m.p. (decomp. 245-247 °C);  $[\alpha]_D^{25}$ : -9.0°;  $\nu_{max}$  ( $\text{cm}^{-1}$ ): 3197-2951 (NH), 1638 (NHC=O), 1627 (CHC=O);  $^1\text{H}$  NMR (500 MHz, DMSO-*d*<sub>6</sub>, 2 rotamers)  $\delta$  ppm 9.42 (1H, s, H<sub>(21)</sub>), 8.37 (3H, s, 3H<sub>(5)</sub>), 6.90 - 7.23 (6H, m, aryl), 6.66 (1H, d,  $J=8.2$  Hz, H<sub>(8)</sub>/H<sub>(10)</sub>), 6.63 (1H, d,  $J=8.2$  Hz, H<sub>(8)</sub>/H<sub>(10)</sub>), 4.50 - 4.80 (1H, m, H<sub>(12)</sub>), 4.50 - 4.66 (2H, m, H<sub>(3)</sub>,H<sub>(12)</sub>), 4.37 (1H, d,  $J=17.1$  Hz, H<sub>(12)</sub>), 3.96 (1H, d,  $J=16.3$  Hz, H<sub>(12)</sub>), 3.69 - 3.78, 3.52 - 3.65, 3.41 - 3.51 (2H, m, H<sub>(20)</sub>), 2.96 - 3.13 (2H, m, H<sub>(4)</sub>,H<sub>(19)</sub>), 2.81 - 2.91 (1H, m, H<sub>(4)</sub>), 2.59 -

2.80, 2.30 - 2.44 (2H, m, H<sub>(19)</sub>); <sup>13</sup>C NMR (126 MHz, DMSO-*d*<sub>6</sub>) δ ppm 167.34 C<sub>(2)</sub>, 167.12 C<sub>(2)</sub>, 156.69 C<sub>(9)</sub> 156.67 C<sub>(9)</sub>, 134.34, 134.11, 132.48 C<sub>(13)</sub>, 132.36 C<sub>(13)</sub>/C<sub>(8)</sub>, 130.49 br. C<sub>(7)</sub>,C<sub>(11)</sub>, 128.32, 128.24, 126.64, 126.47, 126.42, 126.21, 126.14, 126.08, 124.34, 124.14, 115.29 C<sub>(8)</sub>,C<sub>(10)</sub>, 115.20 C<sub>(8)</sub>,C<sub>(10)</sub>, 50.75 C<sub>(3)</sub>, 50.45 C<sub>(3)</sub>, 46.08 C<sub>(12)</sub>, 44.02 C<sub>(12)</sub>, 42.48 C<sub>(20)</sub>, 36.23 C<sub>(4)</sub>, 35.95 C<sub>(4)</sub> 28.40 C<sub>(19)</sub>, 27.60 C<sub>(19)</sub>; HRMS calcd for C<sub>18</sub>H<sub>21</sub>N<sub>2</sub>O<sub>2</sub>: 297.1603, found: 297.1602.

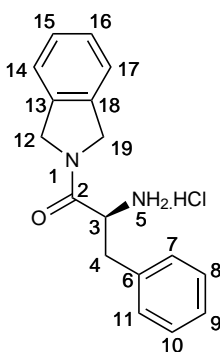
**(*R*)-2-Amino-3-(2,4-dichlorophenyl)-1-(3,4-dihydroisoquinolin-2(1H-yl)propan-1-one hydrochloride (45)**



*N*-Boc protected amide **42** (292 mg, 0.67 mmol) dissolved in ethereal hydrochloric acid (1 M, 10 mL). After 16 h stirring at 20 °C the reaction was heated at reflux for 4 h before the solvent was evaporated to yield **45** (306 mg, 116%).  $\nu_{max}$  (cm<sup>-1</sup>): 2865 br. (NH), 1645 (C=O), 1587; The solid was dissolved in sodium hydrogen carbonate solution (20 mL) and extracted into ethyl acetate (2 x 20 mL), washed with brine (20 mL) and dried over magnesium sulfate. The solvent was evaporated and the residue purified by silica column chromatography (94% ethyl acetate, 5% methanol, 1% ammonia .880) to give the amine **45** as a yellow oil (114 mg, 48%), ethereal hydrochloric acid (2 M, 10 mL) was added and the precipitated solid collected by filtration The precipitate was filtered by gravity filtration through filter paper in a funnel that was on top of a flask of boiling ether **45** as a bright yellow solid, m.p. 187-189 °C; <sup>1</sup>H NMR (500 MHz, DMSO-*d*<sub>6</sub>) δ ppm 6.84 - 7.44 (7H, m, aryl), 4.68 (1H, s, H<sub>(12)</sub>), 4.51 (1H, d, *J*=16.0 Hz, H<sub>(12)</sub>), 4.40 (1H, d, *J*=16.0 Hz, H<sub>(12)</sub>), 4.02

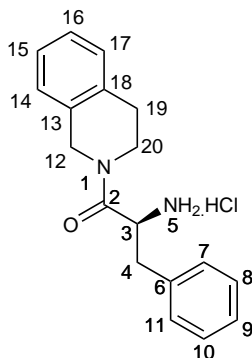
- 4.23 (2H, m, H<sub>(3)</sub>,H<sub>(20)</sub>), 3.59 - 3.71 (1H, m, H<sub>(20)</sub>), 3.40 - 3.54 (1H, m, H<sub>(20)</sub>), 3.00 - 3.08 (1H, m, H<sub>(4)</sub>), 2.55 - 3.09 (3H, m, H<sub>(4)</sub>,2H<sub>(19)</sub>); <sup>13</sup>C NMR (126 MHz, DMSO-*d*<sub>6</sub>) δ ppm 166.77 C<sub>(2)</sub>, 166.29 C<sub>(2)</sub>, 134.56, 134.10, 134.03, 133.84, 133.63, 133.23, 133.07, 132.97, 132.42, 131.84, 131.46, 131.10, 128.82, 128.56, 128.35, 128.17, 127.62, 127.52, 126.65, 126.55, 126.43, 126.25, 126.01, 125.72, 50.49 C<sub>(3)</sub>, 50.17 C<sub>(3)</sub>, 47.09 C<sub>(12)</sub>, 44.74 C<sub>(12)</sub>, 42.91 C<sub>(20)</sub>, 40.46 C<sub>(20)</sub>, 40.38 C<sub>(4)</sub>, 40.03C<sub>(4)</sub>, 29.47 C<sub>(19)</sub>, 28.24 C<sub>(19)</sub>; HRMS calcd for C<sub>18</sub>H<sub>19</sub>N<sub>2</sub>OCl<sub>2</sub>: 349.0884, found: 349.0865.

**(*s*)-2-Amino-1-(isoindolin-2-yl)-3-phenylpropan-1-one hydrochloride (46)<sup>249</sup>**



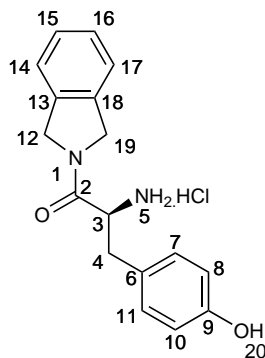
*N*-Boc protected amide **50** (117 mg, 0.32 mmol) was dissolved in ethereal hydrogen chloride (1 M, 10 mL) and the mixture stirred at 20 °C for 16 h. The solvent was evaporated to give **91** (91 mg, 94%) as a cream solid, m.p. (decomp. 235 °C). [ $\alpha$ ]<sub>D</sub><sup>25</sup> methanol +33.0°;  $\nu_{max}$  (cm<sup>-1</sup>): 3100 2700 br. (NH), 1651 (C=O); <sup>1</sup>H NMR (500 MHz, DMSO-*d*<sub>6</sub>) δ ppm 8.63 (3H, br.s, 3H<sub>(5)</sub>), 7.13 - 7.36 (9H, m, aryl), 4.93 (1H, d, *J*=13.9 Hz, H<sub>(12)</sub>/H<sub>(19)</sub>), 4.71 (1H, d, *J*=16.2 Hz, H<sub>(19)</sub>/H<sub>(12)</sub>), 4.51 (1H, d, *J*=16.2 Hz, H<sub>(19)</sub>/H<sub>(12)</sub>), 4.32 (1H, br.s, H<sub>(3)</sub>), 3.96 (1H, d, *J*=13.9 Hz, H<sub>(12)</sub>/H<sub>(19)</sub>), 3.22 (1H, dd, *J*=13.2, 5.5 Hz, H<sub>(4)</sub>), 3.06 (1H, dd, *J*=13.2, 8.7 Hz, H<sub>(4)</sub>); <sup>13</sup>C NMR (126 MHz, DMSO-*d*<sub>6</sub>) δ ppm 166.92 C<sub>(2)</sub>, 135.90 C<sub>(13)</sub>/C<sub>(18)</sub>/C<sub>(6)</sub>, 135.12 C<sub>(13)</sub>/C<sub>(18)</sub>/C<sub>(6)</sub>, 134.80 C<sub>(13)</sub>/C<sub>(18)</sub>/C<sub>(6)</sub>, 129.46 C<sub>(8)</sub>,C<sub>(10)</sub>, 128.52 C<sub>(7)</sub>,C<sub>(11)</sub>, 127.56 C<sub>(15)</sub>/C<sub>(16)</sub>, 127.52 C<sub>(16)</sub>/C<sub>(15)</sub>, 127.30 C<sub>(9)</sub>, 122.98 C<sub>(14)</sub>/C<sub>(17)</sub>, 122.56 C<sub>(17)</sub>/C<sub>(14)</sub>, 51.96 C<sub>(3)</sub>, 51.82 C<sub>(12)</sub>/C<sub>(19)</sub>, 51.53 C<sub>(19)</sub>/C<sub>(12)</sub>, 36.48 C<sub>(4)</sub>. HRMS calcd for C<sub>17</sub>H<sub>19</sub>N<sub>2</sub>O: 267.1497, found 267.1494.

(*s*)-2-Amino-1-(3,4-dihydroisoquinolin-2(1*H*)-yl)-3-phenylpropan-1-one hydrochloride (**47**)<sup>203</sup>



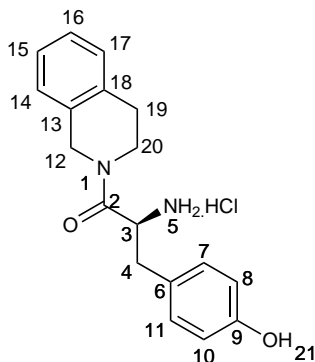
*N*-Boc protected amide **153** (210 mg, 0.55 mmol) was dissolved in dichloromethane (6.7 mL) and cooled to 0 °C. Trifluoroacetic acid was added (0.42 mL) and the mixture stirred overnight. The reaction was concentrated and the residue was dissolved in dichloromethane (10 mL) then neutralised with saturated aqueous sodium hydrogen carbonate (15 mL). The aqueous phase was extracted with dichloromethane (2 x 10 mL), the combined organic layers were combined and washed with brine then dried over magnesium sulfate and solvent evaporated to give a dark orange oil (140 mg, 91%). To obtain the hydrochloride salt the oil was dissolved in diethyl ether (3.0 mL) and ethereal hydrochloric acid was added (2 M, 3.0 mL) and the precipitate filtered.  $[\alpha]_D^{25}$  methanol: +7.2°;  $\nu_{max}$  (cm<sup>-1</sup>): 2910-2810 br. (NH), 1644 (CHC=O); <sup>1</sup>H NMR (600 MHz, DMSO-*d*<sub>6</sub>, 2 rotamers)  $\delta$  ppm 8.44 (3H, br.s, 3H<sub>(5)</sub>), 6.92 - 7.34 (9H, m, aryl), 3.90 - 4.70 (2H, m, H<sub>(2)</sub>), 3.50 - 3.66 (3H, m, H<sub>(3)</sub>, 2H<sub>(20)</sub>), 3.14 - 3.25 (1H, m, H<sub>(4)</sub>), 2.92 - 3.05 (2H, m, H<sub>(4)</sub>, H<sub>(12)</sub>), 2.89 - 3.07 (2H, m, H<sub>(14)</sub>), 2.21 - 2.79 (2H, m, H<sub>(9)</sub>); <sup>13</sup>C NMR (151 MHz, DMSO-*d*<sub>6</sub>, 2 rotamers)  $\delta$  ppm 167.24 C<sub>(2)</sub>, 166.92 C<sub>(2)</sub>, 134.5, 134.28, 134.25, 134.09, 132.39, 132.35, 129.62, 129.51, 128.57, 128.40, 128.28, 127.34, 127.19, 126.64, 126.55, 126.48, 126.28, 126.13, 126.11, 50.41 C<sub>(3)</sub>, 50.21 C<sub>(3)</sub>, 46.17, 44.00, 42.55, 37.03 C<sub>(4)</sub>, 36.81 C<sub>(4)</sub>, 28.36 C<sub>(9)</sub>, 27.60 C<sub>(9)</sub>; HRMS calculated for C<sub>18</sub>H<sub>20</sub>N<sub>2</sub>O+H<sup>+</sup>: 281.1654, found: 281.1665.

(*s*)-2-Amino-3-(4-hydroxyphenyl)-1-(isoindolin-2-yl)propan-1-one hydrochloride (**48**)



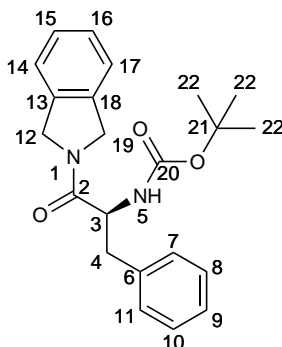
*N*-Boc protected amide **51** (153 mg, 0.48 mmol) was dissolved in ethereal hydrogen chloride and stirred at 20 °C for 16 h. Dichloromethane (2.5 mL) was added and the mixture was then heated at reflux for an additional 2 h before being filtered. The precipitate was filtered by gravity filtration through filter paper in a funnel that was on top of a flask of boiling ether **48** (106 mg, 69%) as a cream solid, m.p. (decomp. 250 °C);  $[\alpha]_D^{25}$   $c=1$  methanol: +32.4°;  $\nu_{max}$  (cm<sup>-1</sup>): 3052 br. (NH), 1650 (C=O); <sup>1</sup>H NMR (500 MHz, DMSO-*d*<sub>6</sub>)  $\delta$  ppm 9.44 (1H, br.s, H<sub>(20)</sub>), 8.51 (3H, s, 3H<sub>(5)</sub>), 7.17 - 7.37 (4H, m, aryl), 7.04 (2H, d,  $J=8.5$  Hz, H<sub>(7)</sub>,H<sub>(11)</sub>), 6.67 (2H, d,  $J=8.5$  Hz, H<sub>(8)</sub>,H<sub>(10)</sub>), 4.92 (1H, d,  $J=14.0$  Hz, H<sub>(12)</sub>/H<sub>(19)</sub>), 4.71 (1H, d,  $J=16.2$  Hz, H<sub>(19)</sub>/H<sub>(12)</sub>), 4.46 - 4.57 (1H, d,  $J=16.2$  Hz, H<sub>(19)</sub>/H<sub>(12)</sub>), 4.17 - 4.28 (1H, m, H<sub>(3)</sub>), 3.99 (1H, d,  $J=14.0$ , H<sub>(12)</sub>/H<sub>(19)</sub>), 3.07 (1H, dd,  $J=13.5$ , 5.8 Hz, H<sub>(4)</sub>), 2.94 (1H, dd,  $J=13.5$ , 8.7 Hz, H<sub>(4)</sub>); <sup>13</sup>C NMR (126 MHz, DMSO-*d*<sub>6</sub>)  $\delta$  ppm 167.09 C<sub>(2)</sub>, 156.64 C<sub>(9)</sub>, 135.95, 135.15, 130.39 C<sub>(7)</sub>,C<sub>(11)</sub>, 127.57, 127.54, 124.54, 123.01, 122.60, 115.32 C<sub>(8)</sub>,C<sub>(10)</sub>, 52.22 C<sub>(3)</sub>, 51.82 C<sub>(12)</sub>/C<sub>(19)</sub>, 51.51 C<sub>(19)</sub>/C<sub>(12)</sub>, 35.78 C<sub>(4)</sub>; HRMS calcd for C<sub>17</sub>H<sub>19</sub>N<sub>2</sub>O<sub>2</sub>: 283.1446, found: 283.1441

(*s*)-2-Amino-1-(3,4-dihydroisoquinolin-2(1*H*)-yl)-3-(4-hydroxyphenyl)propan-1-one hydrochloride (**49**)



*N*-Boc protected amide **154** (166 mg, 0.42 mmol) was dissolved in ethereal hydrogen chloride and stirred for 24 h. Hydrogen chloride was then bubbled through the solution with vigorous stirring for 1 h. The precipitated product was filtered over boiling diethyl ether to give **49** (47 mg, 37%) as a white solid, m.p. (decomp. 220 °C);  $[\alpha]_D^{25}$  *c*=1 methanol: +12.1°;  $\nu_{max}$  (cm<sup>-1</sup>): 3199-2951 (NH), 1638 (C=O), 1623; <sup>1</sup>H NMR (500 MHz, DMSO-*d*<sub>6</sub>, 2 rotamers)  $\delta$  ppm 9.47, 9.40 (1H, s, H<sub>(21)</sub>), 8.38 (3H, s, 3H<sub>(5)</sub>), 6.89 - 7.25 (6H, m, aryl), 6.67 (1H, d, *J*=8.3 Hz, H<sub>(8)</sub>,H<sub>(10)</sub>), 6.63 (1H, d, *J*=8.3 Hz, H<sub>(8)</sub>,H<sub>(10)</sub>), 4.73 (1H, d, *J*=17.2 Hz, H<sub>(12)</sub>), 4.50 - 4.66 (2H, m, H<sub>(3)</sub>,H<sub>(12)</sub>), 4.36 (1H, d, *J*=17.2 Hz, H<sub>(12)</sub>), 3.96 (1H, d, *J*=16.3 Hz, H<sub>(12)</sub>), 3.68 - 3.80 (1H, m, H<sub>(20)</sub>), 3.52 - 3.62 (1H, m, H<sub>(20)</sub>), 3.33 - 3.51 (1H, m, H<sub>(20)</sub>), 2.96 - 3.15 (2H, m, H<sub>(4)</sub>,H<sub>(19)</sub>), 2.80 - 2.94 (1H, m, H<sub>(4)</sub>), 2.58 - 2.78 (1H, m, H<sub>(19)</sub>), 2.29 - 2.42 (1H, m, H<sub>(19)</sub>). <sup>13</sup>C NMR (126 MHz, DMSO-*d*<sub>6</sub>)  $\delta$  ppm 167.34 C<sub>2</sub>, 167.12 C<sub>2</sub>, 156.69 C<sub>9</sub>, 156.67 C<sub>9</sub>, 134.34, 134.11, 132.48, 132.36, 130.49 C<sub>(7)</sub>,C<sub>(11)</sub>, 128.32, 128.24, 126.64, 126.47, 126.42, 126.21, 126.14, 126.08, 124.34, 124.14, 115.29 C<sub>(8)</sub>,C<sub>(11)</sub>, 115.20 C<sub>(8)</sub>,C<sub>(11)</sub>, 50.75 C<sub>(3)</sub>, 50.45 C<sub>(3)</sub>, 46.08 C<sub>(12)</sub>, 44.02 C<sub>(12)</sub>, 42.48 C<sub>(20)</sub>, 40.00 C<sub>(20)</sub>, 36.23 C<sub>(4)</sub>, 35.95 C<sub>(4)</sub>, 28.40 C<sub>(19)</sub>, 27.60 C<sub>(19)</sub>; HRMS calcd for C<sub>16</sub>H<sub>21</sub>N<sub>2</sub>O<sub>2</sub>: 319.1422, measured: 319.1422.

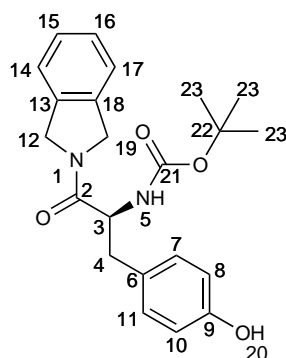
(*s*)-*tert*-Butyl(1-(isoindolin-2-yl)-1-oxo-3-phenylpropan-2-yl)carbamate (**50**)<sup>249</sup>



A literature procedure<sup>249</sup> using triethylamine was adapted for use with *N,N*-diisopropylethylamine, briefly, to isoindoline (0.11 mL, 1.0 mmol), *N*-Boc-(*s*)-phenylalanine (256 mg, 1.0 mmol), 1-ethyl-3-(3-dimethylaminopropyl)carbodiimide (182 mg, 1.0 mmol) and anhydrous 1-hydroxybenzotriazole (203 mg, 1.5 mmol) in dimethylformamide (3.0 mL) was added *N,N*-diisopropylethylamine (1.3 mL, 7.5 mmol). The mixture was stirred for 16 h at 20 °C before the solvent was evaporated, the residue was dissolved in ethyl acetate (20 mL) and washed with water (2 x 20 mL). The combined aqueous fractions were extracted with ethyl acetate (2 x 20 mL) and the combined organic layers were washed with saturated aqueous sodium hydrogen carbonate (2 x 20 mL) and brine (2 x 20 mL) before drying over magnesium sulfate. The solvent was evaporated and the residue was purified by silica column chromatography (70% hexane, 30% ethyl acetate) to give **50** (117 mg, 32%) as a pale cream solid,  $\nu_{max}$  (cm<sup>-1</sup>): 3425 (NH), 3291 (NH), 1707 (NHC=O), 1643 (CHC=O); <sup>1</sup>H NMR (500 MHz, chloroform-*d*)  $\delta$  ppm 7.19 - 7.26 (m, 7H, aryl), 7.13 - 7.18 (1H, m, aryl), 7.08-7.12 (1H, m, aryl), 5.39 (1H, d, *J*=8.5 Hz, H<sub>(5)</sub>), 4.87 (1H, d, *J*=13.6 Hz, H<sub>(12)</sub>/H<sub>(19)</sub>), 4.82 (1H, d, *J*=15.9 Hz, H<sub>(19)</sub>/H<sub>(12)</sub>), 4.72 (1H, m, H<sub>(3)</sub>), 4.63 (1H, d, *J*=15.9 Hz, H<sub>(19)</sub>/H<sub>(12)</sub>), 4.07 (1H, d, *J*=13.6 Hz, H<sub>(12)</sub>/H<sub>(19)</sub>), 2.94 - 3.10 (2H, m, H<sub>(4)</sub>), 1.34 - 1.49 (9H, m, 3 x 3H<sub>(22)</sub>); <sup>13</sup>C NMR (126 MHz, chloroform-*d*)  $\delta$  ppm 170.70 C<sub>(2)</sub>, 155.23 C<sub>(20)</sub>, 136.42 C<sub>(13)</sub>/C<sub>(18)</sub>, 136.00 C<sub>18</sub>/13, 135.76 C<sub>(6)</sub>, 129.42 C<sub>(8)</sub>,C<sub>(10)</sub>, 128.52 C<sub>(7)</sub>,C<sub>(11)</sub>, 127.78 C<sub>(15)</sub>/C<sub>(16)</sub>, 127.57 C<sub>(16)</sub>/C<sub>(15)</sub>, 127.05 C<sub>(9)</sub>,

122.89 C<sub>(14)</sub>/C<sub>(17)</sub>, 122.62 C<sub>(17)</sub>/C<sub>(14)</sub>, 79.86 C<sub>(21)</sub>, 53.44 C<sub>(12)</sub>, 52.21 C<sub>(12)</sub>/C<sub>(19)</sub>, 52.12 C<sub>(19)</sub>/C<sub>(12)</sub>, 39.88 C<sub>(4)</sub>, 28.41 C<sub>(22)</sub>.

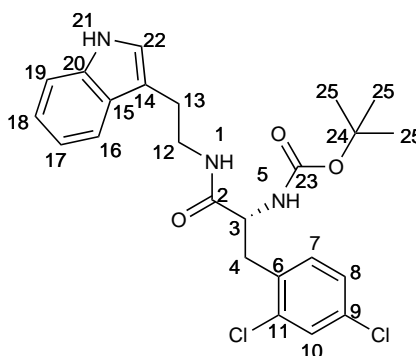
**(*s*)-tert-Butyl(3-(4-hydroxyphenyl)-1-(isoindolin-2-yl)-1-oxopropan-2-yl)carbamate (51)**



To isoindoline (0.11 mL, 1.0 mmol), *N*-Boc-(*s*)-tyrosine (279 mg, 1.0 mmol), 1-ethyl-3-(3-dimethylaminopropyl)carbodiimide (182 mg, 1.0 mmol) and anhydrous 1-hydroxybenzotriazole (203 mg, 1.5 mmol) in dimethylformamide (3.0 mL) was added *N,N*-diisopropylethylamine (1.3 mL, 7.5 mmol), the mixture was then stirred for 16 h at 20 °C. The solvent was evaporated, the residue was dissolved in ethyl acetate (20 mL) and washed with water (2 x 20 mL). The combined aqueous fractions were re-extracted with ethyl acetate (2 x 20 mL) and the combined organic layers were washed with saturated aqueous sodium hydrogen carbonate (2 x 20 mL) and brine (20 mL) before being dried over magnesium sulfate and evaporated. The residue was purified twice by column chromatography (20% ethyl acetate in dichloromethane) to give **51** (168 mg, 44%) as a white foam,  $\nu_{max}$  (cm<sup>-1</sup>): 3290 (NH), 1698 (NHC=O), 1634 (CHC=O); <sup>1</sup>H NMR (500 MHz, chloroform-*d*)  $\delta$  ppm 7.17 - 7.25 (3H, m, aryl), 7.03 - 7.11 (3H, m, aryl), 6.71 (2H, d, *J*=8.4 Hz, H<sub>(8)</sub>,H<sub>(10)</sub>), 5.40 (1H, d, *J*=8.7 Hz, H<sub>(5)</sub>), 4.89 (1H, d, *J*=13.7 Hz, H<sub>(12)</sub>/H<sub>(19)</sub>), 4.81 (1H, d, *J*=15.9 Hz, H<sub>(19)</sub>/H<sub>(12)</sub>), 4.70 (1H, m, H<sub>(3)</sub>), 4.61 (1H, d, *J*=15.9 Hz, H<sub>(19)</sub>/H<sub>(12)</sub>), 4.19 (1H, d, *J*=13.7 Hz, H<sub>(12)</sub>/H<sub>(19)</sub>), 2.99 (1H, dd, *J*=13.5, 8.4 Hz, H<sub>(4)</sub>), 2.91 (1H, dd, *J*=13.5, 5.8 Hz, H<sub>(4)</sub>), 1.74 - 1.87 (1H, br.s, H<sub>(20)</sub>), 1.41 (9H, s, 3 x 3H<sub>(23)</sub>); <sup>13</sup>C NMR (126 MHz,

chloroform-*d*)  $\delta$  ppm 171.01 C<sub>(2)</sub>, 155.46 C<sub>(22)</sub>, C<sub>(10)</sub>, 135.82, 135.59, 130.53 C<sub>(7)</sub>, C<sub>(11)</sub>, 127.83, 127.63, 127.47, 122.90, 122.64, 115.57 C<sub>(8)</sub>, C<sub>(10)</sub>, 80.20 C<sub>(22)</sub>, 53.52 C<sub>(3)</sub>, 52.34 C<sub>(12)</sub>/C<sub>(19)</sub>, 52.23 C<sub>(12)</sub>/C<sub>(19)</sub>, 38.73 C<sub>(4)</sub>, 28.41 C<sub>(23)</sub>.

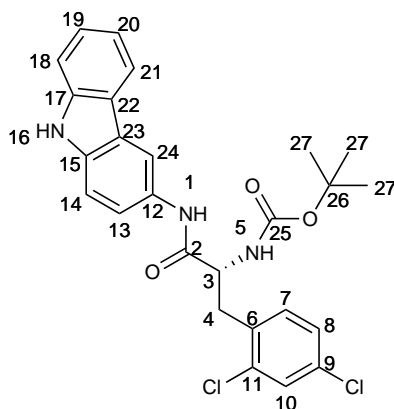
**(*R*)-*tert*-Butyl (*R*)-(1-((2-(1*H*-indol-3-yl)ethyl)amino)-3-(2,4-dichlorophenyl)-1-oxopropan-2-yl)carbamate (54)**



To tryptamine (960 mg, 0.6 mmol), *N*-Boc-(*R*)-2,4-dichlorophenylalanine (201 mg, 0.6 mmol), 1-ethyl-3-(3-dimethylaminopropyl)carbodiimide (109 mg, 0.6 mmol) and anhydrous 1-hydroxybenzotriazole (122 mg, 0.9 mmol) in dimethylformamide (3.0 mL) was added *N,N*-diisopropylethylamine (0.78 mL, 4.5 mmol), the mixture was then stirred for 17 h at 20 °C. The mixture was diluted with ethyl acetate (20 mL) and washed with water (3 x 20 mL). The combined aqueous fractions were re-extracted with ethyl acetate (3 x 20 mL) and the combined organic layers were washed with dilute hydrochloric acid (1 M, 20 mL), saturated aqueous sodium hydrogen carbonate (2 x 20 mL) and brine (20 mL) before being dried over magnesium sulfate and the solvent evaporated. The residue was washed with diethyl ether to give **54** (219 mg, 77%) as a white solid, m.p. 170-174 °C; <sup>1</sup>H NMR (500 MHz, chloroform-*d*)  $\delta$  ppm 10.74 - 10.84 (1H, br.s, H<sub>(21)</sub>), 7.52 (1H, d, *J*=8.0, aryl), 7.33 - 7.37 (1H, m, aryl), 7.28 - 7.31 (1H, m, aryl), 7.15 - 7.21 (1H, m, aryl), 7.05 - 7.14 (3H, m, aryl), 6.84 - 7.00 (1H, m, aryl), 5.95 (1H, t, *J*=5.5 Hz, H<sub>(1)</sub>), 5.09 (1H, d, *J*=7.1 Hz, H<sub>(5)</sub>), 4.30 (1H, d, *J*=8.5 Hz, H<sub>(3)</sub>), 3.40 - 3.67 (2H, m, H<sub>(12)</sub>), 3.15 (1H, dd, *J*=13.9, 6.5 Hz, H<sub>(4)</sub>), 2.93 - 3.04 (1H, m, H<sub>(4)</sub>), 1.15 - 1.32 (9H, m, 3 x 3H<sub>(25)</sub>); <sup>13</sup>C NMR (126

MHz, chloroform-*d*)  $\delta$  ppm 173.65 C<sub>(2)</sub>, 158.28 C<sub>(23)</sub>, 139.41, 138.05, 136.53, 136.35, 135.39, 132.24, 130.15, 125.27, 124.98, 123.27, 122.58, 121.54, 115.60, 114.32, 83.16 C<sub>(24)</sub>, 57.55 C<sub>(3)</sub>, 42.84 C<sub>(12)</sub>, 39.05 C<sub>(4)</sub>, 31.19 3C<sub>(2)</sub>, 28.05 C<sub>(25)</sub>; HRMS calcd for C<sub>24</sub>H<sub>27</sub>Cl<sub>2</sub>N<sub>3</sub>O<sub>3</sub>: 498.1327, found: 498.1323.

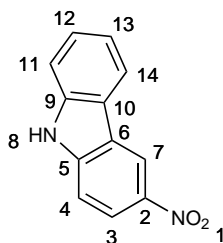
***tert*-Butyl (*R*)-(1-((9*H*-carbazol-3-yl)amino)-3-(2,4-dichlorophenyl)-1-oxopropan-2-yl)carbamate (55)**



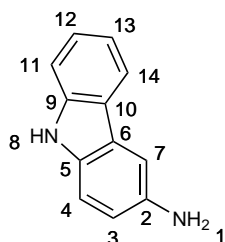
To 9*H*-carbazole-3-amine (**58**) (109 mg, 0.6 mmol), *N*-Boc-(*R*)-2,4-dichlorophenylalanine (201 mg, 0.6 mmol), 1-ethyl-3-(3-dimethylaminopropyl)carbodiimide (109 mg, 0.6 mmol) and anhydrous 1-hydroxybenzotriazole (122 mg, 0.6 mmol) in dimethylformamide (3.0 mL) was added *N,N*-diisopropylethylamine (0.78 mL, 4.5 mmol), the mixture was then stirred for 16 h at 20 °C. The mixture was the diluted with ethyl acetate (20 mL) and washed with water (3 x 20 mL). The combined aqueous fractions were re-extracted with ethyl acetate (3 x 20 mL) and the combined organic layers were washed with saturated aqueous sodium hydrogen carbonate (2 x 20 mL) and brine (20 mL) before being dried over magnesium sulfate and evaporated to give **55** (109 mg, 36%) as a white solid, m.p. 201-203 °C;  $\nu_{max}$  (cm<sup>-1</sup>): 3200-3400 (NH), 1707 (NHC=O), 1655 (CHC=O); <sup>1</sup>H NMR (600 MHz, CD<sub>3</sub>OD-*d*<sub>4</sub>)  $\delta$  ppm 8.02 (1H, d, *J*=7.5 Hz, aryl), 7.92 (1H, d, *J*=7.5 Hz, aryl), 7.40 - 7.52 (2H, m, aryl), 7.34 (2H, d, *J*=8.3 Hz, aryl), 7.24 - 7.30 (1H, m, aryl), 7.07 - 7.19 (3H, m, aryl), 4.52 - 4.71 (1H, m, H<sub>(3)</sub>), 3.32 - 3.46 (1H, dd, *J*= 13.8, 6.8 Hz, H<sub>(4)</sub>), 3.13 - 3.25 (1H, dd, *J*=13.8,

8.7 Hz, H<sub>(4)</sub>), 1.42 (9H, s, 3 x 3H<sub>(27)</sub>); <sup>13</sup>C NMR (126 MHz, CD<sub>3</sub>OD-*d*<sub>4</sub> δ ppm 172.71 C<sub>(2)</sub>, 157.92 C<sub>(25)</sub>, 141.30, 136.50, 135.89, 135.28, 134.54, 134.14, 130.23, 128.28, 127.00, 126.10, 124.39, 122.12, 122.05, 121.10, 120.14, 119.80, 119.24, 111.95, 80.98 C<sub>(26)</sub>, 55.99 C<sub>(4)</sub>, 36.38 C<sub>(3)</sub>, 28.71 3C<sub>(2)</sub>); HRMS calcd for C<sub>26</sub>H<sub>25</sub>Cl<sub>2</sub>N<sub>3</sub>O<sub>3</sub>: 497.1273, found: 497.1284.

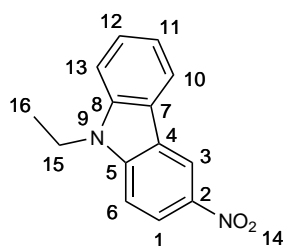
### 3-Nitro-9*H*-carbazole (**57**)<sup>251</sup>



Following the procedure used for **60**, carbazole (3.68g, 22 mmol) was dissolved in glacial acetic acid (70 mL) and stirred at 60 °C for 30 min. The solution was cooled to 20 °C and fuming nitric acid (1 mL) in glacial acetic acid (3 mL) was added dropwise over 30 min, the reaction was then stirred for 1 h at 20 °C before being poured into ice water (100 mL). The precipitate was filtered and dissolved in ethyl acetate and concentrated before purification by column chromatography (10% ethyl acetate 90% hexane) and then recrystallised from acetic acid to give **57** as a yellow crystalline solid (2.76 g, 57%), m.p. 208-210 °C (lit.<sup>252</sup> m.p. 215-216 °C);  $\nu_{max}$  (cm<sup>-1</sup>): 3399 br. (NH); <sup>1</sup>H NMR (500 MHz, chloroform-*d*) δ ppm 10.01 (1H, br.s, H<sub>(8)</sub>), 8.29 - 8.42 (2H, m, aryl), 8.09 (1H, d, *J*=7.9 Hz, aryl), 7.50 - 7.64 (2H, m, H<sub>(11)</sub>,H<sub>(14)</sub>), 7.22 - 7.41 (2H, m, H<sub>(12)</sub>,H<sub>(13)</sub>); <sup>13</sup>C NMR (126 MHz, chloroform-*d*) δ ppm 139.83 C<sub>(2)</sub>, 133.78, 132.22, 127.78, 127.53, 122.30, 122.01, 121.35, 120.74, 118.80, 111.71

**9H-Carbazole-3-amine (58)**<sup>251</sup>

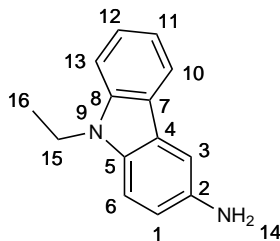
(**57**) (500 mg, 2.36 mmol) and ammonium formate (743 mg, 11.8 mmol) were dissolved in 30 mL methanol. After 10 min stirring under N<sub>2</sub> at 20 °C, 10% palladium on carbon (59 mg) was added and the suspension was heated at reflux for 16 h. The mixture was then filtered over celite and washed with methanol. The filtrate was neutralised with 0.1 M citric acid and extracted with ethyl acetate (3 x 30 mL). The combined organic layers were washed with brine and dried over magnesium sulfate before concentrating. The residue was purified by column chromatography (50% ethyl acetate 50% hexane) to give **58** (135 mg, 31%) as a tan solid,  $\nu_{max}$  (cm<sup>-1</sup>): 3100-3500 (NH), 2300-2700 (NH); <sup>1</sup>H NMR (500 MHz, CD<sub>3</sub>OD)  $\delta$  ppm 7.96 (1H, d,  $J=7.7$  Hz, aryl), 7.47 (1H, dd,  $J=7.8, 1.0$  Hz, aryl), 7.43 (1H, d,  $J=8.2$  Hz, aryl), 7.32 (1H, ddd,  $J=8.2, 7.1, 1.2$  Hz, aryl), 7.10 (1H, m,  $J=7.5, 7.5, 0.9$  Hz, aryl), 6.97 (1H, t,  $J=7.6$  Hz, aryl), 6.78 (1H, dd,  $J=7.6, 1.1$  Hz, aryl); HRMS calcd for C<sub>12</sub>H<sub>11</sub>N<sub>2</sub>: 183.0922 (M+H), found: 183.0920.

**3-Nitro-9-ethyl-9H-carbazole (60)**

To a solution of 9-ethyl-9H-carbazole (4.0 g 14 mmol) in glacial acetic acid (70

mL) was added with stirring fuming nitric acid (1 mL) in glacial acetic acid (3 mL) over 30 min. The mixture was stirred for 1 h at 20 °C before being poured into iced water (100 mL) and stirred for 30 min, the precipitate was extracted into ethyl acetate and purified by column chromatography (20% ethyl acetate 80% hexane) and recrystallised from ethyl acetate to give (**60**) (3.35 g, 99%), m.p. 128-130 °C (Lit 126-127 °C<sup>253</sup>);  $\nu_{max}$  (cm<sup>-1</sup>): 1593 (N=O); <sup>1</sup>H NMR (500 MHz, chloroform-*d*)  $\delta$  ppm 8.91 (1H, d,  $J=2.2$  Hz, H<sub>(3)</sub>), 8.33 (1H, dd,  $J=9.0, 2.2$  Hz, H<sub>(1)</sub>), 8.08 (1H, d,  $J=7.7$  Hz, aryl), 7.56 (1H, ddd,  $J=8.3, 7.1, 1.2$  Hz, aryl), 7.45 (1H, d,  $J=8.4$  Hz, aryl), 7.30 - 7.37 (2H, m, aryl), 4.36 (2H, q,  $J=7.3$  Hz, 2H<sub>(15)</sub>), 1.45 (3H, t,  $J=7.3$  Hz, 3H<sub>(16)</sub>); <sup>13</sup>C NMR (126 MHz, chloroform-*d*)  $\delta$  ppm 143.03, 141.19, 140.60, 127.45, 122.93, 122.64, 121.60, 121.03, 120.78, 117.28, 109.50, 107.99, 38.14 C<sub>(15)</sub>, 13.84 C<sub>(16)</sub>.

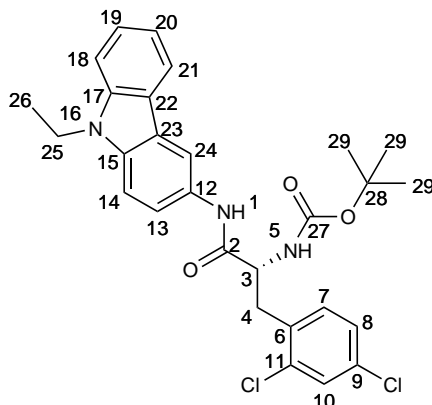
### 9-Ethyl-9*H*-carbazole-3-amine (**61**)



To a solution of 3-nitro-9-ethyl-9*H*-carbazole (**60**) (400 mg, 1.66 mmol) in methanol (20 mL) was added ammonium formate (64.3 mL, 7.9 mmol). After 10 min stirring under nitrogen 10% palladium on carbon (40 mg) was added and the reaction mixture was heated gently to reflux for 2.75 h. The catalyst was filtered through celite and washed with methanol before neutralising with citric acid (0.2 M) and extraction into ethyl acetate (2 x 30 mL) the combined organic layers were concentrated and purified by column chromatography (50% ethyl acetate 50% hexane) to give **61** (143 mg, 41%) as a grey solid which degraded quickly,  $\nu_{max}$  (cm<sup>-1</sup>): 3415 br. (NH), 3342 br. (NH), 2700-2950 (NH); <sup>1</sup>H NMR (500 MHz, chloroform-*d*)  $\delta$  ppm 8.02 (1H, d,  $J=7.7$  Hz, H<sub>(3)</sub>), 7.42 - 7.50 (2H, m, aryl), 7.37 (1H, d,  $J=8.0$  Hz, aryl), 7.14 - 7.28 (1H, m, aryl), 6.93 (1H, dd,  $J=8.5, 2.2$  Hz, aryl), 4.31 (2H, q,  $J=7.2$  Hz, H<sub>(15)</sub>), 3.52 (2H, br.s, H<sub>(14)</sub>), 1.41 (3H, t,  $J=7.2$  Hz), H<sub>(16)</sub>; <sup>13</sup>C NMR (126 MHz,

chloroform-*d*)  $\delta$  ppm 140.53, 138.94, 134.69, 125.54, 123.78, 122.58, 120.51, 118.13, 115.71, 109.10, 108.46, 106.51, 37.59 C<sub>(15)</sub>, 13.90 C<sub>(16)</sub>;

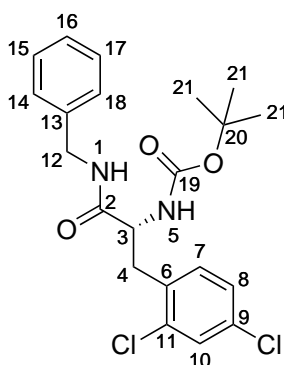
***tert*-Butyl (*R*)-(3-(2,4-dichlorophenyl)-1-((9-ethyl-9*H*-carbazol-3-yl)amino)-1-oxopropan-2-yl)carbamate (62)**



**61** (109 mg, 0.52 mmol), *N*-Boc-(*R*)-2,4-dichlorophenylalanine (201 mg, 0.6 mmol), 1-ethyl-3-(3-dimethylaminopropyl)carbodiimide (109 mg, 0.6 mmol) and anhydrous 1-hydroxybenzotriazole (122 mg, 0.6 mmol) in dimethylformamide (3.0 mL) was added *N,N*-diisopropylethylamine (0.78 mL, 4.5 mmol), the mixture was then stirred for 16 h at 20 °C. The mixture was diluted with ethyl acetate (20 mL) and washed with water (3 x 20 mL). The combined aqueous fractions were re-extracted with ethyl acetate (3 x 20 mL) and the combined organic layers were washed with saturated aqueous sodium hydrogen carbonate (2 x 20 mL) and brine (20 mL) before being dried over magnesium sulfate and evaporated. The residue was purified by column chromatography (20% ethyl acetate/hexane) to give **62** (127 mg, 46%) as a cream solid, m.p. 200-201 °C;  $\nu_{max}$  (cm<sup>-1</sup>): 3295 br. (NH), 1680 (NHC=O), 1651 (CHC=O); <sup>1</sup>H NMR (600 MHz, chloroform-*d*)  $\delta$  ppm 8.19 (1H, br.s, aryl), 7.95 (1H, br.s, aryl), 6.98 - 7.65 (8H, m, aryl), 5.49 (1H, br.s, H<sub>(1)</sub>/H<sub>(5)</sub>), 4.73 (1H, br.s, H<sub>(5)</sub>/H<sub>(1)</sub>), 4.21 (2H, br.s, H<sub>(25)</sub>), 3.38 (1H, br.s, H<sub>(4)</sub>), 3.22 (1H, br.s, H<sub>(4)</sub>), 1.39 (9H, br.s, H<sub>(29)</sub>), 1.32 (3H, br.s, 3H<sub>(26)</sub>); <sup>13</sup>C NMR (151 MHz, chloroform-*d*)  $\delta$  ppm 169.50 C<sub>(2)</sub>, 156.00 C<sub>(30)</sub>, 140.45, 137.41, 135.24, 133.64, 133.57, 132.71, 129.50,

129.07, 127.38, 125.93, 122.98, 122.78, 120.76, 119.69, 118.84, 113.12, 108.58, 108.50, 80.66 C<sub>(33)</sub>, 55.10 C<sub>(4)</sub>, 37.60 C<sub>(5)</sub>/C<sub>(28)</sub>, 35.87 C<sub>(28)</sub>/C<sub>(5)</sub>, 28.38 C<sub>(34)</sub>, C<sub>(35)</sub>, C<sub>36</sub>, 13.89 C<sub>(29)</sub>; HRMS calcd for C<sub>28</sub>H<sub>29</sub>Cl<sub>2</sub>N<sub>3</sub>O<sub>3</sub>: 525.1586, found: 525.1579.

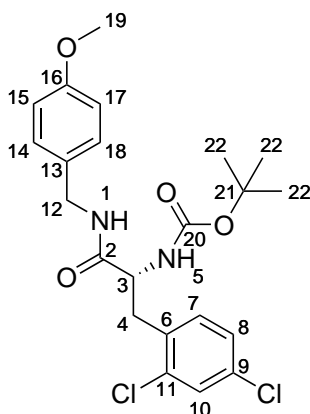
**(*R*)-*tert*-Butyl (1-(benzylamino)-3-(2,4-dichlorophenyl)-1-oxopropan-2-yl) carbamate (63)**



To benzylamine (0.11 mL, 1.0 mmol), *N*-Boc-(*R*)-2,4-dichlorophenylalanine (330 mg, 1.0 mmol), 1-ethyl-3-(3-dimethylaminopropyl)carbodiimide (182 mg, 1.0 mmol) and anhydrous 1-hydroxybenzotriazole (203 mg, 1.5 mmol) in dimethylformamide (3.0 mL) was added *N,N*-diisopropylethylamine (1.3 mL, 7.5 mmol), the mixture was then stirred for 18 h at 20 °C. The mixture was diluted with ethyl acetate (20 mL) and washed with water (3 x 20 mL). The combined aqueous fractions were re-extracted with ethyl acetate (3 x 20 mL) and the combined organic layers were washed with dilute hydrochloric acid (1 M, 20 mL) saturated aqueous sodium hydrogen carbonate (2 x 20 mL) and brine (20 mL) before being dried over magnesium sulfate and evaporated. The residue was purified by silica column chromatography (70% hexane 30% ethyl acetate) to give **63** (405 mg, 96%) as a white solid, m.p. 185 - 186.5 °C;  $[\alpha]_D^{25}$  *c*=1 Dichloromethane, +9.5°; <sup>1</sup>H NMR (500 MHz, chloroform-*d*) δ ppm 7.08 - 7.36 (8H, m, aryl), 6.44 (1H, br.s, H<sub>(1)</sub>), 5.22 (1H, d, *J*=8.7 Hz, H<sub>(5)</sub>), 4.41 - 4.51 (1H, m, H<sub>(3)</sub>), 4.29 - 4.40 (2H, m, H<sub>(12)</sub>), 3.15 - 3.33 (1H, m, H<sub>(4)</sub>), 2.95 - 3.15 (1H, m, H<sub>(4)</sub>), 1.21 - 1.40 (9H, m, 3 x 3H<sub>(21)</sub>); <sup>13</sup>C NMR (126 MHz, chloroform-*d*) δ ppm 170.81 C<sub>(2)</sub>, 155.50 C<sub>(19)</sub>, 137.68 C<sub>(13)</sub>, 135.10 C<sub>(6)</sub>, 133.51, 133.46, 132.59,

129.39 C<sub>(15)</sub>, C<sub>(17)</sub>, 128.73 C<sub>(14)</sub>, C<sub>(18)</sub>, 127.69, 127.60, 127.30, 80.36 C<sub>(20)</sub>, 54.53 C<sub>(3)</sub>, 43.58 C<sub>(12)</sub>, 35.79 C<sub>(4)</sub>, 28.27 3C<sub>(2)</sub>; HRMS calcd for C<sub>21</sub>H<sub>24</sub>Cl<sub>2</sub>N<sub>2</sub>O<sub>3</sub>: 445.1062, found: 445.1051.

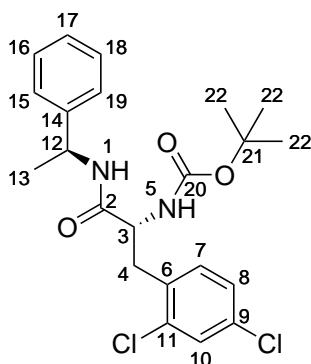
**(*R*)-*tert*-Butyl (3-(2,4-dichlorophenyl)-1-((4-methoxybenzyl)amino)-1-oxopropan-2-yl)carbamate (64)**



To 4-methoxybenzylamine (0.13 mL, 1.0 mmol), *N*-Boc-(*R*)-2,4-dichlorophenylalanine (334 mg, 1.0 mmol), 1-ethyl-3-(3-dimethylaminopropyl)carbodiimide (182 mg, 1.0 mmol) and anhydrous 1-hydroxybenzotriazole (203 mg, 1.5 mmol) in dimethylformamide (3.0 mL) was added *N,N*-diisopropylethylamine (1.3 mL, 7.5 mmol), the mixture was then stirred for 16 h at 30 °C. The mixture was then diluted with ethyl acetate (20 mL) and washed with water (3 x 20 mL). The combined aqueous fractions were re-extracted with ethyl acetate (3 x 20 mL) and the combined organic layers were washed with dilute hydrochloric acid (1 M, 20 mL), saturated aqueous sodium hydrogen carbonate (1 x 20 mL) and brine (20 mL) before being dried over magnesium sulfate and evaporated. The residue was purified by silica column chromatography (30% ethyl acetate 70% hexane) to give **64** (320 mg, 71%) as a white solid, m.p. 175-177 °C; <sup>1</sup>H NMR (500 MHz, chloroform-*d*) δ ppm 7.34 (1H, s, H<sub>(10)</sub>), 7.09 - 7.20 (2H, m, H<sub>(7)</sub>, H<sub>(8)</sub>), 7.04 (2H, d, *J*=8.5 Hz, H<sub>(14)</sub>, H<sub>(18)</sub>), 6.82 (2H, d, *J*=8.5 Hz, H<sub>(15)</sub>, H<sub>(17)</sub>), 6.22 (1H, br.s, H<sub>(1)</sub>), 5.16 (1H, d, *J*=6.3 Hz, H<sub>(5)</sub>), 4.42 (1H, d, *J*=6.3 Hz, H<sub>(3)</sub>), 4.18 - 4.35 (2H, m, 2H<sub>(12)</sub>), 3.79 (3H, s, 3H<sub>(19)</sub>), 3.21 (1H,

m, H<sub>(4)</sub>), 3.08 (1H, m, H<sub>(4)</sub>), 1.27 (9H, s, H<sub>(22)</sub>); <sup>13</sup>C NMR (126 MHz, chloroform-*d*) δ ppm 170.58 C<sub>(2)</sub>, 159.14 C<sub>(16)</sub>, 155.44 C<sub>(20)</sub>, 135.09 C<sub>(6)</sub>, 133.48, 132.58, 129.72, 129.39, 129.09 127.31, 114.12 C<sub>(15)</sub>,C<sub>(17)</sub>, 80.34 C<sub>(21)</sub>, 55.35 C<sub>(19)</sub>, 54.53 C<sub>(3)</sub>, 43.11 C<sub>(12)</sub>, 35.87 C<sub>(4)</sub>, 28.27 3C<sub>(2)</sub>; HRMS calcd for C<sub>22</sub>H<sub>26</sub>Cl<sub>2</sub>N<sub>2</sub>O<sub>4</sub>: 475.1167, found: 475.1166 (M+Na<sup>+</sup>).

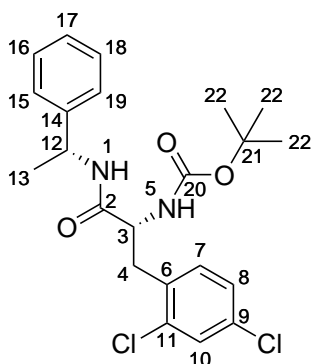
***tert*-Butyl ((*R*)-3-(2,4-dichlorophenyl)-1-oxo-1-(((*S*)-1-phenylethyl)amino)propan-2-yl)carbamate (65)**



To (*S*)-1-phenylethylamine (0.13 mL, 1.0 mmol), *N*-Boc-(*R*)-2,4-dichlorophenylalanine (334 mg, 1.0 mmol), 1-ethyl-3-(3-dimethylaminopropyl)carbodiimide (182 mg, 1.0 mmol) and anhydrous 1-hydroxybenzotriazole (203 mg, 1.5 mmol) in dimethylformamide (3.0 mL) was added *N,N*-diisopropylethylamine (1.3 mL, 7.5 mmol), the mixture was then stirred for 19 h at 20 °C. The mixture was diluted with ethyl acetate (20 mL) and washed with water (3 x 20 mL). The combined aqueous fractions were re-extracted with ethyl acetate (3 x 20 mL) and the combined organic layers were washed with dilute hydrochloric acid (1 M, 20 mL) saturated aqueous sodium hydrogen carbonate (2 x 20 mL) and brine (20 mL) before being dried over magnesium sulfate and evaporated. The residue was purified by silica column chromatography (20% ethyl acetate 80% hexane) to give **65** (221 mg, 51%) as a white solid, m.p. 169-170 °C;  $[\alpha]_D^{25}$  *c*=1 dichloromethane +2.8°; <sup>1</sup>H NMR (500 MHz, chloroform-*d*) δ ppm 7.03 - 7.43 (8H, m, aryl), 6.27 (1H, br.s, H<sub>(1)</sub>), 5.12 (1H, d, *J*=7.9 Hz, H<sub>(12)</sub>), 5.01 (1H, br.s, H<sub>(5)</sub>), 4.40 (1H, d, *J*=5.0 Hz, H<sub>(3)</sub>), 3.30 - 2.97 (2H,

m, H<sub>(5)</sub>), 1.36 (12H, br.s, 3H<sub>(13)</sub>, 3 x 3H<sub>(22)</sub>); <sup>13</sup>C NMR (126 MHz, chloroform-*d*) δ ppm 169.79 C<sub>(2)</sub>, 155.53 C<sub>(20)</sub>, 142.87 C<sub>(14)</sub>, 135.13 C<sub>(6)</sub>, 133.59, 133.50, 132.63, 129.39, 128.73, 127.46, 127.32 126.11, 80.42 C<sub>(21)</sub>, 54.47 C<sub>(12)</sub>, 49.02 C<sub>(3)</sub>, 35.46 C<sub>(4)</sub>, 28.26 3C<sub>(2)</sub>, 21.83 C<sub>(13)</sub>; HRMS calcd for for C<sub>22</sub>H<sub>26</sub>Cl<sub>2</sub>N<sub>2</sub>O<sub>3</sub>: 459.1218, found: 459.1218 (M<sup>+</sup>+Na).

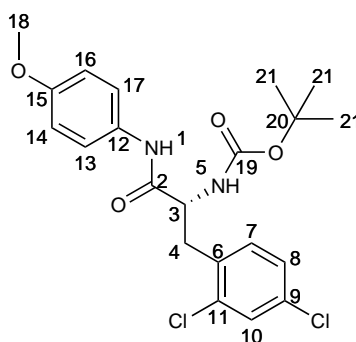
***tert*-Butyl((*R*)-3-(2,4-dichlorophenyl)-1-oxo-1-((*R*)-1-phenylethyl)amino)propan-2-yl)carbamate (**66**)**



To (*R*)-1-phenylethylamine (0.077 mL, 0.6 mmol), *N*-Boc-(*R*)-2,4-dichlorophenylalanine (201 mg, 0.6 mmol), 1-ethyl-3-(3-dimethylaminopropyl)carbodiimide (109 mg, 0.6 mmol) and anhydrous 1-hydroxybenzotriazole (122 mg, 0.9 mmol) in dimethylformamide (3.0 mL) was added *N,N*-diisopropylethylamine (0.78 mL, 4.5 mmol). The mixture was stirred for 20 h at 20 °C. The mixture was diluted with ethyl acetate (20 mL) and washed with water (3 x 20 mL). The combined aqueous fractions were re-extracted with ethyl acetate (3 x 20 mL) and the combined organic layers were washed with dilute hydrochloric acid (1 M, 2 x 20 mL) saturated aqueous sodium hydrogen carbonate (2 x 20 mL) and brine (20 mL) before being dried over magnesium sulfate and evaporated. Amide **66** was obtained as a white solid without further purification (247 mg, 94%), m.p. 178-180 °C;  $[\alpha]_D^{25}$  *c*=1 methanol: +22.1°; <sup>1</sup>H NMR (500 MHz, chloroform-*d*) δ ppm 6.99 - 7.18 (8H, m, aryl), 6.14 - 6.35 (1H, m, H<sub>(1)</sub>), 5.26 (1H, d, *J*=8.7 Hz, H<sub>(12)</sub>), 4.97 - 5.10 (1H, m, H<sub>(5)</sub>), 4.28 - 4.45 (1H, m, H<sub>(3)</sub>), 2.99 - 3.28 (2H, m, H<sub>(4)</sub>), 1.30 - 1.46 (12H, m, 3H<sub>(13)</sub>, 3 x 3H<sub>(22)</sub>);

$^{13}\text{C}$  NMR (126 MHz, chloroform-*d*)  $\delta$  ppm 169.88  $\text{C}_{(2)}$ , 155.48  $\text{C}_{(20)}$ , 142.65  $\text{C}_{(14)}$ , 135.01  $\text{C}_{(6)}$ , 133.43, 133.36, 132.51, 129.33, 128.69, 127.45, 127.28, 126.05, 80.31  $\text{C}_{(21)}$ , 54.56  $\text{C}_{(3)}$ , 48.96  $\text{C}_{(12)}$ , 35.87  $\text{C}_{(4)}$ , 28.29  $\text{C}_{(22)}$ , 21.84  $\text{C}_{(13)}$ ; HRMS calcd for  $\text{C}_{22}\text{H}_{26}\text{Cl}_2\text{N}_2\text{O}_3$ : 437.1399, found: 437.1384.

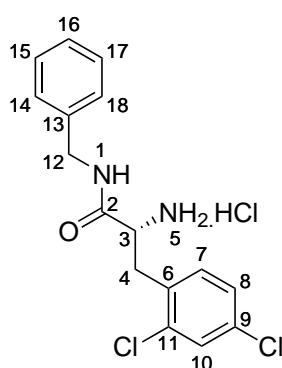
**(*R*)-*tert*-Butyl(3-(2,4-dichlorophenyl)-1-((4-methoxyphenyl)amino)-1-oxopropan-2-yl)carbamate (67)**



To anisidine (74 mg, 0.6 mmol), *N*-Boc-(*R*)-2,4-dichlorophenylalanine (201 mg, 0.6 mmol), 1-ethyl-3-(3-dimethylaminopropyl)carbodiimide (109 mg, 0.6 mmol) and anhydrous 1-hydroxybenzotriazole (122 mg, 0.9 mmol) in dimethylformamide (3.0 mL) was added *N,N*-diisopropylethylamine (0.78 mL, 4.5 mmol), the mixture was then stirred for 16 h at 20 °C. The mixture was diluted with ethyl acetate (20 mL) and washed with water (3 x 20 mL). The combined aqueous fractions were re-extracted with ethyl acetate (3 x 20 mL) and the combined organic layers were washed with dilute hydrochloric acid (1 M, 20 mL), saturated aqueous sodium hydrogen carbonate (2 x 20 mL) and brine (20 mL) before being dried over magnesium sulfate and evaporated. The residue was recrystallised (ethyl acetate/hexane) to give **67** (154 mg, 58%) as a white solid, m.p.(decomp. 180 °C);  $^1\text{H}$  NMR (500 MHz, chloroform-*d*)  $\delta$  ppm 8.08 (1H, br.s,  $\text{H}_{(1)}$ ), 7.38 (1H, s,  $\text{H}_{(10)}$ ), 7.31 (2H, d,  $J=8.6$  Hz,  $\text{H}_{(13)}, \text{H}_{(17)}$ ), 7.23 (1H, d,  $J=8.4$  Hz,  $\text{H}_{(7)}/\text{H}_{(8)}$ ), 7.15 (1H, d,  $J=8.4$  Hz,  $\text{H}_{(8)}/\text{H}_{(7)}$ ), 6.82 (2H, d,  $J=8.6$  Hz,  $\text{H}_{(14)}, \text{H}_{(16)}$ ), 5.30 (1H, d,  $J=8.4$  Hz,  $\text{H}_{(5)}$ ), 4.55 (1H, br.s,  $\text{H}_{(3)}$ ), 3.78 (3H, s,  $\text{H}_{(18)}$ ), 3.32 (1H, m,  $\text{H}_{(4)}$ ), 3.13 (1H, m,  $\text{H}_{(4)}$ ), 1.23 - 1.42 (9H, s, 3 x  $3\text{H}_{(21)}$ );  $^{13}\text{C}$  NMR (126 MHz, chloroform-*d*)  $\delta$  ppm 169.12  $\text{C}_{(2)}$ , 156.75  $\text{C}_{(15)}/\text{C}_{(19)}$

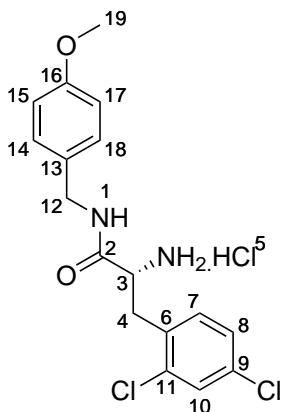
155.67 C<sub>(19)</sub>/C<sub>(15)</sub>, 135.14 C<sub>(6)</sub>, 133.59, 133.46, 132.56, 130.41, 129.45, 127.33, 122.01 C<sub>(13)</sub>, C<sub>(17)</sub>, 114.20 C<sub>(14)</sub>, C<sub>(16)</sub>, 80.73 C<sub>(20)</sub>, 55.51 C<sub>(18)</sub>, 55.09 C<sub>(3)</sub>, 35.53 C<sub>(4)</sub>, 28.26 3C<sub>(2)</sub>; HRMS calcd for for C<sub>21</sub>H<sub>24</sub>Cl<sub>2</sub>N<sub>2</sub>O<sub>4</sub>: 461.1011, found: 461.0992 M<sup>+</sup>+Na.

**(*R*)-2-Amino-*N*-benzyl-3-(2,4-dichlorophenyl)propanamide hydrochloride (68)**



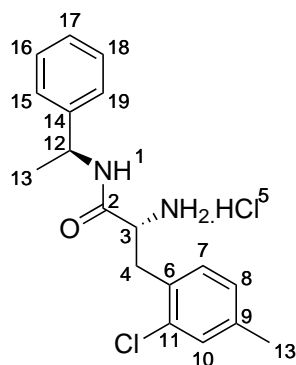
*N*-Boc protected amide **63** (210 mg, 0.5 mmol) was dissolved in dry diethyl ether (20 mL) and dichloromethane (10 mL). Hydrogen chloride was bubbled through the solution with vigorous stirring for 90 min. The precipitate was filtered by gravity filtration through filter paper in a funnel that was on top of a flask of boiling ether **68** (131 mg, 73%) as a white solid, m.p. (decomp. 205 °C);  $[\alpha]_D^{25}$  *c*=1 methanol: -53.5°; <sup>1</sup>H NMR (500 MHz, DMSO-*d*<sub>6</sub>, 2 rotamers) δ ppm 8.96 (1H, t, *J*=5.8 Hz, H<sub>(1)</sub>), 8.72 (3H, s, 3H<sub>(5)</sub>), 7.57 (1H, d, *J*=2.2 Hz, H<sub>(10)</sub>), 7.20 - 7.35 (5H, m, aryl), 7.02 - 7.09 (2H, m, aryl), 4.29 (1H, d, *J*=6.3 Hz, H<sub>(12)</sub>), 4.26 (1H, d, *J*=6.3 Hz, H<sub>(12)</sub>), 4.15 (1H, d, *J*=5.4 Hz, H<sub>(12)</sub>), 4.12 (1H, d, *J*=5.3 Hz, H<sub>(12)</sub>), 4.03 (1H, br.s, H<sub>(3)</sub>), 3.27 (1H, dd, *J*=13.5, 5.7 Hz, H<sub>(4)</sub>), 3.14 (1H, d, *J*=13.5, 9.4 Hz, H<sub>(4)</sub>); <sup>13</sup>C NMR (126 MHz, DMSO-*d*<sub>6</sub>) δ ppm 167.17 C<sub>(2)</sub>, 138.02 C<sub>(13)</sub>, 134.68 C<sub>(6)</sub>, 133.19, 132.70, 131.99, 128.78, 128.13, 127.40, 127.36, 126.91, 51.95 C<sub>(3)</sub>, 42.28 C<sub>(12)</sub>, 33.80 C<sub>(4)</sub>; HRMS calcd for C<sub>16</sub>H<sub>17</sub>Cl<sub>2</sub>N<sub>2</sub>O: 323.0718, found: 323.0720.

**(*R*)-2-Amino-3-(2,4-dichlorophenyl)-*N*-(4-methoxybenzyl)propanamide hydrochloride (69)**

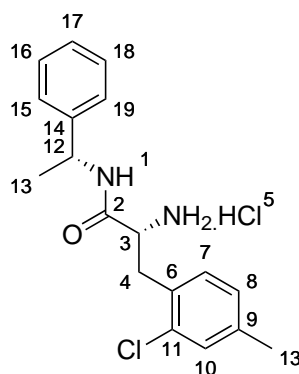


*N*-Boc protected amide **64** (260 mg, 0.67 mmol) was dissolved in dry diethyl ether (20 mL) and dichloromethane (1 mL). Hydrogen chloride was bubbled through the solution with vigorous stirring for 70 min. The precipitate was filtered by gravity filtration through filter paper in a funnel that was on top of a flask of boiling ether **69** (123 mg, 55%) as a white solid, m.p. (decomp. 155 °C);  $[\alpha]_D^{25}$   $c=1$  methanol: -55.9°;  $\nu_{max}$  (cm<sup>-1</sup>): 3216 (NH), 2892 (NH<sub>3</sub>), 1660 (C=O); <sup>1</sup>H NMR (500 MHz, DMSO-*d*<sub>6</sub>)  $\delta$  ppm 8.85 (1H, t,  $J=5.7$  Hz, H<sub>(1)</sub>), 8.70 (3H, br.s, 3H<sub>(5)</sub>), 7.57 (1H, s, H<sub>(10)</sub>), 7.26 - 7.34 (2H, m, H<sub>(7)</sub>,H<sub>(8)</sub>), 6.96 (2H, d,  $J=8.5$  Hz, H<sub>(14)</sub>,H<sub>(18)</sub>), 6.80 (2H, d,  $J=8.7$  Hz, H<sub>(15)</sub>,H<sub>(17)</sub>), 4.21 (1H, dd,  $J=14.8, 6.2$  Hz, H<sub>(12)</sub>), 4.04 (1H, dd,  $J=14.8, 5.1$  Hz, H<sub>(12)</sub>), 3.99 (1H, dd,  $J=9.2, 5.6$  Hz, H<sub>(3)</sub>), 3.71 (3H, s, H<sub>(19)</sub>), 3.25 (1H, dd,  $J=13.5, 5.6$  Hz, H<sub>(4)</sub>), 3.12 (1H, dd,  $J=13.4, 9.5$  Hz, H<sub>(4)</sub>); <sup>13</sup>C NMR (126 MHz, DMSO-*d*<sub>6</sub>)  $\delta$  ppm 166.98 C<sub>(2)</sub>, 158.30 C<sub>(16)</sub>, 134.64 C<sub>(6)</sub>, 133.17, 132.68, 131.96, 129.92, 128.77, 128.72 C<sub>(14)</sub>,C<sub>(18)</sub>, 127.39, 113.52 C<sub>(15)</sub>,C<sub>(17)</sub>, 55.06 C<sub>(19)</sub>, 51.89 C<sub>(3)</sub>, 41.71 C<sub>(12)</sub>, 33.81 C<sub>(4)</sub>; HRMS calcd for C<sub>17</sub>H<sub>19</sub>Cl<sub>2</sub>N<sub>2</sub>O<sub>2</sub>: 353.0824, found: 353.0825.

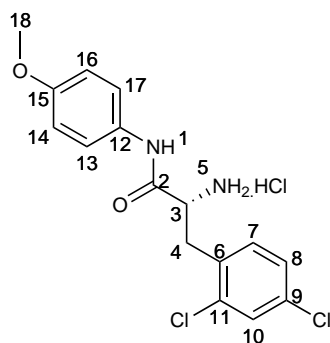
**(*R*)-2-Amino-3-(2,4-dichlorophenyl)-*N*-((*s*)-1-phenylethyl)propanamide hydrochloride (70)**



*N*-Boc protected amide **65** (210 mg, 496  $\mu$ mol) was dissolved in dry diethyl ether (20 mL) and dichloromethane (5 mL). Hydrogen chloride was bubbled through the solution with vigorous stirring for 4 h. The solvent was evaporated to give **70** (151 mg, 92%) as a cream solid, m.p.(decomp. 80 °C);  $[\alpha]_D^{25}$   $c=1$  methanol: -103.5°;  $\nu_{max}$  ( $\text{cm}^{-1}$ ): 2919 (NH)<sub>3</sub>, 1659 (C=O); <sup>1</sup>H NMR (500 MHz, DMSO-*d*<sub>6</sub>)  $\delta$  ppm 8.82 (1H, d,  $J=8.0$  Hz, H<sub>(1)</sub>), 8.56 - 8.75 (3H, br.s, 3H<sub>(5)</sub>), 7.56 - 7.66 (1H, m, H<sub>(10)</sub>), 7.37 - 7.45 (2H, m, aryl), 7.24 - 7.35 (4H, m, aryl), 7.14 - 7.23 (1H, m, H<sub>(12)</sub>), 4.80 (1H, quin,  $J=7.2$  Hz, H<sub>(15)</sub>), 3.95 - 4.04 (1H, m, H<sub>(4)</sub>), 3.30 (1H, dd,  $J=13.6, 5.4$  Hz, H<sub>(5)</sub>), 3.12 (1H, dd,  $J=13.6, 9.5$  Hz, H<sub>(5)</sub>), 1.08 - 1.13 (3H, m, H<sub>(22)</sub>); <sup>13</sup>C NMR (126 MHz, DMSO-*d*<sub>6</sub>)  $\delta$  ppm 166.23 C<sub>(3)</sub>, 143.53 C<sub>(14)</sub>, 134.78 C<sub>(6)</sub>, 133.32, 132.66, 132.13, 128.69, 128.17, 127.33, 126.77, 126.23, 51.95 C<sub>(3)</sub>, 48.26 C<sub>(12)</sub>, 33.91 C<sub>(4)</sub>, 21.96 C<sub>(13)</sub>; HRMS calcd for C<sub>17</sub>H<sub>19</sub>Cl<sub>2</sub>N<sub>2</sub>O: 337.0874, found: 337.0879.

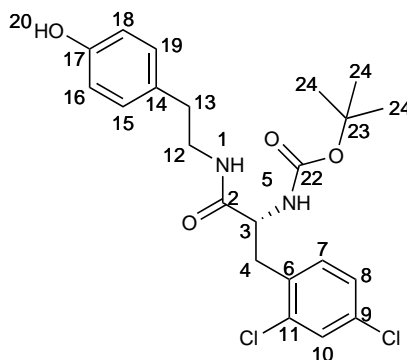
**(*R*)-2-Amino-3-(2,4-dichlorophenyl)-*N*-((*R*)-1-phenylethyl)propanamide hydrochloride (71)**

*N*-Boc protected amide **66** (213 mg, 0.49 mmol) was dissolved in dry diethyl ether (20 mL) and dichloromethane (1 mL). Hydrogen chloride was bubbled through the solution with vigorous stirring for 70 min. The solvent was evaporated to give **71** (175 mg, 63%) as a white solid, m.p. 110-112 °C; <sup>1</sup>H NMR (500 MHz, DMSO-*d*<sub>6</sub>) δ ppm 8.93 (1H, d, *J*=8.2 Hz, H<sub>(1)</sub>), 8.70 (3H, br.s, H<sub>(5)</sub>), 7.49 (1H, d, *J*=2.2 Hz, H<sub>(10)</sub>), 7.18 - 7.30 (4H, m, aryl), 7.14 (1H, dd, *J*= 8.2, 2.2 Hz, H<sub>(8)</sub>), 6.92 - 7.00 (2H, m, aryl), 4.87 (1H, quin *J*=7.1 Hz, H<sub>(12)</sub>), 4.05 (1H, br.s, H<sub>(3)</sub>), 3.19 (1H, dd, *J*=13.6, 5.5 Hz, H<sub>(4)</sub>), 3.08 (1H, dd, *J*=13.6, 9.8 Hz, H<sub>(4)</sub>), 1.32 (3H, d, *J*=7.1 Hz, H<sub>(13)</sub>); <sup>13</sup>C NMR (126 MHz, DMSO-*d*<sub>6</sub>) δ ppm 166.12 C<sub>(2)</sub>, 143.18 C<sub>(14)</sub>, 134.54 C<sub>(6)</sub>, 133.00, 132.57, 131.81, 128.71, 128.02 C<sub>(16)</sub>/C<sub>(18)</sub>, 127.33, 126.66, 125.85 C<sub>(15)</sub>/C<sub>(19)</sub>, 51.86 C<sub>(3)</sub>, 48.02 C<sub>(12)</sub>, 33.64 C<sub>(4)</sub>, 22.11 C<sub>(13)</sub>; HRMS calcd for C<sub>17</sub>H<sub>19</sub>Cl<sub>2</sub>N<sub>2</sub>O: 337.0874, found: 337.0873.

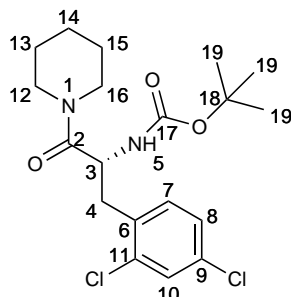
**(*R*)-2-Amino-3-(2,4-dichlorophenyl)-*N*-(4-methoxyphenyl)propanamide hydrochloride (72)**

*N*-Boc protected amide **67** (111 mg, 0.30 mmol) was dissolved in dry diethyl ether (11 mL) and dichloromethane (21 mL). Hydrogen chloride was bubbled through the solution with vigorous stirring for 3 h. The solvent was evaporated and the residue triturated with diethyl ether to give **72** (60 mg, 63%) as a cream solid, m.p. decomp. 115 °C;  $^1\text{H}$  NMR (500 MHz,  $\text{DMSO-}d_6$ )  $\delta$  ppm 10.52 (1H, s,  $\text{H}_{(1)}$ ), 8.59 - 8.79 (3H, s,  $\text{H}_{(5)}$ ), 7.58 (1H, d,  $J=2.0$  Hz,  $\text{H}_{(10)}$ ), 7.46 (1H, d,  $J=8.4$  Hz,  $\text{H}_{(7)}$ ), 7.41 (2H, d,  $J=9.1$  Hz,  $\text{H}_{(13)}, \text{H}_{(17)}$ ), 7.35 (1H, dd,  $J=8.4, 2.0$  Hz,  $\text{H}_{(8)}$ ), 6.87 (2H, d,  $\text{H}_{(14)}, \text{H}_{(16)}$ ), 4.15 - 4.23 (1H, m,  $\text{H}_{(3)}$ ), 3.70 (3H, s,  $\text{H}_{(18)}$ ), 3.29 - 3.35 (1H, m,  $\text{H}_{(4)}$ ), 3.20 - 3.28 (1H, dd,  $J=13.4, 8.7$  Hz,  $\text{H}_{(4)}$ );  $^{13}\text{C}$  NMR (126 MHz,  $\text{DMSO-}d_6$ )  $\delta$  ppm 165.55  $\text{C}_{(2)}$ , 155.83  $\text{C}_{(15)}$ , 134.74  $\text{C}_{(6)}$ , 133.20, 132.73, 131.94, 130.96, 128.78, 127.36, 121.28  $\text{C}_{(13)}, \text{C}_{(17)}$ , 113.93  $\text{C}_{(14)}, \text{C}_{(16)}$ , 55.19  $\text{C}_{(18)}$ , 52.65  $\text{C}_{(3)}$ , 33.76  $\text{C}_{(4)}$ ; HRMS calcd for  $\text{C}_{16}\text{H}_{17}\text{Cl}_2\text{N}_2\text{O}_2$ : 339.0667, found: 339.0666.

*(R)*-*tert*-Butyl (3-(2,4-dichlorophenyl)-1-((4-hydroxyphenethyl)amino)-1-oxopropan-2-yl)carbamate (**73**)

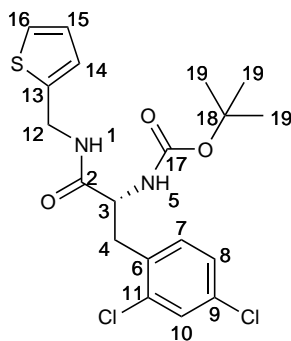


To tyramine hydrochloride (104 mg, 0.6 mmol), *N*-Boc-*(R)*-2,4-dichlorophenylalanine (201 mg, 0.6 mmol), 1-ethyl-3-(3-dimethylaminopropyl)carbodiimide (109 mg, 0.6 mmol) and anhydrous 1-hydroxybenzotriazole (122 mg, 0.9 mmol) in dimethylformamide (3.0 mL) was added *N,N*-diisopropylethylamine (0.78 mL, 4.5 mmol), the mixture was then stirred for 16 h at 20 °C. The mixture was then diluted with ethyl acetate (20 mL) and washed with water (3 x 20 mL). The combined aqueous fractions were re-extracted with ethyl acetate (3 x 20 mL) and the combined organic layers were washed with dilute hydrochloric acid (1 M, 20 mL), saturated aqueous sodium hydrogen carbonate (2 x 20 mL) and brine (20 mL) before being dried over magnesium sulfate and evaporated to give **73** (200 mg, 74%) as a white solid without further purification, m.p. 66-68 °C;  $[\alpha]_D^{25} c=1$  dichloromethane +0.4 °;  $^1\text{H NMR}$  (500 MHz, chloroform-*d*)  $\delta$  ppm 7.30 - 7.36 (1H, s, H<sub>(10)</sub>), 7.04 - 7.19 (2H, m, H<sub>(8)</sub>,H<sub>(9)</sub>), 6.91 (2H, d,  $J=7.8$  Hz, H<sub>(15)</sub>,H<sub>(19)</sub>), 6.74 (2H, d,  $J=8.5$  Hz, H<sub>(16)</sub>,H<sub>(19)</sub>), 6.08 - 6.28 (1H, br.s, H<sub>(1)</sub>), 5.25 (1H, d,  $J=9.5$  Hz, H<sub>(5)</sub>), 4.35 (1H, d,  $J=7.4$  Hz, H<sub>(3)</sub>), 3.27 - 3.48 (2H, m, H<sub>(12)</sub>), 3.09-3.24 (1H, m, H<sub>(4)</sub>), 2.96 - 3.05 (1H, m, H<sub>(4)</sub>), 2.54 - 2.69 (2H, m, H<sub>(13)</sub>), 1.22 - 1.40 (9H, m, 3 x 3H<sub>(24)</sub>);  $^{13}\text{C NMR}$  (126 MHz, chloroform-*d*)  $\delta$  ppm 170.72 C<sub>(2)</sub>, 155.21 C<sub>(22)</sub>, 154.65 C<sub>(17)</sub>, 134.71 C<sub>(6)</sub>, 133.16, 133.00, 132.09, 129.48, 129.35, 128.97, 126.85, 115.31 C<sub>(16)</sub>,C<sub>(18)</sub>, 80.16 C<sub>(23)</sub>, 54.12 C<sub>(3)</sub>, 40.66 C<sub>(12)</sub>, 35.62 C<sub>(4)</sub>, 34.24 C<sub>(13)</sub>, 27.87 C<sub>(24)</sub>; HRMS calcd for C<sub>22</sub>H<sub>26</sub>Cl<sub>2</sub>N<sub>2</sub>O<sub>4</sub>: 475.1167, found: 475.1163.

***tert*-Butyl(*R*)-(3-(2,4-dichlorophenyl)-1-oxo-1-(piperidin-1-yl)propan-2-yl)carbamate (74)**

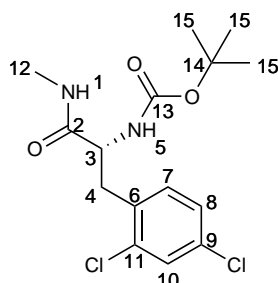
To piperidine (0.59 mL, 0.6 mmol), *N*-Boc-(*R*)-2,4-dichlorophenylalanine (201 mg, 0.6 mmol), 1-ethyl-3-(3-dimethylaminopropyl)carbodiimide (109 mg, 0.6 mmol) and anhydrous 1-hydroxybenzotriazole (122 mg, 0.6 mmol) in dimethylformamide (3.0 mL) was added *N,N*-diisopropylethylamine (0.78 mL, 4.5 mmol), the mixture was then stirred for 16 h at 20 °C. The mixture was diluted with ethyl acetate (20 mL) and washed with water (3 x 20 mL). The combined aqueous fractions were re-extracted with ethyl acetate (3 x 20 mL) and the combined organic layers were washed with saturated aqueous sodium hydrogen carbonate (2 x 20 mL) and brine (20 mL) before being dried over magnesium sulfate and evaporated to give **74** (197 mg, 82%) as a pure white solid, m.p. 104-106 °C;  $\nu_{max}$  (cm<sup>-1</sup>): 3290-4320 (NH), 2930 br. (NH), 1707 (NHC=O), 1628 (CHC=O); <sup>1</sup>H NMR (500 MHz, chloroform-*d*)  $\delta$  ppm 7.23 - 7.35 (1H, s, H<sub>(10)</sub>), 7.03 - 7.15 (2H, m, H<sub>(7)</sub>,H<sub>(8)</sub>), 5.46 - 5.59 (1H, d, *J*=7.7 Hz, H<sub>(5)</sub>), 4.85 - 4.97 (1H, m, H<sub>(3)</sub>), 3.34 - 3.61 (3H, m, 2H<sub>(12)</sub>,2H<sub>(16)</sub>), 3.19 - 3.33 (1H, m, H<sub>(12)</sub>/H<sub>(16)</sub>), 3.02 (1 H, dd, *J*=13.1, 5.0 Hz, H<sub>(4)</sub>), 2.86 (1 H, dd, *J*=13.1, 8.2 Hz, H<sub>(4)</sub>), 1.35 - 1.64 (6H, m, H<sub>(13)</sub>,H<sub>(14)</sub>,H<sub>(15)</sub>), 1.22 - 1.32 (9H, m, 3 x 3H<sub>(19)</sub>); <sup>13</sup>C NMR (126 MHz, chloroform-*d*)  $\delta$  ppm 169.38 C<sub>(2)</sub>, 154.91 C<sub>(17)</sub>, 135.21 C<sub>(6)</sub>, 133.36, 133.30, 132.94, 129.11, 126.84, 79.42 C<sub>(18)</sub>, 48.94 C<sub>(3)</sub>, 46.62 C<sub>(12)</sub>/C<sub>(16)</sub>, 43.23 C<sub>(16)</sub>/C<sub>(12)</sub>, 37.39 C<sub>(4)</sub>, 28.27 C<sub>(19)</sub>, 26.32 C<sub>(13)</sub>/C<sub>(14)</sub>/C<sub>(15)</sub>, 25.48 C<sub>(15)</sub>/C<sub>(13)</sub>/C<sub>(14)</sub>, 24.37 C<sub>(14)</sub>/C<sub>(15)</sub>/C<sub>(13)</sub>; HRMS calcd for C<sub>19</sub>H<sub>26</sub>Cl<sub>2</sub>N<sub>2</sub>O<sub>3</sub>: 400.1320, found: 400.1310.

*(R)*-*tert*-Butyl (3-(2,4-dichlorophenyl)-1-oxo-1-((thiophen-2-ylmethyl)amino)propan-2-yl)carbamate (**75**)



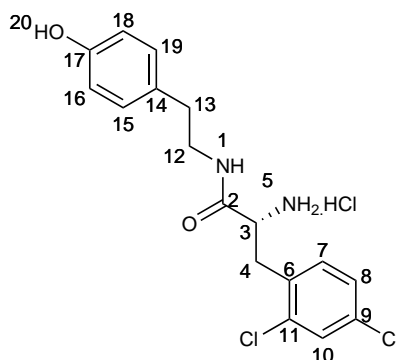
To 2-(thiophenyl)-methylamine (0.05 mL, 0.45 mmol), *N*-Boc-*(R)*-2,4-dichlorophenylalanine (153 mg, 0.6 mmol), 1-ethyl-3-(3-dimethylaminopropyl)carbodiimide (82 mg, 0.45 mmol) and anhydrous 1-hydroxybenzotriazole (91 mg, 67.5 mmol) in dimethylformamide (3.0 mL) was added *N,N*-diisopropylethylamine (0.59 mL, 3.4 mmol), the mixture was then stirred for 21 h at 20 °C. The mixture was diluted with ethyl acetate (20 mL) and washed with water (3 x 20 mL). The combined aqueous fractions were re-extracted with ethyl acetate (3 x 20 mL) and the combined organic layers were washed with saturated aqueous sodium hydrogen carbonate (2 x 20 mL) and brine (20 mL) before being dried over magnesium sulfate. The residue was purified by silica chromatography (28% ethyl acetate 72% hexane) to give **75** (100 mg, 54%) as a white solid, m.p. 162-163.5 °C;  $[\alpha]_D^{25}$  *c*=1 methanol: +11.6°; <sup>1</sup>H NMR (500 MHz, chloroform-*d*)  $\delta$  ppm 7.31 (1H, s, aryl), 7.06 - 7.19 (3H, m, aryl), 6.81 - 6.95 (2H, m, aryl), 6.64 - 6.80 (1H, m, aryl), 5.31 (1H, d, *J*=9.3 Hz H<sub>(1)</sub>), 4.37 - 4.61 (3H, m, H<sub>(3)</sub>, 2H<sub>(12)</sub>), 3.13 - 3.33 (1H, m, H<sub>(4)</sub>), 2.93 - 3.12 (1H, m, H<sub>(4)</sub>), 1.27 - 1.40 (9H, m, 3 x 3H<sub>(19)</sub>); <sup>13</sup>C NMR (126 MHz, chloroform-*d*)  $\delta$  ppm 170.78 C<sub>(2)</sub>, 155.55 C<sub>(17)</sub>, 140.33, 135.08 C<sub>(6)</sub>, 133.46, 133.40, 132.54, 129.34, 127.24, 126.89, 126.12, 125.25, 80.32 C<sub>(18)</sub>, 54.34 C<sub>(3)</sub>, 38.28 C<sub>(12)</sub>, 35.75 C<sub>(4)</sub>, 28.27 3C<sub>(2)</sub>; ; HRMS calcd for C<sub>19</sub>H<sub>23</sub>Cl<sub>2</sub>N<sub>2</sub>O<sub>3</sub>S: 429.0806, found: 429.0793.

*tert*-Butyl (*R*)-(3-(2,4-dichlorophenyl)-1-(methylamino)-1-oxopropan-2-yl)carbamate (**76**)



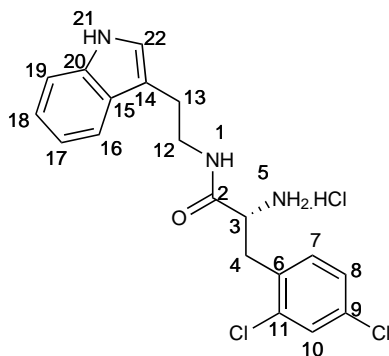
To methylamine (0.075 mL, 0.6 mmol), *N*-Boc-(*R*)-2,4-dichlorophenylalanine (201 mg, 0.6 mmol), 1-ethyl-3-(3-dimethylaminopropyl)carbodiimide (109 mg, 0.6 mmol) and anhydrous 1-hydroxybenzotriazole (122 mg, 0.6 mmol) in dimethylformamide (3.0 mL) was added *N,N*-diisopropylethylamine (0.78 mL, 4.5 mmol), the mixture was then stirred for 16 h at 20 °C. The mixture was diluted with ethyl acetate (20 mL) and washed with water (3 x 20 mL). The combined aqueous fractions were re-extracted with ethyl acetate (3 x 20 mL) and the combined organic layers were washed with saturated aqueous sodium hydrogen carbonate (2 x 20 mL) and brine (20 mL) before being dried over magnesium sulfate and evaporated to give **76** (154 mg, 74%) as a white solid, m.p. 181-183 °C;  $\nu_{max}$  (cm<sup>-1</sup>): 3330 (NH), 1682 (NHC=O), 1651 (CHC=O); <sup>1</sup>H NMR (500 MHz, chloroform-*d*)  $\delta$  ppm 7.31 - 7.38 (1H, m, H<sub>(10)</sub>), 7.11 - 7.21 (2H, m, H<sub>(7)</sub>, H<sub>(8)</sub>), 6.15 (1H, br.s, H<sub>(1)</sub>), 5.15 - 5.25 (1H, d, *J*=8.2 Hz, H<sub>(5)</sub>), 4.32 - 4.43 (1H, m, H<sub>(3)</sub>), 3.15 - 3.35 (1H, m, H<sub>(4)</sub>), 2.96 - 3.08 (1H, m, H<sub>(4)</sub>), 2.65 - 2.80 (3H, m, H<sub>(12)</sub>), 1.30 - 1.38 (9H, m, 3 x 3H<sub>(15)</sub>); <sup>13</sup>C NMR (126 MHz, chloroform-*d*)  $\delta$  ppm 171.54 C<sub>(2)</sub>, 155.46 C<sub>(13)</sub>, 135.12 C<sub>(6)</sub>, 133.62, 133.46, 132.48, 129.34, 127.20, 80.25 C<sub>(14)</sub>, 54.47 C<sub>(3)</sub>, 35.94 C<sub>(4)</sub>, 28.25 3C<sub>(2)</sub>, 26.28 C<sub>(12)</sub>; HRMS calcd for C<sub>15</sub>H<sub>20</sub>Cl<sub>2</sub>N<sub>2</sub>O<sub>3</sub>: 346.0851, Measured: 346.0866.

**(*R*)-2-Amino-3-(2,4-dichlorophenyl)-*N*-(4-hydroxyphenethyl)-propanamide hydrochloride (77)**



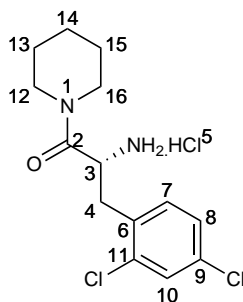
*N*-Boc protected amide **73** (199 mg, 0.5 mmol) was dissolved in dry diethyl ether (15 mL). Hydrogen chloride was bubbled through the solution with vigorous stirring for 135 min. The precipitate was filtered by gravity filtration through filter paper in a funnel that was on top of a flask of boiling ether **68** (219 mg, >100%) as a hygroscopic white solid, m.p. (decomp. 100 °C);  $[\alpha]_D^{26}$  methanol: -48.0°;  $\nu_{max}$  (cm<sup>-1</sup>): 3054 (NH<sub>3</sub>), 2918, 2848, 1663 (C=O); <sup>1</sup>H NMR (500 MHz, DMSO-*d*<sub>6</sub>)  $\delta$  ppm 9.17 - 9.33 (1H, s, H<sub>(1)</sub>), 8.46 - 8.64 (4H, m, H<sub>(5)</sub>,H<sub>(20)</sub>), 7.59 (1H, s, H<sub>(10)</sub>), 7.30 - 7.42 (2H, m, H<sub>(7)</sub>,H<sub>(8)</sub>), 6.90 (2H, d, *J* = 8.4 Hz, H<sub>(16)</sub>,H<sub>(18)</sub>), 6.66 (2H, d, *J* = 8.5 Hz, H<sub>(15)</sub>,H<sub>(19)</sub>), 3.87 - 4.05 (1H, m, H<sub>(3)</sub>), 3.32 - 3.41 (1H, m, H<sub>(12)</sub>), 3.15 - 3.29 (2H, m, H<sub>(4)</sub>,H<sub>(12)</sub>), 3.03 - 3.14 (2H, m, H<sub>(4)</sub>,H<sub>(13)</sub>), 2.37 - 2.46 (1H, m, H<sub>(13)</sub>); <sup>13</sup>C NMR (126 MHz, DMSO-*d*<sub>6</sub>)  $\delta$  ppm 167.08 C<sub>(2)</sub>, 155.80 C<sub>(17)</sub>, 134.69 C<sub>(6)</sub>, 133.18, 132.74, 132.03, 129.34 C<sub>(15)</sub>,C<sub>(19)</sub>, 128.97, 128.77, 127.39, 115.15 C<sub>(16)</sub>,C<sub>(18)</sub>, 51.92 C<sub>(4)</sub>, 40.69 C<sub>(12)</sub>, 33.94 C<sub>(13)</sub>, 33.88 C<sub>(4)</sub>; HRMS calcd for C<sub>17</sub>H<sub>19</sub>Cl<sub>2</sub>N<sub>2</sub>O<sub>2</sub>: 353.0824, found: 353.0822.

**(*R*)-*N*-(2-(1(*H*)-indol-3-yl)ethyl)-2-amino-3-(2,4-dichlorophenyl)propanamide hydrochloride (**78**)**

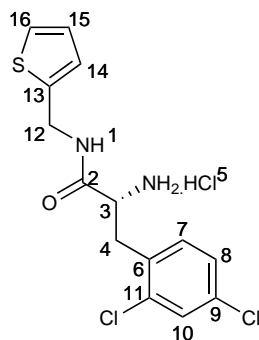


*N*-Boc protected amide **54** (84 mg, 0.2 mmol) was dissolved in dry diethyl ether (5 mL) and dichloromethane (20 mL). Hydrogen chloride was bubbled through the solution with vigorous stirring for 70 min. The solvent was evaporated to give **78** (70 mg, 94%) as a cream solid, m.p. (decomp. 120 °C);  $[\alpha]_D^{25}$   $c=1$  methanol: -53.4°;  $^1\text{H}$  NMR (500 MHz, DMSO- $d_6$ )  $\delta$  ppm 8.50 - 8.7 (5H, m, H<sub>(1)</sub>, 3H<sub>(5)</sub>, H<sub>(21)</sub>), 6.27 - 7.75 (9H, m, aryl), 3.81 - 4.10 (1H, m, H<sub>(3)</sub>), 3.32 - 3.39 (1H, m, H<sub>(12)</sub>), 3.16 - 3.30 (2H, m, H<sub>(4)</sub>, H<sub>(12)</sub>), 3.03 - 3.15 (1H, m, H<sub>(4)</sub>), 2.60 - 2.78 (2H, m, H<sub>(13)</sub>);  $^{13}\text{C}$  NMR (126 MHz, DMSO- $d_6$ )  $\delta$  ppm 167.08 C<sub>(2)</sub>, 136.25, 134.69, 133.20, 132.69, 132.06, 128.74, 127.33, 127.01, 122.72, 120.91, 118.24, 118.03, 111.43, 111.24, 64.89 C<sub>(12)</sub>, 52.00 C<sub>(3)</sub>, 33.86 C<sub>(4)</sub>, 24.73 C<sub>(13)</sub>; HRMS calcd for C<sub>19</sub>H<sub>20</sub>Cl<sub>2</sub>N<sub>3</sub>O: 376.0983, found: 376.0979.

**(*R*)-2-Amino-3-(2,4-dichlorophenyl)-1-(piperidin-1-yl)propan-1-one hydrochloride (79)**

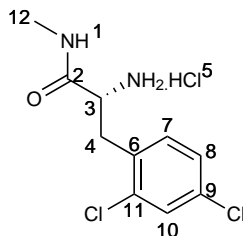


*N*-Boc protected amide **74** (197 mg, 0.58 mmol) was dissolved in dry diethyl ether (15 mL). Hydrogen chloride was bubbled through the solution with vigorous stirring for 60 min. The precipitate was filtered by gravity filtration through filter paper in a funnel that was on top of a flask of boiling ether **79** (139 mg, 83%) as a white solid, m.p. 228 - 229 °C; <sup>1</sup>H NMR (500 MHz, DMSO-*d*<sub>6</sub>) δ ppm 8.57 (3H, br.s, 3H<sub>(5)</sub>), 7.57 - 7.69 (1H, s, H<sub>(10)</sub>), 7.38 - 7.47 (2H, m, H<sub>(7)</sub>,H<sub>(8)</sub>), 4.47 - 4.60 (1H, m, H<sub>(3)</sub>), 3.28 - 3.46 (2H, m, H<sub>(12)</sub>/H<sub>(16)</sub>), 3.15 - 3.27 (2H, m, H<sub>(16)</sub>/H<sub>(12)</sub>), 3.01 - 3.13 (1H, m, H<sub>(4)</sub>), 2.87 - 2.99 (1H, m, H<sub>(4)</sub>), 1.33 - 1.55 (4H, m, 2H<sub>(13)</sub>,2H<sub>(15)</sub>), 1.19 - 1.33 (1H, m, H<sub>(14)</sub>), 0.80 - 0.96 (1H, m, H<sub>(14)</sub>); <sup>13</sup>C NMR (126 MHz, DMSO-*d*<sub>6</sub>) δ ppm 165.87 C<sub>(2)</sub>, 134.59 C<sub>(6)</sub>, 133.74, 133.07, 131.67, 128.85, 127.65, 47.80 C<sub>(3)</sub>, 45.97 C<sub>(12)</sub>/C<sub>(16)</sub>, 42.60 C<sub>(16)</sub>/C<sub>(12)</sub>, 33.94 C<sub>(4)</sub>, 25.34 C<sub>(13)</sub>/C<sub>(14)</sub>/C<sub>(15)</sub>, 24.90 C<sub>(14)</sub>/C<sub>(15)</sub>/C<sub>(13)</sub>, 23.55 C<sub>(15)</sub>/C<sub>(13)</sub>/C<sub>(14)</sub>; HRMS calcd for C<sub>14</sub>H<sub>19</sub>Cl<sub>2</sub>N<sub>2</sub>O: 301.0874, found: 301.0813.

**(*R*)-2-Amino-3-(2,4-dichlorophenyl)-*N*-(thiophen-2-ylmethyl)propanamide hydrochloride (80)**

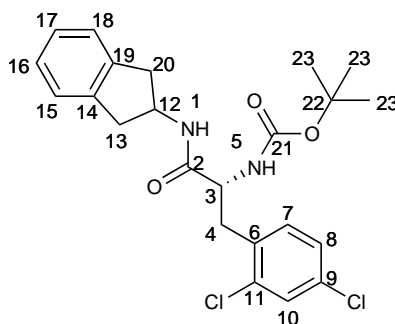
*N*-Boc protected amide **75** (130 mg, 0.35 mmol) was dissolved in dry diethyl ether (20 mL) and dichloromethane (2 mL). Hydrogen chloride was bubbled through the solution with vigorous stirring for 140 min. The precipitate was filtered by gravity filtration through filter paper in a funnel that was on top of a flask of boiling ether **80** (48 mg, 42%) as a white solid, m.p. 191-193 °C; <sup>1</sup>H NMR (500 MHz, DMSO-*d*<sub>6</sub>) δ ppm 9.04 (1H, t, *J*=5.7 Hz, H<sub>(1)</sub>), 8.67 (3H, br.s, H<sub>(5)</sub>), 7.55 (1H, d, *J*=2.1 Hz, aryl), 7.38 (1H, dd, *J*=5.1, 1.3 Hz, aryl), 7.31 (1H, d, *J*= 8.2 Hz, aryl), 7.25 (1H, d, *J*= 8.2, 2.1 Hz, aryl), 6.92 (1H, dd, *J*=5.1, 3.4 Hz, aryl), 6.85 (1H, dd, *J*=3.4, 1.1 Hz, aryl), 4.42 (1H, dd, *J*=15.3, 6.0 Hz, H<sub>(12)</sub>), 4.31 (1H, dd, *J*=15.3, 5.4 Hz, H<sub>(12)</sub>), 3.93 - 4.02 (1H, m, H<sub>(3)</sub>), 3.24 (1H, dd, *J*=13.7, 5.8 Hz, H<sub>(4)</sub>), 3.11 (1H, dd, *J*=13.7, 9.0 Hz, H<sub>(4)</sub>); <sup>13</sup>C NMR (126 MHz, DMSO-*d*<sub>6</sub>) δ ppm 167.05 C<sub>(2)</sub>, 140.44, 134.64, 133.10, 132.69, 131.83, 128.74, 127.32, 126.61, 126.11, 125.31, 51.80 C<sub>(3)</sub>, 37.24 C<sub>(12)</sub>, 33.78 C<sub>(4)</sub>; HRMS calcd for C<sub>14</sub>H<sub>15</sub>Cl<sub>2</sub>N<sub>2</sub>OS: 329.0282, found: 329.0273.

**(*R*)-2-Amino-3-(2,4-dichlorophenyl)-*N*-methylpropanamide hydrochloride (81)**



**76** (154 mg, 0.44 mmol) was dissolved in dry diethyl ether (15 mL) and dichloromethane (5 mL). Hydrogen chloride was bubbled through the solution with vigorous stirring for 4.5 h. The precipitate was filtered by gravity filtration through filter paper in a funnel that was on top of a flask of boiling ether **81** (96 mg, 82%) as a white solid,  $^1\text{H}$  NMR (500 MHz,  $\text{DMSO-}d_6$ )  $\delta$  ppm 8.65 (3H, br.s,  $3\text{H}_{(6)}$ ), 8.48 (1H, q,  $J=4.4$  Hz,  $\text{H}_{(1)}$ ), 7.57 (1H, s,  $\text{H}_{(10)}$ ), 7.33 - 7.42 (2H, s,  $\text{H}_{(7)}$ ,  $\text{H}_{(8)}$ ), 3.90 (1H, br.s,  $\text{H}_{(3)}$ ), 3.23 (1H, dd,  $J=13.7, 5.7$  Hz,  $\text{H}_{(4)}$ ), 3.10 (1H, dd,  $J=13.7, 8.7$  Hz,  $\text{H}_{(4)}$ ), 2.51 (3H, s,  $\text{H}_{(12)}$ );  $^{13}\text{C}$  NMR (126 MHz,  $\text{DMSO-}d_6$ )  $\delta$  ppm 167.58  $\text{C}_{(2)}$ , 134.66 (6), 133.11, 132.64, 132.15, 128.73, 127.35, 51.99  $\text{C}_{(4)}$ , 33.71  $\text{C}_{(3)}$ , 25.49  $\text{C}_{(12)}$ ; HRMS calcd for  $\text{C}_{10}\text{H}_{13}\text{Cl}_2\text{N}_2\text{O}$ : 247.0405, found: 247.0414.

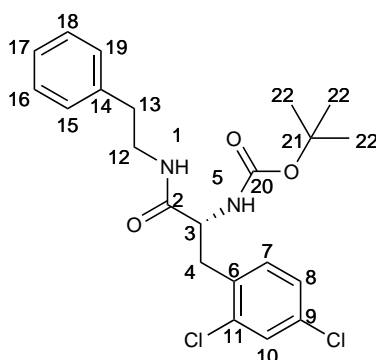
***tert*-Butyl (*R*)-(3-(2,4-dichlorophenyl)-1-((2,3-dihydro-1H-inden-2-yl)amino)-1-oxopropan-2-yl)carbamate (82)**



2-Aminoindane (0.08 mL, 0.6 mmol), *N*-Boc-(*R*)-2,4-dichlorophenylalanine (201 mg,

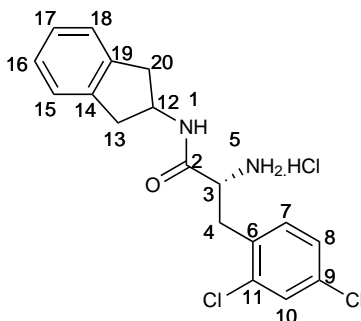
0.6 mmol), 1-ethyl-3-(3-dimethylaminopropyl)carbodiimide (109 mg, 0.6 mmol) and anhydrous 1-hydroxybenzotriazole (122 mg, 0.6 mmol) in dimethylformamide (3.0 mL) was added *N,N*-diisopropylethylamine (0.78 mL, 4.5 mmol), the mixture was then stirred for 16 h at 20 °C. The mixture was diluted with ethyl acetate (20 mL) and washed with water (3 x 20 mL). The combined aqueous fractions were re-extracted with ethyl acetate (3 x 20 mL) and the combined organic layers were washed with saturated aqueous sodium hydrogen carbonate (2 x 20 mL) and brine (20 mL) before being dried over magnesium sulfate and evaporated. The residue was purified by column chromatography (33% ethyl acetate 66% hexane) to give **82** (57 mmol, 96%) as a white solid, m.p. 193-194 °C;  $\nu_{max}$  (cm<sup>-1</sup>): 3200-3400 (NH), 1684 (NHC=O), 1650 (CHC=O); <sup>1</sup>H NMR (500 MHz, chloroform-*d*)  $\delta$  ppm 7.31 - 7.36 (1H, m, H<sub>(10)</sub>), 7.09 - 7.24 (6H, m, aryl), 6.07 (1H, br.s, H<sub>(1)</sub>), 5.14 (1H, br.s, H<sub>(5)</sub>), 4.55 - 4.72 (1H, m, H<sub>(12)</sub>), 4.32 (1H, s, H<sub>(4)</sub>), 3.14 - 3.34 (3H, m, H<sub>(4)</sub>,H<sub>(13)</sub>/H<sub>(20)</sub>), 3.06 (1H, m, H<sub>(4)</sub>), 2.73 (1H, dd, *J*=16.2, 4.8 Hz, H<sub>(20)</sub>/H<sub>(13)</sub>), 2.59 (1H, dd, *J*=16.2, 3.8 Hz, H<sub>(20)</sub>/H<sub>(13)</sub>), 1.31 - 1.38 (9H, m, 3 x 3H<sub>(23)</sub>); <sup>13</sup>C NMR (126 MHz, chloroform-*d*)  $\delta$  ppm 170.45 C<sub>(2)</sub>, 155.40 C<sub>(21)</sub>, 140.54 C<sub>(14)</sub>,C<sub>(19)</sub>, 135.10 C<sub>(6)</sub>, 133.54, 132.49, 129.40, 127.29, 126.90, 124.83, 124.80, 80.34 C<sub>(22)</sub>, 54.48 C<sub>(12)</sub>, 50.68 C<sub>(3)</sub>, 39.96 C<sub>(13)</sub>/C<sub>(20)</sub>, 39.94 C<sub>(20)</sub>/C<sub>(13)</sub>, 35.92 C<sub>(4)</sub>, 28.25 3C<sub>(2)</sub>; HRMS calcd for C<sub>23</sub>H<sub>27</sub>Cl<sub>2</sub>O<sub>3</sub>N<sub>2</sub>: 449.1399 (M+H), found: 449.1385.

***tert*-Butyl (*R*)-(3-(2,4-dichlorophenyl)-1-oxo-1-(phenethylamino)propan-2-yl)carbamate (**83**)**



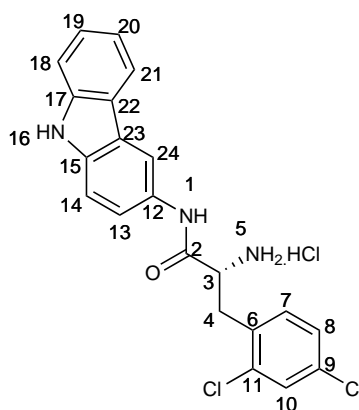
To phenylethylamine (0.76 mL, 0.6 mmol), *N*-Boc-(*R*)-2,4-dichlorophenylalanine (201 mg, 0.6 mmol), 1-ethyl-3-(3-dimethylaminopropyl)carbodiimide (109 mg, 0.6 mmol) and anhydrous 1-hydroxybenzotriazole (122 mg, 0.6 mmol) in dimethylformamide (3.0 mL) was added *N,N*-diisopropylethylamine (0.78 mL, 4.5 mmol), the mixture was then stirred for 16 h at 20 °C. The mixture was then diluted with ethyl acetate (20 mL) and washed with water (3 x 20 mL). The combined aqueous fractions were re-extracted with ethyl acetate (3 x 20 mL) and the combined organic layers were washed with saturated aqueous sodium hydrogen carbonate (2 x 20 mL) and brine (20 mL) before being dried over magnesium sulfate and evaporated. The residue was purified by column chromatography (60% ethyl acetate 40% dichloromethane) to give **83** (117 mg, 45%) as a white solid, m.p. 169-170 °C;  $\nu_{max}$  (cm<sup>-1</sup>): 3338 br. (NH) 2875-3030 (NH) 1682 (NHC=O), 1654 (CHC=O); <sup>1</sup>H NMR (500 MHz, chloroform-*d*)  $\delta$  ppm 7.05 - 7.40 (8H, m, aryl), 5.98 (1H, t, *J*=6.0 Hz, H<sub>(1)</sub>), 5.12 (1H, d, *J*=8.5 Hz, H<sub>(5)</sub>), 4.21 - 4.44 (1H, m, H<sub>(3)</sub>), 3.30 - 3.64 (2H, m, H<sub>(12)</sub>), 3.18 (1H, dd, *J*=13.3, 6.7 Hz, H<sub>(4)</sub>), 2.99 (1H, dd, *J*=13.3, 7.9 Hz, H<sub>(4)</sub>), 2.61 - 2.82 (2H, m, H<sub>(13)</sub>), 1.25 - 1.43 (9H, m, 3 x 3H<sub>(22)</sub>); <sup>13</sup>C NMR (126 MHz, chloroform-*d*)  $\delta$  ppm 170.84 C<sub>(2)</sub>, 155.43 C<sub>(20)</sub>, 138.55 C<sub>(14)</sub>, 135.17 C<sub>(6)</sub>, 133.61, 133.57, 132.58, 129.44, 128.83, 128.80, 127.32, 126.78, 80.32 C<sub>(21)</sub>, 54.56 C<sub>(3)</sub>, 40.78 C<sub>(12)</sub>, 36.12 C<sub>(13)</sub>, 35.63 C<sub>(4)</sub>, 28.34 3C<sub>(2)</sub>; HRMS calcd for C<sub>22</sub>H<sub>27</sub>Cl<sub>2</sub>N<sub>2</sub>O<sub>3</sub>: 437.1399 (M+H), found: 437.1385.

**(*R*)-2-Amino-3-(2,4-dichlorophenyl)-*N*-(2,3-dihydro-1H-inden-2-yl)propanamide hydrochloride (84)**



*N*-Boc protected amide **82** (194 mg, 0.5 mmol) was dissolved in dry diethyl ether (15 mL) and dichloromethane (10 mL). Hydrogen chloride was bubbled through the solution with vigorous stirring for 2 h. The solvent was evaporated to give **84** (158 mg, 95%) as a cream solid, m.p. (decomp. 150 °C);  $[\alpha]_D^{25}$  *c*=1 methanol: -65.0°;  $\nu_{max}$  (cm<sup>-1</sup>): 3199 (NH), 3019 (NH<sub>3</sub>), 3918, 2847, 2658 ; <sup>1</sup>H NMR (500 MHz, DMSO-*d*<sub>6</sub>)  $\delta$  ppm 8.60 - 8.74 (4H, m, H<sub>(1)</sub>,H<sub>(5)</sub>), 7.55 (1H, s, H<sub>(10)</sub>), 7.35 (2H, s, aryl), 7.01 - 7.23 (4H, m, aryl), 4.29 - 4.48 (1H, m, H<sub>(12)</sub>), 3.89 (1H, br.s, H<sub>(3)</sub>), 3.24 (1H, dd, *J*=13.5, 5.3 Hz, H<sub>(4)</sub>), 3.06 - 3.15 (2H, m, H<sub>(4)</sub>,H<sub>(13)</sub>/H<sub>(20)</sub>), 2.98 - 3.06 (1H, dd, (*J*)= 16.2, 7.5 Hz, H<sub>(13)</sub>/H<sub>(20)</sub>), 2.76 (1H, dd, *J*=16.2, 5.2 Hz, H<sub>(20)</sub>/H<sub>(13)</sub>), 2.45 (1H, dd, *J*=16.2, 5.2 Hz, H<sub>(20)</sub>/H<sub>(13)</sub>); <sup>13</sup>C NMR (126 MHz, DMSO-*d*<sub>6</sub>)  $\delta$  ppm 166.86 C<sub>(2)</sub>, 140.81 (14/C<sub>19</sub>), 140.79 C<sub>(19)</sub>/C<sub>(14)</sub>, 134.62 C<sub>(6)</sub>, 133.16, 132.64, 132.01, 128.68, 127.32, 126.42, 124.43, 124.41, 51.77 C<sub>(4)</sub>/C<sub>(12)</sub>, 49.89 C<sub>(12)</sub>/C<sub>(4)</sub>, 38.77 C<sub>(13)</sub>/C<sub>(20)</sub>, 38.61 C<sub>(20)</sub>/C<sub>(13)</sub>, 33.76 C<sub>(4)</sub>;

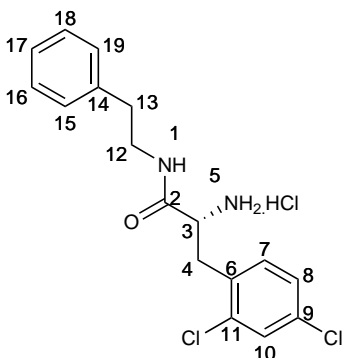
**(*R*)-2-Amino-*N*-(9*H*-carbazol-3-yl)-3-(2,4-dichlorophenyl)propanamide hydro-chloride (**85**)**



*N*-Boc protected amide **55** (109 mg, 0.25 mmol) was dissolved in dry diethyl ether (15 mL). Hydrogen chloride was bubbled through the solution with vigorous stirring for 150 min. The precipitate was filtered by gravity filtration through filter paper in a funnel that was on top of a flask of boiling ether **85** (40 mg, 42%) as a cream solid, <sup>1</sup>H NMR (500 MHz, DMSO-*d*<sub>6</sub>)  $\delta$  ppm 11.46 (1H, s, H<sub>(1)</sub>/H<sub>(16)</sub>), 10.77 (1H, s,

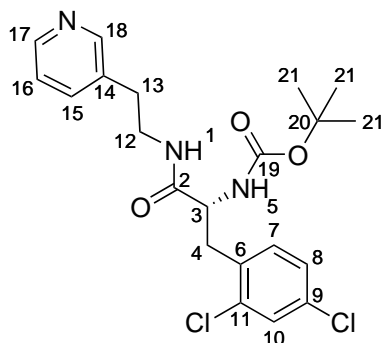
H<sub>(16)</sub>/H<sub>(1)</sub>), 8.78 (3H, br.s, 3H<sub>(5)</sub>), 8.10 (1H, d,  $J=7.7$  Hz, aryl), 7.96 (1H, d,  $J=7.7$  Hz, aryl), 7.60 - 7.70 (1H, m, aryl), 7.33 - 7.59 (5H, m, aryl), 7.08 - 7.22 (2H, m, aryl), 4.49 (1H, s, H<sub>(3)</sub>), 3.33 - 3.66 (2H, m, H<sub>(4)</sub>); <sup>13</sup>C NMR (126 MHz, DMSO-*d*<sub>6</sub>)  $\delta$  ppm 166.50 C<sub>(2)</sub>, 139.28, 134.90, 133.35, 133.16, 132.88, 131.84, 128.91, 127.47, 125.87, 123.65, 122.31, 121.24, 120.31, 119.34, 118.85, 118.52, 117.63, 111.02, 52.47 C<sub>(4)</sub>, 33.79 C<sub>(3)</sub>; HRMS calcd for C<sub>21</sub>H<sub>17</sub>Cl<sub>2</sub>N<sub>3</sub>O: 397.0749, found: 397.0739.

**(*R*)-2-Amino-3-(2,4-dichlorophenyl)-*N*-phenethylpropanamide hydrochloride (86)**



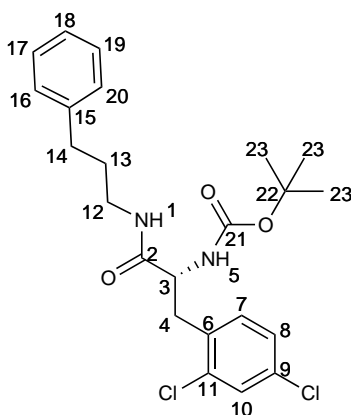
*N*-Boc protected amide **83** (148 mg, 0.34 mmol) was dissolved in dry diethyl ether (20 mL), and dichloromethane (5 mL). Hydrogen chloride was bubbled through the solution with vigorous stirring for 2 h and the solvent was then evaporated, trituration with dry diethyl ether gave **86** (104 mg, 85%) as a sticky white solid, m.p. 96-97 °C <sup>1</sup>H NMR (500 MHz, D<sub>2</sub>O)  $\delta$  ppm 7.58 (1H, s, H<sub>(10)</sub>), 7.37 - 7.45 (2H, m, aryl), 7.34 - 7.45 (4H, m, aryl), 7.14 - 7.25 (3H, m, aryl), 4.19 (1H, dd,  $J=9.5$ , 6.0 Hz, H<sub>(3)</sub>), 3.60 (1H, m, H<sub>(4)</sub>), 3.16 - 3.40 (3H, m, H<sub>(4)</sub>, H<sub>(12)</sub>), 2.60 - 2.79 (2H, m, H<sub>(13)</sub>); <sup>13</sup>C NMR (500 MHz, D<sub>2</sub>O)  $\delta$  ppm 176.77 C<sub>(2)</sub>, 147.27, 143.27, 142.77, 142.68, 142.26, 139.01, 138.04, 137.40, 137.00, 135.17, 61.45 C<sub>(3)</sub>, 49.05 C<sub>(4)</sub>/C<sub>(12)</sub>, 45.19 C<sub>(12)</sub>/C<sub>(4)</sub>, 42.67 C<sub>(13)</sub>; HRMS calcd for C<sub>17</sub>H<sub>19</sub>N<sub>2</sub>Cl<sub>2</sub>O: 337.0874 (M+H), found: 337.0870.

*tert*-Butyl (*R*)-(3-(2,4-dichlorophenyl)-1-oxo-1-((2-(pyridin-3-yl)ethyl)amino)propan-2-yl)carbamate (**87**)



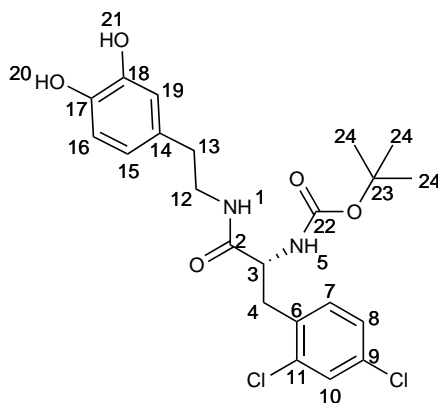
3-(2-Aminoethyl)pyridine dihydrobromide (81 mg, 0.6 mmol), *N*-Boc-(*R*)-2,4-dichlorophenylalanine (201 mg, 0.6 mmol), 1-ethyl-3-(3-dimethylaminopropyl)carbodiimide (109 mg, 0.6 mmol) and anhydrous 1-hydroxybenzotriazole (122 mg, 0.6 mmol) in dimethylformamide (3.0 mL) was added *N,N*-diisopropylethylamine (1.0 mL, 5.7 mmol), the mixture was then stirred for 16 h at 20 °C. The mixture was diluted with ethyl acetate (20 mL) and washed with water (3 x 20 mL). The combined aqueous fractions were re-extracted with ethyl acetate (3 x 20 mL) and the combined organic layers were washed with saturated aqueous sodium hydrogen carbonate (2 x 20 mL) and brine (20 mL) before being dried over magnesium sulfate and evaporated. The residue was purified by column chromatography (25% ethyl acetate 75% hexane) to yield **87** as a white solid (110 mg, 42%), m.p. 154 - 154.5 °C;  $[\alpha]_D^{26}$  chloroform: +5.9°;  $\nu_{max}$  (cm<sup>-1</sup>): 3370 br. (NH), 2966 (NH), 1681 (NHC=O), 1650 (CHC=O); <sup>1</sup>H NMR (500 MHz, chloroform-*d*)  $\delta$  ppm 8.29 - 8.49 (2H, m, H<sub>(17)</sub>,H<sub>(18)</sub>), 7.48 (1H, d, *J*=8.2 Hz, aryl), 7.29 - 7.38 (1H, m, aryl), 7.08 - 7.24 (3H, m, aryl), 6.61 (1H, t, *J*=6.0 Hz, H<sub>(1)</sub>), 5.33 (1H, d, *J*=9.0 Hz, H<sub>(5)</sub>), 4.30 - 4.41 (1H, m, H<sub>(3)</sub>), 3.44 (1H, q, *J*=7.0 Hz, H<sub>(12)</sub>), 3.09 - 3.30 (1H, m, H<sub>(4)</sub>), 2.93 - 3.05 (1H, m, H<sub>(4)</sub>), 2.67 - 2.81 (2H, m, H<sub>(13)</sub>), 1.26 - 1.36 (9H, m, 3 x 3H<sub>(21)</sub>); <sup>13</sup>C NMR (126 MHz, chloroform-*d*)  $\delta$  ppm 171.27 C<sub>(2)</sub>, 155.56 C<sub>(19)</sub>, 149.49 C<sub>(19)</sub>, 147.47, 136.78, 135.10, 134.50, 133.53, 133.46, 132.49, 129.33, 127.18, 123.73, 80.29 C<sub>(20)</sub>, 54.38 br. C<sub>(3)</sub>, 40.37 C<sub>(12)</sub>, 35.75 br. C<sub>(4)</sub>, 32.83 C<sub>(13)</sub>, 28.26 C<sub>(21)</sub>; HRMS calcd for C<sub>21</sub>H<sub>26</sub>N<sub>3</sub>Cl<sub>2</sub>O<sub>3</sub>: 438.13512, found: 438.135409.

*tert*-Butyl (*R*)-(3-(2,4-dichlorophenyl)-1-oxo-1-((3-phenylpropyl)-amino)propan-2-yl)carbamate (**88**)



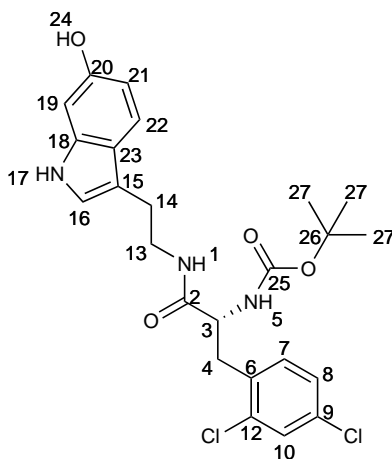
3-Phenylpropan-1-amine (85 mg, 0.6 mmol) *N*-Boc-(*R*)-2,4-dichlorophenylalanine (201 mg, 0.6 mmol), 1-ethyl-3-(3-dimethylaminopropyl)carbodiimide (109 mg, 0.6 mmol) and anhydrous 1-hydroxybenzotriazole (122 mg, 0.6 mmol) in dimethylformamide (3.0 mL) was added *N,N*-diisopropylethylamine (0.78 mL, 4.5 mmol), the mixture was then stirred for 16 h at 20 °C. The mixture was diluted with ethyl acetate (20 mL) and washed with water (3 x 20 mL). The combined aqueous fractions were re-extracted with ethyl acetate (3 x 20 mL) and the combined organic layers were washed with saturated aqueous sodium hydrogen carbonate (2 x 20 mL) and brine (20 mL) before being dried over magnesium sulfate and evaporated. The residue was purified by column chromatography (66% hexane 33% ethyl acetate) to give **88** (133 mg, 49%) as a white solid, m.p. 133-133.5 °C; <sup>1</sup>H NMR (500 MHz, chloroform-*d*) δ ppm 7.34 (1H, d, *J*=1.6 Hz, H<sub>(10)</sub>), 7.23 - 7.30 (2H, m, aryl), 7.15 - 7.21 (2H, m, aryl), 7.10 - 7.15 (3H, m, aryl), 6.39 (1H, br.s, H<sub>(1)</sub>), 5.31 (1H, d, *J*=9.1 Hz, H<sub>(5)</sub>), 4.31 - 4.46 (1H, m, H<sub>(3)</sub>), 3.14 - 3.28 (3H, m, H<sub>(4)</sub>, 2H<sub>(12)</sub>), 2.96 - 3.09 (1H, m, H<sub>(4)</sub>), 2.51 - 2.63 (2H, m, H<sub>(14)</sub>), 1.68 - 1.82 (2H, m, H<sub>(13)</sub>), 1.35 (9H, br.s, 3 x 3H<sub>(23)</sub>); <sup>13</sup>C NMR (126 MHz, chloroform-*d*) δ ppm 171.02 C<sub>(2)</sub>, 155.59 C<sub>(21)</sub>, 141.32 C<sub>(14)</sub>, 135.14 C<sub>(6)</sub>, 133.65, 133.43, 132.61, 129.33, 128.54, 128.39, 127.19, 126.09, 80.18 C<sub>(21)</sub>, 54.44 C<sub>(3)</sub>, 39.21 C<sub>(15)</sub>, 35.92 C<sub>(4)</sub>, 33.18 C<sub>(14)</sub>, 30.94 C<sub>(13)</sub>, 28.31 3C<sub>(2)</sub>; HRMS calcd for C<sub>23</sub>H<sub>29</sub>Cl<sub>2</sub>N<sub>2</sub>O<sub>3</sub> 451.1556 (M+H), found 451.1552.

*tert*-Butyl (*R*)-(3-(2,4-dichlorophenyl)-1-((3,4-dihydroxyphenethyl)amino)-1-oxopropan-2-yl)carbamate (**89**)



Dopamine hydrochloride (114 mg, 0.6 mmol), *N*-Boc-(*R*)-2,4-dichlorophenylalanine (201 mg, 0.6 mmol), 1-ethyl-3-(3-dimethylaminopropyl)carbodiimide (109 mg, 0.6 mmol) and anhydrous 1-hydroxybenzotriazole (122 mg, 0.6 mmol) in dimethylformamide (3.0 mL) was added *N,N*-diisopropylethylamine (0.78 mL, 4.5 mmol), the mixture was then stirred for 18 h at 20 °C. The mixture was diluted with ethyl acetate (20 mL) and washed with water (3 x 20 mL). The combined aqueous fractions were re-extracted with ethyl acetate (3 x 20 mL) and the combined organic layers were washed with saturated aqueous sodium hydrogen carbonate (2 x 20 mL) and brine (20 mL) before being dried over magnesium sulfate and evaporated. The residue was purified by column chromatography (33% ethyl acetate 66% hexane) to give **89** as a glassy solid (177 mg, 63%), m.p. 64-65 °C; <sup>1</sup>H NMR (500 MHz, chloroform-*d*) δ ppm 7.29 - 7.38 (1H, s, H<sub>(10)</sub>), 7.09 - 7.14 (2H, m, H<sub>(7)</sub>, H<sub>(8)</sub>), 6.76 (1H, d, *J*=8.0 Hz, H<sub>(15)</sub>), 6.63 (1H, s, H<sub>(19)</sub>), 6.52 (1H, br.s, H<sub>(1)</sub>), 6.46 (1H, d, *J*=8.0 Hz, H<sub>(16)</sub>), 5.32 - 5.70 (1H, m, H<sub>(5)</sub>), 4.30 - 4.69 (1H, m, H<sub>(3)</sub>), 3.29 - 3.45 (2H, m, 2H<sub>(12)</sub>), 3.08 - 3.22 (1H, m, H<sub>(4)</sub>), 2.96 - 3.06 (1H, m, H<sub>(4)</sub>), 2.56 (2H, m, H<sub>(13)</sub>), 1.29 - 1.42 (9H, m, H<sub>(24)</sub>); <sup>13</sup>C NMR (126 MHz, chloroform-*d*) δ ppm 171.71 (2), 155.85 C<sub>(22)</sub>, 144.14 C<sub>(17)</sub>/C<sub>(18)</sub>, 143.12 C<sub>(18)</sub>/C<sub>(17)</sub>, 135.07 C<sub>(6)</sub>, 133.59, 133.20, 132.40, 130.66, 129.39, 127.28, 120.77, 115.84, 115.55, 80.86 C<sub>(23)</sub>, 54.60 C<sub>(3)</sub>, 41.14 C<sub>(12)</sub>, 35.94 C<sub>(4)</sub>, 34.70 C<sub>(13)</sub>, 28.25 C<sub>(24)</sub>.

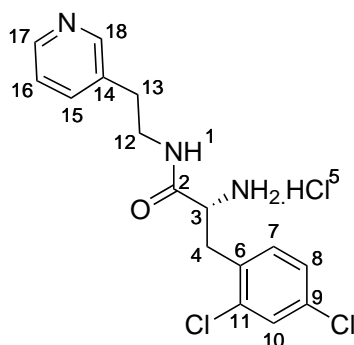
*tert*-Butyl (*R*)-(3-(2,4-dichlorophenyl)-1-((2-(6-hydroxy-2*H*-indol-3-yl)ethyl)amino)-1-oxopropan-2-yl)carbamate(**90**)



Serotonin hydrochloride (128 mg, 0.6 mmol) *N*-Boc-(*R*)-2,4-dichlorophenylalanine (201 mg, 0.6 mmol), 1-ethyl-3-(3-dimethylaminopropyl)carbodiimide (109 mg, 0.6 mmol) and anhydrous 1-hydroxybenzotriazole (122 mg, 0.6 mmol) in dimethylformamide (3.0 mL) was added *N,N*-diisopropylethylamine (0.78 mL, 4.5 mmol), the mixture was then stirred for 18 h at 20 °C. The mixture was diluted with ethyl acetate (20 mL) and washed with water (3 x 20 mL). The combined aqueous fractions were re-extracted with ethyl acetate (3 x 20 mL) and the combined organic layers were washed with saturated aqueous sodium hydrogen carbonate (2 x 20 mL) and brine (20 mL) before being dried over magnesium sulfate and evaporated. The residue was purified by column chromatography to give **90** (220 mg, 72%) as a white solid, m.p. 85 °C;  $\nu_{max}$  (cm<sup>-1</sup>): 3242 (br. OH), 2866 (br. NH), 1665 (C=O); <sup>1</sup>H NMR (500 MHz, chloroform-*d*)  $\delta$  ppm 8.22 (1H, br.s, H<sub>(17)</sub>), 7.27 (1H, s, aryl), 7.14 (1H, d, *J*=8.7 Hz, aryl), 7.01 - 7.09 (2H, m, aryl), 6.93 (1H, s, aryl), 6.76 - 6.85 (2H, m, aryl), 6.36 (1H, t, *J*=6.0 Hz, H<sub>(1)</sub>), 5.49 (1H, d, *J*=9.0 Hz, H<sub>(5)</sub>), 4.24 - 4.49 (1H, m, H<sub>(3)</sub>), 3.41 - 3.53 (1H, m, H<sub>(13)</sub>), 3.24 (1H, m, H<sub>(13)</sub>), 3.11 (1H, dd, *J*=13.8, 5.0 Hz, H<sub>(4)</sub>), 2.96 (1H, dd, *J*=13.6, 8.5 Hz, H<sub>(4)</sub>), 2.62 - 2.81 (2H, m, H<sub>(14)</sub>), 1.28 - 1.39 (9H, m, 3 x 3H<sub>(27)</sub>); <sup>13</sup>C NMR (126 MHz, chloroform-*d*)  $\delta$  ppm 171.12 C<sub>(2)</sub>, 155.77 C<sub>(25)</sub>, 150.34 C<sub>(20)</sub>, 135.07 C<sub>(6)</sub>, 133.41, 133.31, 132.34, 131.43, 129.31, 128.11,

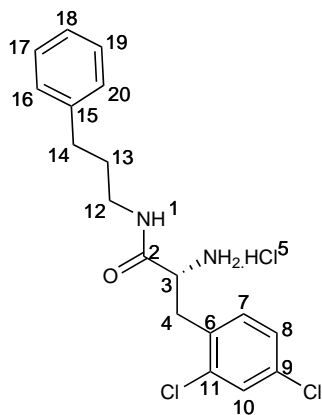
127.17, 123.15, 112.49, 112.10, 103.27, 80.73 C<sub>(26)</sub>, 54.57 C<sub>(3)</sub>, 40.98 C<sub>(13)</sub>, 36.18 C<sub>(4)</sub>, 28.30 3C<sub>(2)</sub>, 25.42 C<sub>(14)</sub>.

**(*R*)-2-Amino-3-(2,4-dichlorophenyl)-*N*-(2-(pyridin-3-yl)ethyl)propanamide hydrochloride (91)**

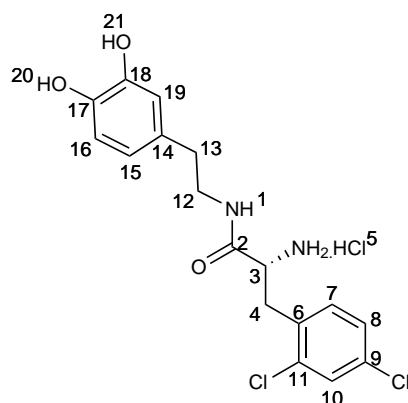


*N*-Boc protected amide **87** (110 mg, 0.25 mmol) was dissolved in dry diethyl ether (10 mL), dichloromethane (2 mL) and ethyl acetate (1 mL). Hydrogen chloride was bubbled through the solution with vigorous stirring for 1 h. The solvent was evaporated to give **91** (105 mg) as a damp solid, <sup>1</sup>H NMR (600 MHz, DMSO-*d*) δ ppm 8.92 (1H, s, H<sub>(19)</sub>), 8.84 (1H, t, *J*=5.3 Hz, H<sub>(1)</sub>), 8.79 (1H, d, *J*=5.5 Hz, H<sub>(17)</sub>), 8.74 (3H, br. s 3H<sub>(5)</sub>), 8.48 (1H, d, *J*=8.1 Hz, H<sub>(15)</sub>), 7.97 (1H, dd, *J*=8.1, 5.5 Hz, H<sub>(16)</sub>), 7.55 (1H, d, *J*=2.1 Hz, H<sub>(10)</sub>), 7.38 (1H, d, *J*=8.5 Hz, H<sub>(7)</sub>), 7.34 (1H, dd, *J*=8.5, 2.1 Hz, H<sub>(8)</sub>), 3.92 (1H, br.s, H<sub>(3)</sub>), 3.39 - 3.47 (1H, m, H<sub>(12)</sub>), 3.24 - 3.32 (1H, m, H<sub>(3)</sub>), 3.18 (1H, dd, *J*=13.7, 6.0 Hz, H<sub>(4)</sub>), 3.07 (1H, dd, *J*=13.7, 8.6 Hz, H<sub>(4)</sub>), 2.81 - 2.97 (2H, m, H<sub>(13)</sub>); <sup>13</sup>C NMR (151 MHz, DMSO-*d*<sub>6</sub>) δ ppm 167.53 C<sub>(2)</sub>, 146.45, 141.50, 139.40, 139.27, 134.65, 133.15, 132.64, 132.05, 128.75, 127.38, 126.78, 64.95 C<sub>(12)</sub>, 51.93 C<sub>(3)</sub>, 33.71 C<sub>(4)</sub>, 31.32 C<sub>(13)</sub>; HRMS calcd for C<sub>16</sub>H<sub>18</sub>N<sub>3</sub>OCl<sub>2</sub>: 338.0827 (M+H), found: 338.0822.

**(*R*)-2-Amino-3-(2,4-dichlorophenyl)-*N*-(3-phenylpropyl)propanamide hydrochloride (92)**

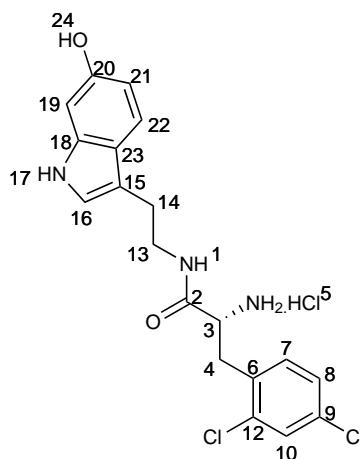


*N*-Boc protected amide **88** (100 mg, 22 mmol) was dissolved in dry diethyl ether (15 mL), dichloromethane (0.5 mL). Hydrogen chloride was bubbled through the solution with vigorous stirring for 2 h. The solvent was evaporated to give **92** (96 mg),  $^1\text{H}$  NMR (600 MHz,  $\text{DMSO-}d_6$ )  $\delta$  ppm 8.71 (3H, br.s,  $3\text{H}_{(5)}$ ), 8.59 (1H, s, 1), 7.57 (1H, d,  $J=2.0$  Hz,  $\text{H}_{(10)}$ ), 7.41 (1H, d,  $J=8.3$  Hz,  $\text{H}_{(7)}$ ), 7.36 (1H, dd,  $J=8.3$ , 2.0 Hz,  $\text{H}_{(7)}$ ), 7.26 (2H, m, aryl), 7.10 - 7.19 (3H, m, aryl), 3.95 - 4.04 (1H, m,  $\text{H}_{(3)}$ ), 3.26 (1H, dd,  $J=13.6$ , 5.6 Hz,  $\text{H}_{(4)}$ ), 3.12 (1H, dd,  $J=13.6$ , 9.4 Hz,  $\text{H}_{(4)}$ ), 3.02 - 3.09 (1H, m,  $\text{H}_{(12)}$ ), 2.90 - 2.98 (1H, m,  $\text{H}_{(12)}$ ), 2.37 - 2.46 (2H, m,  $\text{H}_{(14)}$ ), 1.49 - 1.61 (2H, m,  $\text{H}_{(13)}$ );  $^{13}\text{C}$  NMR (151 MHz,  $\text{DMSO-}d_6$ )  $\delta$  ppm 167.08  $\text{C}_{(2)}$ , 141.53  $\text{C}_{(15)}$ , 134.68  $\text{C}_{(6)}$ , 133.21, 132.70, 132.15, 128.76, 128.28, 127.39, 125.76, 51.97  $\text{C}_{(3)}$ , 38.25  $\text{C}_{(15)}$ , 33.79  $\text{C}_{(4)}$ , 32.26  $\text{C}_{(14)}$ , 30.31  $\text{C}_{(13)}$ ; HRMS calcd for  $\text{C}_{18}\text{H}_{21}\text{Cl}_2\text{N}_2\text{O}$ : 351.1031 (M+H), found: 351.1039.

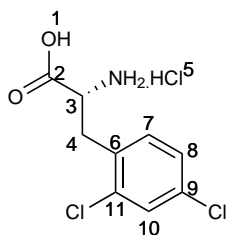
**(*R*)-2-Amino-3-(2,4-dichlorophenyl)-*N*-(3,4-dihydroxyphenethyl)propanamide hydrochloride (93)**

*N*-Boc protected amide **89** (177 mg, 0.38 mmol) was dissolved in dry diethyl ether (10 mL). Hydrogen chloride was bubbled through the solution with vigorous stirring for 35 min. The precipitate was filtered by gravity filtration through filter paper in a funnel that was on top of a flask of boiling ether **93** (147 mg, 95%) as a white solid, m.p. (decomp. 175 °C);  $[\alpha]_D^{25}$   $c=1$  methanol:  $-57.3^\circ$ ;  $\nu_{max}$  ( $\text{cm}^{-1}$ ): 2967 (OH/NH<sub>3</sub>), 1664 (C=O); <sup>1</sup>H NMR (600 MHz, DMSO-*d*<sub>6</sub>)  $\delta$  ppm 8.86 (1H, s, H<sub>(20)</sub>/H<sub>(21)</sub>), 8.76 (1H, s, H<sub>(21)</sub>/H<sub>(20)</sub>), 8.57 (3H, br.s, 3H<sub>(5)</sub>), 8.53 (1H, t,  $J=5.6$  Hz, H<sub>(1)</sub>), 7.61 (1H, d,  $J=2.2$  Hz, H<sub>(10)</sub>), 7.39 (1H, dd,  $J=8.3, 2.2$  Hz, H<sub>(8)</sub>), 7.34 (1H, d,  $J=8.3$  Hz, H<sub>(7)</sub>), 6.63 (1H, d,  $J=8.0$  Hz, H<sub>(15)</sub>), 6.58 (1H, d,  $J=2.2$  Hz, H<sub>(19)</sub>), 6.35 (1H, dd,  $J=8.0, 2.2$  Hz, H<sub>(16)</sub>), 3.91 (1H, dd,  $J=8.6, 6.1$  Hz, H<sub>(3)</sub>), 3.14 - 3.25 (2H, m, H<sub>(4)</sub>, H<sub>(12)</sub>), 3.03 - 3.14 (2H, m, H<sub>(4)</sub>, H<sub>(12)</sub>), 2.39 - 2.46 (1H, m, H<sub>(13)</sub>), 2.33 - 2.39 (1H, m, H<sub>(13)</sub>); <sup>13</sup>C NMR (151 MHz, DMSO-*d*<sub>6</sub>)  $\delta$  ppm 167.10 C<sub>(2)</sub>, 145.16 C<sub>(17)</sub>/C<sub>(18)</sub>, 143.69 C<sub>(18)</sub>/C<sub>(17)</sub>, 134.73 C<sub>(6)</sub>, 133.26, 132.77, 132.04, 129.69, 128.81, 127.43, 119.14, 115.98, 115.59, 51.95 C<sub>(3)</sub>, 40.74 C<sub>(12)</sub>, 34.24 C<sub>(13)</sub>, 33.94 C<sub>(4)</sub>; HRMS calcd for C<sub>17</sub>H<sub>19</sub>N<sub>2</sub>Cl<sub>2</sub>O<sub>3</sub>: 369.0772 (M+H), found: 369.0777.

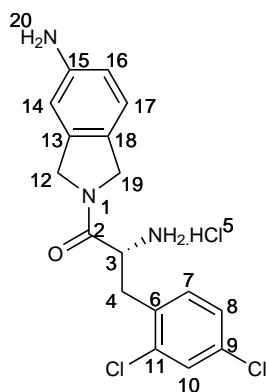
*(R)*-2-Amino-3-(2,4-dichlorophenyl)-*N*-(2-(6-hydroxy-2H-indol-3-yl)ethyl)propanamide hydrochloride (**94**)



*N*-Boc protected amide **90** (158 mg, 0.3 mmol) was dissolved in dry diethyl ether (10 mL). Hydrogen chloride was bubbled through the solution with vigorous stirring for 35 min. The precipitate was filtered by gravity filtration through filter paper in a funnel that was on top of a flask of boiling ether **94** (105 mg, 0.24 mmol, 79%) as a white solid, m.p. (decomp. 150 °C);  $[\alpha]_D^{25} c=1$  methanol: -47.2°;  $^1\text{H}$  NMR (600 MHz,  $\text{DMSO-}d_6$ )  $\delta$  ppm 10.57 (1H, br.s,  $\text{H}_{(17)}$ ), 8.50 - 8.66 (5H, m, aryl), 7.61 (1 H, s), 7.33 - 7.36 (2H, m, aryl), 7.12 (1H, d,  $J=8.6$  Hz, aryl), 7.00 (1H, d,  $J=1.9$  Hz, aryl), 6.80 (1H, d,  $J=2.4$  Hz, aryl), 6.60 (1H, dd,  $J=8.6, 2.4$  Hz, aryl), 3.90 - 3.97 (1H, m,  $\text{H}_{(3)}$ ), 3.28 - 3.35 (1H, m,  $\text{H}_{(11)}$ ), 3.16 - 3.25 (2H, m,  $\text{H}_{(11)}, \text{H}_{(4)}$ ), 3.12 (1 H, dd,  $J=13.7, 8.7$  Hz,  $\text{H}_{(4)}$ ), 2.52 - 2.67 (2H, m,  $\text{H}_{(14)}$ );  $^{13}\text{C}$  NMR (151 MHz,  $\text{DMSO-}d_6$ )  $\delta$  ppm 167.09  $\text{C}_{(2)}$ , 150.27  $\text{C}_{(20)}$ , 134.74  $\text{C}_{(6)}$ , 133.26, 132.76, 132.05, 130.79, 128.81, 127.70, 127.41, 123.19, 111.73, 111.34, 110.26, 102.08, 52.01  $\text{C}_{(3)}$ , 33.95  $\text{C}_{(4)}$ , 24.92  $\text{C}_{(14)}$ ; HRMS calcd for  $\text{C}_{19}\text{H}_{20}\text{N}_3\text{Cl}_2\text{O}_2$ : 392.0933 (M+H), found: 392.0936.

**(*R*)-2-Amino-3-(2,4-dichlorophenyl)propanoic acid hydrochloride (95)**

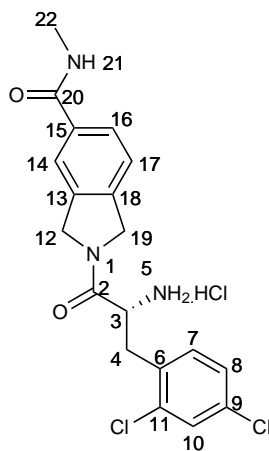
*N*-Boc-(*R*)-2,4-dichlorophenylalanine (134 mg, 0.4 mmol) was dissolved in dry diethyl ether (15 mL). Hydrogen chloride was bubbled through the solution with vigorous stirring for 140 min. The precipitate was filtered by gravity filtration through filter paper in a funnel that was on top of a flask of boiling ether **95** (89 mg, 82%) as a white solid,  $^1\text{H}$  NMR (500 MHz, DMSO- $d_6$ )  $\delta$  ppm 13.35 - 14.24 (1H, m, H<sub>(1)</sub>), 8.55 - 8.76 (3H, m, H<sub>(5)</sub>), 7.61 (1H, d,  $J$  = 2.0 Hz, H<sub>(10)</sub>), 7.48 (1H, d,  $J$  = 8.3 Hz, H<sub>(8)</sub>), 7.41 (1H, dd,  $J$  = 8.3, 2.0 Hz, H<sub>(7)</sub>), 4.03 (1H, t,  $J$  = 7.5 Hz, H<sub>(3)</sub>), 3.25 (2H, d,  $J$  = 7.5, H<sub>(4)</sub>);  $^{13}\text{C}$  NMR (126 MHz, DMSO- $d_6$ )  $\delta$  ppm 169.88 C<sub>(2)</sub>, 134.52 C<sub>(6)</sub>, 133.31, 132.78, 132.27, 128.81, 127.52, 51.58 C<sub>(3)</sub>, 33.11 C<sub>(4)</sub>;

**(*R*)-2-Amino-1-(5-aminoisindolin-2-yl)-3-(2,4-dichlorophenyl)propan-1-one hydrochloride 97**

*N*-Boc protected amide **136** (100 mg, 0.22 mmol) was dissolved in dry diethyl ether

(20 mL). Hydrogen chloride was bubbled through the solution with vigorous stirring for 30 min and the precipitate was filtered. The precipitate was filtered by gravity filtration through filter paper in a funnel that was on top of a flask of boiling ether **97** (20 mg, 22%) as a white solid,  $^1\text{H}$  NMR (600 MHz,  $\text{D}_2\text{O}$ , 2 rotamers)  $\delta$  ppm 7.39 - 7.44 (1H, m, aryl), 7.13 - 7.35 (5H, m, aryl), 4.63 (1H, m,  $\text{H}_{(12)}/\text{H}_{(19)}$ ), 4.08 (1H, t,  $J=15.0$  Hz,  $\text{H}_{(4)}$ ), 3.38 (1H, ddd,  $J=13.7, 6.1, 3.0$  Hz  $\text{H}_{(4)}$ ), 3.27 (1H, ddd,  $J=13.7, 9.0, 2.5$  Hz,  $\text{H}_{(4)}$ ).  $^{13}\text{C}$  NMR (126 MHz,  $\text{D}_2\text{O}$ , 2 rotamers)  $\delta$  ppm 167.72  $\text{C}_{(2)}$ , 167.69  $\text{C}_{(2)}$ , 137.61, 137.35, 136.62, 136.42, 135.08, 135.05, 134.77, 134.76, 133.04, 130.34, 130.30, 129.98, 129.79, 129.74, 128.12, 124.80, 124.57, 123.10, 122.92, 117.99, 117.71, 52.61  $\text{C}_{(12)}/\text{C}_{(19)}$ , 52.46  $\text{C}_{(12)}/\text{C}_{(19)}$ , 52.24  $\text{C}_{(19)}/\text{C}_{(12)}$ , 52.14  $\text{C}_{(19)}/\text{C}_{(12)}$ , 50.98  $\text{C}_{(4)}$ , 50.96  $\text{C}_{(4)}$ , 34.30  $\text{C}_{(3)}$ ; HRMS calcd for  $\text{C}_{18}\text{H}_{20}\text{N}_2\text{Cl}_2\text{O}$ : 350.0952 (M+H), found: 350.0951.

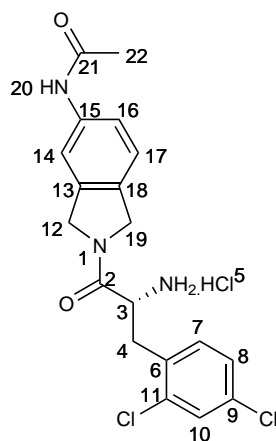
**(*R*)-2-(2-Amino-3-(2,4-dichlorophenyl)propanoyl)-*N*-methylisoindoline-5-carboxamide hydrochloride (**98**)**



*N*-Boc protected amide **130** (45 mg, 0.09 mmol) was dissolved in diethyl ether (5 mL) and dichloromethane (4 mL) and hydrogen chloride was bubbled through the solution with vigorous stirring for 2 h. The solvent was evaporated to give **98** (37 mg, 95%) as a white solid, m.p. decomp (190 °C);  $^1\text{H}$  NMR (600 MHz,  $\text{CD}_3\text{OD}$ , 2 rotamers)  $\delta$  ppm 7.64 - 7.82 (2H, m, aryl), 7.46 (1H, s, aryl), 7.24 - 7.44 (3H,

m, aryl), 4.98 - 5.08 (1H, m, H<sub>(12)</sub>/H<sub>(19)</sub>), 4.85 (1H, d,  $J=16.2$  Hz, H<sub>(19)</sub>/H<sub>(12)</sub>), 4.68 (1H, d,  $J=16.2$  Hz, H<sub>(19)</sub>/H<sub>(12)</sub>), 4.82 - 4.93 (1H, m, H<sub>(12)</sub>/H<sub>(19)</sub>), 4.21 (1H, t,  $J=13.0$  Hz, H<sub>(3)</sub>), 3.38 (2 H, d,  $J=6.8$  Hz, H<sub>(4)</sub>), 2.94 (3H, s, 3 x 3H<sub>(26)</sub>); <sup>13</sup>C NMR (151 MHz, CD<sub>3</sub>OD, 2 rotamers)  $\delta$  ppm 170.24 C<sub>(2)</sub>, 170.14 C<sub>(2)</sub>, 168.16 C<sub>(20)</sub>, 168.15 C<sub>(20)</sub>, 140.51, 140.20, 137.43, 137.07, 136.44, 135.93, 135.40, 135.20, 134.48, 132.12, 130.64, 129.08, 128.30, 128.15, 124.21, 124.07, 122.98, 122.86, 53.57 C<sub>(12)</sub>/C<sub>(19)</sub>, 53.48 C<sub>(12)</sub>/C<sub>(19)</sub>, 53.27 C<sub>(19)</sub>/C<sub>(12)</sub>, 53.17 C<sub>(19)</sub>/C<sub>(12)</sub>, 52.14 C<sub>(3)</sub>, 52.11 C<sub>(3)</sub>, 35.31 C<sub>(4)</sub>, 35.27 C<sub>(4)</sub>, 27.15 C<sub>(22)</sub>; HRMS calcd for C<sub>19</sub>H<sub>20</sub>N<sub>3</sub>Cl<sub>2</sub>O<sub>2</sub>: 392.0927 (M+H), found: 392.0933.

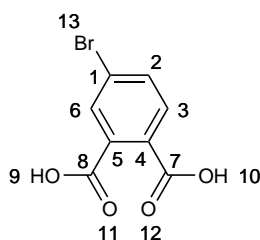
**(*R*)-*N*-(2-(2-Amino-3-(2,4-dichlorophenyl)propanoyl)isoindolin-5-yl)-acetamide hydrochloride (99)**



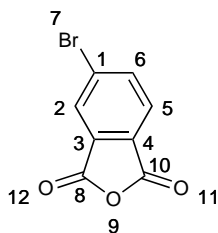
*N*-Boc protected amide **138** (84 mg, 0.17 mmol) was dissolved in dry diethyl ether (10 mL) and dichloromethane (10 mL). Hydrogen chloride was bubbled through the solution with vigorous stirring for 150 min. The precipitate was filtered by gravity filtration through filter paper in a funnel that was on top of a flask of boiling ether **99** (65 mg, 89%) as a cream solid, m.p. (decomp. 200 °C);  $[\alpha]_D^{26}$  methanol:  $-28.8^\circ$ ;  $\nu_{max}$  (cm<sup>-1</sup>): 2861 (NH<sub>3</sub>), 1651 (C=O), 1649 (C=O); <sup>1</sup>H NMR (500 MHz, chloroform-*d*, 2 rotamers)  $\delta$  ppm 10.25 (1H, d,  $J=4.5$  Hz, H<sub>(20)</sub>), 8.63 (3H, d,  $J=4.1$  Hz, 3H<sub>(5)</sub>), 7.67 (1H, d,  $J=18.4$  Hz, aryl), 7.61 (1H, t,  $J=2.3$  Hz, aryl), 7.42 - 7.50 (2H, m, aryl), 7.39 (1H, ddd,  $J=8.3, 3.8, 2.3$  Hz, aryl), 7.21

(1H, m, aryl), 4.99 (1H, m,  $J=13.9$  Hz,  $H_{(12)}/H_{(19)}$ ), 4.69 (1H, m,  $J=16.2$  Hz,  $H_{(19)}/H_{(12)}$ ), 4.50 (1H, m,  $J=16.2$  Hz,  $H_{(19)}/H_{(12)}$ ), 4.32 - 4.42 (1H, m,  $H_{(3)}$ ), 4.22 (1H, m,  $J=13.9$  Hz,  $H_{(12)}/H_{(19)}$ ), 3.27 (2H, s,  $H_{(4)}$ ), 2.04 (3H, s,  $H_{(22)}$ );  $^{13}\text{C}$  NMR (126 MHz, chloroform-*d*, 2 rotamers)  $\delta$  ppm 168.44  $C_{(2)}/C_{(21)}$ , 166.48  $C_{(21)}/C_{(2)}$ , 166.46  $C_{(21)}/C_{(2)}$ , 139.15, 139.08, 136.26, 135.64, 134.64, 134.61, 133.61, 133.59, 133.11, 133.10, 131.58, 129.99, 129.42, 128.90, 127.69, 123.14, 122.89, 118.63, 118.60, 113.29, 112.93, 52.24  $C_{(12)}/C_{(19)}$ , 51.84  $C_{(12)}/C_{(19)}$ , 51.79  $C_{(19)}/C_{(12)}$ , 51.36  $C_{(19)}/C_{(12)}$ , 49.98  $C_{(3)}$ , 33.36  $C_{(4)}$ , 33.25  $C_{(4)}$ , 24.02  $C_{(22)}$ , 24.01  $C_{(22)}$ . HRMS calcd for  $\text{C}_{19}\text{H}_{20}\text{N}_3\text{Cl}_2\text{O}_2$ : 392.0933 (M+H), found: 392.0938.

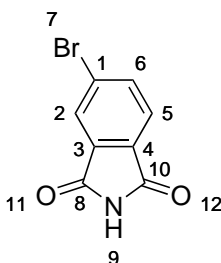
### 5-Bromophthalic acid (**102**)<sup>218,254</sup>



To a solution of phthalic anhydride (17.76 g, 120 mmol) and sodium hydroxide (9.6 g, 240 mmol) in water (80 mL) was added bromine (12 mL, 466 mmol) dropwise with stirring over 4 h. The mixture was heated to 90 °C and allowed to reflux for 9 h. The mixture was then cooled slowly and allowed to stand at 20 °C overnight before cooling to 4 °C for 48 h and the crystallised solids were collected by filtration to give the mono-sodium salt of **102** (13.56 g, 42%) as an off white solid, m.p. >295 °C; The filtrate was concentrated, acidified with hydrochloric acid (4M) and extracted into ethyl acetate (50 mL), washed with brine and evaporated to give a small amount of **102** as a free acid, m.p. 157-158 °C (lit.<sup>254</sup> m.p. 166 - 168 °C);  $^1\text{H}$  NMR (600 MHz, DMSO-*d*)  $\delta$  ppm 8.27 (1H, d,  $J=2.4$  Hz,  $H_{(6)}$ ), 8.09 (1H, d,  $J=8.4$  Hz,  $H_{(3)}$ ), 7.74 (1H, dd,  $J=8.4, 2.4$  Hz,  $H_{(2)}$ ).

**5-Bromophthalic anhydride (103)<sup>218</sup>**

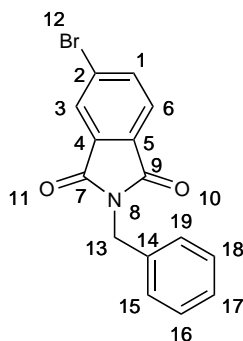
Phthalic acid **102** (9.59 g, 35 mmol) was dissolved in thionyl chloride (60 mL) was heated at reflux at 80 °C for 3 h. The solvent was evaporated and the residue was recrystallised from ethyl acetate to give **103** as a white solid (5.63 g, 58%), m.p. 97-99 °C (lit.<sup>255</sup> m.p. 104-106 °C); <sup>1</sup>H NMR (500 MHz, chloroform-*d*) δ ppm 8.15 (1H, d, *J*=1.4 Hz, H<sub>(2)</sub>), 8.04 (1H, dd, *J*=8.0, 1.4 Hz, H<sub>(6)</sub>), 7.88 (1H, d, *J*=8.0 Hz, H<sub>(5)</sub>); <sup>13</sup>C NMR (126 MHz, chloroform-*d*) δ ppm 161.94 C<sub>(8)</sub>/C<sub>(10)</sub>, 161.45 C<sub>(10)</sub>/C<sub>(8)</sub>, 139.40 C<sub>(1)</sub>, 132.95, 131.56, 129.86, 128.97, 126.96.

**5-Bromoisindoline-1,3-dione (104a)<sup>218</sup>**

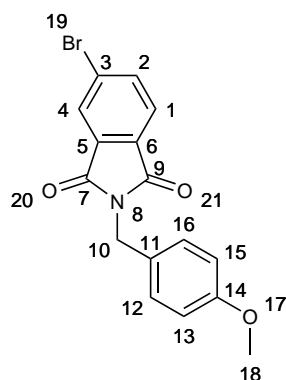
5-Bromophthalic anhydride **103** (5.4 g, 24 mmol) was heated at reflux in formamide (7.8 mL) for 2 h. The mixture was poured into ice/water and stirred for 1 h, the precipitate was collected by filtration and dried in a desiccator to give **104a** (5.31 g, 97%) as an off white solid, m.p. 232-235 °C (lit.<sup>256</sup> m.p. 221 °C); <sup>1</sup>H NMR (500 MHz, DMSO-*d*<sub>6</sub>) δ ppm 11.42 (1H, s, H<sub>(9)</sub>), 7.88 (1H, dd, *J*=7.9, 1.5 Hz, H<sub>(6)</sub>), 7.81 (1H, d, *J*=1.5 Hz, H<sub>(2)</sub>), 7.63 (1H, d, *J*=7.9 Hz, H<sub>(5)</sub>); <sup>13</sup>C NMR (126 MHz, DMSO-*d*<sub>6</sub>) δ

168.40 C<sub>(8)</sub>/C<sub>(10)</sub>, 167.80 C<sub>(10)</sub>/C<sub>(8)</sub>, 136.93, 134.52, 131.46, 127.78, 125.72, 124.77; HRMS calcd for C<sub>15</sub>H<sub>12</sub>N<sub>2</sub>O<sub>2</sub>Br: 331.0082 (M+H), found: 331.0086.

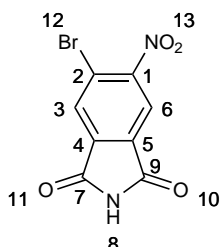
### 2-Benzyl-5-bromoisindoline-1,3-dione (104b)<sup>257</sup>



To intermediate **103** (5.67 g, 24 mmol) in acetic acid (27 mL) was added benzylamine (2.62 g, 24 mmol). The mixture was heated at reflux for 1 h before pouring into ice-water (200 mL) and stirred for 1 h. The product was filtered off and dried in a vacuum oven to give a white solid (6.84 g, 90%), m.p. 124.5 - 125 °C;  $\nu_{max}$  (cm<sup>-1</sup>): 1696 (C=O); <sup>1</sup>H NMR (300 MHz, chloroform-*d*)  $\delta$  ppm 7.96 (1H, d,  $J=1.7$  Hz, H<sub>(3)</sub>), 7.82 (1H, dd,  $J=7.9, 1.7$  Hz, H<sub>(1)</sub>), 7.69 (1H, d,  $J=7.9$  Hz, H<sub>(6)</sub>), 7.36 - 7.48 (2H, m, aryl), 7.25 - 7.36 (3H, m, aryl), 4.83 (2H, s, H<sub>(13)</sub>); <sup>13</sup>C NMR (75 MHz, DMSO-*d*<sub>6</sub>)  $\delta$  ppm 167.36 C<sub>(7)</sub>/C<sub>(9)</sub>, 166.82 C<sub>(9)</sub>/C<sub>(7)</sub>, 137.14, 136.16, 133.87, 130.75, 129.05, 128.88 C<sub>(16)</sub>,C<sub>(18)</sub>, 128.78 C<sub>(15)</sub>,C<sub>(19)</sub>, 128.11, 126.88, 124.88, 41.98 C<sub>(13)</sub>.

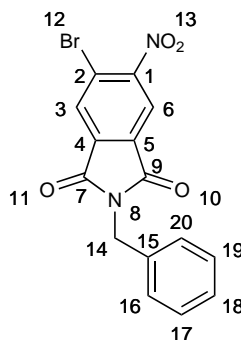
**5-Bromo-2-(4-methoxybenzyl)isoindoline-1,3-dione (104c)**

To a solution of anhydride (**103**) (3.0 g, 13.0 mmol) in acetic acid (15 mL) was added 4-methoxybenzylamine (1.73 mL, 13.0 mmol) the mixture was heated at reflux for 2.5 h. The reaction mixture was then poured into cold water and the precipitate was dried in a desiccator to give **104c** (3.91g, 87%) as an off white solid, m.p. 116-117 °C;  $\nu_{max}$  ( $\text{cm}^{-1}$ ): 1769 (C=O), 1710 (C=O);  $^1\text{H}$  NMR (300 MHz, chloroform-*d*)  $\delta$  ppm 7.93 (1H, d,  $J=1.7$  Hz,  $\text{H}_{(4)}$ ), 7.81 (1H, dd,  $J=7.9, 1.7$  Hz,  $\text{H}_{(2)}$ ), 7.67 (1H, d,  $J=7.9$  Hz,  $\text{H}_{(1)}$ ), 7.31 - 7.40 (2H, m,  $\text{H}_{(12)}, \text{H}_{(16)}$ ), 6.77 - 6.86 (2H, m,  $\text{H}_{(15)}, \text{H}_{(13)}$ ), 4.75 (2H, s,  $\text{H}_{(10)}$ ), 3.75 (3H, s,  $\text{H}_{(18)}$ );  $^{13}\text{C}$  NMR (75 MHz, chloroform-*d*)  $\delta$  ppm 167.35  $\text{C}_{(7)}/\text{C}_{(9)}$ , 166.80  $\text{C}_{(9)}/\text{C}_{(7)}$ , 159.42  $\text{C}_{(14)}$ , 137.04, 133.92, 130.81, 130.31  $\text{C}_{(12)}, \text{C}_{(16)}$ , 128.94, 128.45, 126.79, 124.79, 114.16  $\text{C}_{(13)}, \text{C}_{(15)}$ , 55.38  $\text{C}_{(18)}$ , 41.42  $\text{C}_{(10)}$ ; HRMS calcd for  $\text{C}_{16}\text{H}_{12}\text{NO}_3$ : 344.9995 (M+H), found: 344.9998.

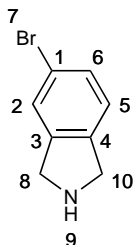
**5-Bromo-6-nitroisoindoline-1,3-dione (105a)<sup>218</sup>**

Sulfuric acid (14.4 mL) was added slowly to fuming nitric acid (6.2 mL) at -10 °C with stirring, **104a** (3.4 g, 15 mmol) was added portionwise with stirring to the mixture at -10 °C then stirred at 20 °C for 16 h. The mixture was poured into a water/ice bath, the mixture was made basic (pH 10) with sodium hydroxide (4 M) and stirred for 30 min. The precipitate was collected and dried to give **105a** (4.06 g, 70%) as a white solid, m.p. 201-203 °C (lit 215 - 216 °C)<sup>258</sup> <sup>1</sup>H NMR (500 MHz, DMSO-*d*<sub>6</sub>)  $\delta$  ppm 12.00 (1H, br.s, H<sub>(8)</sub>), 8.59 (1H, s, H<sub>(3)</sub>), 8.51 (1H, s, H<sub>(6)</sub>); <sup>13</sup>C NMR (126 MHz, DMSO-*d*<sub>6</sub>)  $\delta$  ppm 167.02 C<sub>(7)</sub>/C<sub>(9)</sub>, 166.83 C<sub>(9)</sub>/C<sub>(7)</sub>, 153.59 C<sub>(1)</sub>, 135.94 C<sub>(4)</sub>, 133.27, 129.15, 119.60, 119.24 C<sub>(2)</sub>.

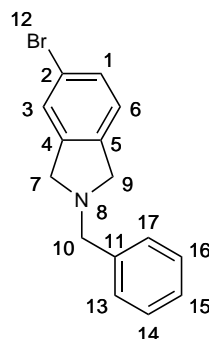
### 2-Benzyl-5-bromo-6-nitroisindoline-1,3-dione (**105b**)<sup>218</sup>



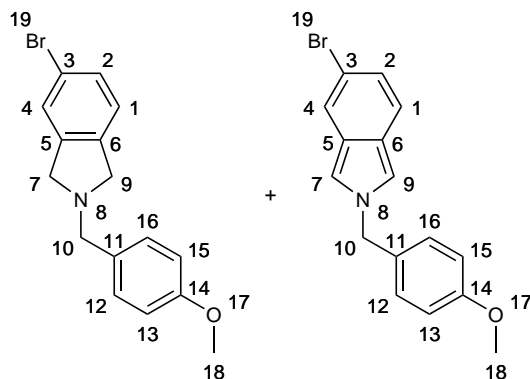
To imide **105a** (500 mg, 1.8 mmol) and potassium carbonate (650 mg, 4.63 mmol) in dimethylformamide (3.0 mL) was added benzyl bromide (330 mg, 2.8 mmol) was added and the mixture stirred for 16 h at 20 °C. The mixture was then diluted with ethyl acetate (10 mL) and washed with water (3 x 10 mL), the aqueous fractions were re-extracted with ethyl acetate (30 mL). The combined organic fractions were washed with brine (50 mL), dried over magnesium sulfate and evaporated. The residue was purified by column chromatography (40% dichloromethane 60% hexane) to give **105b** (580 mg, 87%) as a white solid, m.p. 149-152 °C; <sup>1</sup>H NMR (500 MHz, chloroform-*d*)  $\delta$  ppm 8.18 - 8.23 (1H, s, H<sub>(3)</sub>/H<sub>(6)</sub>), 8.13 - 8.17 (1H, s, H<sub>(6)</sub>/H<sub>(3)</sub>), 7.23 - 7.45 (5H, m, aryl), 4.86 (2H, s, H<sub>(14)</sub>); <sup>13</sup>C NMR (126 MHz, chloroform-*d*)  $\delta$  ppm 165.09 C<sub>(7)</sub>/C<sub>(9)</sub>, 164.93 C<sub>(9)</sub>/C<sub>(7)</sub>, 135.40, 134.81, 131.92, 130.21, 129.02, 128.93, 128.81, 128.36, 120.99, 120.17, 42.52 C<sub>(14)</sub>.

**5-Bromoisoindoline (106a)**<sup>221</sup>

Sodium borohydride (378 mg, 10 mmol) was added with stirring to (**104a**) (226 mg, 1.0 mmol) in tetrahydrofuran (10 mL). The suspension was cooled to -10 °C and boron trifluoride diethyletherate (1.43 mL 11.6 mmol) was added dropwise before and then heated at reflux at 70 °C for 16 h. The mixture was quenched dropwise with cold water (10 mL) and diluted with ethyl acetate (70 mL), the aqueous layer was basified with sodium hydroxide (6 M) to pH 10. The organic layer was washed with brine (20 mL) then dried over sodium sulfate and the solvent evaporated. The residue was dissolved in ethyl acetate (20 mL) and water was added (10 mL). The aqueous layer was acidified with HCl (6 M) to pH 1.0. The aqueous layer was extracted with ethyl acetate (2 x 20 mL). The combined organic layers were washed with brine (30 mL) and dried (sodium sulfate) and the solvent was evaporated. The residue was purified by column chromatography (94: 5: 1 ethyl acetate:methanol:0.880 ammonia) to give **106a** (108 mg, 54%) as a pale pink solid. The literature<sup>221</sup> describes this compound as a pale green oil, <sup>1</sup>H NMR (500 MHz, CD<sub>3</sub>OD) δ ppm 7.62 (1H, s, H<sub>(2)</sub>), 7.53 (1H, dd, *J*=8.1, 2.0 Hz, H<sub>(6)</sub>), 7.35 (1H, d, *J*=8.1 Hz, H<sub>(5)</sub>), 4.65 (2H, s, H<sub>(2)</sub>/H<sub>(10)</sub>), 4.61 (2H, s, H<sub>(10)</sub>/H<sub>(8)</sub>); <sup>13</sup>C NMR (126 MHz, CD<sub>3</sub>OD) δ ppm 138.30 C<sub>(1)</sub>, 135.06 C<sub>(4)</sub>, 132.96 C<sub>(3)</sub>, 127.37 C<sub>(5)</sub>/C<sub>(6)</sub>, 125.86 C<sub>(6)</sub>/C<sub>(5)</sub>, 123.42 C<sub>(2)</sub>, 51.64 C, 51.56 C. This compound degraded rapidly and further steps were achieved without isolation of **106a**

**2-Benzyl-5-bromoisoindoline (106b)**

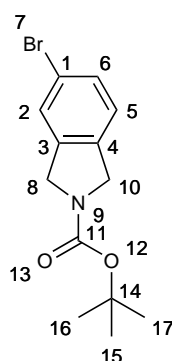
To phthalimide **104b** (2.0 g, 6.3 mmol) in dry tetrahydrofuran (100 mL), sodium borohydride (3.29 g, 87 mmol) was added and the suspension was cooled to -10 °C. Borontrifluoride diethyletherate (12.0 mL 101 mmol) was added dropwise with stirring and the mixture was stirred at 24°C for 16 h. Excess sodium borohydride and borontrifluoride diethyletherate was quenched with water (15 mL) at 0 °C and the mixture was neutralised with saturated aqueous sodium hydrogen carbonate solution then extracted with diethyl ether (3 x 50 mL). The organic layers were washed with brine (100 mL), dried over magnesium sulfate and concentrated to give a white solid which was dissolved in dichloromethane and passed through a silica plug to give **106b** (1.50 g, 82%) as a white solid, m.p. 104-108 °C;  $\nu_{max}$  (cm<sup>-1</sup>): 2379-2273 (NH<sub>3</sub><sup>+</sup> stretch); <sup>1</sup>H NMR (500 MHz, chloroform-*d*)  $\delta$  ppm 7.32 - 7.39 (6H, m, aryl), 7.30 (1H, s, aryl), 7.03 (1H, d, *J*=8.0 Hz, aryl), 4.23 - 4.47 (4H, m, H<sub>(7)</sub>,H<sub>(9)</sub>), 4.08 - 4.20 (2H, m, H<sub>(10)</sub>); <sup>13</sup>C NMR (126 MHz, chloroform-*d*)  $\delta$  ppm 139.23, 135.96, 132.50 C<sub>(13)</sub>,C<sub>(17)</sub>, 131.71, 131.08, 129.28, 128.44 C<sub>(14)</sub>,C<sub>(16)</sub>, 125.94, 124.18, 121.70, 65.50 C<sub>(10)</sub>, 64.32 C<sub>(7)</sub>/C<sub>(9)</sub>, 64.20 C<sub>(9)</sub>/C<sub>(7)</sub>; HRMS calcd for C<sub>15</sub>H<sub>15</sub>NBr: 288.0388(M+H), found: 288.0390.

**5-Bromo-2-(4-methoxybenzyl)isoindoline (106c), and  
5-bromo-2-(4-methoxybenzyl)-2*H*-isoindole, (113)**

To phthalimide **104c** (2.0 g, 5.78 mmol) and sodium borohydride (2.25 g, 58 mmol) in tetrahydrofuran (100 ml) was added borontrifluoride diethyletherate (4.5 mL, 63.6 mmol) dropwise with stirring at  $-10\text{ }^{\circ}\text{C}$ , the mixture was brought to  $20\text{ }^{\circ}\text{C}$  and stirred for 16 h. Excess sodium borohydride and borontrifluoride diethyletherate were quenched with water. The mixture was extracted with diethyl ether (3 x 30 mL), the combined organic layers were washed with brine and dried over magnesium sulfate. The solvent was evaporated to give a yellow oil which was purified by silica column chromatography (60% dichloromethane 40% hexane) to give **106c** (620 mg, 33%) as a white solid;  $\nu_{max}$  ( $\text{cm}^{-1}$ ): 2932, 2381, 2349, 2325;  $^1\text{H}$  NMR (500 MHz, chloroform-*d*)  $\delta$  ppm 7.36 (1H, dd,  $J=8.0, 1.2$  Hz,  $\text{H}_{(2)}$ ), 7.23 - 7.33 (3H, m, aryl), 7.03 (1H, d,  $J=8.0$  Hz,  $\text{H}_{(1)}$ ), 6.83-6.89 (2H, m,  $\text{H}_{(13)}, \text{H}_{(15)}$ ), 4.21 - 4.39 (4H, m,  $\text{H}_{(7)}, \text{H}_{(9)}$ ), 4.07 (2H, s,  $\text{H}_{(10)}$ ), 3.78 - 3.81 (3H, m,  $\text{H}_{(18)}$ );  $^{13}\text{C}$  NMR (126 MHz, chloroform-*d*)  $\delta$  ppm 160.28  $\text{C}_{(14)}$ , 139.31, 136.03, 133.80  $\text{C}_{(12)}, \text{C}_{(16)}$ , 131.07, 125.97, 124.23, 123.82, 121.67, 113.78  $\text{C}_{(13)}, \text{C}_{(15)}$ , 64.84  $\text{C}_{(10)}$ , 64.11  $\text{C}_{(7)}/\text{C}_{(9)}$ , 63.97  $\text{C}_{(9)}/\text{C}_{(7)}$ , 55.40  $\text{C}_{(18)}$ . This reaction had not gone to completion; a second, less polar product was purified and identified as the isoindole intermediate. This compound is interesting as it contains a 10  $\pi$  electron system -  $^1\text{H}$  NMR (500 MHz, chloroform-*d*) 7.64 - 7.67 (1H, m, aryl), 7.35 - 7.41 (1H, m, aryl), 7.08 - 7.14 (3H, m, aryl), 7.03 - 7.07 (1H, m, aryl), 6.96 (1H, dd,  $J=9.0, 1.7$  Hz, aryl), 6.84 - 6.90 (2H, m, aryl), 5.26 (2H, s,  $2\text{H}_{(10)}$ ), 3.80 (3H, s,  $3\text{H}_{(18)}$ )  $^{13}\text{C}$  NMR (126 MHz, chloroform-*d*)  $\delta$  ppm

159.59 C<sub>14</sub>, 128.94 C<sub>12</sub>,C<sub>16</sub> , 125.44, 124.28, 122.75, 121.70, 121.45, 114.68, 114.31 C<sub>13</sub>,C<sub>15</sub>, 111.80, 110.69, 55.40 C<sub>18</sub>, 54.47 C<sub>10</sub>.

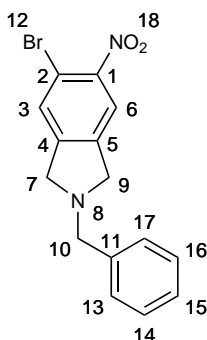
***tert*-Butyl 5-bromoisindoline-2-carboxylate **106d**<sup>221</sup>**



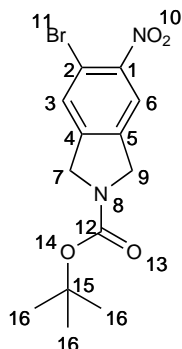
Using an adapted literature<sup>221</sup> procedure, **104a** (4.52 g, 20 mmol) was dissolved in dry tetrahydrofuran (150 mL), sodium borohydride (7.56 g, 200 mmol) was added and the mixture was stirred at -10 °C. Borontrifluoride diethyletherate (29.6 mL, 240 mmol) was added dropwise over 2 h. The mixture was then heated at reflux for 16 h before quenching with 20 mL water at 0 °C. The quenched reaction was stirred for 30 min until all solids had dissolved before diluting with ethyl acetate (50 mL), the aqueous layer was basified to pH 10-12 with sodium hydroxide (4 M), and washed with brine (pH 10). The organic layer was dried over sodium sulfate and evaporated to give crude (**106a**). This was dissolved in dimethylformamide (50 mL), di-*tert*-butyl dicarbonate (5.5 mL) and a few crystals of 4-dimethylaminopyridine were added. The mixture was stirred for 16 h at 20 °C, diluted with ethyl acetate (25 mL) and washed with water (3 x 30 mL) and brine (1 x 30 mL) and then dried over magnesium sulfate. The solvent was evaporated and the residue was purified by column chromatography (10% diethyl ether 90% hexane) to give **106d** (2.28 g, 38 % over 2 steps) as a pink oil. The literature<sup>221</sup> describes this compound as a pale yellow solid, <sup>1</sup>H NMR (500 MHz, chloroform-*d*)  $\delta$  ppm 7.31 - 7.44 (2H, m aryl), 7.03 - 7.17 (1H, m aryl), 4.56 - 4.67 (4H, H<sub>(8)</sub>,H<sub>(10)</sub>), 1.48 - 1.54 (9H, m, H<sub>(15)</sub>,H<sub>(16)</sub>,H<sub>(18)</sub>); <sup>13</sup>C NMR (126 MHz, chloroform-*d*)  $\delta$  ppm 154.39 C<sub>(11)</sub>, 139.69, 139.32, 136.39, 136.04,

126.10, 125.85 C, 124.41, 124.16, 122.83, 122.60, 121.19, 121.11, 80.01 C<sub>(14)</sub>, 51.97 C<sub>(8)</sub>/C<sub>(10)</sub>, 51.72 C<sub>(10)</sub>/C<sub>(8)</sub>, 51.69 C<sub>(10)</sub>/C<sub>(8)</sub>, 28.58 C<sub>(15)</sub>,C<sub>(16)</sub>,C<sub>(17)</sub>. HRMS calcd for C<sub>13</sub>H<sub>16</sub>BrNO<sub>2</sub>: 297.0364 (M+H), found: 297.0362.

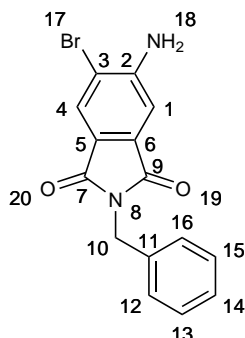
## 2-Benzyl-5-bromo-6-nitroisindoline (107b)



Phthalimide **105b** (320 mg, 0.88 mmol) was dissolved in dry tetrahydrofuran (15 mL), sodium borohydride (333 mg, 8.8 mmol) was added and the suspension was cooled to -10 °C. Borontrifluoride diethyletherate (1.3 mL 10.3 mmol) was added dropwise with stirring and the mixture was allowed to stir at rt for 16 h. Excess sodium borohydride and boron trifluoride diethyletherate was quenched with water (2.5 mL) and extracted with diethyl ether (20 mL) the organic layers were washed with brine, dried over magnesium sulfate and concentrated to give a white solid which was purified by silica column chromatography (chloroform) to give **107b** as a yellow/orange oil (128 mg, 43%), <sup>1</sup>H NMR (600 MHz, chloroform-*d*) δ ppm 7.66 (1H, s, aryl), 7.52 (1H, s, aryl), 7.28 - 7.40 (6H, m, aryl), 3.96 (2H, s, 2H<sub>(7)</sub>/2H<sub>(9)</sub>), 3.94 (2H, s, 2H<sub>(9)</sub>/2H<sub>(7)</sub>), 3.91 (2H, s, H<sub>(10)</sub>); <sup>13</sup>C NMR (151 MHz, chloroform-*d*) δ ppm 167.76 C<sub>(7)</sub>/C<sub>(9)</sub>, 167.15 C<sub>(9)</sub>/C<sub>(7)</sub>, 149.25 C<sub>(2)</sub>, 136.59, 133.59, 128.77, 128.62, 128.51, 127.88, 121.45, 112.80, 109.01, 41.71 C<sub>(10)</sub>; HRMS calcd for C<sub>15</sub>H<sub>14</sub>N<sub>2</sub>O<sub>2</sub>Br: 333.0239 (M+H), found: 333.0236.

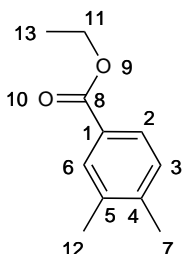
*tert*-Butyl 5-bromo-6-nitroisoindoline-2-carboxylate (**107c**)

Sodium borohydride (3.04 g, 80 mmol) was added with stirring to phthalimide **105a** (2.17 g, 8.0 mmol) in tetrahydrofuran (15 mL). The mixture was cooled to  $-10\text{ }^{\circ}\text{C}$  and boron trifluoride diethyletherate (1.26 mL, 10.26 mmol) was added dropwise over 2 h. The mixture was heated to  $70\text{ }^{\circ}\text{C}$  for 16 h before quenching slowly with cold water (15 mL). The mixture was stirred until all solids had dissolved. Aqueous sodium hydroxide (20%, 20 mL) was added and the mixture stirred for 2 h, then extracted with ethyl acetate (1 x 50 mL, 1 x 100 mL). The combined organic layers were washed with basified brine (pH 12) and dried over sodium sulfate. After evaporation the residue was dissolved in 15 mL dimethylformamide and di-*tert*-butyl dicarbonate (2.2 mL, 9.6 mmol) was added. A few crystals of 4-dimethylaminopyridine were added and the mixture was stirred at  $20\text{ }^{\circ}\text{C}$  for 16 h. The mixture was diluted with ethyl acetate (50 mL) and washed with brine (4 x 30 mL) the organic layer was dried over magnesium sulfate and the solvent evaporated. The residue was purified by column chromatography (40% diethyl ether 60% hexane) to give **107c** (654 mg, 24%) as a cream solid,  $^1\text{H}$  NMR (500 MHz, chloroform-*d*)  $\delta$  ppm 7.68 - 7.80 (1H, m, H<sub>(3)</sub>/H<sub>(6)</sub>), 7.53 - 7.67 (1H, m, H<sub>(6)</sub>/H<sub>(3)</sub>), 4.61 - 4.76 (4H, m, 2H<sub>(7)</sub>, 2H<sub>(9)</sub>), 1.46 - 1.53 (9H, m, 3 x 3H<sub>(16)</sub>);  $^{13}\text{C}$  NMR (126 MHz, chloroform-*d*)  $\delta$  ppm 154.07 C<sub>(12)</sub>, 154.03 C<sub>(12)</sub>, 149.38 C<sub>(8)</sub>, 149.35 C<sub>(8)</sub>, 143.61, 143.29, 138.39, 138.06, 129.37, 129.14, 120.33, 120.13, 113.66, 113.56, 80.65 C<sub>(15)</sub>, 51.66 C<sub>(7)</sub>/C<sub>(9)</sub>, 51.51 C<sub>(9)</sub>/C<sub>(7)</sub>, 51.48 C<sub>(9)</sub>/C<sub>(7)</sub>.

**5-Amino-2-benzyl-6-bromoisindoline-1,3-dione (110)**

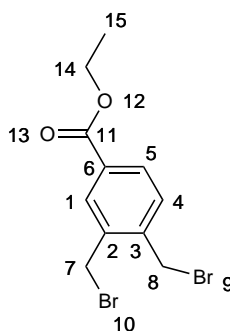
To a stirred solution of iron sulfate heptahydrate (4.64 g, 16.68 mmol) in water (10 mL) and 0.880 ammonia (10 mL) at 60 °C was added a solution of 2-benzyl-5-bromo-6-nitroisindoline-1,3-dione (**105b**) (376 mg, 1.39 mmol) in methanol (10 mL). The mixture was heated at 60 °C for 1 h before being extracted with dichloromethane (2 x 30 mL) and the solvent was evaporated to give **110** (270 mg, 59%) as a yellow solid, m.p. (decomp. 221 °C); <sup>1</sup>H NMR (600 MHz, chloroform-*d*) δ ppm 7.88 (1H, s, H<sub>(4)</sub>), 7.40 (2H, d, *J*=7.5 Hz, H<sub>(12)</sub>,H<sub>(16)</sub>), 7.28 - 7.35 (3H, m, H<sub>(13)</sub>,H<sub>(14)</sub>,H<sub>(15)</sub>), 7.12 (1H, s, H<sub>(1)</sub>), 4.82 (2H, br.s, H<sub>(18)</sub>), 4.79 (2H, s, H<sub>(10)</sub>); <sup>13</sup>C NMR (151 MHz, chloroform-*d*) δ ppm 167.76 C<sub>(7)</sub>/C<sub>(9)</sub>, 167.15 C<sub>(9)</sub>/C<sub>(7)</sub>, 149.25, 136.59, 133.59, 128.77 C<sub>(12)</sub>,C<sub>(16)</sub>, 128.62 C<sub>(16)</sub>,C<sub>(12)</sub>, 128.51, 127.88, 121.45, 112.80, 109.01, 41.71 C<sub>(10)</sub>, HRMS calcd for C<sub>20</sub>H<sub>20</sub>N<sub>2</sub>O<sub>2</sub>Br: 331.0082 (M+H), found: 331.0086.

For 113 see 106c

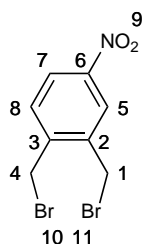
**Ethyl 3,4-dimethylbenzoate (115)<sup>259</sup>**

Following a literature<sup>259</sup> procedure, 3,4-dimethylbenzoic acid (10.0 g, 66.6 mmol) was dissolved in ethanol (200 mL) and sulfuric acid (3.0 mL) was added. The mixture was heated to 65 °C for 6 h before being concentrated and the residue dissolved in ethyl acetate (50 mL), washed with saturated sodium hydrogen carbonate (3 x 50 mL) and then with brine (50 mL) the organic layer was dried over magnesium sulfate and the solvent evaporated to give **115** (20.9 g, 88%) as an orange oil and used without further purification. <sup>1</sup>H NMR (600 MHz, chloroform-*d*) δ ppm 7.81 (1H, s, H<sub>(6)</sub>), 7.77 (1H, d, *J*=7.9 Hz, H<sub>(3)</sub>), 7.15 (1H, d, *J*=7.9 Hz, H<sub>(2)</sub>), 4.35 (2H, q, *J*=7.2 Hz, H<sub>(11)</sub>), 2.27 (6H, s, H<sub>(7)</sub>,H<sub>(12)</sub>), 1.38 (3H, t, *J*=7.2 Hz, H<sub>(13)</sub>); <sup>13</sup>C NMR (151 MHz, chloroform-*d*) δ ppm 166.93 C<sub>(8)</sub>, 142.16, 136.68, 130.66, 129.68, 128.15, 127.22 C(aryl), 60.76 C<sub>(11)</sub>, 20.03 C<sub>(7)</sub>/C<sub>(12)</sub>, 19.72 C<sub>(12)</sub>/C<sub>(7)</sub>, 14.45 C<sub>(13)</sub>.

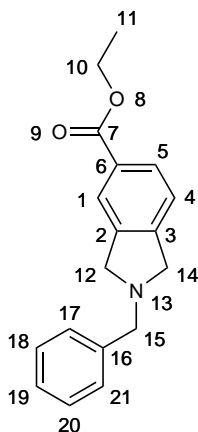
### Ethyl 3,4-bis(bromomethyl)benzoate (**117**)



Ethyl 3,4-dimethylbenzoate (**115**) (1.44 g, 8.1 mmol), *N*-bromosuccinimide (3.17 g, 17.8 mmol) and 2-2'azobis(isobutylnitrile) (10 mg, 0.06 mmol) were dissolved in carbon tetrachloride (10 mL) and heated at reflux for 2 h. The mixture was cooled to 20 °C and the precipitate filtered and washed with carbon tetrachloride. The filtrate was evaporated to give **117** as an orange oil which was used without further purification in the next step (3.28 g, 64% by NMR), <sup>1</sup>H NMR (500 MHz, chloroform-*d*) δ ppm 8.02 (1H, s, H<sub>(1)</sub>), 7.93 (1H, d, *J*=8.1 Hz, H<sub>(4)</sub>/H<sub>(5)</sub>), 7.41 (1H, d, *J*=8.1 Hz, H<sub>(5)</sub>/H<sub>(4)</sub>), 4.64 (4H, d, *J*=4.9 Hz, H<sub>(7)</sub>/H<sub>(8)</sub>), 4.26 - 4.42 (2H, m, H<sub>(14)</sub>), 1.26 - 1.44 (3H, s, H<sub>(15)</sub>);

**1,2-Bis(bromomethyl)-4-nitrobenzene (118)**<sup>259</sup>

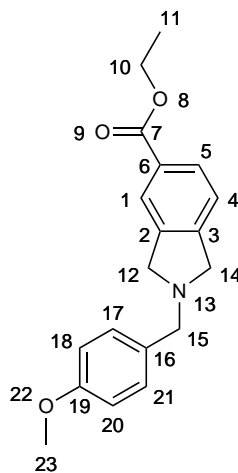
To 1,2-dimethyl-4-nitrobenzene (8.0 g, 53 mmol) in carbon tetrachloride (80 mL) was added *N*-bromosuccinimide (18.8 g, 106 mmol) followed by 2-2'-azobis(isobutyronitrile) (100 mg, 0.6 mmol) and the mixture was heated at reflux for 18 h. The precipitated solids were filtered and washed with carbon tetrachloride and the filtrate was evaporated to give **118** as a yellow oil (13.7 g, 84%) which was used without further purification, <sup>1</sup>H NMR (500 MHz, chloroform-*d*)  $\delta$  ppm 8.18 - 8.26 (1H, m, H<sub>(5)</sub>), 8.11 (1H, d, *J* = 8.4 Hz, H<sub>(8)</sub>), 7.54 (1H, d, *J* = 8.4 Hz, H<sub>(7)</sub>), 4.58 - 4.68 (4H, m, 2H<sub>(1)</sub>, 2H<sub>(2)</sub>).

**Ethyl 2-benzylisoindoline-5-carboxylate (119a)**

Ethyl 3,4-dimethylbenzoate (9.43 g, 53 mmol), *N*-bromosuccinimide (20.7 g 116 mmol) and benzoyl peroxide (0.8 g, 3.3 mmol) were dissolved in carbon tetrachlo-

ride (40 mL) and heated at reflux for 44 h. The mixture was allowed to cool and the reprecipitated solids were removed by filtration. The solvent was evaporated and the residue was dissolved in tetrahydrofuran (250 mL), triethylamine (14.7 mL, 106 mmol) was added and benzylamine (5.6 mL, 51 mmol) in tetrahydrofuran (30 mL) was added very slowly with stirring. The mixture was stirred for 16 h and the precipitate was filtered and washed with tetrahydrofuran. The solvent was evaporated and the residue was purified by column chromatography (7% ethyl acetate 93% dichloromethane) to give **119a** (6.6 g, 43%) as a brown oil,  $\nu_{max}$  (cm<sup>-1</sup>): 2920, 2850, 1716 (C=O); <sup>1</sup>H NMR (500 MHz, chloroform-*d*)  $\delta$  ppm 7.90 (1H, dd,  $J=7.8, 1.4$  Hz, H<sub>(5)</sub>), 7.86 (1H, s, H<sub>(1)</sub>), 7.39 - 7.42 (2H, m, aryl), 7.2 - 7.43 (8H, m,  $J=7.3$  Hz, aryl), 4.36 (2H, q,  $J=7.1$  Hz, H<sub>(10)</sub>), 3.97 (4H, s, H<sub>(12)</sub>, H<sub>(14)</sub>), 3.92 (2H, s, H<sub>(15)</sub>), 1.38 (3H, t,  $J=7.2$  Hz, H<sub>(11)</sub>); <sup>13</sup>C NMR (126 MHz, chloroform-*d*)  $\delta$  ppm 166.74 C<sub>(7)</sub>, 145.56 C<sub>(3)</sub>, 140.64 C<sub>(2)</sub>, 138.75 C<sub>(16)</sub>, 129.38, 128.85, 128.64, 128.53, 127.34, 123.59, 122.25, 60.94 C<sub>(10)</sub>/C<sub>(12)</sub>/C<sub>(14)</sub>/C<sub>(14)</sub>/C<sub>(15)</sub>, 60.25 C<sub>(10)</sub>/C<sub>(12)</sub>, C<sub>(14)</sub>/C<sub>(15)</sub>, 58.85 C<sub>(10)</sub>/C<sub>(12)</sub>, C<sub>(14)</sub>/C<sub>(15)</sub>, 58.62 C<sub>(10)</sub>/C<sub>(12)</sub>, C<sub>(14)</sub>/C<sub>(15)</sub>, 14.39 C<sub>(11)</sub>.

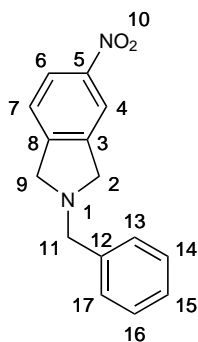
### Ethyl 2-(4-methoxybenzyl)isoindoline-5-carboxylate (**119b**)



Crude ethyl 3,4-bis(bromomethyl)benzoate (**117**) (3.281 g, 64% by NMR, 6.2 mmol) was dissolved in tetrahydrofuran (80 mL) and treated with triethylamine (4.6 mL, 32.6 mmol). 4-Methoxybenzylamine (2.1 mL, 16.1 mmol) was dissolved in tetrahy-

drofuran (17.9 mL) and added dropwise to the solution with stirring and stirring was continued for 16 h. The precipitate was filtered and washed with tetrahydrofuran and the solvent was evaporated. The residue was purified by column chromatography (50% hexane 50% diethylether) to give **119b** (1.02 g, 40%) as a dark yellow oil,  $^1\text{H}$  NMR (300 MHz, chloroform-*d*)  $\delta$  ppm 7.91 (1H, dd,  $J=7.7$ , 0.9 Hz, H<sub>(5)</sub>), 7.86 (1H, s, H<sub>(1)</sub>), 7.32 (2H, d,  $J=8.7$  Hz, H<sub>(17)</sub>,H<sub>(21)</sub>), 7.23 (1H, d,  $J=7.7$  Hz, H<sub>(4)</sub>), 6.90 (2H, d,  $J=8.7$  Hz, H<sub>(18)</sub>,H<sub>(20)</sub>), 4.37 (2H, q,  $J=7.1$  Hz, H<sub>(10)</sub>), 3.94 (4H, s, H<sub>(12)</sub>,H<sub>(14)</sub>), 3.86 (2H, s, H<sub>(15)</sub>), 3.82 (3H, s, H<sub>(23)</sub>), 1.39 (2H, t,  $J=7.1$  Hz, H<sub>(11)</sub>);  $^{13}\text{C}$  NMR (75 MHz, chloroform-*d*)  $\delta$  ppm 166.64 C<sub>(7)</sub>, 158.78 C<sub>(19)</sub>, 145.59, 140.65, 130.85, 129.85 C<sub>(17)</sub>,C<sub>(21)</sub>, 129.18, 128.47, 123.46, 122.13, 113.75 C<sub>(18)</sub>,C<sub>(20)</sub>, 60.81 C, 59.45 C<sub>(12)</sub>/C<sub>(14)</sub>/C<sub>(15)</sub>, 58.63 C<sub>(14)</sub>/C<sub>(15)</sub>/C<sub>(12)</sub>, 58.39 C<sub>(15)</sub>/C<sub>(12)</sub>/C<sub>(14)</sub>, 55.21 C<sub>(23)</sub>, 14.28 C<sub>(11)</sub>; HRMS calcd for C<sub>19</sub>H<sub>22</sub>NO<sub>3</sub>: 312.1600 (M+H), found: 312.1599.

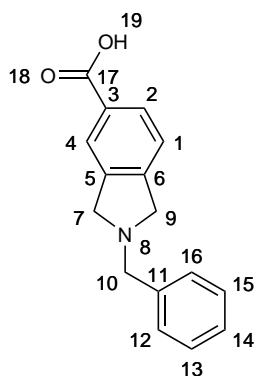
## 2-Benzyl-5-nitroisindoline (120)<sup>259</sup>



To sodium carbonate (20.2 g, 190 mmol) was added water (30 mL). The mixture was briefly sonicated and acetone (60 mL) was added. Benzylamine was dissolved in acetone (10 mL) and added to the stirred suspension over 3 h and the mixture was stirred for 18 h. The mixture was concentrated before being extracted into ethyl acetate (2 x 75 mL). The organic layers were then extracted with hydrochloric acid (2 M, 3 x 75 mL) and the aqueous layers were neutralised with saturated aqueous sodium hydrogen carbonate solution and the product was extracted into ethyl acetate (2 x 50 mL) washed with brine and dried over magnesium sulfate. The solvent was evaporated and the residue purified by column chromatography (20%

ethyl acetate 80% hexane) to give **120** (1.17 g, 20%) as a yellow solid, m.p. 79.5-80 °C (lit.<sup>227</sup> 77.5-78 °C);  $\nu_{max}$  (cm<sup>-1</sup>): 2809 (CH), 1516 (NO asym), 1340 (NO sym); <sup>1</sup>H NMR (500 MHz, chloroform-*d*)  $\delta$  ppm 8.09 (1H dd,  $J=8.4, 2.0$  Hz, H<sub>(6)</sub>), 8.02 (1H, s, H<sub>(4)</sub>), 7.27 - 7.44 (6H, m, aryl), 3.99 (4H, d,  $J=1.6$  Hz, H<sub>(2)</sub>,H<sub>(9)</sub>), 3.93 (2H, s, 2H<sub>(11)</sub>); <sup>13</sup>C NMR (126 MHz, chloroform-*d*)  $\delta$  ppm 147.98 C<sub>(5)</sub>, 147.55 C<sub>(8)</sub>, 142.20 C<sub>(3)</sub>, 138.48 C<sub>(12)</sub>, 128.79 C<sub>(13)</sub>,C<sub>(17)</sub>, 128.63 C<sub>(14)</sub>,C<sub>(16)</sub>, 127.48 C<sub>(7)</sub>, 122.94 C<sub>(4)</sub>/C<sub>(15)</sub>, 122.76 C<sub>(15)</sub>/C<sub>(4)</sub>, 117.80 C<sub>(6)</sub>, 60.07 C<sub>(11)</sub>, 58.56 C<sub>(2)</sub>/C<sub>(9)</sub>, 58.38 C<sub>(9)</sub>/C<sub>(2)</sub>.

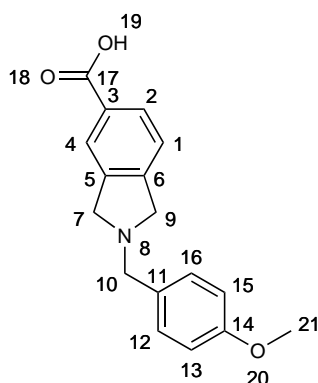
### 2-Benzylisoindoline-5-carboxylic acid (**125a**)



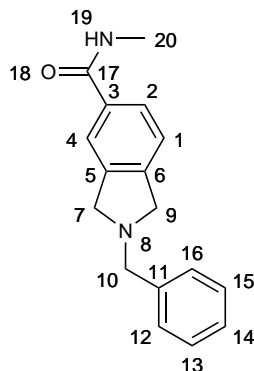
To isoindoline **106b** (327 mg, 1.13 mmol) in tetrahydrofuran (7 mL) at -78 °C was added *n*-BuLi in hexane (0.60 mL, 1.2 mmol) dropwise with stirring. The mixture was stirred at -78 °C for 2 h after which gaseous carbon dioxide evolved from the sublimation of dry ice was bubbled into the mixture for 2 h. The reaction was quenched at 0 °C with water, and slightly acidified (pH 4-5) with hydrochloric acid (1 M) to pH 2-3. The product was extracted into ethyl acetate (2 x 20 mL) and the combined organic fractions were washed with brine (1 x 30 mL) before drying over magnesium sulfate and evaporating. The residue was loaded onto a silica plug in dichloromethane, washed with dichloromethane and eluted with 1% acetic acid in dichloromethane. The solvent was evaporated to give **125a** as a white solid (277 mg, 79%), m.p. (decomp 151 °C);  $\nu_{max}$  (cm<sup>-1</sup>): 3400 (OH), 2378, 2325, 2282, 1676 (C=O); <sup>1</sup>H NMR (600 MHz, chloroform-*d*)  $\delta$  ppm 7.99 (1H, d,  $J=7.9$  Hz, H<sub>(2)</sub>), 7.88 (1H, s, H<sub>(4)</sub>), 7.32 - 7.41 (5H, m, aryl), 7.24 (1H, d,  $J=7.9$  Hz, H<sub>(1)</sub>), 4.34 - 4.54 (4H,

m, H<sub>(7),H(9)</sub>), 4.19 (2H, s, H<sub>(10)</sub>); <sup>13</sup>C NMR (151 MHz, chloroform-*d*) δ ppm 171.23 C<sub>(17)</sub>, 142.98 C<sub>(6)</sub>, 137.61, 132.55 C<sub>(12),C(16)</sub>, 131.65, 130.41, 129.61, 129.37, 128.56 C<sub>(13),C(15)</sub>, 124.44, 122.74, 65.66 C<sub>(10)</sub>, 64.50 C<sub>(7)/C(9)</sub>, 64.23 C<sub>(9)/C(7)</sub>; HRMS calcd for C<sub>16</sub>H<sub>15</sub>NO<sub>2</sub>: 254.1179 (M+H), found: 254.1179.

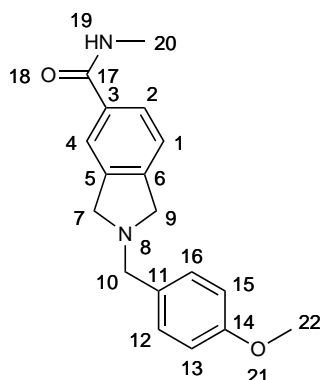
## 2-(4-Methoxybenzyl)isoindoline-5-carboxylic acid (**125b**)



To isoindoline **106c** (620 mg, 1.95 mmol) in tetrahydrofuran (12 mL) was added *n*-BuLi (0.94 mL, 2.34 mmol) dropwise at -78 °C. The mixture was stirred at -78 °C for 2 h then carbon dioxide evolved from sublimation of dry ice was bubbled through the reaction for 2 h. The reaction was quenched at 0 °C with water and extracted into diethyl ether before being slightly acidified (pH 4-5) with hydrochloric acid (2 M) and extracted into ethyl acetate (2 x 30 mL) the ethyl acetate layers were combined and dried over sodium sulfate to give **125b** (539 mg, 98%) as a white solid, m.p. (decomp. 175 °C);  $\nu_{max}$  (cm<sup>-1</sup>): 3122 br. (OH) 2379, 2283, 2223 1676 (C=O); <sup>1</sup>H NMR (600 MHz, chloroform-*d*) δ ppm 8.01 (1H, d, *J*=8.1 Hz, H<sub>(2)</sub>), 7.90 (1H, s, H<sub>(4)</sub>), 7.25 - 7.31 (4H, m, aryl), 6.87 (1H, d, *J*=8.1 Hz, H<sub>(1)</sub>), 4.35 - 4.50 (4H, m, H<sub>(7),H(9)</sub>), 4.13 (2H, s, H<sub>(10)</sub>), 3.80 (3H, s, H<sub>(21)</sub>); <sup>13</sup>C NMR (126 MHz, chloroform-*d*) δ ppm 169.96 C<sub>(17)</sub>, 160.33 C<sub>(14)</sub>, 143.15, 137.74, 133.83 C<sub>(12),C(16)</sub>, 130.45, 129.18, 124.48, 123.72, 122.84, 113.88 C<sub>(13),C(15)</sub>, 64.99 C<sub>(10)</sub>, 64.31 C<sub>(7),C(9)</sub>, 63.99 C<sub>(9)/C(7)</sub>, 55.42 C<sub>(21)</sub>; HRMS calcd for C<sub>17</sub>H<sub>17</sub>NO<sub>3</sub>: 284.1290 (M+H), found: 284.1287.

**2-Benzyl-*N*-methylisoindoline-5-carboxamide (126a)**

Isoindoline **125a** (506 mg, 2.0 mmol), *N*-(3-dimethylaminopropyl)-*N'*-ethylcarbodiimide hydrochloride (767 mg, 4 mmol) and anhydrous hydroxybenzotriazole (540 mg, 4 mmol) were dissolved in dimethylformamide (6.0 mL) and the mixture was stirred for 30 min. Methylamine in tetrahydrofuran (10 mL, 20 mmol) was added and the mixture stirred for 16 h. The mixture was then diluted with ethyl acetate (30 mL) and washed with water (3 x 30 mL) the aqueous fractions were re-extracted with ethyl acetate (50 mL). The combined organic layers were washed with brine (50 mL), dried over magnesium sulfate and evaporated. The residue was purified by column chromatography (3% methanol 97% ethyl acetate) to give **126a** (396 mg, 74%) as a white solid, m.p. (decomp. 141-143 °C);  $\nu_{max}$  (cm<sup>-1</sup>): 3324 (NH), 3022, 2892, 2806, 1655 (C=O); <sup>1</sup>H NMR (600 MHz, chloroform-*d*)  $\delta$  ppm 7.60 (1H, s, H<sub>(4)</sub>), 7.57 (1H, d,  $J$ =7.9 Hz, H<sub>(2)</sub>), 7.39 - 7.44 (2H, m, H<sub>(16)</sub>,H<sub>(12)</sub>), 7.36 (2H, t,  $J$ =7.3 Hz, H<sub>(13)</sub>,H<sub>(15)</sub>), 7.27 - 7.32 (1H, m, H<sub>(14)</sub>), 7.22 (1H, d,  $J$ =7.9 Hz, H<sub>(1)</sub>), 6.10 (1H, br.s, H<sub>(16)</sub>), 3.95 (4H, s, H<sub>(7)</sub>/H<sub>(9)</sub>), 3.92 (2H, s, H<sub>(10)</sub>), 3.00 (3H, d,  $J$ =4.5 Hz, H<sub>(20)</sub>); <sup>13</sup>C NMR (126 MHz, chloroform-*d*)  $\delta$  ppm 168.38 C<sub>(17)</sub>, 143.91 C<sub>(6)</sub>, 140.90 C<sub>(5)</sub>, 138.78 C<sub>(11)</sub>, 133.57, 128.85 C<sub>(12)</sub>,C<sub>(16)</sub>, 128.53 C<sub>(13)</sub>,C<sub>(15)</sub>, 127.33, 125.67, 122.41, 121.12, 60.24 C<sub>(10)</sub>, 58.74 C<sub>(7)</sub>/C<sub>(9)</sub>, 58.68 C<sub>(9)</sub>/C<sub>(7)</sub>, 26.90 C<sub>(20)</sub>; HRMS calcd for C<sub>17</sub>H<sub>19</sub>NO<sub>2</sub>: 267.1497, found: 267.1497.

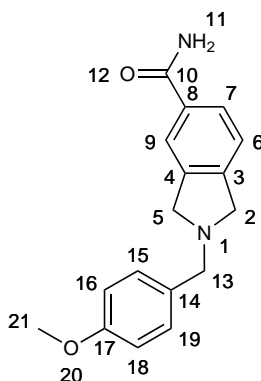
**2-(4-Methoxybenzyl)-*N*-methylisoindoline-5-carboxamide (126b)**

Ethylester (**119a**), (400 mg, 1.28 mmol) and 40% aqueous methylamine (4 mL) were sealed in a tube and stirred at 100 °C for 16 h. The reaction was allowed to cool to 20 °C and the solvent evaporated. The residue was purified by column chromatography (5% methanol 95% ethyl acetate) to give **126b** (288 mg, 75%) as a white solid.

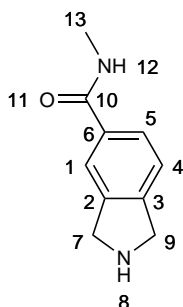
Using *N*-(3-dimethylaminopropyl)-*N*'-ethylcarbodiimide hydrochloride, isoindoline **125b** (320 mg, 1.1 mmol) in dimethylformamide (5 mL), *N*-(3-dimethylaminopropyl)-*N*'-ethylcarbodiimide hydrochloride (499 mg, 2.6 mmol) and anhydrous hydroxybenzotriazole (351 mg, 2.6 mmol) were stirred at rt for 30 min. Methylamine in tetrahydrofuran (6.5 mL, 13 mmol) was added and the mixture stirred for 16 h. The mixture was then diluted with ethyl acetate (30 mL) and washed with water (3 x 30 mL) the aqueous fractions were re-extracted with ethyl acetate (50 mL), the combined organic layers were washed with brine (50 mL), dried over magnesium sulfate and evaporated. The residue was purified by column chromatography (3% methanol 97% ethyl acetate to give **126b** (295 mg, 86%) as a white solid, m.p. 138-140 °C;  $\nu_{max}$  (cm<sup>-1</sup>): 3273 (NH), 2934, 2892, 2803, 1633 (C=O); <sup>1</sup>H NMR (600 MHz, chloroform-*d*)  $\delta$  ppm 7.49 - 7.66 (2H, m, H<sub>(2)</sub>,H<sub>(4)</sub>), 7.30 (2H, d,  $J$ =8.7 Hz, H<sub>(12)</sub>,H<sub>(16)</sub>), 7.17 (1H, d,  $J$ =8.1 Hz, H<sub>(1)</sub>), 6.88 (2H, d,  $J$ =8.7 Hz, H<sub>(13)</sub>,H<sub>(15)</sub>), 6.33 (1H, d,  $J$ =3.0 Hz, H<sub>(19)</sub>), 3.90 (4H, s, H<sub>(7)</sub>,H<sub>(9)</sub>), 3.83 (2H, s, H<sub>(10)</sub>), 3.80 (3H, s, 3H<sub>(22)</sub>), 2.96 (3H, d,  $J$ =4.7 Hz, 3H<sub>(20)</sub>); <sup>13</sup>C NMR (126 MHz, chloroform-*d*)  $\delta$  ppm 168.46 C<sub>(17)</sub>, 158.95 C<sub>(14)</sub>, 144.08 C<sub>(6)</sub>, 141.06 C<sub>(5)</sub>, 133.57, 131.08, 130.03 C<sub>(12)</sub>,C<sub>(16)</sub>, 125.70, 122.44,

121.19, 113.94 C<sub>(13)</sub>,C<sub>(15)</sub>, 59.65 C<sub>(10)</sub>, 58.73 C<sub>(7)</sub>/C<sub>(9)</sub>, 58.66 C<sub>(9)</sub>/C<sub>(7)</sub>, 55.42 C<sub>(22)</sub>, 26.97 C<sub>(20)</sub>; HRMS calcd for C<sub>18</sub>H<sub>19</sub>N<sub>2</sub>O<sub>2</sub>: 297.1603 (M+H), found: 297.1602.

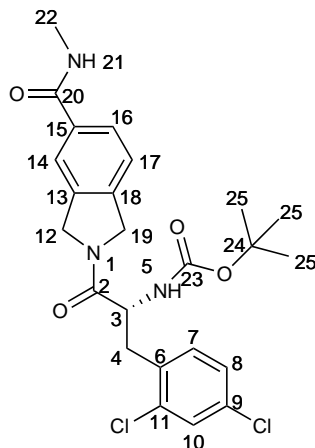
### 2-(4-Methoxybenzyl)isoindoline-5-carboxamide (**127**)



To isoindoline **119b** (746 mg, 2.40 mmol) in ethanol (4 mL) was slowly added concentrated 0.880 ammonia (10 mL). The tube was sealed and heated to 100 °C for 16 h. The solvent was evaporated and the residue was purified by column chromatography (5% methanol 95% ethyl acetate) to give **127** (181 mg, 26%) as a white solid, m.p. 177-178 °C;  $\nu_{max}$  (cm<sup>-1</sup>): 3347 br. (NH), 3198 br. (NH), 1662 (C=O); <sup>1</sup>H NMR (500 MHz, CD<sub>3</sub>OD)  $\delta$  ppm 7.73 (1H, dd,  $J$ =7.8, 1.5 Hz, H<sub>(7)</sub>), 7.71 (1H, s, H<sub>(9)</sub>), 7.26 - 7.34 (3H, m, H<sub>(6)</sub>,H<sub>(15)</sub>,H<sub>(19)</sub>), 6.90 (2H, d,  $J$ =8.7 Hz, H<sub>(16)</sub>,H<sub>(18)</sub>), 3.91 (4H, s, H<sub>(2)</sub>,H<sub>(5)</sub>), 3.84 (2H, s, H<sub>(13)</sub>), 3.78 (3H, s, H<sub>(21)</sub>); <sup>13</sup>C NMR (126 MHz, CD<sub>3</sub>OD)  $\delta$  ppm 172.27 C<sub>(10)</sub>, 160.65 C<sub>(17)</sub>, 145.23, 141.56, 134.08, 131.51 C<sub>(15)</sub>,C<sub>(19)</sub>, 131.13, 127.92, 123.43, 122.71, 114.89 C<sub>(16)</sub>,C<sub>(18)</sub>, 60.37 C<sub>(13)</sub>, 59.41 C<sub>(2)</sub>/C<sub>(5)</sub>, 59.27 C<sub>(5)</sub>/C<sub>(2)</sub>, 55.68 C<sub>(21)</sub>; HRMS calcd for C<sub>17</sub>H<sub>19</sub>N<sub>2</sub>O<sub>2</sub>: 283.1447 (M+H), found: 283.1457.

***N*-Methylisindoline-5-carboxamide (128)**

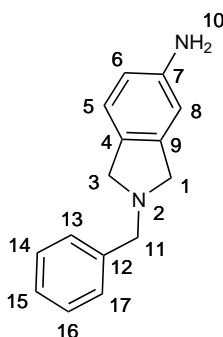
**126a** (288 mg, 0.971.0 mmol) was dissolved in methanol (10 mL) and 30% palladium on carbon (50 mg) was added. A hydrogen balloon was attached and the solution was stirred at 30 °C, after 24 h Pearlman's catalyst (50 mg) was added, and the mixture was stirred for a further 48 h under hydrogen at 30 °C. The mixture was filtered through celite celite and the filtrate was concentrated to give a purple, minty-smelling oil. This was purified by column chromatography (90% ethyl acetate 6% methanol 4% 0.880 ammonia) to give **128** (48 mg, 28%) as a white solid. Starting material (130 mg, 45%) was recovered.  $^1\text{H}$  NMR (600 MHz,  $\text{CD}_3\text{OD}$ )  $\delta$  ppm 7.70 (1H, s,  $\text{H}_{(1)}$ ), 7.68 (1H, d,  $J=7.7$  Hz,  $\text{H}_{(5)}$ ), 7.34 (1H, d,  $J=7.7$  Hz,  $\text{H}_{(4)}$ ), 4.19 (4H, s,  $\text{H}_{(7)}$ ,  $\text{H}_{(9)}$ ), 2.90 (3H, s,  $\text{H}_{(13)}$ );  $^{13}\text{C}$  NMR (126 MHz,  $\text{CD}_3\text{OD}$ )  $\delta$  ppm 170.64  $\text{C}_{(10)}$ , 145.88  $\text{C}_{(3)}$ , 142.67  $\text{C}_{(2)}$ , 134.79, 127.41, 123.48, 122.31, 52.96  $\text{C}_{(7)}/\text{C}_{(9)}$ , 52.84  $\text{C}_{(9)}/\text{C}_{(7)}$ , 26.93  $\text{C}_{(13)}$ ; HRMS calcd for  $\text{C}_{10}\text{H}_{13}\text{N}_2\text{O}$ : 177.1028 (M+H), found: 177.0988.

***tert*-Butyl (*R*)-3-(2,4-dichlorophenyl)-1-(5-(methylcarbamoyl)isoindolin-2-yl)-1-oxopropan-2-yl)carbamate (**130**)**

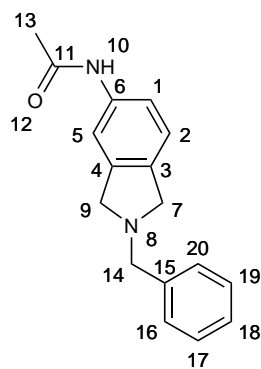
To isoindoline **128** (48 mg, 0.27 mmol), *N*-Boc-(*R*)-2,4-dichlorophenylalanine (91 mg, 0.27 mmol), 1-ethyl-3-(3-dimethylaminopropyl)carbodiimide (59 mg, 0.33 mmol) and anhydrous 1-hydroxybenzotriazole (55 mg, 0.41 mmol) in dimethylformamide (3 mL) was added *N,N*-diisopropylethylamine (0.4 mL, 2.3 mmol), the mixture was then stirred for 24 h at 20 °C. The mixture was diluted with ethyl acetate (20 mL) and washed with water (3 x 20 mL). The combined aqueous fractions were re-extracted with ethyl acetate (3 x 20 mL) and the combined organic layers were dried over magnesium sulfate and evaporated. The residue was purified by column chromatography (94% ethyl acetate 6% methanol) (100 mg, 75%) and then recrystallised from chloroform to yield **130** (48 mg, 36%), m.p. 167-168 °C;  $\nu_{max}$  (cm<sup>-1</sup>): 3550-3180 (br.) 2971, 2927, 2865, 1699 (NHC=O), 1639 (CHC=O), 1583; <sup>1</sup>H NMR (600 MHz, chloroform-*d*, 2 rotamers)  $\delta$  ppm 7.62 - 7.72 (2H, m, aryl), 7.32 (1H, d, *J*=1.7 Hz, aryl), 7.20 - 7.28 (1H, m, aryl), 7.15 - 7.18 (1H, m, aryl), 7.11 (1H, m, *J*=1.7 Hz, aryl), 6.69 - 6.81 (1H, m, H<sub>(21)</sub>), 5.48 (1H, d, *J*=8.7 Hz, H<sub>(5)</sub>), 4.98 (1H, d, *J*=14.3 Hz, H<sub>(12)</sub>/H<sub>(19)</sub>), 4.76 - 4.87 (2H, m, H<sub>(3)</sub>,H<sub>(19)</sub>/H<sub>(12)</sub>), 4.57 - 4.68 (2H, m, H<sub>(12)</sub>,H<sub>(19)</sub>), 3.13 (1H, dd, *J*=13.7, 6.2 Hz, H<sub>(4)</sub>), 2.94 - 3.03 (4H, m, H<sub>(4)</sub>,H<sub>(22)</sub>), 1.27 - 1.38 (9H, m, 3 x 3H<sub>(25)</sub>); <sup>13</sup>C NMR (151 MHz, chloroform-*d*, 2 rotamers) 170.39 C<sub>(2)</sub>, 167.85 C<sub>(15)</sub>, 155.22 C<sub>(23)</sub>, 139.22, 139.10, 136.51, 136.30, 135.09, 134.79, 134.62, 133.73, 132.87, 132.84, 129.34, 127.16, 126.79, 126.72, 123.06, 122.96, 121.84, 121.80,

80.08 C<sub>(24)</sub>, 52.27 C<sub>(3)</sub>, 52.19 C<sub>(12)</sub>/C<sub>(19)</sub>, 52.16 C<sub>(12)</sub>/C<sub>(19)</sub>, 51.08 C<sub>(19)</sub>/C<sub>(12)</sub>, 51.05 C<sub>(19)</sub>/C<sub>(12)</sub>, 36.54 C<sub>(4)</sub>, 28.34 3C<sub>(2)</sub>, 27.03 C<sub>(22)</sub>; HRMS calcd for C<sub>24</sub>H<sub>28</sub>N<sub>3</sub>Cl<sub>2</sub>O<sub>4</sub>: 492.1433 (M+H), found: 492.1457.

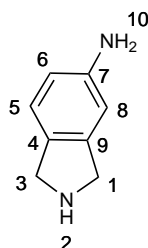
## 2-Benzylisoindolin-5-amine (**132**)<sup>227</sup>



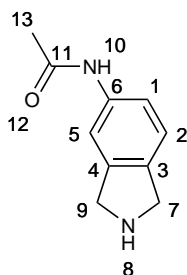
Following an adapted literature<sup>227</sup> procedure, **120** (515 mg, 2.0 mmol) was dissolved in methanol (15 mL) 10% palladium on carbon (29 mg) was added and the mixture stirred vigorously under an atmosphere of hydrogen for 1.5 h. The catalyst was removed by filtration through celite and the filtrate was concentrated to give **132** (445 mg, 89%) as a cream solid, m.p. 137-139 °C (Lit<sup>227</sup> 110-115 °C); <sup>1</sup>H NMR (500 MHz, chloroform-*d*)  $\delta$  ppm 7.42 - 7.47 (2H, m, aryl), 7.26 - 7.40 (3H, m, aryl), 6.93 (1H, d,  $J=7.9$  Hz, aryl), 6.47 - 6.54 (2H, m, aryl), 3.94 (2H, s, H<sub>(11)</sub>), 3.90 (4H, s, 2H<sub>(1)</sub>, 2H<sub>(3)</sub>); <sup>13</sup>C NMR (126 MHz, chloroform-*d*)  $\delta$  ppm 145.43, 141.63, 139.40, 130.47, 128.86, 128.40, 127.09, 122.96, 113.80, 109.40, 60.48 C<sub>(11)</sub>, 59.14 C<sub>(1)</sub>/C<sub>(3)</sub>, 58.58 C<sub>(3)</sub>/C<sub>(1)</sub>.

***N*-(2-Benzylisoindolin-5-yl)acetamide (133)**

To a mixture of amine **132** (443 mg, 1.8 mmol) and triethylamine (1.5 mL, 10 mmol) in dichloromethane (15 mL) was added acetic anhydride (1.5 mL, 15.8 mmol) dropwise and the mixture was stirred for 135 min at 22 °C. The organic phase was washed with saturated aqueous sodium hydrogen carbonate (4 x 30 mL) and dried over magnesium sulfate before evaporating. The residue was purified by silica column chromatography (ethyl acetate) to give **133** (425 mg, 88%) as a white solid, <sup>1</sup>H NMR (500 MHz, chloroform-*d*) δ ppm 7.56 (1H, br.s, H<sub>(10)</sub>), 7.38 - 7.44 (3H, m, aryl), 7.34 (2H, t, *J*=7.4, H<sub>(17)</sub>,H<sub>(19)</sub>), 7.28 (1H, d, *J*=7.1 Hz, aryl), 7.17 (1H, d, *J*=8.0 Hz, H<sub>(1)</sub>/H<sub>(2)</sub>), 7.07 (1H, d, *J*=8.0 Hz, H<sub>(2)</sub>/H<sub>(1)</sub>), 3.89 (4H, s, H<sub>(7)</sub>,H<sub>(9)</sub>), 3.86 (2H, s, H<sub>(14)</sub>), 2.12 (3H, s, H<sub>(13)</sub>); <sup>13</sup>C NMR (126 MHz, chloroform-*d*) δ ppm 168.54 C<sub>(11)</sub>, 141.23, 139.07, 136.79 C<sub>(16)</sub>,C<sub>(20)</sub>, 128.87 C<sub>(17)</sub>,C<sub>(19)</sub>, 127.23, 122.63, 118.74, 114.65, 60.35 C<sub>(7)</sub>/C<sub>(9)</sub>/C<sub>(14)</sub>, 59.08 C<sub>(9)</sub>/C<sub>(14)</sub>/C<sub>(7)</sub>, 58.60 C<sub>(14)</sub>/C<sub>(7)</sub>/C<sub>(9)</sub>, 24.57 C<sub>(13)</sub>.

**Isoindolin-5-amine (134)**<sup>259</sup>

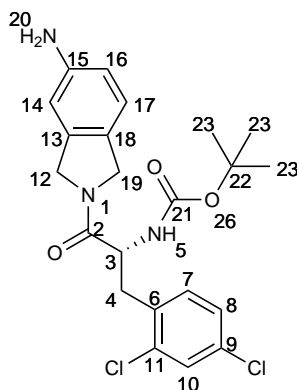
**120** (200 mg, 0.79 mmol) was dissolved in a mixture of methanol (8 mL) and ethanol (5 mL), 10% palladium on carbon (42 mg) was added and the suspension was stirred vigorously under an atmosphere of hydrogen for 48 h. The catalyst was removed by filtration through celite and the filtrate was concentrated and purified by column chromatography (85% ethyl acetate 10% methanol 2% 0.880 ammonia) to give **134** (54 mg, 51%) as a pale brown solid, <sup>1</sup>H NMR (500 MHz, CD<sub>3</sub>OD) δ ppm 6.97 (1H, d, *J*=8.0 Hz, H<sub>(5)</sub>), 6.63 (1H, s, H<sub>(8)</sub>), 6.59 (1H, dd, *J*=8.0, 2.0 Hz, H<sub>(6)</sub>), 4.05 (4H, d, *J*=5.5 Hz, H<sub>(1)</sub>,H<sub>(3)</sub>); <sup>13</sup>C NMR (126 MHz, chloroform-*d*) δ ppm 147.99 C<sub>(7)</sub>, 142.71 C<sub>(9)</sub>, 131.14 C<sub>(4)</sub>, 123.71 C<sub>(5)</sub>, 115.92 C<sub>(6)</sub>/C<sub>(8)</sub>, 110.47 C<sub>(8)</sub>/C<sub>(6)</sub>, 53.03 C<sub>(1)</sub>/C<sub>(3)</sub>, 52.46 C<sub>(3)</sub>/C<sub>(1)</sub>; HRMS calcd for C<sub>8</sub>H<sub>10</sub>N<sub>2</sub>[M<sup>+</sup>]: 134.0844, found: 134.0848.

***N*-(Isoindolin-5-yl)acetamide (135)**

To **133** (290 mg, 1.1 mmol), 30% palladium on carbon (20 mg) and Pearlman's catalyst (40 mg) under an inert atmosphere was added methanol (10 mL). The mixture was then stirred vigorously under an atmosphere of hydrogen for 16 h at 30

°C. The catalyst was removed by filtration through celite and the filtrate evaporated to give **128** as a tan solid (207 mg, **107%**), m.p. 153-155 °C;  $\nu_{max}$  (cm<sup>-1</sup>): 3432 br. (NH) 3296 (NH), 1673 (C=O); <sup>1</sup>H NMR (600 MHz, CD<sub>3</sub>OD)  $\delta$  ppm 7.53 (1H, s, H<sub>(5)</sub>), 7.31 (1H, d,  $J=7.9$  Hz, H<sub>(1)</sub>/H<sub>(2)</sub>), 7.19 (1H, d,  $J=7.9$  Hz, H<sub>(2)</sub>/H<sub>(1)</sub>), 4.05 - 4.17 (4H, m, H<sub>(7)</sub>,H<sub>(9)</sub>), 2.10 (3H, s, H<sub>(13)</sub>); <sup>13</sup>C NMR (151 MHz, chloroform-*d*)  $\delta$  ppm 171.59 C<sub>(11)</sub>, 142.80 C<sub>(4)</sub>/C<sub>(6)</sub>/C<sub>(3)</sub>, 139.00 C<sub>(4)</sub>/C<sub>(6)</sub>/C<sub>(3)</sub>, 137.69 C<sub>(6)</sub>/C<sub>(3)</sub>/C<sub>(4)</sub>, 123.49 C<sub>(1)</sub>/C<sub>(2)</sub>/C<sub>(5)</sub>, 120.21 C<sub>(2)</sub>/C<sub>(5)</sub>/C<sub>(1)</sub>, 115.40 C<sub>(5)</sub>/C<sub>(1)</sub>/C<sub>(2)</sub>, 53.14 C<sub>(7)</sub>/C<sub>(9)</sub>, 52.69 C<sub>(9)</sub>/C<sub>(7)</sub> 23.77 C<sub>(13)</sub>. HRMS calcd for C<sub>10</sub>H<sub>12</sub>N<sub>2</sub>O: 177.1028 (M+H), found: 117.1031.

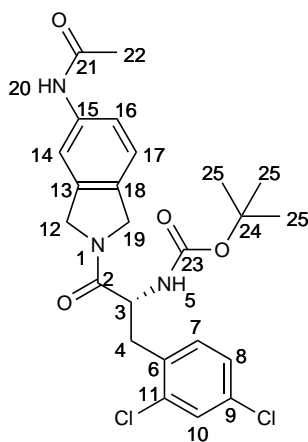
**(*R*)-tert-Butyl (1-(5-aminoisindolin-2-yl)-3-(2,4-dichlorophenyl)-1-oxopropan-2-yl)carbamate**  
**(136)**



**134** (68 mg, 0.5 mmol) *N*-Boc-(*R*)-2,4-dichlorophenylalanine (201 mg, 0.6 mmol), 1-ethyl-3-(3-dimethylaminopropyl)carbodiimide (109 mg, 0.6 mmol) and anhydrous 1-hydroxybenzotriazole (122 mg, 0.6 mmol) in dimethylformamide (3.0 mL) was added *N,N*-diisopropylethylamine (0.78 mL, 4.5 mmol), the mixture was then stirred for 16 h at 20 °C. The mixture was diluted with ethyl acetate (20 mL) and washed with water (3 x 20 mL). The combined aqueous fractions were re-extracted with ethyl acetate (3 x 20 mL) and the combined organic layers were washed with saturated aqueous sodium hydrogen carbonate (2 x 20 mL) and brine (20 mL) before being dried over magnesium sulfate and evaporated. The residue was purified by column

chromatography (25% ethyl acetate 75% hexane) to yield **136** (100 mg, 44%) as a white solid,  $^1\text{H}$  NMR (500 MHz, chloroform-*d*, 2 rotamers)  $\delta$  ppm 7.34 (1H, s, H<sub>(10)</sub>), 7.10 - 7.20 (1H, m, aryl), 6.99 (1H, m, aryl), 6.44 - 6.67 (2H, m, aryl), 5.44 (1H, br.s, H<sub>(6)</sub>), 4.79 - 5.01 (2H, m, H<sub>(3)</sub>/H<sub>(12)</sub>/H<sub>(19)</sub>), 4.71 (1H, m, H<sub>(12)</sub>/H<sub>(19)</sub>), 4.48 - 4.63 (2H, m, H<sub>(12)</sub>/H<sub>(19)</sub>), 3.76 (2H, br.s, H<sub>(20)</sub>), 3.15 (1H, dd,  $J=13.7, 6.1$  Hz, H<sub>(4)</sub>), 3.00 (1H, dd,  $J=13.7, 8.0$  Hz, H<sub>(4)</sub>), 1.34 (9H, s, 3 x 3H<sub>(23)</sub>);  $^{13}\text{C}$  NMR (500 MHz, chloroform-*d*, 2 rotamers)  $\delta$  ppm 170.15 (2), 170.06 C<sub>(2)</sub>, 155.07 C<sub>(21)</sub>, 155.04 C<sub>(21)</sub>, 146.58, 146.38, 137.06, 137.01, 135.17, 135.14, 133.55, 133.04, 132.85, 129.26, 127.02, 125.47, 123.60, 123.46, 115.20 C<sub>(14)</sub>/C<sub>(16)</sub>, 114.94 C<sub>(14)</sub>/C<sub>(16)</sub>, 108.94 C<sub>(16)</sub>/C<sub>(14)</sub>, 108.75 C<sub>(16)</sub>/C<sub>(14)</sub>, 79.79 C<sub>(22)</sub>, 52.43 C<sub>(12)</sub>/C<sub>(19)</sub>, 52.38 C<sub>(12)</sub>/C<sub>(19)</sub>, 52.00 C<sub>(19)</sub>/C<sub>(12)</sub>, 51.90 C<sub>(19)</sub>/C<sub>(12)</sub>, 51.01 C<sub>(3)</sub>, 36.64 C<sub>(4)</sub>, 28.32 C<sub>(23)</sub>; HRMS calcd for C<sub>22</sub>Cl<sub>2</sub>H<sub>(26)</sub>N<sub>3</sub>O<sub>3</sub>: 450.1351, found: 450.1351.

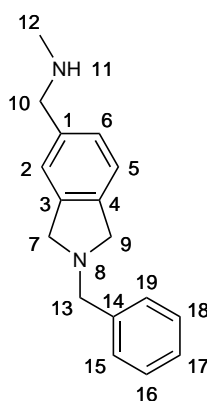
***tert*-Butyl (*R*)-(1-(5-acetamidoisoindolin-2-yl)-3-(2,4-dichlorophenyl)-1-oxopropan-2-yl)carbamate (138)**



To isoindoline **135** (100 mg, 0.58 mmol), *N*-Boc-(*R*)-2,4-dichlorophenylalanine (201 mg, 0.6 mmol), 1-ethyl-3-(3-dimethylaminopropyl)carbodiimide (109 mg, 0.6 mmol) and anhydrous 1-hydroxybenzotriazole (122 mg, 0.9 mmol) in dimethylformamide (3 mL) was added *N,N*-diisopropylethylamine (0.8 mL, 4.5 mmol), the mixture was then stirred for 24 h at 20 °C. The mixture was diluted with ethyl acetate (20 mL) and washed with water (3 x 20 mL). The combined aqueous fractions

were re-extracted with ethyl acetate (3 x 20 mL) and the combined organic layers were washed with saturated aqueous sodium hydrogen carbonate (2 x 20 mL) and brine (20 mL) before being dried over magnesium sulfate and evaporated. The residue was purified by silica column chromatography (ethyl acetate) to give **138** (143 mg, 52%) as a white solid, m.p. 196 - 197 °C;  $\nu_{max}$  (cm<sup>-1</sup>): 3281 (NH), 2920, 2850 (CH), 1703 (NHC=O), 1640 (CHC=O); <sup>1</sup>H NMR (500 MHz, chloroform-*d*, 2 rotamers)  $\delta$  ppm 8.26, 8.08 (1H, br.s, aryl), 7.65, 7.50 (1H, s, aryl), 7.34 (1H, d, *J*=6.3 Hz, aryl), 7.00 - 7.21 (3H, m, aryl), 5.45 (1H, t, *J*=9.0 Hz, H<sub>(5)</sub>), 4.48 - 4.86 (5H, m, H<sub>(3)</sub>,H<sub>(12)</sub>,H<sub>(19)</sub>), 3.14 (1H, dd, *J*=13.6, 5.8 Hz, H<sub>(4)</sub>), 2.85 - 3.02 (1H, m, H<sub>(4)</sub>), 2.15 (3H, d, *J*=7.4 Hz, H<sub>(22)</sub>), 1.26 - 1.37 (9H, m, 3H<sub>(25)</sub>); <sup>13</sup>C NMR (126 MHz, chloroform-*d*, 2 rotamers)  $\delta$  ppm 170.07 C<sub>(2)</sub>/C<sub>(21)</sub>, 170.01 C<sub>(2)</sub>/C<sub>(21)</sub>, 168.96 C<sub>(21)</sub>/C<sub>(2)</sub>, 168.84 C<sub>(21)</sub>/C<sub>(2)</sub>, 155.32 C<sub>(23)</sub>, 155.18 C<sub>(23)</sub>, 138.26, 138.08, 136.73, 136.54, 135.14, 133.73, 133.68, 132.84, 132.75, 131.28, 130.96, 129.32, 129.27, 127.09, 123.16, 123.07, 119.55, 119.35 C, 114.45, 114.32, 80.16 C<sub>(24)</sub>, 80.05 C<sub>(24)</sub>, 52.46 C<sub>(12)</sub>/C<sub>(19)</sub>, 52.30 C<sub>(12)</sub>/C<sub>(19)</sub>, 52.03 C<sub>(19)</sub>/C<sub>(12)</sub>, 51.95 C<sub>(19)</sub>/C<sub>(12)</sub>, 51.03 C<sub>(3)</sub>, 36.62 C<sub>(4)</sub>, 36.58 C<sub>(4)</sub>, 28.32 3C<sub>(2)</sub>, 24.53 C<sub>(22)</sub>, 24.47 C<sub>(22)</sub>; HRMS calcd for C<sub>24</sub>H<sub>27</sub>N<sub>3</sub>Cl<sub>2</sub>O<sub>4</sub>: 4923.1457 (M+H), found: 492.1460.

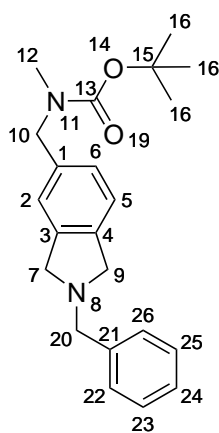
### 1-(2-Benzylisoindolin-5-yl)-*N*-methylmethanamine (140)



To amide **126a** (255 mg, 0.96 mmol) in dry tetrahydrofuran was added lithium aluminium hydride in tetrahydrofuran (1.5 mL, 1.5 mmol) dropwise at 0 °C with

stirring under an atmosphere of nitrogen. The solution was allowed to reach 23 °C and stirred for 30 min. The mixture was heated at reflux for 19 h and additional tetrahydrofuran was added (5 mL), after a further 7.5 h at reflux the mixture was cooled to 0 °C and was quenched with water (1 mL). The product was extracted with ethyl acetate (2 x 20 mL), washed with brine, dried over magnesium sulfate and the solvent evaporated. the residue was purified by silica column chromatography (92% ethyl acetate 5% methanol 2% ammonia .880) to give **140** (169 mg, 75%) as a white solid, <sup>1</sup>H NMR (500 MHz, chloroform-*d*) δ ppm 7.22 - 7.54 (5H, m, aryl), 7.02 - 7.21 (3H, m, aryl), 3.91 (6H, d, *J*=1.9 Hz, H<sub>(7)</sub>,H<sub>(9)</sub>,H<sub>(10)</sub>), 3.71 (2H, d, *J*=1.9 Hz, H<sub>(13)</sub>), 2.33 - 2.53 (3H, m, H<sub>(12)</sub>), 1.47 - 1.85 (1H, br.s, H<sub>(11)</sub>); <sup>13</sup>C NMR (126 MHz, chloroform-*d*) δ ppm 140.67 C<sub>(14)</sub>, 139.21 C<sub>(3)</sub>/C<sub>(4)</sub>, 138.66 C<sub>(4)</sub>/C<sub>(3)</sub>, 128.86 C<sub>(15)</sub>,C<sub>(19)</sub>, 128.46 C<sub>(16)</sub>,C<sub>(18)</sub>, 127.18, 126.89, 122.34, 122.28, 60.40 C<sub>(13)</sub>, 58.97 C<sub>(7)</sub>/C<sub>(9)</sub>, 58.80 C<sub>(9)</sub>/C<sub>(7)</sub>, 56.03 C<sub>(10)</sub>, 35.88 C<sub>(12)</sub>; HRMS calcd for C<sub>17</sub>H<sub>21</sub>N<sub>2</sub>: 253.1705, found: 253.1704.

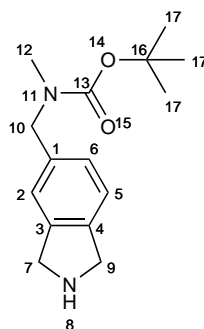
***tert*-Butyl ((2-benzylisoindolin-5-yl)methyl)(methyl)carbamate(141)**



To amine **140** (169 mg, 0.67 mmol) in *tert*-butanol (2 mL) was added dropwise with stirring, di-*tert*-butyl dicarbonate (161 mg, 0.74 mmol) in *tert*-butanol (1 mL). the mixture was stirred for 2.5 h and the solvent was evaporated. The residue was purified by silica column chromatography (50% hexane 50% diethyl ether) to give **141** (138 mg, 58%) as a yellow oil,  $\nu_{max}$  (cm<sup>-1</sup>): 3080 (CH), 2783 br. (NH), 1687

(C=O);  $^1\text{H}$  NMR (500 MHz, chloroform-*d*, 2 rotamers)  $\delta$  ppm 7.43 (2H, d,  $J=7.5$  Hz,  $\text{H}_{(22)},\text{H}_{(26)}$ ), 7.36 (2H, t,  $J=7.5$  Hz,  $\text{H}_{(23)},\text{H}_{(25)}$ ), 7.27 - 7.32 (1H, m, aryl), 7.14 (1H, d,  $J=7.2$  Hz, aryl), 7.00 - 7.10 (2H, m, aryl), 4.34 - 4.46 (2H, m,  $\text{H}_{(10)}$ ), 3.92 (6H, d,  $J=2.3$  Hz,  $\text{H}_{(7)},\text{H}_{(9)},\text{H}_{(20)}$ ), 2.64 - 2.94 (3H, m,  $3\text{H}_{(12)}$ ), 1.40 - 1.62 (9H, m,  $3\text{H}_{(16)}$ );  $^{13}\text{C}$  NMR (126 MHz, chloroform-*d*, 2 rotamers)  $\delta$  ppm 156.29  $\text{C}_{(13)}$ , 155.89  $\text{C}_{(13)}$ , 140.84, 139.44, 139.16, 136.84, 128.94, 128.89, 128.55, 127.29, 122.48, 79.82  $\text{C}_{(15)}$ , 79.65  $\text{C}_{(15)}$ , 60.43  $\text{C}_{(20)}$ , 58.99  $\text{C}_{(7)}/\text{C}_{(9)}$ , 58.81  $\text{C}_{(9)}/\text{C}_{(7)}$ , 52.65  $\text{C}_{(10)}$ , 51.94  $\text{C}_{(10)}$ , 33.85  $\text{C}_{(12)}$ , 28.62  $3\text{C}_{(2)}$ ; HRMS calcd for  $\text{C}_{22}\text{H}_{28}\text{N}_2\text{O}$ : 352.2145 (M+H), found: 352.2144.

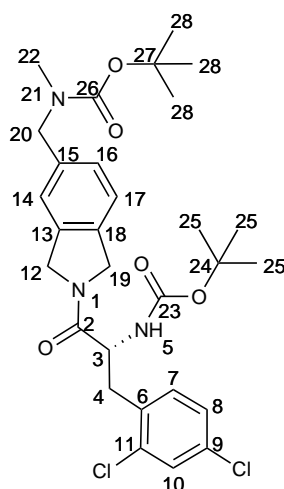
### *tert*-Butyl (isoindolin-5-ylmethyl)(methyl)carbamate (**142**)



To **141** (315 mg, 0.89 mmol in methanol (5 mL) was added 30% palladium on carbon (20 mg) and Pearlman's catalyst (20 mg). The suspension was stirred vigorously under an atmosphere of hydrogen for 24 h at 30 °C. The catalyst was removed by filtration through celite and the filtrate evaporated. The residue was purified by silica column chromatography (90% ethyl acetate 7% methanol 3% 0.880 ammonia) to give **142** (161 mg, 69%) as a dark yellow oil,  $\nu_{max}$  ( $\text{cm}^{-1}$ ): 2970 (CH), 1683 (C=O);  $^1\text{H}$  NMR 500 MHz, chloroform-*d*, 2 rotamers)  $\delta$  ppm 7.16 (1H, d,  $J=7.5$  Hz, aryl), 6.98 - 7.13 (2H, m, aryl), 4.38 (2H, s,  $\text{H}_{(10)}$ ), 4.17 (4H, s,  $\text{H}_{(7)},\text{H}_{(9)}$ ), 2.68 - 2.89 (3H, m,  $\text{H}_{(12)}$ ), 2.45 - 2.61 (1H, m,  $\text{H}_{(8)}$ ), 1.45 (9H, s,  $\text{H}_{(17)}$ );  $^{13}\text{C}$  NMR (126 MHz, chloroform-*d*, 2 rotamers)  $\delta$  ppm 156.24  $\text{C}_{(13)}$ , 155.87  $\text{C}_{(13)}$ , 142.39, 140.94, 136.86, 126.48, 126.00, 122.39, 121.78, 121.29, 79.74  $\text{C}_{(16)}$ , 79.68  $\text{C}_{(16)}$ , 52.97  $\text{C}_{(7)}/\text{C}_{(9)}$ ,

52.81 C<sub>(9)</sub>/C<sub>(7)</sub>, 52.58 C<sub>(10)</sub>, 51.89 C<sub>(10)</sub>, 33.90 C<sub>(12)</sub>, 28.56 C<sub>(17)</sub>; HRMS calcd for C<sub>15</sub>H<sub>23</sub>N<sub>2</sub>O<sub>2</sub>: 263.1760, found: 263.1763.

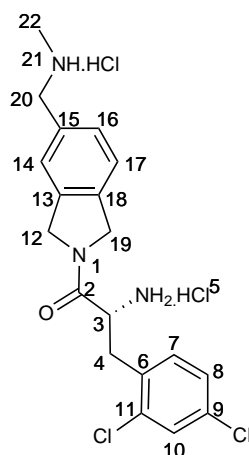
*tert*-Butyl (*R*)-((2-(2-((*tert*-butoxycarbonyl)amino)-3-(2,4-dichlorophenyl)propanoyl)isoindolin-5-yl)methyl)(methyl)carbamate (143)



To isoindoline **142** (158 mg, 0.6 mmol), *N*-Boc-(*R*)-2,4-dichlorophenylalanine (201 mg, 0.6 mmol), 1-ethyl-3-(3-dimethylaminopropyl)carbodiimide (131 mg, 0.72 mmol) and anhydrous 1-hydroxybenzotriazole (122 mg, 0.9 mmol) in dimethylformamide (5 mL) was added *N,N*-diisopropylethylamine (0.89 mL, 5.12 mmol), the mixture was then stirred for 24 h h at 20 °C. The mixture was the diluted with ethyl acetate (20 mL) and washed with water (3 x 20 mL). The combined aqueous fractions were re-extracted with ethyl acetate (3 x 20 mL) and the combined organic layers were washed with saturated aqueous sodium hydrogen carbonate (2 x 20 mL) and brine (20 mL) before being dried over magnesium sulfate and evaporated. The residue was purified by silica column chromatography (50% ethyl acetate 50% hexane) to give **143** (291 mg, 84%) as a white solid;  $\nu_{max}$  (cm<sup>-1</sup>): 3294 br. (NH), 2973, 1690 (NHC=O), 1640 (CHC=O); <sup>1</sup>H NMR (500 MHz, chloroform-*d*, mixture of rotamers)  $\delta$  ppm 7.34 - 7.40 (1H, m, aryl), 7.19 (5H, m, aryl), 5.35 (1H, d, *J*=9.0 Hz, H<sub>(5)</sub>), 5.01 (1H, d, *J*=13.6 Hz, H<sub>(12)</sub>/H<sub>(19)</sub>), 4.88 (1H, s, H<sub>(4)</sub>), 4.82 (1H, d,

$J=15.8$  Hz,  $H_{(19)}/H_{(12)}$ ), 4.58 - 4.71 (2H, m,  $H_{(12)},H_{(19)}$ ), 4.42 (2H, s,  $H_{(20)}$ ), 3.17 (1H, dd,  $J=13.4, 6.0$  Hz,  $H_{(4)}$ ), 3.04 (1H, dd,  $J=13.4, 7.9$  Hz,  $H_{(4)}$ ), 2.81 (3H, s,  $H_{(22)}$ ), 1.48 (9H, s, 3 x  $3H_{(28)}$ ), 1.27 - 1.40 (9H, s, 3 x  $3H_{(22)}$ );  $^{13}\text{C}$  NMR (126 MHz, chloroform-*d*, mixture of rotamers)  $\delta$  ppm 170.26  $C_{(2)}$ , 155.08  $C_{(23)},C_{(26)}$ , 138.43, 138.18, 136.39, 136.33, 135.20, 134.89, 133.68, 132.99, 132.85, 129.35, 127.12, 127.32 br., 123.09, 122.93, 121.99 br., 79.95  $C_{(24)},C_{(27)}$ , 52.38  $C_{(12)}/C_{(19)}$ , 52.32  $C_{(12)}/C_{(19)}$ , 52.26  $C_{(19)}/C_{(12)}$ , 52.20  $C_{(19)}/C_{(12)}$ , 51.06  $C_{(3)}$ , 36.73  $C_{(4)}$ , 34.11  $C_{(20)}$ , 34.07  $C_{(20)}$ , 28.57 ( $3C_{25}/3C_{28}$ ), 28.56 ( $3C_{28}/3C_{25}$ ), 28.36  $3C_{(2)}$ ; HRMS calcd for  $\text{C}_{29}\text{H}_{37}\text{N}_3\text{O}_5$ : 577.2105, found: 577.2108.

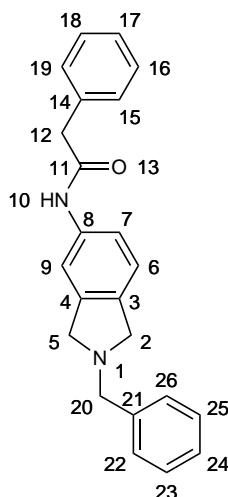
**(*R*)-2-Amino-3-(2,4-dichlorophenyl)-1-(5-((methylamino)methyl)-isoindolin-2-yl)propan-1-one dihydrochloride (144)**



*N*-Boc protected amide **143** (291 mg, 0.5 mmol) was dissolved in dry diethyl ether (10 mL). Hydrogen chloride was bubbled through the solution with vigorous stirring for 1 h. The precipitate was filtered by gravity filtration through filter paper in a funnel that was on top of a flask of boiling ether **144** (196 mg, 87%) as a cream solid,  $[\alpha]_D^{26}$  methanol:  $-34.2^\circ$ ;  $\nu_{max}$  ( $\text{cm}^{-1}$ ): 3437 br. ( $\text{NH}_3$ ), 2789 br. ( $\text{NH}_3$ ), 1649 ( $\text{C}=\text{O}$ );  $^1\text{H}$  NMR (500 MHz,  $\text{DMSO-}d_6$ )  $\delta$  ppm 9.62 (2H, br.s,  $H_{(24)}$ ), 8.75 (3H, br.s,  $H_{(6)}$ ), 7.60 (1H, t,  $J=1.9$  Hz, aryl), 7.50 (3H, s, aryl), 7.37 - 7.42 (2H, m, aryl), 7.34 (1H, d,  $J=7.9$  Hz, aryl), 5.09 (1H, m,  $J=17.3, 15.4$  Hz,  $H_{(15)}/H_{(22)}$ ), 4.74 (1H,

dd,  $J=16.2, 3.8$  Hz,  $H_{(22)}/H_{(15)}$ ), 4.54 (1H, dd,  $J=16.2, 4.5$  Hz,  $H_{(22)}/H_{(15)}$ ), 4.33 - 4.46 (1H, m,  $H_{(4)}$ ), 4.25 (1H, dd,  $J=15.4, 12.0$  Hz,  $H_{(15)}/H_{(22)}$ ), 4.07 (2H, br.s,  $H_{(23)}$ ), 3.30 - 3.35 (1H, m,  $H_{(5)}$ ), 3.26 (1H, dd,  $J=13.6, 7.9$  Hz,  $H_{(5)}$ );  $^{13}\text{C}$  NMR (151 MHz,  $\text{DMSO-}d_6$ )  $\delta$  ppm 166.59  $\text{C}_{(2)}$ , 136.61, 136.28, 136.00, 135.61, 134.59, 134.56, 133.60, 133.58, 133.08, 133.07, 131.73, 131.67, 129.64, 129.55, 128.88, 127.69, 124.70, 124.43, 123.29, 123.04, 51.94  $\text{C}_{(23)}$ , 51.59  $\text{C}_{(5)}$ , 51.57  $\text{C}_{(5)}$ , 50.80  $\text{C}_{(15)}/\text{C}_{(22)}$ , 50.76  $\text{C}_{(15)}/\text{C}_{(22)}$ , 50.03  $\text{C}_{(22)}/\text{C}_{(15)}$ , 49.97  $\text{C}_{(22)}/\text{C}_{(15)}$ , C, 33.32  $\text{C}_{(5)}/\text{C}_{(25)}$ , 33.28  $\text{C}_{(5)}/\text{C}_{(25)}$ , 31.77  $\text{C}_{(25)}/\text{C}_{(5)}$ , 31.72  $\text{C}_{25}/5$ ; HRMS calcd for  $\text{C}_{19}\text{H}_{22}\text{N}_3\text{Cl}_2\text{O}_2$ : 378.1140 (M+H), found: 378.1144.

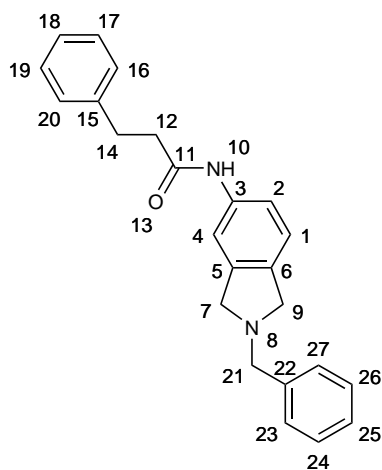
### *N*-(2-Benzylisoindolin-5-yl)-2-phenylacetamide (145)



Nitroisoindoline **120** (520 mg, 1.9 mmol) in methanol (10 mL) was stirred with 10% palladium on carbon (20 mg) under an atmosphere of hydrogen for 1 h. The catalyst was removed by filtration through celite and the solvent was evaporated. The residue was dissolved in dichloromethane and triethylamine (0.8 mL, 5.7 mmol) was added. Phenylacetyl chloride (0.28 mL, 2.1 mmol) was added dropwise and the solution was stirred for 1 h. The mixture was diluted with dichloromethane (10 mL), washed with aqueous saturated sodium hydrogen carbonate, dried over magnesium sulfate and the solvent evaporated. The residue was purified by silica

column chromatography (75% ethyl acetate 25% hexane) to give **145** as a white solid (368 mg, 54%), m.p. 150-152 °C;  $^1\text{H}$  NMR (500 MHz, chloroform-*d*)  $\delta$  ppm 7.27 - 7.45 (10H, m, aryl), 6.96 - 7.19 (3H, m, aryl), 3.88 (4H, s, H<sub>(2)</sub>,H<sub>(5)</sub>), 3.86 (2H, s, H<sub>(20)</sub>), 3.72 (2H, s, H<sub>(12)</sub>);  $^{13}\text{C}$  NMR (126 MHz, chloroform-*d*)  $\delta$  ppm 169.06 C<sub>(11)</sub>, 141.21, 138.97, 136.50, 136.43, 134.55, 129.61, 129.31, 128.85, 128.48 C, 127.73, 127.24, 122.60, 118.56, 114.45, 60.32 C<sub>(20)</sub>, 59.05 C<sub>(2)</sub>/C<sub>(5)</sub>, 58.57 C<sub>(5)</sub>/C<sub>(2)</sub>, 44.90 C<sub>12</sub>; HRMS calcd for C<sub>23</sub>H<sub>22</sub>N<sub>2</sub>O): 343.1810 (M+H), found: 343.1811.

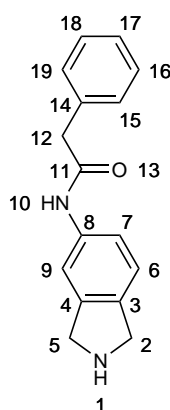
### *N*-(2-Benzylisoindolin-5-yl)-3-phenylpropanamide (**146**)



Nitroisoindoline **120** (210 mg, 0.74 mmol) was dissolved in methanol and stirred vigorously with 10% Pd/c catalyst under an atmosphere of hydrogen for 2 h. The catalyst was removed by filtration through celite and the filtrate was evaporated to give a cream solid (174 mg). This was dissolved in dichloromethane (10 mL), triethylamine (0.31 mL, 2.2 mmol) was added and the solution was cooled to 0 °C before dropwise addition of hydrocinnamoyl chloride (0.14 mL, 0.77 mmol), the mixture was then stirred for 15 min at 20 °C. The reaction was quenched with the addition of water (5 mL) and the organic phase was washed with saturated aqueous sodium hydrogen carbonate, dried over magnesium sulfate and the solvent was evaporated. The crude residue was purified by column chromatography (25% hexane 75% ethyl acetate) to give **146** (238 mg, 90%) as a cream solid, m.p. 138-

139.5 °C;  $\nu_{max}$  (cm<sup>-1</sup>): 3286 br. (NH), 2782, 1665 (C=O); <sup>1</sup>H NMR (500 MHz, chloroform-*d*)  $\delta$  ppm 7.39 - 7.44 (2H, m, aryl), 7.33 - 7.39 (3H, m, aryl), 7.27 - 7.32 (3H, m, aryl), 7.18 - 7.24 (3H, m, aryl), 7.11 (1H, dd,  $J=8.1, 1.5$  Hz, H<sub>(2)</sub>), 7.05 (1H, d,  $J=8.1$  Hz, H<sub>(1)</sub>), 3.90 (2H, s, H<sub>(21)</sub>), 3.87 (4H, s, 2H<sub>(7)</sub>, 2H<sub>(9)</sub>), 3.03 (2H, t,  $J=7.7$  Hz, 2H<sub>(12)</sub>), 2.62 (2H, t,  $J=7.7$  Hz, 2H<sub>(14)</sub>); <sup>13</sup>C NMR (151 MHz, chloroform-*d*)  $\delta$  ppm 170.62 C<sub>(11)</sub>, 141.23, 140.81, 139.09, 136.66, 136.33, 128.93, 128.75, 128.56, 128.53, 127.31, 126.49, 122.66, 118.84, 114.75, 60.40 C<sub>(21)</sub>, 59.11 C<sub>(7)</sub>/C<sub>(9)</sub>, 58.65 C<sub>(9)</sub>/C<sub>(7)</sub>, 39.50 C<sub>(12)</sub>, 31.73 C<sub>(14)</sub>; HRMS calcd for C<sub>24</sub>H<sub>24</sub>N<sub>2</sub>O 356.2883, found: 356.1881.

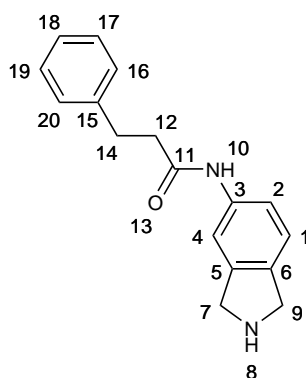
### *N*-(Isoindolin-5-yl)-2-phenylacetamide (147)



*N*-benzylisoindoline **145** (368 mg, 1.03 mmol) was stirred in methanol (5 mL) with 30% palladium on carbon (37 mg) and Pearlman's catalyst (37 mg) and stirred vigorously under an atmosphere of hydrogen for 22 h. The catalyst was removed by filtration through celite and the solvent evaporated. The residue was purified by silica column chromatography (85% ethyl acetate 10% methanol 5% 0.880 ammonia) to give **147** (164 mg, 63%) as a white solid which degrades rapidly upon exposure to air, <sup>1</sup>H NMR (500 MHz, CD<sub>3</sub>OD)  $\delta$  ppm 7.54 (1H, s, H<sub>(9)</sub>), 7.29 - 7.38 (5H, m, aryl), 7.21 - 7.27 (1H, m, aryl), 7.19 (1H, d,  $J=7.9$  Hz, aryl), 4.11 (4H, d,  $J=6.4$  Hz, H<sub>(2)</sub>, H<sub>(5)</sub>), 3.65 (2H, s, H<sub>(12)</sub>); <sup>13</sup>C NMR (126 MHz, CD<sub>3</sub>OD)  $\delta$  ppm 172.28 C<sub>(11)</sub>,

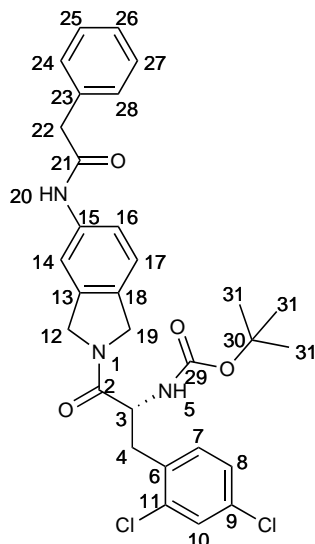
142.78, 138.96, 137.80, 136.87, 130.13, 129.60, 127.95, 123.53, 120.36, 115.53, 53.11 C<sub>(2)</sub>/C<sub>(5)</sub>, 52.69 C<sub>(5)</sub>/C<sub>(2)</sub>, 44.67 C<sub>(12)</sub>.

***N*-(Isoindolin-5-yl)-3-phenylpropanamide (148)**



*N*-Benzylisoindoline **146** (283 mg, 0.67 mmol), 30% palladium on carbon (30 mg) and Pearlman's catalyst (50 mg) and in methanol (12 mL) was stirred vigorously at 30 °C under an atmosphere of hydrogen for 24 h. The catalyst was removed by filtration through celite and the solvent evaporated. The residue was purified by silica chromatography (85% ethyl acetate 10% methanol 5% ammonia .880) to give the amine **148** (125 mg, 70%) as a cream solid, m.p. 137-138.5 °C;  $\nu_{max}$  (cm<sup>-1</sup>): 3200-3400 (NH), 3128-2576 (NH), 1658 (C=O); <sup>1</sup>H NMR (600 MHz, CD<sub>3</sub>OD)  $\delta$  ppm 7.50 (1H, s, H<sub>(4)</sub>), 7.29 (1H, dd, *J*=8.1, 1.7 Hz, H<sub>(2)</sub>), 7.19 - 7.26 (4H, m, aryl), 7.10 - 7.18 (2H, m, aryl), 4.02 - 4.13 (4H, m, 2H<sub>(7)</sub>, 2H<sub>(9)</sub>), 2.96 (2H, t, *J*=7.7 Hz, H<sub>(12)</sub>), 2.63 (2H, t, *J*=7.7 Hz, H<sub>(14)</sub>); <sup>13</sup>C NMR (151 MHz, chloroform-*d*)  $\delta$  ppm 173.53 C<sub>(11)</sub>, 142.78, 142.19, 138.92, 137.70, 129.53, 129.43, 127.27, 123.51, 120.35, 115.54, 53.15 C<sub>(7)</sub>/C<sub>(9)</sub>, 52.72 C<sub>(9)</sub>/C<sub>(7)</sub>, 39.83 C<sub>(12)</sub>, 32.85 C<sub>(14)</sub>. HRMS calcd for C<sub>17</sub>H<sub>18</sub>N<sub>2</sub>O: 266.1414, found: 266.1417.

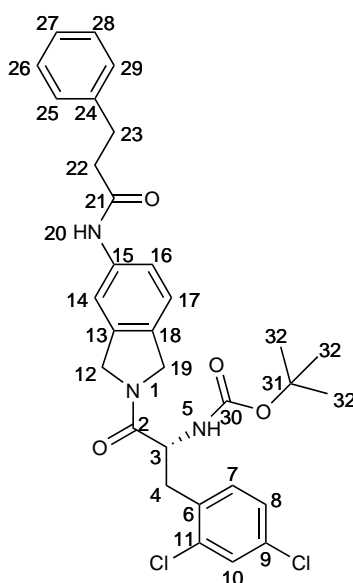
***tert*-Butyl (*R*)-(3-(2,4-dichlorophenyl)-1-oxo-1-(5-(2-phenylacetamido)-isoindolin-2-yl)propan-2-yl)carbamate (**149**)**



To isoindoline **147** (164 mg, 0.65 mmol), *N*-Boc-(*R*)-2,4-dichlorophenylalanine (217 mg, 0.65 mmol), 1-ethyl-3-(3-dimethylaminopropyl)carbodiimide (142 mg, 0.78 mmol) and anhydrous 1-hydroxybenzotriazole (131 mg, 0.98 mmol) in dimethylformamide (3 mL) was added *N,N*-diisopropylethylamine (0.96 mL, 5.53 mmol), the mixture was then stirred for 24 h at 20 °C. The mixture was then diluted with ethyl acetate (20 mL) and washed with water (3 x 20 mL). The combined aqueous fractions were re-extracted with ethyl acetate (2 x 20 mL) and the combined organic layers were washed with brine (50 mL) before being dried over magnesium sulfate and evaporated. The residue was purified by silica column chromatography (65% ethyl acetate 35% hexane) and recrystallised from ethyl acetate to give **149** (192 mg, 52%) as a white solid, m.p. (223-224 °C);  $[\alpha]_D^{26}$  chloroform: 25.2°;  $\nu_{max}$  (cm<sup>-1</sup>): 3292 br. (NH), 1687 (NHC=O), 1636 (CHC=O); <sup>1</sup>H NMR (500 MHz, chloroform-*d*)  $\delta$  ppm 7.52 (1H, br.s, H<sub>(14)</sub>), 7.38 - 7.46 (2H, m, aryl), 7.34 (4H, m, aryl), 7.06 - 7.22 (5H, m, aryl), 5.33 (1H, d, *J*=8.35 Hz, H<sub>(5)</sub>), 4.94 (1H, d, *J*=12.93 Hz, H<sub>(12)</sub>/H<sub>(19)</sub>), 4.80 - 4.88 (1H, m, H<sub>(19)</sub>/H<sub>(12)</sub>), 4.71 - 4.80 (1H, m, H<sub>(19)</sub>/H<sub>(12)</sub>), 4.50 - 4.66 (2H, m, H<sub>(12)</sub>,H<sub>(19)</sub>), 3.74 (2H, s, H<sub>(22)</sub>), 3.15 (1H, dd, *J*=13.48, 6.23 Hz, H<sub>(4)</sub>), 2.92 - 3.08 (1H, m, H<sub>(4)</sub>), 1.60 (1H, br.s, H<sub>(20)</sub>), 1.28 - 1.44 (9H, m, 3 x 3H<sub>(31)</sub>); <sup>13</sup>C NMR (126

MHz, chloroform-*d*)  $\delta$  ppm 170.19 C<sub>(2)</sub>, 169.29 C<sub>(21)</sub>, 155.08 C<sub>(29)</sub>, 137.69, 137.50, 136.87, 136.80, 135.18, 134.35, 133.71, 132.95, 132.91, 132.84, 131.76, 131.73, 129.62, 129.42, 129.34, 127.89, 127.12, 123.28, 123.17, 119.72, 119.56, 114.55, 114.45, 79.98 C<sub>(30)</sub>, 52.40 C<sub>(12)</sub>/C<sub>(19)</sub>, 52.07 C<sub>(19)</sub>/C<sub>(12)</sub>, 51.07 C<sub>(3)</sub>, 44.93 C<sub>(22)</sub>, 36.73 C<sub>(4)</sub>, 28.36 3C<sub>(2)</sub>, HRMS calcd for C<sub>30</sub>H<sub>32</sub>N<sub>3</sub>Cl<sub>2</sub>O<sub>4</sub>: 568.1770 (M+H), found: 568.1746.

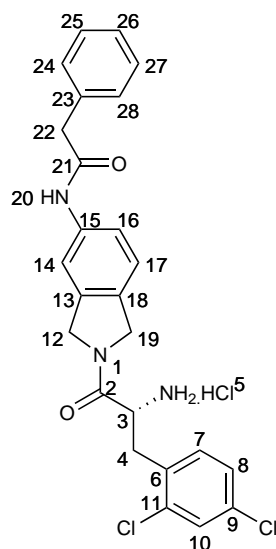
***tert*-Butyl (*R*)-(3-(2,4-dichlorophenyl)-1-oxo-1-(5-(3-phenylpropan-amido)isoindolin-2-yl)propan-2-yl)carbamate (**150**)**



Isoindoline **148** (125 mg, 0.47 mmol), *N*-Boc-(*R*)-2,4-dichlorophenylalanine (156 mg, 0.47 mmol), 1-ethyl-3-(3-dimethylaminopropyl)carbodiimide (80 mg, 0.52 mmol) and anhydrous 1-hydroxybenzotriazole (86 mg, 0.56 mmol) in dimethylformamide (3 mL) was added *N,N*-diisopropylethylamine (0.67 mL, 4.0 mmol), the mixture was then stirred for 24 h at 20 °C. The mixture was diluted with ethyl acetate (20 mL) and washed with water (3 x 20 mL). The combined aqueous fractions were re-extracted with ethyl acetate (2 x 20 mL) and the combined organic layers were washed with brine (50 mL) before being dried over magnesium sulfate and evaporated. The residue was purified by silica column chromatography (35% hexane 65% ethyl acetate) to give **150** (143 mg, 52%) as a cream solid, m.p. 195-197 °C;  $\nu_{max}$

( $\text{cm}^{-1}$ ): 3424-3300 (NH), 1687 (NHC=O), 1638 (CHC=O);  $^1\text{H}$  NMR (600 MHz, chloroform-*d*, mixture of rotamers)  $\delta$  ppm 7.60 - 7.79 (1H, m, aryl), 7.41 - 7.54 (1H, m, aryl), 7.27 - 7.40 (3H, m, aryl), 7.07 - 7.26 (6H, m, aryl), 6.97 (1H, d,  $J=7.5$  Hz, aryl), 5.35 - 5.46 (1H, m,  $\text{H}_{(5)}$ ), 4.52 - 4.85 (5H, m,  $\text{H}_{(3)}$ ,  $\text{H}_{(12)}$ ,  $\text{H}_{(19)}$ ), 3.12 - 3.20 (1H, m,  $\text{H}_{(4)}/\text{H}_{(22)}$ ), 3.02 - 3.11 (2H, m,  $\text{H}_{(4)}$ ,  $\text{H}_{(22)}$ ), 2.88 - 3.02 (1H, m,  $\text{H}_{(22)}/\text{H}_{(4)}$ ), 2.59 - 2.76 (2H, m,  $\text{H}_{(23)}$ ), 1.23 - 1.40 (9 H, m, 3 x  $3\text{H}_{(32)}$ )  $^{13}\text{C}$  NMR (151 MHz, chloroform-*d*, mixture of rotamers)  $\delta$  ppm 170.89  $\text{C}_{(2)}/\text{C}_{(21)}$ , 170.71  $\text{C}_{(2)}/\text{C}_{(21)}$ , 170.13  $\text{C}_{(21)}/\text{C}_{(2)}$ , 170.01  $\text{C}_{(21)}/\text{C}_{(2)}$ , 155.32  $\text{C}_{(30)}$ , 155.15  $\text{C}_{(30)}$ , 140.78, 140.68, 137.91, 137.82, 136.85, 136.70, 135.20, 135.18, 133.78, 133.73, 132.91, 132.89, 132.78, 131.48, 131.12, 129.40, 129.34, 128.79, 128.52, 128.50, 127.15, 127.13, 126.54, 126.52, 123.25, 123.16, 119.58, 119.35, 114.55, 114.47, 80.19  $\text{C}_{(31)}$ , 80.06  $\text{C}_{(31)}$ , 52.48  $\text{C}_{(12)}/\text{C}_{(19)}$ , 52.32  $\text{C}_{(12)}/\text{C}_{(19)}$ , 52.07  $\text{C}_{(19)}/\text{C}_{(12)}$ , 52.03  $\text{C}_{(19)}/\text{C}_{(12)}$ , 51.01  $\text{C}_{(4)}$ , 39.54  $\text{C}_{(22)}$ , 36.77  $\text{C}_{(23)}$ , 31.75  $\text{C}_{(4)}$ , 31.63  $\text{C}_{(4)}$ , 28.38  $\text{C}_{(32)}$ ; HRMS calcd for  $\text{C}_{31}\text{H}_{33}\text{N}_3\text{Cl}_2\text{O}_4$ : 581.1843, found: 581.1843.

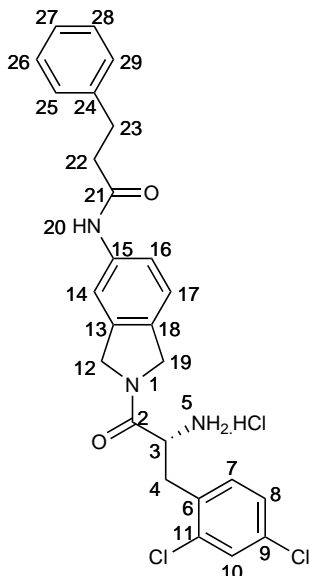
**(*R*)-*N*-(2-(2-Amino-3-(2,4-dichlorophenyl)propanoyl)isoindolin-5-yl)-2-phenylacetamide hydrochloride (151)**



*N*-Boc protected amide **149** (150 mg, 0.26 mmol) was dissolved in diethyl ether (10 mL) and dichloromethane (15 mL) and hydrogen chloride was bubbled through

the solution with vigorous stirring for 1 h. The precipitate was filtered by gravity filtration through filter paper in a funnel that was on top of a flask of boiling ether **151** (125 mg, 95%) as a grey solid, m.p. (decomp. 130 °C);  $[\alpha]_D^{25}$   $c=1$  methanol: -30.9°;  $\nu_{max}$  (cm<sup>-1</sup>): 2858 br. (NH<sub>3</sub>), 1644 (C=O); <sup>1</sup>H NMR (500 MHz, chloroform-*d* mixture of rotamers)  $\delta$  ppm 10.46 (1H, d,  $J=3.2$  Hz, H<sub>(20)</sub>), 8.49 (3H, d,  $J=2.6$  Hz, H<sub>(5)</sub>), 7.66 - 7.75 (1H, m, aryl), 7.62 (1H, d,  $J=1.1$  Hz, aryl), 7.43 - 7.52 (2H, m, aryl), 7.39 (1H, dt,  $J=8.3, 1.9$  Hz, aryl), 7.33 - 7.37 (2H, m, aryl), 7.31 (2H, t,  $J=7.5$  Hz, aryl), 7.16 - 7.28 (2H, m, aryl), 4.93 - 5.05 (1H, m, H<sub>(12)</sub>/H<sub>(19)</sub>), 4.64 - 4.76 (1H, m, H<sub>(19)</sub>/H<sub>(12)</sub>), 4.45 - 4.58 (1H, m, H<sub>(19)</sub>/H<sub>(12)</sub>), 4.34 - 4.45 (1H, m, H<sub>(3)</sub>), 4.17 - 4.30 (1H, m, H<sub>(12)</sub>/H<sub>(19)</sub>), 3.65 (2H, d,  $J=3.2$  Hz, H<sub>(22)</sub>), 3.26 (2H, d,  $J=6.8$  Hz, H<sub>(4)</sub>); <sup>13</sup>C NMR (126 MHz, chloroform-*d*)  $\delta$  ppm 169.29 C<sub>(2)</sub>/C<sub>(21)</sub>, 166.50 C<sub>(21)</sub>/C<sub>(2)</sub>, 166.47 C<sub>(21)</sub>/C<sub>(2)</sub>, 139.06, 139.00, 136.31, 136.12, 136.11, 135.69, 134.62, 133.62, 133.59, 133.12, 131.55, 130.22, 129.66, 129.16, 129.15, 128.92, 128.29, 127.69, 126.53, 123.19, 122.93, 118.82, 118.75, 113.47, 113.15, 64.96, 52.25 C<sub>(12)</sub>/C<sub>(19)</sub>, 51.86 C<sub>(12)</sub>/C<sub>(19)</sub>, 51.76 C<sub>(12)</sub>/C<sub>(19)</sub>, 51.36 C<sub>(12)</sub>/C<sub>(19)</sub>, 49.99 C<sub>(3)</sub>, 43.27 C<sub>(22)</sub>, 40.04 C<sub>(22)</sub>, 33.36 C<sub>(4)</sub>, 33.28 C<sub>(4)</sub>, HRMS calcd for C<sub>25</sub>H<sub>23</sub>N<sub>3</sub>Cl<sub>2</sub>O<sub>2</sub>: 468.1246 (M+H), found: 468.1236.

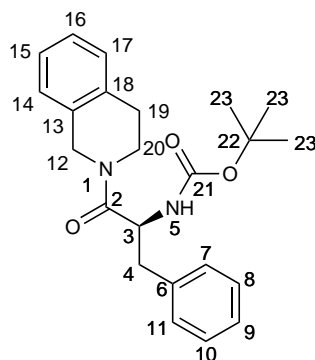
**(*R*)-*N*-(2-(2-Amino-3-(2,4-dichlorophenyl)propanoyl)isoindolin-5-yl)-3-phenylpropanamide hydrochloride (**152**)**



**150** (143 mg, 0.24 mmol) was dissolved in a mixture of diethyl ether (5 mL) and dichloromethane (13 mL). hydrogen chloride was bubbled through the stirred solution for 1.5 h. The precipitate was filtered by gravity filtration through filter paper in a funnel that was on top of a flask of boiling ether **152** (76 mg, 61%) as a white solid, m.p. (decomp. 170 °C) ;  $[\alpha]_D^{26}$  methanol: -30.5°;  $\nu_{max}$  (cm<sup>-1</sup>): 2855 br. (NH<sub>3</sub>), 1649 (C=O); <sup>1</sup>H NMR (600 MHz, DMSO-*d*<sub>6</sub>, 2 rotamers)  $\delta$  ppm 10.23 (1H, s, H<sub>(20)</sub>), 8.59 (3H, br.s, 3H<sub>(5)</sub>), 7.70 (1H, d, *J*=18.4 Hz, aryl), 7.63 (1H, t, *J*=2.4 Hz, aryl), 7.42 - 7.51 (2H, m, aryl), 7.38 - 7.42 (1H, m, aryl), 7.15 - 7.32 (6H, m, aryl), 5.02 (1H, d, *J*=13.7 Hz, H<sub>(12)</sub>/H<sub>(19)</sub>), 4.97 (1H, d, *J*=13.7 Hz, H<sub>(12)</sub>/H<sub>(19)</sub>), 4.72 (1H, d, *J*=16.0 Hz, H<sub>(19)</sub>/H<sub>(12)</sub>), 4.69 (1H, d, *J*=16.0 Hz, H<sub>(19)</sub>/H<sub>(12)</sub>), 4.53 (1H, d, *J*=16.0 Hz, H<sub>(19)</sub>/H<sub>(12)</sub>), 4.49 (1H, d, *J*=16.0 Hz, H<sub>(19)</sub>/H<sub>(12)</sub>), 4.33 - 4.44 (1H, m, H<sub>(3)</sub>), 4.28 (1H, d, *J*=13.7 Hz, H<sub>(12)</sub>/H<sub>(19)</sub>), 4.22 (1H, d, *J*=13.7 Hz, H<sub>(12)</sub>/H<sub>(19)</sub>), 3.20 - 3.33 (2H, m, 2H<sub>(4)</sub>), 2.90 (2H, t, *J*=7.7 Hz, 2H<sub>(22)</sub>), 2.64 (2H, t, *J*=7.7 Hz, H<sub>(23)</sub>); <sup>13</sup>C NMR (151 MHz, DMSO-*d*<sub>6</sub>, 2 rotamers)  $\delta$  ppm 170.54 C<sub>(2)</sub>, 166.50 C<sub>(21)</sub>, 166.47 C<sub>(21)</sub>, 141.19, 139.06, 138.98, 136.31, 135.67, 134.65, 134.63, 133.62, 133.60, 133.13, 131.56, 130.04, 129.48, 128.93, 128.34, 128.29, 127.70, 125.97, 123.17, 122.92, 118.72,

118.67, 113.38, 113.04, 52.27 C<sub>(12)</sub>/C<sub>(19)</sub>, 51.86 C<sub>(12)</sub>/C<sub>(19)</sub>, 51.78 C<sub>(19)</sub>/C<sub>(12)</sub>, 51.36 C<sub>(19)</sub>/C<sub>(12)</sub>, 50.00 C<sub>(3)</sub>, 37.94 C<sub>(22)</sub>, 37.91 C<sub>(22)</sub>, 33.37 C<sub>(4)</sub>, 33.28 C<sub>(4)</sub>, 30.86 C<sub>(23)</sub>; HRMS calcd for C<sub>26</sub>H<sub>25</sub>N<sub>3</sub>Cl<sub>2</sub>O<sub>2</sub>: 481.1318 (M+H), found: 481.1319.

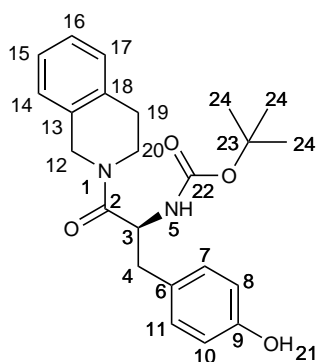
**(*s*)-tert-Butyl (1-(3,4-dihydroisoquinolin-2(1*H*))-yl)-1-oxo-3-phenylpropan-2-yl)carbamate (153)<sup>250</sup>**



To tetrahydroisoquinoline (0.13 mL, 1.0 mmol), *N*-Boc-(*R*)-phenylalanine (265 mg, 1.0 mmol), 1-ethyl-3-(3-dimethylaminopropyl)carbodiimide (182 mg, 1.0 mmol) and anhydrous 1-hydroxybenzotriazole (203 mg, 1.5 mmol) in dimethylformamide (3.0 mL) was added *N,N*-diisopropylethylamine (1.3 mL, 7.5 mmol), the mixture was then stirred for 16 h at 20 °C. The solvent was evaporated, the residue was dissolved in ethyl acetate (20 mL) and washed with water (2 x 20 mL). The combined aqueous fractions were re-extracted with ethyl acetate (2 x 20 mL) and the combined organic layers were washed with saturated aqueous sodium hydrogen carbonate (2 x 20 mL) and brine (20 mL) before being dried over magnesium sulfate and evaporated. The residue was purified by silica column chromatography (25% ethyl acetate, 75% hexane) to give **33** (221 mg, 58%) as a colourless oil,  $\nu_{max}$  (cm<sup>-1</sup>): 3304 (NH), 1701 (NHC=O), 1637 (CHC=O); <sup>1</sup>H NMR (500 MHz, chloroform-*d*, 2 rotamers)  $\delta$  ppm 6.97 - 7.30 (8H, m, aryl), 6.75 - 9.63 (1H, m, aryl), 5.52 - 5.66 (1H, m, H<sub>(5)</sub>), 4.83 - 5.00 (1H, m, H<sub>(3)</sub>), 4.73, 4.55 (*J* = 17.0 Hz), 4.48, 3.98 (*J* = 16.0 Hz, 2H, H<sub>(12)</sub>) 3.09 - 3.85 (2H, m, 2H<sub>(20)</sub>), 2.91 - 3.05 (2H, m, H<sub>(4)</sub>,H<sub>(19)</sub>), 2.26 - 2.80 (2H, m, H<sub>(4)</sub>,H<sub>(19)</sub>), 1.34 - 1.45 (9H, m, 3 x 3H<sub>(23)</sub>); <sup>13</sup>C NMR (126 MHz, chloroform-*d*, 2

rotamers)  $\delta$  ppm 170.77 C<sub>(2)</sub>, 170.47 C<sub>(2)</sub>, 155.15 C<sub>(21)</sub>, 149.40 C<sub>(21)</sub>, 136.49, 136.24, 134.55, 134.10, 132.79, 132.10, 129.51, 129.37, 128.65, 128.52, 128.3, 128.29, 126.96, 126.90, 126.86, 126.64, 126.60, 126.57, 126.31, 126.15, 79.78 C<sub>(22)</sub>, 51.84 C<sub>(3)</sub>, 51.61 C<sub>(3)</sub>, 47.08, 44.55, 43.10, 40.61, 40.49, 40.24, 29.15 C<sub>(19)</sub>, 28.43 C<sub>(23)</sub>, 28.35 C<sub>(19)</sub>; HRMS calcd for C<sub>23</sub>H<sub>28</sub>N<sub>2</sub>O<sub>3</sub>+H<sup>+</sup>: 381.2180, found: 381.2182.

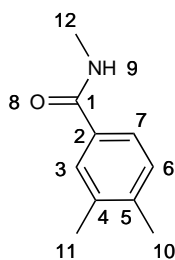
**(*s*)-*tert*-Butyl (1-(3,4-dihydroisoquinolin-2(1*H*)-yl)-3-(4-hydroxyphenyl)-1-oxopropan-2-yl)carbamate (154)**



To tetrahydroisoquinoline (0.11 mL, 1.0 mmol), *N*-Boc-(*s*)-tyrosine (281 mg, 1.0 mmol), 1-ethyl-3-(3-dimethylaminopropyl)carbodiimide (182 mg, 1.0 mmol) and anhydrous 1-hydroxybenzotriazole (203 mg, 1.5 mmol) in dimethylformamide (3.0 mL) was added *N,N*-diisopropylethylamine (1.3 mL, 7.5 mmol), the mixture was then stirred for 24 h at 20 °C. The mixture was diluted with ethyl acetate (20 mL) and washed with water (2 x 20 mL). The combined aqueous fractions were re-extracted with ethyl acetate (2 x 20 mL) and the combined organic layers were washed with saturated aqueous sodium hydrogen carbonate (2 x 20 mL) and brine (20 mL) before being dried over magnesium sulfate and evaporated. The residue was purified by silica column chromatography (20% ethyl acetate 80% dichloromethane) to give **154** (220 mg, 55%) as a pale yellow solid,  $\nu_{max}$  (cm<sup>-1</sup>): 3297 (NH), 1695 (NHC=O), 1628 (CHC=O); <sup>1</sup>H NMR (500 MHz, chloroform-*d*, 2 rotamers)  $\delta$  ppm 7.83, 7.65 (1H, s, H<sub>(21)</sub>) 6.81 - 7.20 (6H, m, aryl), 6.60 - 6.74 (2H, m, H<sub>(8)</sub>,H<sub>(10)</sub>), 5.58 (1H, d, *J*=9.0 Hz, H<sub>(5)</sub>), 4.82 - 4.95 (1H, m, H<sub>(3)</sub>), 3.90 - 4.81 (2H, m, 2H<sub>(12)</sub>),

3.60 - 3.80 (1H, m, H<sub>(20)</sub>), 3.50 - 3.61, 3.09-3.22 (1H, m, H<sub>(20)</sub>), 2.82 - 2.98 (2H, m, H<sub>(4)</sub>,H<sub>(19)</sub>), 2.63 - 2.80 (1H, m, H<sub>(4)</sub>), 2.38 (1H, m, H<sub>(19)</sub>), 1.42 (9H, s, 3 x 3H<sub>(24)</sub>); <sup>13</sup>C NMR (126 MHz, chloroform-*d*, 2 rotamers) δ ppm 170.15 C<sub>(2)</sub>, 170.86 C<sub>(2)</sub>, 155.80 C<sub>(9)</sub>/C<sub>(22)</sub>, 155.72 C<sub>(9)</sub>/C<sub>(22)</sub>, 155.51 C<sub>(22)</sub>/C<sub>(9)</sub>, 155.49 C<sub>(22)</sub>/C<sub>(9)</sub>, 134.48, 134.07, 132.56, 132.04, 128.57, 130.56 C<sub>(7)</sub>,C<sub>(11)</sub>, 130.47 C<sub>(7)</sub>,C<sub>(11)</sub>, 128.32, 127.28, 127.12 126.99 126.73, 126.59, 126.44, 126.18, 115.58 C<sub>(8)</sub>,C<sub>(10)</sub> 115.49 C<sub>(8)</sub>/C<sub>(10)</sub>, 80.02 C<sub>(23)</sub>, 52.06 C<sub>(3)</sub>, 51.83 C<sub>(3)</sub>, 47.20 C<sub>(12)</sub>, 44.70 C<sub>(12)</sub>, 43.21 C<sub>(20)</sub>, 40.62 C<sub>(20)</sub>, 39.48 C<sub>(4)</sub>, 39.43 C<sub>(4)</sub> 29.14 C<sub>(19)</sub>, 28.45 3C<sub>(2)</sub>, 28.29 C<sub>(9)</sub>; HRMS calcd for C<sub>23</sub>H<sub>28</sub>N<sub>2</sub>O<sub>4</sub>: 397.2127, found 397.2121.

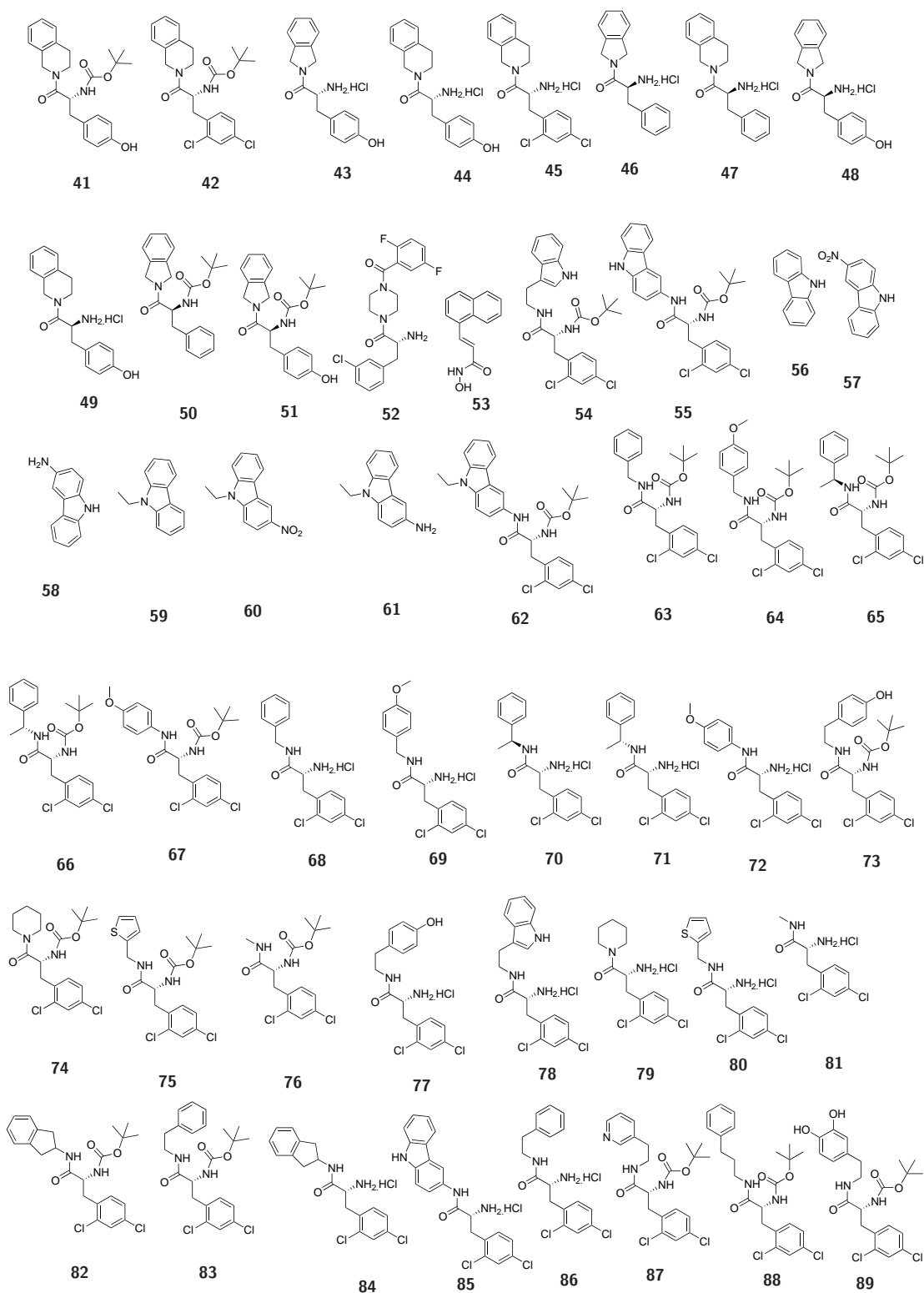
### *N*,3,4-Trimethylbenzamide (155)

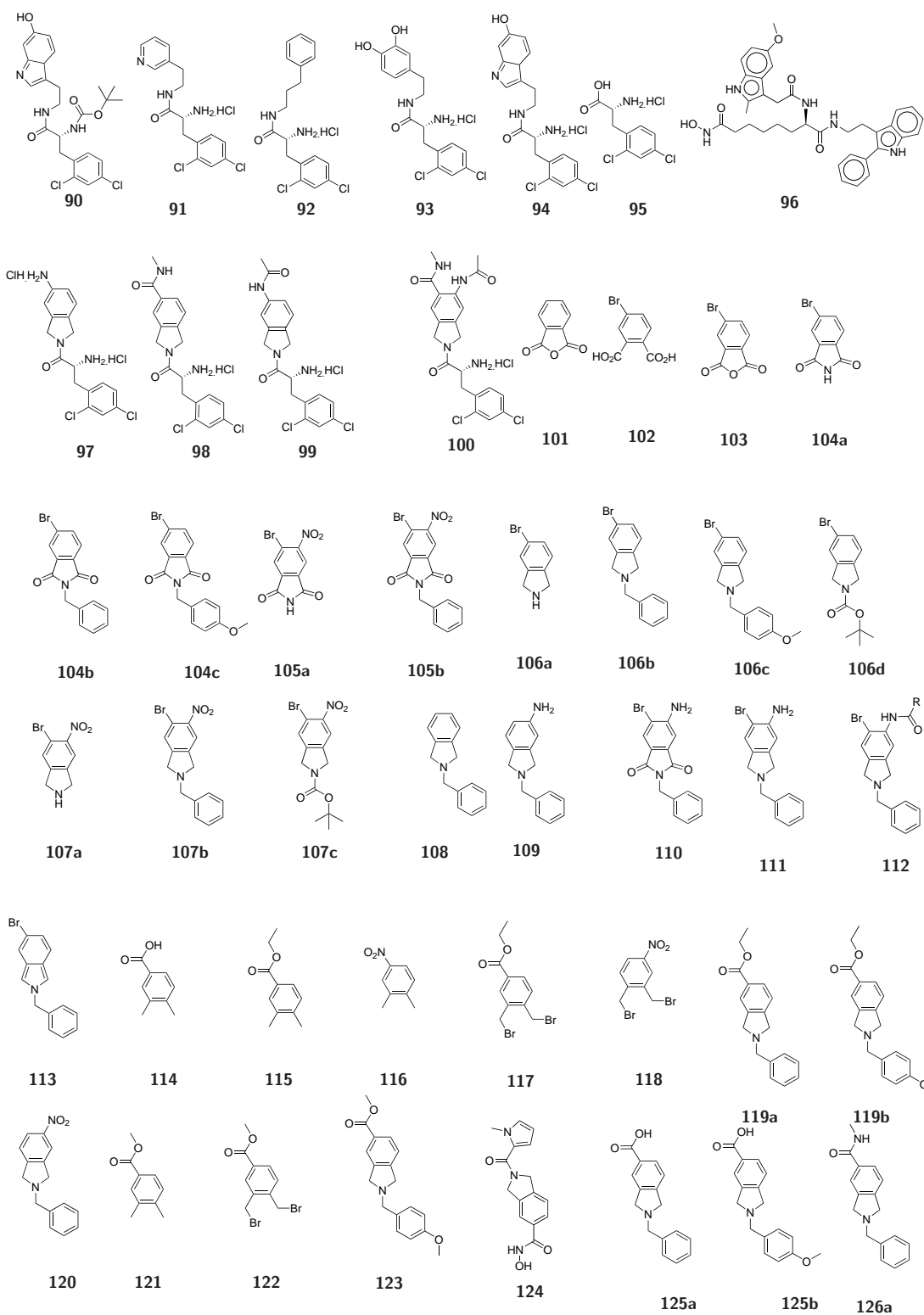


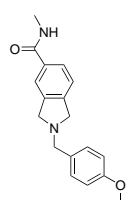
Ethyl 3,4-dimethylbenzoate (**115**) (534 mg, 4.37 mmol) and aqueous methylamine (40%, 10 mL) were added to a tube which was then sealed. The mixture was stirred for 16 h at 100 °C. The mixture was cooled to 20 °C and the solvent evaporated. The residue was then extracted into dichloromethane, washed with brine and dried over magnesium sulfate. The solvent was then evaporated to give crude **155** as a pale yellow solid (558 mg, 78%), <sup>1</sup>H NMR (600 MHz, chloroform-*d*) δ ppm 7.55 (1H, s, H<sub>(3)</sub>), 7.48 (1H, d, *J*=7.9 Hz, H<sub>(6)</sub>/H<sub>(7)</sub>), 7.12 (1H, d, *J*=7.9 Hz, H<sub>(7)</sub>/H<sub>(6)</sub>), 6.58 (1H, br.s, H<sub>(9)</sub>), 2.96 (3H, d, *J*=4.9 Hz, H<sub>(12)</sub>), 2.26 (3H, s, H<sub>(10)</sub>/H<sub>(11)</sub>), 2.25 (3H, s, H<sub>(11)</sub>/H<sub>(10)</sub>); <sup>13</sup>C NMR (151 MHz, DMSO-*d*<sub>6</sub>) δ ppm 168.79 C<sub>(1)</sub>, 140.41, 136.88, 132.12, 129.74, 128.36, 124.43, 26.90 C<sub>(12)</sub>, 19.88 C<sub>(10)</sub>/C<sub>(11)</sub>, 19.82 C<sub>(11)</sub>/C<sub>(10)</sub>.



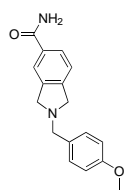




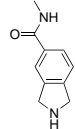




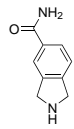
126b



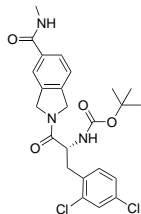
127



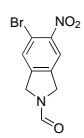
128



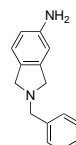
129



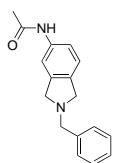
130



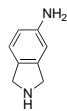
131



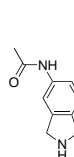
132



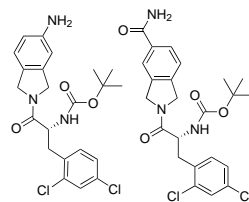
133



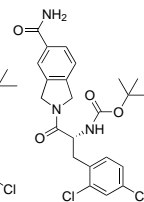
134



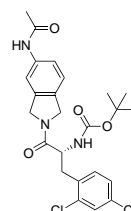
135



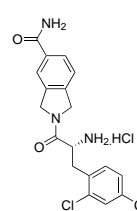
136



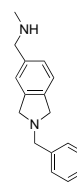
137



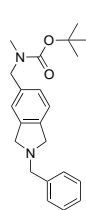
138



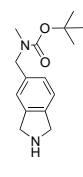
139



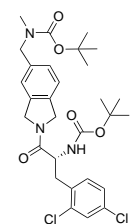
140



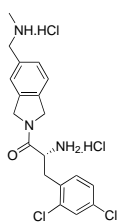
141



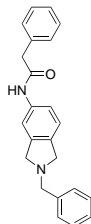
142



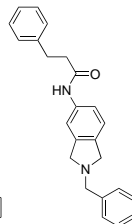
143



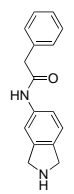
144



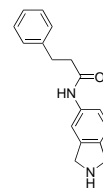
145



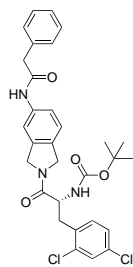
146



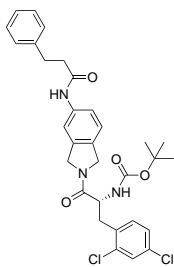
147



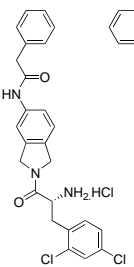
148



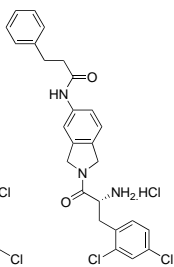
149



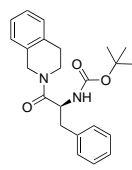
150



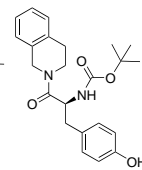
151



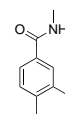
152



153



154



155

# Bibliography

- (1) Kouzarides, T. *EMBO J.* **2000**, *19*, 1176–1179.
- (2) Choudhary, C.; Kumar, C.; Gnad, F.; Nielsen, M. L.; Rehman, M.; Walther, T. C.; Olsen, J. V.; Mann, M. *Science* **2009**, *325*, 834–840.
- (3) Zeng, L.; Zhou, M. M. *FEBS Lett.* **2002**, *513*, 124–128.
- (4) Dey, a; Ellenberg, J; Farina, a; Coleman, a. E.; Maruyama, T; Sciortino, S; Lippincott-Schwartz, J; Ozato, K *Mol. Cell. Biol.* **2000**, *20*, 6537–6549.
- (5) Filippakopoulos, P.; Picaud, S.; Mangos, M.; Keates, T.; Lambert, J. P.; Barsyte-Lovejoy, D.; Felletar, I.; Volkmer, R.; Müller, S.; Pawson, T.; Gingras, A. C.; Arrowsmith, C. H.; Knapp, S. *Cell* **2012**, *149*, 214–231.
- (6) Waterborg, J. H. *Biochem. cell Biol.* **2002**, *80*, 363–378.
- (7) Ruijter, A. J. M. de; Gennip, A. H. van; Caron, H. N.; Kemp, S.; Kuilenburg, A. B. P. van *Biochem. J.* **2003**, *370*, 737–49.
- (8) Tsai, S.-C.; Seto, E. *J. Biol. Chem.* **2002**, *277*, 31826–33.
- (9) Ahringer, J. *Trends Genet.* **2000**, *16*, 351–356.
- (10) You, A.; Tong, J. K.; Grozinger, C. M.; Schreiber, S. L. *Proc. Natl. Acad. Sci.* **2001**, *98*, 1454–1458.
- (11) Khan, O.; La Thangue, N. B. *Immunol. Cell Biol.* **2012**, *90*, 85–94.
- (12) Petrie, K.; Guidez, F.; Howell, L.; Healy, L.; Waxman, S.; Greaves, M.; Zelent, A. *J. Biol. Chem.* **2003**, *278*, 16059–72.
- (13) Bertos, N. R.; Wang, A. H.; Yang, X.-J. *Biochem. Cell Biol.* **2001**, *79*, 243–252.
- (14) Yang, X.-J.; Gregoire, S. *Mol. Cell. Biol.* **2005**, *25*, 2873–2884.

- (15) Haggarty, S. S. J.; Koeller, K. *Proc. Natl. Acad. Sci.* **2003**, *100*, 4389–94.
- (16) Joshi, P.; Greco, T. M.; Guise, A. J.; Luo, Y.; Yu, F.; Nesvizhskii, A. I.; Cristea, I. M. *Mol. Syst. Biol.* **2013**, *9*, 672.
- (17) Gregoretto, I. V.; Lee, Y.-M.; Goodson, H. V. *J. Mol. Biol.* **2004**, *338*, 17–31.
- (18) Emiliani, S.; Fischle, W.; Van Lint, C.; Al-Abed, Y.; Verdin, E. *Proc. Natl. Acad. Sci.* **1998**, *95*, 2795–800.
- (19) Miska, E. a.; Langley, E.; Wolf, D.; Karlsson, C.; Pines, J.; Kouzarides, T. *Nucleic Acids Res.* **2001**, *29*, 3439–3447.
- (20) Verdin, E.; Dequiedt, F.; Kasler, H. G. *Trends Genet.* **2003**, *19*, 286–93.
- (21) Buggy, J. J.; Sideris, M. L.; Mak, P.; Lorimer, D. D.; McIntosh, B.; Clark, J. M. *Biochem. J.* **2000**, *350 Pt 1*, 199–205.
- (22) Hu, E.; Chen, Z.; Fredrickson, T.; Zhu, Y.; Kirkpatrick, R.; Zhang, G.-f. F.; Johanson, K.; Sung, C.-m. M.; Liu, R.; Winkler, J. *J. Biol. Chem.* **2000**, *275*, 15254–64.
- (23) Waltregny, D.; De Leval, L.; Glénisson, W.; Ly Tran, S.; North, B. J.; Belhahcène, A.; Weidle, U.; Verdin, E.; Castronovo, V. *Am. J. Pathol.* **2004**, *165*, 553–64.
- (24) Waltregny, D.; Glénisson, W.; Tran, S. L.; North, B. J.; Verdin, E.; Colige, A.; Castronovo, V. *FASEB J.* **2005**, *19*, 966–8.
- (25) Yang, Y.-c.; Chen, C.-n.; Wu, C.-i.; Huang, W.-J.; Kuo, T.-y.; Kuan, M.-c.; Tsai, T.-h.; Huang, J.-S.; Huang, C.-y. *Evid. Based. Complement. Alternat. Med.* **2013**, *2013*, 514908.
- (26) Wolfson, N. a.; Ann Pitcairn, C.; Fierke, C. A. *Biopolymers* **2013**, *99*, 112–26.
- (27) Lager, G.; O’Carroll, D.; Rembold, M.; Khier, H.; Tischler, J.; Weitzer, G.; Schuettengruber, B.; Hauser, C.; Brunmeir, R.; Jenuwein, T.; Seiser, C. *EMBO J.* **2002**, *21*, 2672–81.
- (28) Montgomery, R. L.; Davis, C. a.; Potthoff, M. J.; Haberland, M.; Fielitz, J.; Qi, X.; Hill, J. a.; Richardson, J. a.; Olson, E. N. *Genes Dev.* **2007**, *21*, 1790–1802.

- (29) Trivedi, C. M.; Luo, Y.; Yin, Z.; Zhang, M.; Zhu, W.; Wang, T.; Floss, T.; Goettlicher, M.; Noppinger, P. R.; Wurst, W.; Ferrari, V.; Abrams, C. S.; Gruber, P. J.; Epstein, J. A. *Nat. Med.* **2007**, *13*, 324–331.
- (30) Knutson, S. K.; Chyla, B. J.; Amann, J. M.; Bhaskara, S.; Huppert, S. S.; Hiebert, S. W. *EMBO J.* **2008**, *27*, 1017–1028.
- (31) Montgomery, R. L.; Potthoff, M. J.; Haberland, M.; Qi, X.; Matsuzaki, S.; Humphries, K. M.; Richardson, J. a.; Bassel-Duby, R.; Olson, E. N. *J. Clin. Invest.* **2008**, *118*, 3588–3597.
- (32) Vega, R. B.; Matsuda, K.; Oh, J.; Barbosa, A. C.; Yang, X.; Meadows, E.; McAnally, J.; Pomajzl, C.; Shelton, J. M.; Richardson, J. A.; Karsenty, G.; Olson, E. N. *Cell* **2004**, *119*, 555–566.
- (33) Chang, S.; McKinsey, T. a.; Zhang, C. L.; Richardson, J. a.; Hill, J. a.; Olson, E. N. *Mol. Cell. Biol.* **2004**, *24*, 8467–8476.
- (34) Zhang, Y.; Kwon, S.; Yamaguchi, T.; Cubizolles, F.; Rousseaux, S.; Kneissel, M.; Cao, C.; Li, N.; Cheng, H.-L.; Chua, K.; Lombard, D.; Mizeracki, A.; Matthias, G.; Alt, F. W.; Khochbin, S.; Matthias, P. *Mol. Cell. Biol.* **2008**, *28*, 1688–1701.
- (35) Chang, S.; Young, B. D.; Li, S.; Qi, X.; Richardson, J. a.; Olson, E. N. *Cell* **2006**, *126*, 321–334.
- (36) Haberland, M.; Mokalled, M. H.; Montgomery, R. L.; Olson, E. N. *Genes Dev.* **2009**, *23*, 1625–1630.
- (37) Chatterjee, T. K.; Basford, J. E.; Knoll, E.; Tong, W. S.; Blanco, V.; Blomkalns, A. L.; Rudich, S.; Lentsch, A. B.; Hui, D. Y.; Weintraub, N. L. *Diabetes* **2014**, *63*, 176–187.
- (38) Sahakian, E.; Powers, J. J.; Chen, J.; Deng, S. L.; Cheng, F.; Distler, A.; Woods, D. M.; Rock-Klotz, J.; Sodre, A. L.; Youn, J.-I.; Woan, K. V.; Villagra, A.; Gabrilovich, D.; Sotomayor, E. M.; Pinilla-Ibarz, J. *Mol. Immunol.* **2015**, *63*, 579–585.

- (39) Witt, O.; Deubzer, H. E.; Milde, T.; Oehme, I.; Witter, D. J.; Belvedere, S.; Chen, L.; Secrist, J. P.; Mosley, R. T.; Miller, T. a. *Cancer Lett.* **2009**, *277*, 8–21.
- (40) Deubzer, H. E.; Schier, M. C.; Oehme, I.; Lodrini, M.; Haendler, B.; Sommer, A.; Witt, O. *Int. J. Cancer* **2013**, *132*, 2200–2208.
- (41) Pflum, M. K.; Tong, J. K.; Lane, W. S.; Schreiber, S. L. *J. Biol. Chem.* **2001**, *276*, 47733–41.
- (42) Liang, B.; Bushweller, J. H.; Tamm, L. K. *J. Am. Chem. Soc.* **2006**, *128*, 4389–97.
- (43) Chien, W.; Lee, D. H.; Zheng, Y.; Wuensche, P.; Alvarez, R.; Wen, D. L.; Aribi, A. M.; Thean, S. M.; Doan, N. B.; Said, J. W.; Koeffler, H. P. *Mol. Carcinog.* **2014**, *53*, 722–735.
- (44) Park, J.-H.; Kim, S.-H.; Choi, M.-C.; Lee, J.; Oh, D.-Y.; Im, S.-A.; Bang, Y.-J.; Kim, T.-Y. *Biochem. Biophys. Res. Commun.* **2008**, *368*, 318–22.
- (45) Karagianni, P; Wong, J *Oncogene* **2007**, *26*, 5439–5449.
- (46) Lin, Y.-y.; Kiihl, S.; Suhail, Y.; Liu, S.-Y.; Chou, Y.-h.; Kuang, Z.; Lu, J.-y.; Khor, C. N.; Lin, C.-L.; Bader, J. S.; Irizarry, R.; Boeke, J. D. *Nature* **2012**, *482*, 251–5.
- (47) Luo, J; Su, F; Chen, D; Shiloh, a; Gu, W *Nature* **2000**, *408*, 377–81.
- (48) Wilson, B. J.; Tremblay, A. M.; Deblois, G.; Sylvain-Drolet, G.; Giguère, V. *Mol. Endocrinol.* **2010**, *24*, 1349–58.
- (49) Karolczak-Bayatti, M.; Sweeney, M.; Cheng, J.; Edey, L.; Robson, S. C.; Ulrich, S. M.; Treumann, A.; Taggart, M. J.; Europe-Finner, G. N. *J. Biol. Chem.* **2011**, *286*, 34346–55.
- (50) Deardorff, M. A.; Bando, M.; Nakato, R.; Watrin, E.; Itoh, T.; Minamino, M.; Saitoh, K.; Komata, M.; Katou, Y.; Clark, D.; Cole, K. E.; De Baere, E.; Decroos, C.; Di Donato, N.; Ernst, S.; Francey, L. J.; Gyftodimou, Y.; Hirashima, K.; Hullings, M.; Ishikawa, Y.; Jaulin, C.; Kaur, M.; Kiyono, T.; Lombardi, P. M.; Magnaghi-Jaulin, L.; Mortier, G. R.; Nozaki, N.; Petersen, M. B.; Seimiya, H.; Siu, V. M.; Suzuki, Y.; Takagaki, K.; Wilde, J.

- J.; Willems, P. J.; Prigent, C.; Gillessen-Kaesbach, G.; Christianson, D. W.; Kaiser, F. J.; Jackson, L. G.; Hirota, T.; Krantz, I. D.; Shirahige, K. *Nature* **2012**, *489*, 313–7.
- (51) Yan, W; Liu, S; Xu, E; Zhang, J; Zhang, Y; Chen, X *Oncogene* **2012**, *32*, 1–11.
- (52) Lee, H.; Sengupta, N.; Villagra, A.; Rezai-Zadeh, N.; Seto, E. *Mol. Cell. Biol.* **2006**, *26*, 5259–69.
- (53) Durst, K. L.; Lutterbach, B.; Kummalue, T.; Friedman, A. D.; Hiebert, S. W. *Mol. Cell. Biol.* **2003**, *23*, 607–619.
- (54) Watamoto, K.; Towatari, M.; Ozawa, Y.; Miyata, Y.; Okamoto, M.; Abe, A.; Naoe, T.; Saito, H. *Oncogene* **2003**, *22*, 9176–84.
- (55) Yuan, Z.; Peng, L.; Radhakrishnan, R.; Seto, E. *J. Biol. Chem.* **2010**, *285*, 39329–39338.
- (56) Scroggins, B. T.; Robzyk, K.; Wang, D.; Marcu, M. G.; Tsutsumi, S.; Beebe, K.; Cotter, R. J.; Felts, S.; Toft, D.; Karnitz, L.; Rosen, N.; Neckers, L. *Mol. Cell* **2007**, *25*, 151–9.
- (57) Hubbert, C.; Guardiola, A.; Shao, R.; Kawaguchi, Y.; Ito, A.; Nixon, A.; Yoshida, M.; Wang, X.-F.; Yao, T.-P. *Nature* **2002**, *417*, 455–458.
- (58) Juan, L. J.; Shia, W. J.; Chen, M. H.; Yang, W. M.; Seto, E; Lin, Y. S.; Wu, C. W. *J. Biol. Chem.* **2000**, *275*, 20436–43.
- (59) Luo, J; Su, F; Chen, D; Shiloh, A; Gu, W *Nature* **2000**, *408*, 377–81.
- (60) Bantscheff, M.; Hopf, C.; Savitski, M. M.; Dittmann, A.; Grandi, P.; Michon, A.-M.; Schlegl, J.; Abraham, Y.; Becher, I.; Bergamini, G.; Boesche, M.; Delling, M.; Dümpelfeld, B.; Eberhard, D.; Huthmacher, C.; Mathieson, T.; Poeckel, D.; Reader, V.; Strunk, K.; Sweetman, G.; Kruse, U.; Neubauer, G.; Ramsden, N. G.; Drewes, G. *Nat. Biotechnol.* **2011**, *29*, 255–65.
- (61) Madsen, A. S.; Olsen, C. a. *Angew. Chem. Int. Ed. Engl.* **2012**, *51*, 9083–7.
- (62) Du, J.; Zhou, Y.; Su, X.; Yu, J. J.; Khan, S.; Jiang, H.; Kim, J. H.; Woo, J.; Kim, J. H.; Choi, B. H.; He, B.; Chen, W.; Zhang, S.; Cerione, R. a.; Auwerx, J.; Hao, Q.; Lin, H. *Science* **2011**, *334*, 806–809.

- (63) Bradner, J. E.; Mak, R.; Tanguturi, S. K.; Mazitschek, R.; Haggarty, S. J.; Ross, K.; Chang, C. Y.; Bosco, J.; West, N.; Morse, E.; Lin, K.; Shen, J. P.; Kwiatkowski, N. P.; Gheldof, N.; Dekker, J.; DeAngelo, D. J.; Carr, S. a.; Schreiber, S. L.; Golub, T. R.; Ebert, B. L. *Proc. Natl. Acad. Sci.* **2010**, *107*, 12617–22.
- (64) Bouche-careilh, M.; Hutt, D. M.; Szajner, P.; Flotte, T. R.; Balch, W. E. *J. Biol. Chem.* **2012**, *287*, 38265–78.
- (65) Hutt, D. M.; Olsen, C. a.; Vickers, C. J.; Herman, D.; Chalfant, M.; Montero, A.; Leman, L. J.; Burkle, R.; Maryanoff, B. E.; Balch, W. E.; Ghadiri, M. R. *ACS Med. Chem. Lett.* **2011**, *2*, 703–707.
- (66) Zhang, Z.; Cai, Y.-q.; Zou, F.; Bie, B.; Pan, Z. Z. *Nat. Med.* **2011**, *17*, 1448–55.
- (67) Halili, M. a.; Andrews, M. R.; Sweet, M. J.; Fairlie, D. P. *Curr. Top. Med. Chem.* **2009**, *9*, 309–19.
- (68) Ha, S.-D.; Han, C. Y.; Reid, C.; Kim, S. O. *J. Immunol.* **2014**, *193*, 1333–43.
- (69) Andrews, K. T.; Tran, T. N.; Wheatley, N. C.; Fairlie, D. P. *Curr. Top. Med. Chem.* **2009**, *9*, 292–308.
- (70) Savarino, A.; Mai, A.; Norelli, S.; El Daker, S.; Valente, S.; Rotili, D.; Altucci, L.; Palamara, A. T.; Garaci, E. *Retrovirology* **2009**, *6*, 52.
- (71) Xu, K.; Dai, X.-L.; Huang, H.-C.; Jiang, Z.-F. *Oxid. Med. Cell. Longev.* **2011**, *2011*, 143269.
- (72) Fass, D. M.; Reis, S. a.; Ghosh, B.; Hennig, K. M.; Joseph, N. F.; Zhao, W.-N.; Nieland, T. J. F.; Guan, J.-S.; Kuhnle, C. E. G.; Tang, W.; Barker, D. D.; Mazitschek, R.; Schreiber, S. L.; Tsai, L.-H.; Haggarty, S. J. *Neuropharmacology* **2013**, *64*, 81–96.
- (73) Huangfu, D.; Maehr, R.; Guo, W.; Eijkelenboom, A.; Snitow, M.; Chen, A. E.; Melton, D. A. *Nat. Biotechnol.* **2008**, *26*, 795–7.
- (74) Van den Wyngaert, I; Vries, W de; Kremer, a; Neefs, J; Verhasselt, P; Luyten, W. H.; Kass, S. U. *FEBS Lett.* **2000**, *478*, 77–83.
- (75) Lee, H.; Rezai-Zadeh, N.; Seto, E. *Mol. Cell. Biol.* **2004**, *24*, 765–73.

- (76) Oehme, I.; Deubzer, H. E.; Wegener, D.; Pickert, D.; Linke, J.-p.; Hero, B.; Kopp-schneider, A.; Westermann, F.; Ulrich, S. M.; Deimling, A. von; Fischer, M.; Witt, O.; Deimling, A. V. *Clin. Cancer Res.* **2009**, *15*, 91–99.
- (77) Balasubramanian, S; Ramos, J; Luo, W; Sirisawad, M; Verner, E; Buggy, J. J. *Leukemia* **2008**, *22*, 1026–34.
- (78) Brodeur, G. M. *Nat. Rev. Cancer* **2003**, *3*, 203–216.
- (79) Maris, J. M.; Hogarty, M. D.; Bagatell, R.; Cohn, S. L. *Lancet* **2007**, *369*, 2106–2120.
- (80) Liu, D. P.; Song, H; Xu, Y *Oncogene* **2010**, *29*, 949–56.
- (81) Nobeli, I.; Favia, A. D.; Thornton, J. M. *Nat. Biotechnol.* **2009**, *27*, 157–67.
- (82) Somoza, J. R.; Skene, R. J.; Katz, B. a.; Mol, C.; Ho, J. D.; Jennings, A. J.; Luong, C.; Arvai, A.; Buggy, J. J.; Chi, E.; Tang, J.; Sang, B.-C.; Verner, E.; Wynands, R.; Leahy, E. M.; Dougan, D. R.; Snell, G.; Navre, M.; Knuth, M. W.; Swanson, R. V.; McRee, D. E.; Tari, L. W. *Structure* **2004**, *12*, 1325–34.
- (83) David, G.; Neptune, M. a.; DePinho, R. a. *J. Biol. Chem.* **2002**, *277*, 23658–63.
- (84) Vannini, A.; Volpari, C.; Gallinari, P.; Jones, P.; Mattu, M.; Francesco, R. D.; Steinkühler, C.; Marco, S. D.; Carfí, A.; De Francesco, R.; Di Marco, S.; Steinkühler, C.; Di Marco, S.; Francesco, R. D.; Steinkühler, C.; Marco, S. D.; Carfí, A.; De Francesco, R.; Di Marco, S. *EMBO Rep.* **2007**, *8*, 879–84.
- (85) Dowling, D. P.; Gantt, S. L.; Gattis, S. G.; Fierke, C. A.; Christianson, D. W. *Biochemistry* **2008**, *47*, 13554–63.
- (86) Bressi, J. C.; Jennings, A. J.; Skene, R.; Wu, Y.; Melkus, R.; De Jong, R.; O’Connell, S.; Grimshaw, C. E.; Navre, M.; Gangloff, A. R. *Bioorg. Med. Chem. Lett.* **2010**, *20*, 3142–5.
- (87) Watson, P. J.; Fairall, L.; Santos, G. M.; Schwabe, J. W. R. *Nature* **2012**, *481*, 335–40.
- (88) Bottomley, M. J.; Lo Surdo, P. L.; Di Giovine, P. D.; Cirillo, A.; Scarpelli, R.; Ferrigno, F.; Jones, P.; Neddermann, P.; De Francesco, R.; Steinkühler, C.; Gallinari, P.; Carfí, A. *J. Biol. Chem.* **2008**, *283*, 26694–704.

- (89) Schuetz, A.; Min, J.; Allali-Hassani, A.; Schapira, M.; Shuen, M.; Loppnau, P.; Mazitschek, R.; Kwiatkowski, N. P.; Lewis, T. A.; Maglathin, R. L.; Mclean, T. H.; Bochkarev, A.; Plotnikov, A. N.; Vedadi, M.; Arrowsmith, C. H. *J. Biol. Chem.* **2008**, *283*, 11355–63.
- (90) KrennHrubec, K.; Marshall, B. L.; Hedglin, M.; Verdin, E.; Ulrich, S. M. *Bioorg. Med. Chem. Lett.* **2007**, *17*, 2874–8.
- (91) Wernimont, A.; Edwards, A. *PLoS One* **2009**, *4*, ed. by Song, H., e5094.
- (92) Kunze, M. B. A.; Wright, D. W.; Werbeck, N. D.; Kirkpatrick, J.; Coveney, P. V.; Hansen, D. F. *J. Am. Chem. Soc.* **2013**, *135*, 17862–17868.
- (93) Decroos, C.; Bowman, C. M.; Moser, J.-a. S.; Christianson, K. E.; Deardor, M. a.; Christianson, D. W. **2015**.
- (94) Estiu, G.; West, N.; Mazitschek, R.; Greenberg, E.; Bradner, J. E.; Wiest, O. *Bioorg. Med. Chem.* **2010**, *18*, 4103–10.
- (95) Fatkins, D. G.; Zheng, W. *Anal. Biochem.* **2008**, *372*, 82–8.
- (96) Lombardi, P. M.; Cole, K. E.; Dowling, D. P.; Christianson, D. W. *Curr. Opin. Struct. Biol.* **2011**, *21*, 735–743.
- (97) Madsen, A. S.; Kristensen, H. M. E.; Lanz, G.; Olsen, C. A. *ChemMedChem* **2014**, *9*, 614–626.
- (98) Higuchi, T.; Nakayama, T.; Arao, T.; Nishio, K.; Yoshie, O. *Blood* **2013**, *121*, 3640–9.
- (99) Li, X.; Song, S.; Liu, Y.; Ko, S.-H.; Kao, H.-Y. *J. Biol. Chem.* **2004**, *279*, 34201–8.
- (100) Sengupta, N.; Seto, E. *J. Cell. Biochem.* **2004**, *93*, 57–67.
- (101) Haider, S.; Joseph, C. G.; Neidle, S.; Fierke, C. A.; Fuchter, M. J. *Bioorg. Med. Chem. Lett.* **2011**, *21*, 2129–32.
- (102) Gupta, R.; Jung, E.; Brunak., S. Prediction of N-glycosylation sites in human proteins., 2004.

- (103) Qiu, Y.; Zhao, Y.; Becker, M.; John, S.; Parekh, B. S.; Huang, S.; Hendarwanto, A.; Martinez, E. D.; Chen, Y.; Lu, H.; Adkins, N. L.; Stavreva, D. a.; Wiench, M.; Georgel, P. T.; Schiltz, R. L.; Hager, G. L. *Mol. Cell* **2006**, *22*, 669–79.
- (104) Gantt, S. L.; Joseph, C. G.; Fierke, C. A. *J. Biol. Chem.* **2010**, *285*, 6036–6043.
- (105) Singh, R. K.; Mandal, T.; Balsubramanian, N.; Viaene, T.; Leedahl, T.; Sule, N.; Cook, G.; Srivastava, D. K. *Bioorg. Med. Chem. Lett.* **2011**, *21*, 5920–3.
- (106) Vogelauer, M.; Krall, a. S.; McBrian, M. a.; Li, J.-Y.; Kurdistani, S. K. *J. Biol. Chem.* **2012**, *287*, 32006–32016.
- (107) Millard, C. J. J.; Watson, P. J. J.; Celardo, I.; Gordiyenko, Y.; Cowley, S. M. M.; Robinson, C. V. V.; Fairall, L.; Schwabe, J. W. R. *Mol. Cell* **2013**, *51*, 57–67.
- (108) Wilmott, J. S.; Colebatch, A. J.; Kakavand, H.; Shang, P.; Carlino, M. S.; Thompson, J. F.; Long, G. V.; Scolyer, R. a.; Hersey, P. *Mod. Pathol.* **2015**, *2*, 1–11.
- (109) Gantt, S. L.; Gattis, S. G.; Fierke, C. A. *Biochemistry* **2006**, *45*, 6170–8.
- (110) Dowling, D. P.; Gattis, S. G.; Fierke, C. A.; Christianson, D. W. *Biochemistry* **2010**, *49*, 5048–56.
- (111) Chang, C. J.; Jaworski, J.; Nolan, E. M.; Sheng, M.; Lippard, S. J. *Proc. Natl. Acad. Sci.* **2004**, *101*, 1129–34.
- (112) Bozym, R. a.; Thompson, R. B.; Stoddard, A. K.; Fierke, C. A. *ACS Chem. Biol.* **2006**, *1*, 103–11.
- (113) Wang, D.; Hosteen, O.; Fierke, C. A. *J. Inorg. Biochem.* **2012**, *111*, 173–81.
- (114) Werbeck, N. D.; Kirkpatrick, J.; Hansen, D. F. *Angew. Chemie Int. Ed.* **2013**, *52*, 3145–3147.
- (115) Lodish, H.; Berk, A.; Kaiser, C. A.; Krieger, M.; Scott, M. P.; Bretscher, A.; Ploegh, H.; Matsudaira, P. In *Mol. Cell Biol.* 4th; W. H. Freeman: New York, 2000, p 15.4.

- (116) Bolden, J. E.; Shi, W.; Jankowski, K.; Kan, C.-Y.; Cluse, L.; Martin, B. P.; Mackenzie, K. L.; Smyth, G. K.; Johnstone, R. W. *Cell Death Dis.* **2013**, *4*, e519.
- (117) Piekarz, R. L.; Frye, A. R.; Wright, J. J.; Steinberg, S. M.; Liewehr, D. J.; Rosing, D. R.; Sachdev, V.; Fojo, T.; Bates, S. E. *Clin. Cancer Res.* **2006**, *12*, 3762–73.
- (118) Tsuji, N.; Kobayashi, M.; Nagashima, K.; Wakisaka, Y.; Koizumi, K. *J. Antibiot. (Tokyo)*. **1976**, *29*, 1–6.
- (119) Geddes, J. R.; Goodwin, G. M.; Rendell, J.; Morriss, R.; Alder, N.; Juszcak, E.; Azorin, J. M.; Cipriani, A.; Ostacher, M. J.; Lewis, S.; Attenburrow, M. J.; Carter, B.; Hainsworth, J.; Healey, C.; Stevens, W.; Van Gucht, E. D.; Young, H.; Davies, C.; Peto, R.; Barnes, T. R. E.; Curtis, V.; Johnson, T.; Marven, M.; Arif, M.; Bruce, J.; Drybala, G.; Hayden, E.; Jhingan, H. P.; Marudkar, M.; Hillier, R.; Barrett, S.; Lidder, J. S.; McCartney, M.; Middleton, H.; Ononye, F.; Solanki, R. D.; Agell, I.; Anjum, R.; Hunt, N.; Jones, P.; Ramana, R.; Chase, J.; Ayuba, L.; Macmillan, I.; Michael, A.; Frangou, S.; Gijnsman, H.; Parker, E.; Phillips, M.; Behr, G.; Tyrer, P.; Conway, A.; Ferrier, N.; Oakley, T.; Tower, N.; Young, A.; Chitty, R.; Littlejohns, C.; Suri, A.; Iqbal, M.; Zikis, P.; Anderson, I.; O’Driscoll, D.; Robbins, N.; Ash, G.; Chaudhry, I.; Duddu, V.; Reed, P.; Van Wyk, S.; Vohra, A.; Zingela, Z.; Mahmood, T.; Diedricks, H.; Faizal, M. a.; McCarthy, J.; Briess, D.; Ceccherini-Nelli, A.; Clifford, E.; Croos, R.; Davis, J. D. R.; De Silva, L.; Eranti, S.; Mahmoud, R.; Maurya, A.; Partovi-Tabar, P.; Rahimi, Y.; Tuson, J.; Greening, J.; Campbell, C.; Grewal, J. S.; Kumar, A.; Schultewolter, D.; Baldwin, D.; Best, N.; Herod, N.; Polson, R.; Shawcross, C.; Khan, U.; Almoshmosh, N.; El-Adl, M.; Rao, C.; Timmins, B.; Bale, R.; Bansal, S.; Bhagwagar, Z.; Carre, A.; Cartright, J.; Chalmers, J.; Chisuse, A.; Davison, P.; Elwell, D.; Fazel, S.; Geaney, D.; Hampson, S.; Harrison, P.; Henderson, E.; Johnson, S.; Massey, C.; Ogilvie, A.; O’Leary, D.; Oppenheimer, C.; Orr, M.; Quested, D.; Sargent, P.; Wilkinson, P.; Hussain, T.; Franklin, S.; King, J.; White, J.; Anagnosti, O.; Bruce-Jones, B.; Evans, J.; Woodin, G.; Kirov, G.; Laugharne, R.; Blewett, A. E.; Gupta, S.; Saluja, B.; Kelly, C.; Leeman,

- T.; Macauley, M.; Shields, D.; Anderson, J.; McRae, A.; Taylor, M.; Carrick, L.; Hare, E.; Morrison, D.; Maurel, M.; Derouet, J.; Garzic, N. L.; Millet, B.; Droulout, T.; Henry, C.; Leboyer, M.; Meary, A.; Barbui, C.; Imperadore, G.; Tansella, M.; Sachs, G. *Lancet* **2010**, *375*, 385–395.
- (120) Ylisastigui, L.; Archin, N. M.; Lehrman, G.; Bosch, R. J.; Margolis, D. M. *AIDS* **2004**, *18*, 1101–1108.
- (121) Gotfryd, K.; Skladchikova, G.; Lepekhin, E. a.; Berezin, V.; Bock, E.; Walmod, P. S. *BMC Cancer* **2010**, *10*, 383.
- (122) Marks, P. A.; Breslow, R. *Nat. Biotechnol.* **2007**, *25*, 84–90.
- (123) Furumai, R.; Matsuyama, A.; Kobashi, N.; Lee, K.-H.; Nishiyama, M.; Nakajima, H.; Tanaka, A.; Komatsu, Y.; Nishino, N.; Yoshida, M.; Horinouchi, S. *Cancer Res.* **2002**, *62*, 4916–21.
- (124) Plumb, J. a.; Finn, P. W.; Williams, R. J.; Bandara, M. J.; Romero, M. R.; Watkins, C. J.; La Thangue, N. B.; Brown, R. *Mol. Cancer Ther.* **2003**, *2*, 721–728.
- (125) Jones, P.; Steinkühler, C. *Curr. Pharm. Des.* **2008**, *14*, 545–61.
- (126) Khan, N.; Jeffers, M.; Kumar, S.; Hackett, C.; Boldog, F.; Khramtsov, N.; Qian, X.; Mills, E.; Berghs, S. C.; Carey, N.; Finn, P. W.; Collins, L. S.; Tumber, A.; Ritchie, J. W.; Jensen, P. B.; Lichenstein, H. S.; Sehested, M. *Biochem. J.* **2008**, *409*, 581–9.
- (127) Brush, M. H.; Guardiola, A.; Connor, J. H.; Yao, T. P.; Shenolikar, S. *J. Biol. Chem.* **2004**, *279*, 7685–7691.
- (128) Bertrand, P. *Eur. J. Med. Chem.* **2010**, *45*, 2095–2116.
- (129) Silvestri, L.; Ballante, F.; Mai, A.; Marshall, G. R.; Ragno, R.; Silvestri, L.; Ballante, F.; Mai, A.; Marshall, G. R.; Ragno, R. *J. Chem. Inf. Model.* **2012**, *52*, 2215–35.
- (130) Olsen, C. a.; Ghadiri, M. R. *J. Med. Chem.* **2009**, *52*, 7836–46.
- (131) Hanessian, S.; Auzzas, L.; Larsson, A.; Zhang, J.; Giannini, G.; Gallo, G.; Ciacci, A.; Cabri, W. *ACS Med. Chem. Lett.* **2010**, *1*, 70–74.

- (132) Estiu, G.; Greenberg, E.; Harrison, C. B.; Kwiatkowski, N. P.; Mazitschek, R.; Bradner, J. E.; Wiest, O. *J. Med. Chem.* **2008**, *51*, 2898–906.
- (133) Jones, P.; Altamura, S.; De Francesco, R.; Paz, O. G.; Kinzel, O.; Mesiti, G.; Monteagudo, E.; Pescatore, G.; Rowley, M.; Verdirame, M.; Steinkühler, C. *J. Med. Chem.* **2008**, *51*, 2350–3.
- (134) Vaidya, A. S.; Neelarapu, R.; Madriaga, A.; Bai, H.; Mendonca, E.; Abdelkarim, H.; Breemen, R. B. van; Blond, S. Y.; Petukhov, P. a. *Bioorg. Med. Chem. Lett.* **2012**, *22*, 6621–7.
- (135) Bowers, A. A.; West, N.; Newkirk, T. L.; Troutman-Youngman, A. E.; Schreiber, S. L.; Wiest, O.; Bradner, J. E.; Williams, R. M. *Org. Lett.* **2009**, *11*, 1301–1304.
- (136) Hu, E.; Dul, E.; Sung, C.-M.; Chen, Z.; Kirkpatrick, R.; Zhang, G.-F.; Johanson, K.; Liu, R.; Lago, A.; Hofmann, G.; Macarron, R.; Frailes, M. de los; Perez, P.; Krawiec, J.; Winkler, J.; Jaye, M. *J. Pharmacol. Exp. Ther.* **2003**, *307*, 720–728.
- (137) Fournel, M.; Bonfils, C.; Hou, Y.; Yan, P. T.; Trachy-Bourget, M.-C.; Kalita, A.; Liu, J.; Lu, A.-H.; Zhou, N. Z.; Robert, M.-F.; Gillespie, J.; Wang, J. J.; Ste-Croix, H.; Rahil, J.; Lefebvre, S.; Moradei, O.; Delorme, D.; MacLeod, A. R.; Besterman, J. M.; Li, Z. *Mol. Cancer Ther.* **2008**, *7*, 759–768.
- (138) Mazitschek, R.; Patel, V.; Wirth, D. F. D.; Clardy, J. *Bioorg. Med. Chem. Lett.* **2008**, *18*, 2809–2812.
- (139) Jones, P.; Altamura, S.; De Francesco, R.; Gallinari, P.; Lahm, A.; Neddermann, P.; Rowley, M.; Serafini, S.; Steinkühler, C. *Bioorg. Med. Chem. Lett.* **2008**, *18*, 1814–9.
- (140) Wang, C.; Henkes, L. M.; Doughty, L. B.; He, M.; Wang, D.; Meyer-Almes, F.-J.; Cheng, Y.-Q. *J. Nat. Prod.* **2011**, *74*, 2031–8.
- (141) Bowers, A. A.; Greshock, T. J.; West, N.; Estiu, G.; Schreiber, S. L.; Wiest, O.; Williams, R. M.; Bradner, J. E. *J. Am. Chem. Soc.* **2009**, *131*, 2900–5.
- (142) Kalin, J. H.; Bergman, J. a. *J. Med. Chem.* **2013**, *56*, 6297–6313.

- (143) Santo, L.; Hideshima, T.; Kung, A. L.; Tseng, J. C.; Tamang, D.; Yang, M.; Jarpe, M.; Van Duzer, J. H.; Mazitschek, R.; Ogier, W. C.; Cirstea, D.; Rodig, S.; Eda, H.; Scullen, T.; Canavese, M.; Bradner, J.; Anderson, K. C.; Jones, S. S.; Rajee, N. *Blood* **2012**, *119*, 2579–2589.
- (144) Schroeder, F. a.; Lewis, M. C.; Fass, D. M.; Wagner, F. F.; Zhang, Y.-L.; Hennig, K. M.; Gale, J.; Zhao, W.-N.; Reis, S.; Barker, D. D.; Berry-Scott, E.; Kim, S. W.; Clore, E. L.; Hooker, J. M.; Holson, E. B.; Haggarty, S. J.; Petryshen, T. L. *PLoS One* **2013**, *8*, ed. by Homberg, J., e71323.
- (145) Marek, L.; Hamacher, A.; Hansen, F. K.; Kuna, K.; Gohlke, H.; Kassack, M. U.; Kurz, T. *J. Med. Chem.* **2013**, *56*, 427–436.
- (146) Tang, W.; Luo, T.; Greenberg, E. F.; Bradner, J. E.; Schreiber, S. L. *Bioorg. Med. Chem. Lett.* **2011**, *21*, 2601–5.
- (147) Whitehead, L.; Dobler, M. R.; Radetich, B.; Zhu, Y.; Atadja, P. W.; Claiborne, T.; Grob, J. E.; McRiner, A.; Pancost, M. R.; Patnaik, A.; Shao, W.; Shultz, M.; Tichkule, R.; Tommasi, R. A.; Vash, B.; Wang, P.; Stams, T. *Bioorg. Med. Chem.* **2011**, *19*, 4626–4634.
- (148) Suzuki, T.; Muto, N.; Bando, M.; Itoh, Y.; Masaki, A.; Ri, M.; Ota, Y.; Nakagawa, H.; Iida, S.; Shirahige, K.; Miyata, N. *ChemMedChem* **2014**, *149*, 1–9.
- (149) Wang, H.; Yu, N.; Chen, D.; Lee, K. C. L.; Lye, P. L.; Chang, J. W. W.; Deng, W.; Ng, M. C. Y.; Lu, T.; Khoo, M. L.; Poulsen, A.; Sangthongpitag, K.; Wu, X.; Hu, C.; Goh, K. C.; Wang, X.; Fang, L.; Goh, K. L.; Khng, H. H.; Goh, S. K.; Yeo, P.; Liu, X.; Bonday, Z.; Wood, J. M.; Dymock, B. W.; Ethirajulu, K.; Sun, E. T. *Journal of Medicinal Chemistry* **2011**, *54*, 4694–4720.
- (150) Richon, V. M.; Webb, Y.; Merger, R.; Sheppard, T.; Jursic, B.; Ngo, L.; Civoli, F.; Breslow, R.; Rifkind, R. a.; Marks, P. a. *Proc. Natl. Acad. Sci.* **1996**, *93*, 5705–5708.
- (151) Vickers, C. J.; Olsen, C. A.; Leman, L. J.; Ghadiri, M. R. *ACS Med. Chem. Lett.* **2012**, *3*, 505–508.

- (152) Jacobsen, F. Bioinorganic tools and zinc selective inhibitors for matrix metalloproteinases., PhD, University of California, San Diego, 2007.
- (153) Darkin-Rattray, S. J.; Gurnett, a. M.; Myers, R. W.; Dulski, P. M.; Crumley, T. M.; Allocco, J. J.; Cannova, C; Meinke, P. T.; Colletti, S. L.; Bednarek, M. a.; Singh, S. B.; Goetz, M. a.; Dombrowski, a. W.; Polishook, J. D.; Schmatz, D. M. *Proc. Natl. Acad. Sci.* **1996**, *93*, 13143–13147.
- (154) Wen, S.; Carey, K. L.; Nakao, Y.; Fusetani, N.; Packham, G.; Ganesan, a. *Org. Lett.* **2007**, *9*, 1105–1108.
- (155) Konsoula, Z.; Cao, H.; Velena, A.; Jung, M. *Mol. Cancer Ther.* **2009**, *8*, 2844–2851.
- (156) Muthyala, R.; Shin, W. S.; Xie, J.; Sham, Y. Y. *Bioorg. Med. Chem. Lett.* **2015**, 2–6.
- (157) Ilies, M.; Dowling, D. P.; Lombardi, P. M.; Christianson, D. W. *Bioorg. Med. Chem. Lett.* **2011**, *21*, 5854–8.
- (158) Lobera, M.; Madauss, K. P.; Pohlhaus, D. T.; Wright, Q. G.; Trocha, M.; Schmidt, D. R.; Baloglu, E.; Trump, R. P.; Head, M. S.; Hofmann, G. a.; Murray-Thompson, M.; Schwartz, B.; Chakravorty, S.; Wu, Z.; Mander, P. K.; Kruidenier, L.; Reid, R. a.; Burkhart, W.; Turunen, B. J.; Rong, J. X.; Wagner, C.; Moyer, M. B.; Wells, C.; Hong, X.; Moore, J. T.; Williams, J. D.; Soler, D.; Ghosh, S.; Nolan, M. a. *Nat. Chem. Biol.* **2013**, *9*, 319–25.
- (159) Laitaoja, M.; Valjakka, J.; Jänis, J. *Inorg. Chem.* **2013**, *52*, 10983–10991.
- (160) Mai, A.; Massa, S.; Cerbara, I.; Valente, S.; Ragno, R.; Bottoni, P.; Scatena, R.; Loidl, P.; Brosch, G. *J. Med. Chem.* **2004**, *47*, 1098–109.
- (161) Sleiman, S. F.; Olson, D. E.; Bourassa, M. W.; Karuppagounder, S. S.; Zhang, Y.-L.; Gale, J.; Wagner, F. F.; Basso, M.; Coppola, G.; Pinto, J. T.; Holson, E. B.; Ratan, R. R. *The Journal of Neuroscience* **2014**, *34*, 14328–14337.
- (162) Weisburger, J. H.; Weisburger, E. K. *Pharmacol. Rev.* **1973**, *25*, 1–66.
- (163) McDonnel, S. J.; Tell, L. A.; Murphy, B. G. *Journal of Veterinary Pharmacology and Therapeutics* **2014**, *37*, 196–200.

- (164) Jiang, J.; Thyagarajan-Sahu, A.; Krchnak, V.; Jedinak, A.; Sandusky, G. E.; Sliva, D. *PLoS One* **2012**, *7*, ed. by Ahmad, A., e34283.
- (165) Türkel, N. *J. Chem. Eng. Data* **2011**, *56*, 2337–2342.
- (166) Brown, D.; Glass, W.; McGardle, S. *Inorganica Chim. Acta* **1983**, *80*, 13–18.
- (167) Brown, D.; McKeith (née Byrne), D.; Glass, W. *Inorganica Chim. Acta* **1979**, *35*, 5–10.
- (168) Haratake, M.; Fukunaga, M.; Ono, M.; Nakayama, M. *J. Biol. Inorg. Chem.* **2005**, *10*, 250–258.
- (169) O'Brien, E.; Farkas, E.; Gil, M. *J. Inorg. ...* **2000**, *79*, 47–51.
- (170) Miller, M. *J. Chem. Rev.* **1989**, *89*, 1563–1579.
- (171) Končić, M. Z.; Barbarić, M.; Perković, I.; Zorc, B. *Molecules* **2011**, *16*, 6232–6242.
- (172) Frey, R. R.; Wada, C. K.; Garland, R. B.; Curtin, M. L.; Michaelides, M. R.; Li, J.; Pease, L. J.; Glaser, K. B.; Marcotte, P. a.; Bouska, J. J.; Murphy, S. S.; Davidsen, S. K. *Bioorg Med. Chem. Lett.* **2002**, *12*, 3443–3447.
- (173) Wu, S.; Zhang, C.; Xu, D.; Guo, H. *J. Phys. Chem. B* **2010**, *114*, 9259–9267.
- (174) Trial E2112 - ECOG-ACRIN Opens Phase III Trial of Syndax's Entinostat in Advanced Breast Cancer., 2014.
- (175) Lauffer, B. E. L.; Mintzer, R.; Fong, R.; Mukund, S.; Tam, C.; Zilberleyb, I.; Flicke, B.; Ritscher, A.; Fedorowicz, G.; Vallero, R.; Ortwine, D. F.; Gunzner, J.; Modrusan, Z.; Neumann, L.; Koth, C. M.; Kaminker, J. S.; Heise, C. E.; Steiner, P. *J. Biol. Chem.* **2013**, *288*, 26926–26943.
- (176) Moradei, O. M.; Mallais, T. C.; Frechette, S.; Paquin, I.; Tessier, P. E.; Leit, S. M.; Fournel, M.; Bonfils, C.; Trachy-Bourget, M.-C.; Liu, J.; Yan, T. P.; Lu, A.-h.; Rahil, J.; Wang, J.; Lefebvre, S.; Li, Z.; Vaisburg, A. F.; Besterman, J. M. *J. Med. Chem.* **2007**, *50*, 5543–5546.
- (177) Cole, K. E.; Dowling, D. P.; Boone, M. a.; Phillips, A. J.; Christianson, D. W. *J. Am. Chem. Soc.* **2011**, *133*, 12474–7.
- (178) Konstantinopoulos, P. a.; Vandoros, G. P.; Papavassiliou, A. G. *Cancer Chemother. Pharmacol.* **2006**, *58*, 711–5.

- (179) Page-McCaw, A.; Ewald, A. J.; Werb, Z. *Nat. Rev. Mol. Cell Biol.* **2007**, *8*, 221–233.
- (180) Wang, C.; Henkes, L. M.; Doughty, L. B.; He, M.; Wang, D.; Meyer-Almes, F.-J.; Cheng, Y.-Q. *J. Nat. Prod.* **2011**, *74*, 2031–8.
- (181) Kijima, M.; Yoshida, M.; Sugita, K.; Horinouchi, S.; Beppu, T. *J. Biol. Chem.* **1993**, *268*, 22429–35.
- (182) Qian, Z.; Upadhyaya, P.; Pei, D. In *Methods Mol. Biol.* Springer New York: 2015, pp 39–53.
- (183) Rettig, I.; Koeneke, E.; Trippel, F.; Mueller, W. C.; Burhenne, J.; Kopp-Schneider, a; Fabian, J.; Schober, a; Fernekorn, U; Deimling, a von; Deubzer, H. E.; Milde, T; Witt, O; Oehme, I *Cell Death Dis.* **2015**, *6*, e1657.
- (184) Kalyaanamoorthy, S.; Chen, Y.-P. P. *J. Comput. Chem.* **2013**, 1–14.
- (185) Wilcken, R.; Zimmermann, M. O.; Lange, A.; Joerger, A. C.; Boeckler, F. M. *J. Med. Chem.* **2013**, *56*, 1363–1388.
- (186) Liu, Y.; Xu, Z.; Yang, Z.; Chen, K.; Zhu, W. *J. Mol. Model.* **2013**, *19*, 5015–5030.
- (187) Verdin, E.; Dequiedt, F.; Fischle, W.; Frye, R.; Marshall, B.; North, B. In *Methods Enzymol.* 2002, 2003; Vol. 377, pp 180–196.
- (188) Wegener, D.; Wirsching, F.; Riestler, D.; Schwienhorst, A. *Chem. Biol.* **2003**, *10*, 61–68.
- (189) Gurard-Levin, Z. a.; Mrksich, M. *Biochemistry* **2008**, *47*, 6242–50.
- (190) Fatkins, D. G.; Monnot, A. D.; Zheng, W. *Bioorg. Med. Chem. Lett.* **2006**, *16*, 3651–6.
- (191) Gurard-Levin, Z. a.; Kim, J.; Mrksich, M. *ChemBioChem* **2009**, *10*, 2159–61.
- (192) Enzo Life Sciences *Fluor De Lys - HDAC8 Fluorimetric Drug Discovery Kit*; tech. rep.; Enzo Life Sciences, Product #: BML–AK518.
- (193) Schultz, B. E.; Misialek, S.; Wu, J.; Tang, J.; Conn, M. T.; Tahilramani, R.; Wong, L. *Biochemistry* **2004**, *43*, 11083–91.

- (194) Chou, K. C.; Zhou, G. P. *J. Am. Chem. Soc.* **1982**, *104*, 1409–1413.
- (195) Heltweg, B.; Dequiedt, F.; Marshall, B. L.; Brauch, C.; Yoshida, M.; Nishino, N.; Verdin, E.; Jung, M. *J. Med. Chem.* **2004**, *47*, 5235–43.
- (196) Heltweg, B.; Dequiedt, F.; Verdin, E.; Jung, M. *Anal. Biochem.* **2003**, *319*, 42–48.
- (197) Schultz, B. E.; Misialek, S.; Wu, J.; Tang, J.; Conn, M. T.; Tahilramani, R.; Wong, L. *Biochemistry* **2004**, *43*, 11083–91.
- (198) Singh, R. K.; Mandal, T.; Balasubramanian, N.; Cook, G.; Srivastava, D. K. *Anal. Biochem.* **2011**, *408*, 309–15.
- (199) Administration, U. S. F. D. FDA approves Farydak for treatment of multiple myeloma., 2015.
- (200) Bruserud, O.; Stapnes, C; Ersvær, E; Gjertsen, B. T.; Rynningen, A; Bruserud, O; Ersvaer, E *Curr. Pharm. Biotechnol.* **2007**, *8*, 388–400.
- (201) Tan, M.; Luo, H.; Lee, S.; Jin, F.; Yang, J. S.; Montellier, E.; Buchou, T.; Cheng, Z.; Rousseaux, S.; Rajagopal, N.; Lu, Z.; Ye, Z.; Zhu, Q.; Wysocka, J.; Ye, Y.; Khochbin, S.; Ren, B.; Zhao, Y. *Cell* **2011**, *146*, 1016–1028.
- (202) Montalbetti, C. a. G. N.; Falque, V. *Tetrahedron* **2005**, *61*, 10827–10852.
- (203) Aissaoui, H.; Boss, C.; Corminboeuf, O.; Frantz, M.-C. US2011/0281869 -1 Tetrahydroisoquinolines as Antimalarial Agents., 2009.
- (204) Yung-Chi, C.; Prusoff, W. H. *Biochem. Pharmacol.* **1973**, *22*, 3099–3108.
- (205) Chetan, B.; Bunha, M.; Jagrat, M.; Sinha, B. N.; Saiko, P.; Graser, G.; Szekeres, T.; Raman, G.; Rajendran, P.; Moorthy, D.; Basu, A.; Jayaprakash, V. *Bioorg Med. Chem. Lett.* **2010**, *20*, 3906–3910.
- (206) Canzoneri, J. C.; Chen, P. C.; Oyelere, A. K. *Bioorg. Med. Chem. Lett.* **2009**, *19*, 6588–6590.
- (207) Weerasinghe, S. V. W.; Estiu, G.; Wiest, O.; Pflum, M. K. H. *J. Med. Chem.* **2008**, *51*, 5542–5551.
- (208) Hanwell, M. D.; Curtis, D. E.; Lonie, D. C.; Vandermeersch, T.; Zurek, E.; Hutchison, G. R. *J. Cheminform.* **2012**, *4*, 1–17.

- (209) Huo, Z.; Li, Z.; Wang, T.; Zeng, H. *Tetrahedron* **2013**, *69*, 8964–8973.
- (210) Myslinski, J. M.; DeLorbe, J. E.; Clements, J. H.; Martin, S. F. *J. Am. Chem. Soc.* **2011**, *133*, 18518–18521.
- (211) Chang, C.-e. a.; Chen, W.; Gilson, M. K. *Proc. Natl. Acad. Sci.* **2007**, *104*, 1534–9.
- (212) Shimizu, S.; Watanabe, N.; Kataoka, T.; Shoji, T.; Abe, N.; Morishita, S.; Ichimura, H. In *Ullmann's Encycl. Ind. Chem.* Wiley-VCH Verlag GmbH & Co. KGaA: Weinheim, Germany, June 2000, pp 183–228.
- (213) Kulandaivelu, U.; Chilakamari, L. M.; Jadav, S. S.; Rao, T. R.; Jayaveera, K.; Shireesha, B.; Hauser, A.-T.; Senger, J.; Marek, M.; Romier, C.; Jung, M.; Jayaprakash, V. *Bioorg. Chem.* **2014**, *57*, 116–120.
- (214) Uffer, A; Schlittler, E. *Helv. Chim. Acta* **1948**, *31*, 1397–1400.
- (215) Anastasiadis, C.; Hogarth, G.; Wilton-Ely, J. D. E. T. *Inorganica Chim. Acta* **2010**, *363*, 3222–3228.
- (216) Micallef, A. S.; Bott, R. C.; Bottle, S. E.; Smith, G.; White, J. M.; Matsuda, K.; Iwamura, H. *J. Chem. Soc. Perkin Trans. 2* **1999**, 65–72.
- (217) Fairfull-Smith, K. E.; Brackmann, F.; Bottle, S. E. *European J. Org. Chem.* **2009**, 1902–1915.
- (218) Milan, C.; Engel, S. R.; Fang, Q. K.; Spear, K. L.; Chytil, M.; Us, M. A.; Engel, S. R.; Milan Chytil; Fang, Q. K.; Spear, K. L.; Us, M. A.; Milan Chytil US 2010/0204214 A1 - Histamine H3 inverse agonists and antagonists and methods of use thereof., Aug. 2010.
- (219) Cook, E. W.; France, W. G. *J. Phys. Chem.* **1931**, *36*, 2383–2389.
- (220) Gawley, R. E.; Chemburkar, S. R.; Smith, A. L.; Anklekar, T. V. *J. Org. Chem.* **1988**, *53*, 5381–5383.
- (221) Patel, B. H.; Barrett, A. G. M. *J. Org. Chem.* **2012**, *77*, 11296–301.
- (222) Prasad, A.; Kanth, J.; Periasamy, M. *Tetrahedron* **1992**, *48*, 4623–4628.
- (223) Neumeyer, J. L. *J. Pharm. Sci.* **1964**, *53*, 981–982.

- (224) Li, Y.; Manickam, G.; Ghoshal, A.; Subramaniam, P. *Synth. Commun.* **2006**, *36*, 925–928.
- (225) Blackburn, C.; Barrett, C.; Chin, J.; Garcia, K.; Gigstad, K.; Gould, A.; Gutierrez, J.; Harrison, S.; Hoar, K.; Lynch, C.; Rowland, R. S.; Tsu, C.; Ringeling, J.; Xu, H. *J. Med. Chem.* **2013**, *56*, 7201–11.
- (226) Han, W; Koch, S; Lam, P; Li, Y.; Orwat, M; Pinto, D Lactam-containing compounds and derivatives thereof as factor Xa inhibitors., 2002.
- (227) Yatsunami, T.; Yazaki, A.; Inoue, S.; Yamamoto, H.; Yokomoto, M.; Nomiya, J.; Noda, S. US5026856 - Isoindoline Derivative., 1991.
- (228) Blackstock, D. J.; Hartshorn, M. P.; Lewis, A. J.; Richards, K. E.; Vaughan, J.; Wright, G. J. *J. Chem. Soc. B Phys. Org.* **1971**, 1212.
- (229) Jo, Y.; Ju, J.; Choe, J.; Song, K. H.; Lee, S.; Kwang, H. S.; Lee, S. *J. Org. Chem.* **2009**, *74*, 6358–61.
- (230) Caldwell, T. M.; Gao, Y.; Han, B.; Xie, L.; Xu, Y. WO2007/106349 - Piperazinyl oxoalkyl tetrahydroisoquinolines and related analogues., 2007.
- (231) Williams, M. A.; Ladbury, J. E. In *Protein-Ligand Interact. From Mol. Recognit. to Drug Des.* Jan. 2005, pp 137–161.
- (232) Pervushin, K; Riek, R; Wider, G; Wüthrich, K *Proc. Natl. Acad. Sci.* **1997**, *94*, 12366–71.
- (233) Tugarinov, V.; Kay, L. E. *J. Am. Chem. Soc.* **2003**, *125*, 13868–78.
- (234) Harding, M. M.; Nowicki, M. W.; Walkinshaw, M. D. *Crystallogr. Rev.* **2010**, *16*, 247–302.
- (235) Hansen, D. F.; Neudecker, P.; Kay, L. E. *J. Am. Chem. Soc.* **2010**, *132*, 7589–7591.
- (236) Cala, O.; Guillière, F.; Krimm, I. *Anal. Bioanal. Chem.* **2014**, *406*, 943–956.
- (237) Dalvit, C; Fogliatto, G; Stewart, a; Veronesi, M; Stockman, B *J. Biomol. NMR* **2001**, *21*, 349–59.
- (238) Viegas, A.; Manso, J.; Nobrega, F. L.; Cabrita, E. J. *J. Chem. Educ.* **2011**, *88*, 990–994.

- (239) Hajduk, P. J.; Greer, J. *Nat. Rev. Drug Discov.* **2007**, *6*, 211–219.
- (240) West, A. C.; Johnstone, R. W. *J. Clin. Invest.* **2014**, *124*, 30–39.
- (241) Lopez, G.; Bill, K. L. J.; Bid, H. K.; Braggio, D.; Constantino, D.; Prudner, B.; Zewdu, A.; Batte, K.; Lev, D.; Pollock, R. E. *PLoS One* **2015**, *10*, ed. by Hofmann, T. G., e0133302.
- (242) Jones, P.; Altamura, S.; Chakravarty, P. K.; Cecchetti, O.; De Francesco, R.; Gallinari, P.; Ingenito, R.; Meinke, P. T.; Petrocchi, A.; Rowley, M.; Scarpelli, R.; Serafini, S.; Steinkühler, C. *Bioorg. Med. Chem. Lett.* **2006**, *16*, 5948–52.
- (243) Sixto-López, Y.; Gómez-Vidal, J. a.; Correa-Basurto, J. *Appl. Biochem. Biotechnol.* **2014**, DOI: 10.1007/s12010-014-0976-1.
- (244) Wang, D.-F.; Helquist, P.; Wiech, N. L.; Wiest, O. *J. Med. Chem.* **2005**, *48*, 6936–47.
- (245) Zang, L.-L.; Wang, X.-J.; Li, X.-B.; Wang, S.-Q.; Xu, W.-R.; Xie, X.-B.; Cheng, X.-c.; Ma, H.; Wang, R.-L. *J. Mol. Graph. Model.* **2014**, *54C*, 10–18.
- (246) Brunsteiner, M.; Petukhov, P. a. *J. Mol. Model.* **2012**, *18*, 3927–39.
- (247) Fielding, L *Prog. Nucl. Magn. Reson. Spectrosc.* **2007**, *51*, 219–242.
- (248) Schrödinger, LLC The {PyMOL} Molecular Graphics System, Version~1.3r1., Aug. 2010.
- (249) Hoover, D. J.; Hulin, B.; Martin, W. H.; Phillips, D.; Treadway, J. L. US006107329A - Substituted -(indole-2-carbonyl)glycinamides and derivatives as glycogen phosphorylase inhibitors., 2000.
- (250) Dutta, S.; Basak, A.; Dasgupta, S. *Bioorg. Med. Chem.* **2009**, *17*, 3900–8.
- (251) Alisi, M. A.; Dragone, P.; Furlotti, G.; Cazzolla, N.; Russo, V.; Mangano, G.; Coletta, I.; Lorenzo, P. WO 2007014687 A1 - 3-aminocarbazole compounds, pharmaceutical composition containing the same and method for the preparation thereof., 2007.
- (252) Nagarajan, R.; Muralidharan, D.; Perumal, P. T. *Synth. Commun.* **2004**, *34*, 1259–1264.

- (253) Iles, D. H.; Ledwith, A. *J. Chem. Soc. D Chem. Commun.* **1969**, 364.
- (254) Yang, M.-J. J.; Shao, T.; Men, J.; Gao, G.-w. W.; Chen, H. *J. Chem. Res.* **2012**, *36*, 379–380.
- (255) Zhang, Z.; Li, X.; Song, T.; Zhao, Y.; Feng, Y. *J. Med. Chem.* **2012**, *55*, 10735–41.
- (256) Elvidge, J. A.; Golden, J. H.; Linstead, R. P. *J. Chem. Soc.* **1957**, 2466 – 2472.
- (257) Blanck, S.; Maksimoska, J.; Baumeister, J.; Harms, K.; Marmorstein, R.; Meggers, E. *Angew. Chemie - Int. Ed.* **2012**, *51*, 5244–5246.
- (258) Shishkina, O. V.; Maizlish, V. E.; Shaposhnikov, G. P. *Russ. J. Org. Chem.* **1997**, *67*, 789–792.
- (259) Carpino, P. P. A.; Dasilva-Jardine, P.; Dasilba-Jardine, P. A.; Lefker, B. A.; Ragan, J. A.; Dasilva-Jardine, P. US 5936089 - Dipeptides which promote release of growth hormone., New York, Aug. 1999.